



THE HONG KONG
POLYTECHNIC UNIVERSITY

香港理工大學

Pao Yue-kong Library

包玉剛圖書館

Copyright Undertaking

This thesis is protected by copyright, with all rights reserved.

By reading and using the thesis, the reader understands and agrees to the following terms:

1. The reader will abide by the rules and legal ordinances governing copyright regarding the use of the thesis.
2. The reader will use the thesis for the purpose of research or private study only and not for distribution or further reproduction or any other purpose.
3. The reader agrees to indemnify and hold the University harmless from and against any loss, damage, cost, liability or expenses arising from copyright infringement or unauthorized usage.

IMPORTANT

If you have reasons to believe that any materials in this thesis are deemed not suitable to be distributed in this form, or a copyright owner having difficulty with the material being included in our database, please contact lbsys@polyu.edu.hk providing details. The Library will look into your claim and consider taking remedial action upon receipt of the written requests.

SOUND PROPAGATION IN PERFORMANCE HALLS WITH BALCONIES

CHEUNG LIU YEE

Ph.D

The Hong Kong Polytechnic University

2017

The Hong Kong Polytechnic University

Department of Building Services Engineering

**Sound Propagation in Performance Halls with
Balconies**

CHEUNG Liu Yee

A thesis submitted in partial fulfilment of the requirements for the degree of Doctor of
Philosophy

September 2015

This page is blank.

CERTIFICATE OF ORIGINALITY

I hereby declare that this thesis is my own work and that, to the best of my knowledge and belief, it reproduces no material previously published or written, nor material that has been accepted for the award of any other degree or diploma, except where due acknowledgement has been made in the text.

Cheung Liu Yee

This page is blank

ABSTRACT

The development of the West Kowloon Cultural District and the growing demand of performing facilities for the locals, more world-class performance halls with balconies are expected to be built in the future in Hong Kong. This urges the need to understand more about halls with balconies. Nowadays, to understand the variation of the acoustics in large performance hall in a detailed manner, seats to seats measurement is unavoidable. However, full scale measurements are very time consuming.

This study started with real hall measurements as a hall survey aiming at building a hall database locally for this study and future research. Four different performing halls with different sizes and designs were measured using impulse method using Room Acoustic software. In three of the halls, both its concert and proscenium setting were measured.

The measurement results was then reviewed and commented. With the hall geometric data and the first reflection path difference calculated from the point of reflection, the measured hall data were then used for establishing a simple framework using neural network analysis. Testing the four training schemes with a simple feed-forward network, an artificial neural network for the evaluation of performance hall acoustics was successfully established. This network predicted the parameters measured in Hall A successfully. Hall B's data was used to validate this prediction approach. With the validation results, this framework of using a small number of training/measured inputs to predict other hall parameters were founded reliable for halls with similar level of reverberance.

Furthermore, the real hall measurements results of Hall A were used to test and build various regression model. For simplicity, the regression models generated are formed by linear combinations of polynomials of these parameters without any inclusion of cross-products of different parameters. Once the source-to-receiver distance, azimuthal and elevation angle are included, the regression model predicts more accurately than the neural network approach. However, the symmetry of the hall affected the formation of the best performing model. A model consisting of quadratic polynomials in source-to-receiver distance and elevation angle and a linear function of the azimuthal angle

magnitude performed best in symmetrical halls while a quadratic function of source-to-receiver distance and a linear function of elevation angle, a polynomial in azimuthal angle is the best for asymmetrical hall. Since asymmetrical hall design yet common in Hong Kong and lack of measurement data, further validation is required.

To study the design of the balcony to various parameters in a hall, a 1/10 scale model of Hall A was done to evaluate the balcony effect. The model architecture was based on the geometry of Hall A. Plywood panels were used to construct the model on top of a raised timbre framework that allow access from below. Both the concert and proscenium setting of the hall was tested with and without the balcony. The results show that the balcony affect the energy received at different location of hall, especially the seats underneath the balcony.

Keywords: Performance hall; balconies; Hall acoustics

PUBLICATIONS

The following publications arise from this thesis work:

L.Y. Cheung and S.K. Tang, (2010) “Sound Propagation and Scattering in Performance Halls with Balconies” *Proceedings of 20th International Congress on Acoustics, ICA 2010*, page 33-38, 2010.

L.Y. Cheung and S.K. Tang, (2012) “How the design of a balcony affects the acoustics in an auditorium?” *Abstract book of Acoustics 2012 Hong Kong*, Hong Kong (The Journal of the Acoustical Society of America, vol. 131, issue 4, p. 3358)

L.Y. Cheung and S.K. Tang, (2013) “3D Computer Modeling on Balconies In Auditorium” *Proceedings of the 19th International Congress on Sound and Vibration*, Vilnius, Lithuania.

L.Y. Cheung and S.K. Tang, (2013) “Sound Propagation to and around the balcony in a performance hall, “*Meeting abstract, the 166th Meeting of the Acoustical Society of America*.”

L.Y. Cheung and S.K. Tang, (2013). “Neural network predictions of acoustical parameters in multi-purpose performance halls”. *Journal of Acoustical Society of America*, 134(3), 2049-65.

L.Y. Cheung and S.K. Tang, (2016). “Geometrical parameter combinations that correlate with early interaural cross-correlation coefficients in a performance hall”. *Journal of Acoustical Society of America*, 139, 2741-2753.

This page is blank

ACKNOWLEDGEMENT

First of all, it is very grateful that I can have Professor Tang Shiu-Keung as my supervisor for my PhD studies. Without him, I would not have been able to extend my interest in music and staging to acoustics, merging my interests to my career. The guidance, advice, resources, support and opportunities given from Prof. Tang are valuable and precious to my research and career development.

Special thanks to my family, especially my mother giving me the freedom with unconditional support to persuade my study and feeling proud of me. Many thanks to my best friends accompanying me in going through all the challenges.

Also, I would like to acknowledge the Leisure and Cultural Department, HKSAR, the Hong Kong Polytechnic University and the Chinese University of Hong Kong for allowing me to use their halls as measurement venues; the PolyU Student Hall of Residence, Hung Hom for providing me the lecture room for my scale model experiment.

Finally, many thanks to my research group teammates who helped me so much in my measurements and experiments. Without them, the experiment cannot be completed.

This page is blank

Table of Content

Chapter 1	Introduction	1
1.1	Background	1
1.2	Aims and objectives	1
1.3	Outline of this thesis	2
Chapter 2	Literature review and background	5
2.1	Halls	5
2.2	Fundamental acoustical parameters	5
2.2.1	Reverberation Time RT	6
2.2.2	Early time, definition, steepness Energy building up in a hall	7
2.2.3	<i>Sound pressure level</i>	9
2.2.4	<i>Sound strength G, Loudness</i>	9
2.2.5	<i>Spaciousness and envelopment – IACC, ASW, LEV</i>	10
2.2.6	<i>Intimacy- initial-time-delay-gap</i>	12
2.3	Subjective parameters	12
2.3.1	Pitch and brightness	12
2.3.2	Loudness	12
2.3.3	Liveness and fullness of tone	12
2.3.4	Intimacy or presence	13
2.3.5	Timbre	13
2.3.6	Spaciousness	13
2.3.7	Definition and Clarity	13
2.3.8	Warmth	13
2.3.9	Ensemble	13
2.4	Balcony	14
2.5	Impulse response Measurement method	17
2.5.1	<i>Maximum Length Sequences, MLS</i>	18
2.5.2	<i>Impulse source</i>	19
2.5.3	<i>Measurement locations</i>	19
2.6	Neural Network	21
2.6.1	Theory and how	21
2.6.2	Application in Acoustics	23
2.7	Conclusion	24

Chapter 3	Methodology	25
3.1	Real hall measurements	25
3.2	Scale down model	27
3.2.1	Model	27
3.2.2	Measurement Cases	28
3.2.3	Source signal	31
3.2.4	Measurement locations	33
3.2.5	Receiver and recording	34
3.2.6	Analysis using Integrated-impulse method.....	36
3.3	Neural network analysis.....	38
3.4	Regression analysis	40
3.4.1	Point of reflection and path difference.....	40
3.4.2	Regression inputs	42
3.5	Conclusions	43
Chapter 4	Hall measurements.....	45
4.1	Introduction.....	45
4.2	The Halls	45
4.3	Hall details	46
4.3.1	Hall A.....	46
4.3.2	Hall B.....	48
4.3.3	Hall C	49
4.3.4	Hall D.....	51
4.4	Measurement setup	52
4.4.1	Binaural measurement	52
4.4.2	Mono-aural measurements around the balcony edge.....	53
4.5	Measurement points and survey results	53
4.5.1	Hall A measurement points.....	54
4.5.2	Hall B measurement points.....	55
4.5.3	Hall C measurement points.....	56
4.6	Binaural Measurement Results	56
4.6.1	Hall A Binaural Results	57
4.6.1.1	Early decay time, EDT.....	57
4.6.1.2	T30	58
4.6.1.3	Clarity, C80 and Definition, D50.....	58

4.6.1.4	G_{relative}	59
4.6.2	Hall B Binaural Results.....	61
4.6.2.1	EDT	61
4.6.2.2	T30	63
4.6.2.3	C80 and D50	63
4.6.2.4	G_{relative}	65
4.6.3	Hall C Binaural Results.....	65
4.6.3.1	EDT	65
4.6.3.2	T30	67
4.6.3.3	C80 and D50	67
4.6.3.4	G_{relative}	67
4.6.4	Hall D Binaural Results	70
4.6.4.1	EDT	70
4.6.4.2	T30	70
4.6.4.3	C80	71
4.6.4.4	D50.....	71
4.6.4.5	G_{relative}	72
4.7	Balcony Edge Mono Measurement.....	72
4.7.1	Balcony edge points, high level points in Hall A	72
4.7.2	Results.....	72
4.8	Analysis and discussion	77
4.9	Conclusions.....	80
Chapter 5	Neural network.....	81
5.1	Introduction.....	81
5.2	Neural Network Analysis.....	81
5.3	Results and Discussion.....	84
5.3.1	Hall A	87
5.3.1.1	Concert setting	87
5.3.1.2	Proscenium setting	95
5.3.2	Hall B	99
5.3.2.1	Concert setting	99
5.3.2.2	Proscenium setting	104
5.4	Conclusions.....	107

Chapter 6	The influence of geometrical parameters on early interaural cross-correlation coefficients, $IACC_{E3}$	109
6.1	Introduction	109
6.2	The Surveyed Hall and Measurements	110
6.3	Regression Analyses	112
6.3.1	$IACC_{E3}$ and distance	112
6.3.2	Regression fitting	113
6.4	Conclusions	127
Chapter 7	The effect of balcony design	129
7.1	Introduction	129
7.2	The scale model and measurement setup	129
7.3	Spark source	134
7.4	Results	136
7.4.1	Student t-test/ difference between with and without balcony	139
7.4.2	Proscenium setting	139
7.4.2.1	Early decay time and Reverberation time	139
7.4.2.2	Energy ratios, Clarity and Definition	145
7.4.3	Concert setting	151
7.4.3.1	Early decay time and Reverberation time	151
7.4.3.2	Early energy ratios, Clarity and Definition	156
7.5	Balcony Effect	161
7.5.1	Proscenium Setting	161
7.5.1.1	Early Decay Time and reverberation time	161
7.5.1.2	Early energy ratios, Clarity and Definition	165
7.5.2	Concert Setting	168
7.5.2.1	Early decay time and reverberation time	168
7.5.2.2	Energy ratios, Clarity and Definition	171
7.6	Effects on the early energy and reflections	175
7.6.1	Proscenium setting	175
7.6.2	Concert hall setting	176
7.7	3D ray tracing model for comparison	180
7.7.1	Balcony effect in 3D simulation model	181
7.7.1.1	Effect of removing the balcony	181
7.7.1.2	Effect of a reduced size balcony	183

7.8	Conclusions.....	186
Chapter 8	Conclusions and Recommendation for Future Work.....	189
8.1	Conclusions.....	189
8.2	Limitations of the present study.....	191
8.3	Recommendations for future work.....	192
	BIBLIOGRAPHIC REFERENCES.....	193

This page is blank

List of Figures

Figure 2-1 Examples of build-up curves measured by Jordon in Concert Studio(Copenhagen) and New York State Theatre.[14, p. 60]	8
Figure 2-2 Structure of a single layer feedforward neural network.....	22
Figure 3-1 Dual Channel dummy head connection system	26
Figure 3-2 Exterior of the scale model from the side.....	27
Figure 3-3 Interior of the scale model with a proscenium setting, view from the audience	29
Figure 3-4 Case 2 with balcony and with sound canopy	30
Figure 3-5 The balcony in the scale model in case 1 and case 2	30
Figure 3-6 View from the stage inside the scale model seeing the rear part of the scale model without the balcony structure.....	31
Figure 3-7 The probe of the electric spark	32
Figure 3-8 Spark source mounted at the source position.	32
Figure 3-9 Points measured in scale model.....	33
Figure 3-10 Microphones mounted on the tailor-made measurement rack at one of the balcony edge positions	34
Figure 3-11 1/8 inch microphones at measurement position	35
Figure 3-12 High frequency LAN-XI data acquisition hardware, Pulse system used in scale model measurement	35
Figure 3-13 The schematic of the sound source, point of reflection, receiver and image	42
Figure 3-14 Definitions of the Geometrical parameters	42
Figure 4-1 Interior of Hall A with concert setting	46
Figure 4-2 Sectional and layout views of Hall A extracted from technical drawings of Hall A, available on the owner's website.....	47
Figure 4-3 Interior of Hall B viewing from the stage	48
Figure 4-4 Sectional and layout views of Hall B extracted from the technical drawings of Hall B, available on the owner's website.....	49
Figure 4-5 Interior view of Hall C from the stage	50
Figure 4-6(b) Sectional view and layout view of Hall C, from drawings from the hall owner.....	51
Figure 4-7 Interior of Hall D [89]	52

Figure 4-8 Tailor-made measurement rack for the balcony edge of Hall A 53

Figure 4-9 Binaural Measurement points (seats market with blue dots) in Hall 54

Figure 4-10 Locations of balcony measurement and high level points from the source to the balcony rack 55

Figure 4-11 Measurement points (seats market with blue dots) in Hall B 56

Figure 4-12 Measurement points (seats market with blue dots) in Hall C, (a) is balcony plan and (b) is stall area plan. Filled points are points measured. 56

Figure 4-13 Spectrum of means of EDT in each seating zone of Hall B in concert setting 62

Figure 4-14 Spectrum of means of EDT in each seating zone of Hall B in proscenium setting 62

Figure 4-15 Contour plots of measured C80 around the balcony edge at point 2 in Hall A 76

Figure 5-1 Measurement point distributions in performance halls and the four training schemes adopted 83

Figure 5-2 Comparison between simulated $IACC_{0,80}$ and measurements for Hall A under concert setting 88

Figure 5-3 Comparison between simulated EDT_L and measured EDT for Hall A under concert setting 89

Figure 5-4 Statistical distributions of acoustical parameters under concert setting of Hall A 90

Figure 5-5 Statistical distributions of acoustical parameters under proscenium setting of Hall A 97

Figure 5-6 Comparison between simulated $IACC_{0,80}$ and measurements for Hall B under concert setting 99

Figure 5-7 Statistical distributions of acoustical parameters under concert setting of Hall B 101

Figure 5-8 Statistical distributions of acoustical parameters under proscenium setting of Hall B 105

Figure 6-1 Layout and dimensions of Hall A 110

Figure 6-2 Two different settings of Hall A 111

Figure 6-3 Definitions of the Geometrical parameters 112

Figure 6-4 Variation of $IACC_{E3}$ with distance from source D in Hall A 113

Figure 6-5 Measurement Schemes adopted in Hall A 115

Figure 6-6 Regression model residue distributions of Hall A under proscenium stage setting	118
Figure 6-7 Regression model residue distributions of Hall A under concert hall setting..	122
Figure 6-8 $ \Delta $ distributions of Hall B	125
Figure 7-1 Sectional drawing of the scale model with the balcony removed	130
Figure 7-2 View from the seating area to the stage in the scale model with the acoustic shell	131
Figure 7-3 View from the seating area to the stage in the scale model without the acoustic shell, ie proscenium setting	131
Figure 7-4 Location of spark source (marked as a red cross) and balcony edge measuring racks mark in blue line.	133
Figure 7-5 The exterior view of the scale model after the conversion.....	133
Figure 7-6 Measurement points in the scale model are marked with blue dots.....	134
Figure 7-7 Directivity plots of the spark source measured in anechoic chamber, at 1m, 1.5m 2m and 3m from the source	135
Figure 7-8 Measured pressure spectrum at 2m at 90 degree of the spark source and its background pressure spectrum.....	136
Figure 7-9 Measured impulse at 1000Hz in case 1	137
Figure 7-10 Measured impulse at 1000Hz in case 2	138
Figure 7-11 Measured EDT (in sec) spectrum of the scaled-model with balcony and a proscenium stage setting (Case 1).....	141
Figure 7-12 Measured EDT (in sec) spectrum of the scaled-model without balcony with a proscenium stage setting (Case 3).....	142
Figure 7-13 Measured T30 (in sec) spectrum of the scaled-model with balcony and a proscenium stage setting (Case 1).....	143
Figure 7-14 Measured T30 (in sec) spectrum of the scaled-model without balcony with a proscenium stage setting (Case 3).....	144
Figure 7-15 Measured C80 (in dB) spectrum of the scaled-model without balcony with a proscenium stage setting (Case 1).....	146
Figure 7-16 Measured C80 (in dB) spectrum of the scaled-model without balcony with a proscenium stage setting (Case 3).....	147
Figure 7-17 Measured D50 spectrum of the scaled-model without balcony with a proscenium stage setting (Case 1).....	149

Figure 7-18 Measured D50 spectrum of the scaled-model without balcony with a proscenium stage setting (Case 3)..... 150

Figure 7-19 Measured EDT (in sec) spectrum of the scaled-model without balcony with a proscenium stage setting (Case 2)..... 152

Figure 7-20 Measured EDT (in sec) spectrum of the scaled-model without balcony with a proscenium stage setting (Case 4)..... 153

Figure 7-21 Measured T30 (in sec) spectrum of the scaled-model without balcony with a proscenium stage setting (Case 2)..... 154

Figure 7-22 Measured T30 (in sec) spectrum of the scaled-model without balcony with a proscenium stage setting (Case 4)..... 155

Figure 7-23 Measured C80 (in dB) spectrum of the scaled-model without balcony with a proscenium stage setting (Case 2)..... 157

Figure 7-24 Measured C80 (in dB) spectrum of the scaled-model without balcony with a proscenium stage setting (Case 4)..... 158

Figure 7-25 Measured D50 spectrum of the scaled-model without balcony with a proscenium stage setting (Case 2)..... 159

Figure 7-26 Measured D50 spectrum of the scaled-model without balcony with a proscenium stage setting (Case 4)..... 160

Figure 7-27 The balcony effect in EDT (in sec) spectrum of the scaled-model with balcony with a proscenium stage setting (Case 1 – Case 3) 163

Figure 7-28 The balcony effect in T30 (in sec) spectrum of the scaled-model with balcony with a proscenium stage setting (Case 1 – Case 3)..... 164

Figure 7-29 The balcony effect in C80 (in dB) spectrum of the scaled-model with balcony with a proscenium stage setting (Case 1 – Case 3)..... 166

Figure 7-30 The balcony effect in D50 spectrum of the scaled-model with balcony with a proscenium stage setting (Case 1 – Case 3)..... 167

Figure 7-31 The balcony effect in EDT (in sec) spectrum of the scaled-model with balcony with a proscenium stage setting (Case 2 – Case 4) 169

Figure 7-32 The balcony effect in T30 (in sec) spectrum of the scaled-model with balcony with a proscenium stage setting (Case 2 – Case 4)..... 170

Figure 7-33 The balcony effect in C80 (in dB) spectrum of the scaled-model with balcony with a proscenium stage setting (Case 2 – Case 4) 173

Figure 7-34 The balcony effect in D50 spectrum of the scaled-model with balcony with a proscenium stage setting (Case 2 – Case 4)..... 174

Figure 7-35 Impulse response measured at M31 in mid-stall on the side within the first 200msec.	177
Figure 7-36 Impulse response measured at O28 in mid-stall in the middle within the first 200msec.	179
Figure 7-37 Impulse response measured at Y16 under the balcony within the first 200msec.	179
Figure 7-38 The balcony effect in T30 (in sec) spectrum of the ray-tracing model with a concert stage setting, comparison between with and without balcony.	182
Figure 7-39 The balcony effect in C80 (in dB) spectrum of the ray-tracing model with a concert stage setting, comparison between a full balcony and a half-ly reduced balcony	184
Figure 7-40 The balcony effect in D50 spectrum of the ray-tracing model with a concert stage setting, comparison between a full balcony and a half-ly reduced balcony	185

This page is blank

List of Tables

Table 2-1 Minimum number of receiver positions as a function of auditorium size [13]	21
Table 4-1 Summary of the halls measured.....	46
Table 4-2 Summary of number of binaural measurement points done in each hall	54
Table 4-3 Mean and Stand deviation of averaged EDT (in sec) measured in Hall A with different settings. Numbers are averages of 2 channels, underlined and in italic are standard deviations while the other are means of each zone	57
Table 4-4 Mean and Stand deviation of averaged T30 (in sec) measured in Hall A with different settings. Numbers are averages of 2 channels, underlined and in italic are standard deviations while the other are means of each zone	58
Table 4-5 Mean and Stand deviation of averaged C80 (in dB) measured in Hall A with different settings. Numbers are averages of 2 channels, underlined and in italic are standard deviations while the other are means of each zone	59
Table 4-6 Mean and Stand deviation of averaged D50 measured in Hall A with different settings. Numbers are averages of 2 channels, underlined and in italic are standard deviations while the other are means of each zone	60
Table 4-7 Mean and Stand deviation of averaged G-relative (in dB) measured in Hall A with different settings. Numbers are averages of 2 channels, underlined and in italic are standard deviations while the other are means of each zone	60
Table 4-8 Mean and Stand deviation of averaged EDT (in sec) measured in Hall B with different settings. Numbers are averages of 2 channels, underlined and in italic are standard deviations while the other are means of each zone	61
Table 4-9 Mean and Stand deviation of averaged T30 (in sec) measured in Hall B with different settings. Numbers are averages of 2 channels, underlined and in italic are standard deviations while the other are means of each zone	63
Table 4-10 Mean and Stand deviation of averaged C80 (in dB) measured in Hall B with different settings. Numbers are averages of 2 channels, underlined and in italic are standard deviations while the other are means of each zone	64
Table 4-11 Mean and Stand deviation of averaged D50 measured in Hall B with different settings. Numbers are averages of 2 channels, underlined and in italic are standard deviations while the other are means of each zone	64

Table 4-12 Mean and Stand deviation of averaged G-relative (in dB) measured in Hall B with different settings. Numbers are averages of 2 channels, underlined and in italic are standard deviations while the other are means of each zone 65

Table 4-13 Mean and Stand deviation of averaged EDT (in sec) measured in Hall C with different settings. Numbers are averages of 2 channels, underlined and in italic are standard deviations while the other are means of each zone 66

Table 4-14 Mean and Stand deviation of averaged T30 (in sec) measured in Hall C with different settings. Numbers are averages of 2 channels, underlined and in italic are standard deviations while the other are means of each zone 66

Table 4-15 Mean and Stand deviation of averaged C80 (in dB) measured in Hall C with different settings. Numbers are averages of 2 channels, underlined and in italic are standard deviations while the other are means of each zone 68

Table 4-16 Mean and Stand deviation of averaged D50 measured in Hall C with different settings. Numbers are averages of 2 channels, underlined and in italic are standard deviations while the other are means of each zone 68

Table 4-17 Mean and Stand deviation of averaged G-relative (in dB) measured in Hall C with different settings. Numbers are averages of 2 channels, underlined and in italic are standard deviations while the other are means of each zone 69

Table 4-18 Mean and Stand deviation of averaged EDT (in seconds) measured in Hall D. Numbers are averages of 2 channels, underlined and in italic are standard deviations while the other are means of each zone 70

Table 4-19 Mean and Stand deviation of averaged T30 (in seconds) measured in Hall D. Numbers are averages of 2 channels, underlined and in italic are standard deviations while the other are means of each zone 70

Table 4-20 Mean and Stand deviation of averaged C80 (in dB) measured in Hall D. Numbers are averages of 2 channels, underlined and in italic are standard deviations while the other are means of each zone 71

Table 4-21 Mean and Stand deviation of averaged D50 measured in Hall D. Numbers are averages of 2 channels, underlined and in italic are standard deviations while the other are means of each zone 72

Table 4-22 Mean and Stand deviation of averaged Sound Strength, G_{rel} (in dB) measured in Hall D. Numbers are averages of 2 channels, underlined and in italic are standard deviations while the other are means of each zone 72

Table 4-23 Mean and Standard deviation of EDT and T30 (in sec) measured in Hall A at the balcony edge. Numbers are averages of all angles while underlined and in italic are standard deviations.....	73
Table 4-24 Mean and Stand deviation of C80 (in dB), D50 and G_{rel} (in dB) measured in Hall A at the balcony edge. Numbers are averages of all angles while underlined and in italic are standard deviations.....	74
Table 5-1 Results of paired comparison t-test for vanishing differences (95% confidence level).....	84
Table 5-2 Simple statistics of the acoustical parameters of Hall A	85
Table 5-3. Simple statistics of the acoustical parameters of Hall B.....	86
Table 5-4. Root-mean-square differences between simulations and measurements for Hall A	93
Table 5-5 Paired t-test statistics for vanishing differences between simulations and measurements under concert setting of Hall A (95% confidence level).....	94
Table 5-6 Paired t-test statistics for vanishing differences between simulations and measurements under proscenium setting of Hall A (95% confidence level).....	98
Table 5-7 Root-mean-square differences between simulations and measurements for Hall B	102
Table 5-8. Paired t-test statistics for vanishing differences between simulations and measurements under concert setting of Hall B (95% confidence level).....	103
Table 5-9. Paired t-test statistics for vanishing differences between simulations and measurements under proscenium setting of Hall B(95% confidence level)	106
Table 6-1 Regression Analysis at 95% confidence level for the proscenium stage case of Hall A with all 182 data included	114
Table 6-2 Regression Analysis at 95% confidence level for the proscenium case of Hall A (Scheme B).....	116
Table 6-3 Regression Analysis at 95% confidence level for the proscenium stage case of Hall A (Scheme C).....	117
Table 6-4 Regression Analysis at 95% confidence level for the proscenium stage case of Hall A (Scheme D).....	117
Table 6-5 Coefficients of the regression models for Hall A	119
Table 6-6 Regression Analysis at 95% confidence level for the concert hall setting of Hall A (Scheme A).....	119

Table 6-7 Regression Analysis at 95% confidence level for the concert hall setting of Hall A (Scheme B).....	120
Table 6-8 Regression Analysis at 95% confidence level for the concert hall setting of Hall A (Scheme C).....	121
Table 6-9 Regression Analysis at 95% confidence level for the concert hall setting of Hall A (Scheme D).....	121
Table 6-10 Regress Analysis at 95% confidence level for Hall B under Scheme C	124
Table 7-1 Model setting for 4 scale model measurement cases.....	132
Table 7-2 The ratio of mean BE of EDT to the mean of values with the balcony measured	162
Table 7-3 The ratios of mean BE of T30 to the mean of values with the balcony measured	162
Table 7-4 The ratios of mean BE of T60 to the mean of values with the balcony measured	162
Table 7-5 The ratios of mean BE of C80 to the mean of values with the balcony measured	168
Table 7-6 The ratios of mean BE of D50 to the mean of values with the balcony measured	168
Table 7-7 The ratios of mean BE of EDT to the mean of values with the balcony measured in concert setting	171
Table 7-8 The ratios of mean BE of T30 to the mean of values with the balcony measured in concert setting	171
Table 7-9 The ratios of mean BE of T60 to the mean of values with the balcony measured in concert setting	171
Table 7-10 Mean and standard deviation of BE of C80 in Concert setting	172
Table 7-11 The ratios of mean BE of C80 to the mean of values with the balcony measured in concert setting	175
Table 7-12 The ratios of mean BE of D50 to the mean of values with the balcony measured in concert setting.....	175

Abbreviations

Hz	Hertz
RT, T30	Reverberation time
EDT	Early Decay Time
C ₅₀ , C ₈₀	Clarity, subscripts denote the time concerned in milliseconds
D ₅₀ , D ₈₀	Definition, subscripts denote the time concerned in milliseconds
SPL	Sound Pressure Level
G	Sound Strength
G _{relative} G _{rel}	Relative Sound Strength
IACC	Interaural cross correlation
IACC _{E3}	Early interaural cross correlation
ASW	Apparent source width
LEV	Listener envelopment
ITDG	Initial time delay gap
BQI	Binaural quality index
BR	Bass ratio
MLS	Maximum length sequences
NNA	Neural network analysis
ϕ	Azimuthal angle
θ	Elevation angle
D	Source-to-receiver distance

δ	Path difference
HATS	Head and Torso Simulator
sec	Second
Eq.	Equation
ISO	International standard organization
dB	Decibels
Pa	Pascal
mid	Middle
R	Right, as subscripts for parameters
L	Left, as subscripts
0,80	Range of time, from 0 milliseconds to 80 milliseconds, as subscripts for parameters
80,+	Range of time, from 80 milliseconds to infinity, as subscripts for parameters
CH	Channel
S	Scheme
Δ	Difference
V	Volume
A	Area

Chapter 1 Introduction

1.1 Background

Performing arts has played a significant role in human's life since centuries ago. To ensure a performance beautifully done, proper sound transmission in the performing venue is as crucial as the visual presentation. Music and opera are the two major forms of indoor performance in the western world in the past. This encourages the construction of many concert halls and opera houses around the world. Ancient halls are usually purposely designed; therefore classical shapes were very popular.

As culture evolves, modern performances are with many varieties, artist and architects are having more and more brilliant ideas in their innovations. These bring the needs of building more multi-functional halls with sophisticated designs. Unlike the classically-designed halls, the acoustics inside these halls are much more complicated.

In Hong Kong, there is a growing demand in cultural and performance facilities from the locals. There have been developments on cultural districts which include a number of world-class performance spaces. To match this growing need, a study on the current situation and research on hall acoustics are needed.

In this thesis, large performance halls are referring to those that can accommodate more than hundreds people, usually up to 1000 or even more than 2000. Various local halls were measured and the data collected would kick off a formation of a local hall databank. With the hall parameter prediction methods developed, the requirement in measurement and monitoring resource should be reduced. Such that in accessing and constructing new halls, the process can be more efficient.

1.2 Aims and objectives

The major aim of this study is to understand the sound propagation in a large performance hall through real hall measurements and scale model experiments.

The aim and objectives of this study are as follows:

- Understand the sound propagation and the relationship between different parameters in a larger performance hall by local hall survey

- Understand the effects of the balcony on the acoustics of a hall by measurements and scale model experiment
- Develop prediction models for hall parameters that requires simple inputs

1.3 Outline of this thesis

This thesis contains seven chapters. They are outlined as below:

Chapter 2 first starts with literature review describing the development in research in hall acoustics. This provides the background information for this study. This chapter also includes the explanation of some common and relevant acoustical parameters, measurement methods and evaluation algorithm.

Chapter 3 introduces the methodology used in this study. The details of the equipment used, setup, selection of source and receiver points for real hall measurements are discussed at the beginning of this chapter. Followed by the experiment planning for the scale down model measurements from model construction to preparing the sound source to measurements and to analysis.

Chapter 4 details the halls being measured in this study, explains the measurement setups, and presents the results of the halls with analysis and discussions. Four different halls were measured in this study.

Extensive measurements as in chapter 4 are very time consuming. The hall parameters vary from hall to hall and from seat to seat. For easier evaluation, neural network analysis in Chapter 5 investigates the relationships between the different geometrical and measured parameters including the reverberation time, early decay time, clarity, definition, bass ratio and inter-aural cross correlation. Thus, a neural network analysis is presented in the Chapter 6 for further examining the effectiveness of predictions using limited number of measurements.

Chapter 7 presents the results of a 1/10 scale model experiment in an attempt to understand the effects of balcony on the hall acoustical parameters. The measured results with and without the balcony was compared for investigating the balcony effects in this chapter.

The major findings of the present study are summarized in Chapter 8 together with recommendations and direction for future works.

This page is blank.

Chapter 2 Literature review and background

2.1 Halls

In a room, once a note is played, the sound travels along the shortest distance and reaches the listener as direct sound. It also travels to different reflecting surfaces of the room, partly absorbed, reflected or scattered and finally reaches the listener as reverberation sound. This reverberation part of the total perceived sound depends on the absorption and the geometry of the room as well as the source and receiver position. This is the interesting but complex part that worth investigation. In another words, the acoustic energy starts to build up once the sound is ignited. After reaching the peak level, it starts to decay with time.

The characteristics of music or the type of performance to be conducted and the seating capacity would affect the design of a performance hall. The musical requirements changed from time to time from baroque period to classical period, then from romantic to modern period. Baroque music requires the melody and details to be heard, that needs a hall with high clarity. Classical music started the trend of classical symphony and sonata, requiring more fullness of tone. Romantic music emphasizes the harmony between the melody and the backing-up by the other parts of the orchestra that requires a balance between fullness of tone and clarity. Modern music is with a very large variety. New century music needs higher definition to differentiate each parts while passionate music needs a high fullness of tone. This brings the need of a variable acoustic design for a hall with the use of electronic systems. Also, the growth in the orchestra size and audience size starting from classical period urges the need of larger halls. Opera house would need another kind of acoustics: less reverberant condition that provides a higher clarity for language intelligibility.

Other than classic shoebox or rectangle shape concert halls and horseshoe-shape opera house, there are some modern hall designs with fan shape, vineyard, spread and even asymmetrical layouts. The more complicated the hall layout, the more sophisticated the acoustic design needs.

2.2 Fundamental acoustical parameters

Not much attention was paid to hall acoustics and there was not much breakthrough till the early 20th century.

2.2.1 Reverberation Time RT

In 30's of the 20th century, Sabine found that the reverberation time (RT) of a room depends on the volume and the absorption of the space. It is the first acoustical parameter developed and used in performance space design. Sabine then developed the Sabine's equation to calculate the reverberation time. [1], [2]

$$RT = 0.161 \frac{V}{A} \quad \text{Eq. 2-1}$$

where V is the net cubic volume in m^3 of the hall while A is the total internal sound absorption in m^2 for both the room surfaces with air absorption. The total internal sound absorption in m^2 ,

$$A = S_T \alpha_T + S_R \alpha_R + S_{M1} \alpha_{M1} + S_{M2} \alpha_{M2} + \dots + 4mV, \quad \text{Eq. 2-2}$$

where S_T is the sum of the area of where the audience chairs sit and the orchestra area, a maximum of $180m^2$, on the stage; S_{M1} , S_{M2} , S_{M3} , etc., are the areas of the specially designed absorbing materials like carpet, curtains, acoustical tiles and absorptive surfaces; S_R is the area of the remaining surfaces of the hall including the under-balcony soffits and aisles ceilings. Each of the area S has its associated absorption coefficient α . The term $4mV$ is the air absorption term and $4m$ is the air attenuation coefficient multiplied by 4 as stated in ISO standard.[3] [4] the air absorption coefficient can be calculated by Eq. 2-3 [5]

$$m = 5.5 \times 10^{-4} (50/h)(f/1000)^{1.7} \quad \text{Eq. 2-3}$$

Measured RT is defined as the time in second that it takes for a loud sound to decay by 60dB after the source is cut off. RT is usually determined separately at a number of frequencies in octave bands, such as 63, 125, 250, 500, 1000, 2000 and 4000Hz. [6]

The equation is good for estimating RT in halls with simple and regular shapes such as shoebox shape. Later in 1960's, hall designers started finding measured RT in newly-built halls different from the predicted one using the equation.[2], [7]. By using computer aided ray-tracing calculations, Schroeder [8] found that 20% error in calculating the RT using classical formulas is common. Such deviation in RT is very significant in hall acoustics. The formulas are particularly inaccurate in rooms with irregular shape and large absorption coefficients. [9], [10]

2.2.2 Early time, definition, steepness Energy building up in a hall

RT describes the energy decay inside a room. The variation of acoustic energy in a room can be further separated by time. In the mid of 20th century, researcher started looking at the energy content with respect to time. It can be measured by using an impulse or a maximum length sequence signal. The RT can be traced from the impulse response of the room. Apart from RT, Early decay time (EDT) is another important parameter to describe the decay of sound in a space. EDT is the reverberation time based on the first 10dB portion of the decay. RT and EDT are usually the same in a very reverberant space. [11]

Definition is proposed by Thiele in 1953 [12]. It is defined as the ratio of early energy arriving with the first 50 milliseconds to the total energy. Definition D_{50} is used in speech while 50 milliseconds is a reasonable figure for speech articulation. [12], [13]

$$D_{50} = \frac{\int_0^{0.05} p^2(t) dt}{\int_0^{\infty} p^2(t) dt} \quad \text{Eq. 2-4}$$

$p(t)$ is the instantaneous pressure measured at the measurement point. Clarity is the ratio of the early energy to the late energy arrive at a point, the following equation is the mathematical definition. Clarity C_{80} is used in music. C_{80} is the ratio of early energy received within the first 80 milliseconds to that received afterwards.

$$C_{80} = 10 \log \frac{\int_0^{0.08} p^2(t) dt}{\int_{0.08}^{\infty} p^2(t) dt} \quad \text{Eq. 2-5}$$

While clarity C_{50} is used for speech, the relationship of clarity C_{50} and definition D_{50} is defined using Eq. 2-6 [13]

$$C_{50} = 10 \log \left(\frac{D_{50}}{1 - D_{50}} \right) \quad (dB) \quad \text{Eq. 2-6}$$

In the old days, hall measurements were done with a high speed level recorder. Jordon [14] measured the pulse generated in Concert Studio (Copenhagen) and New York Theatre. Examples of the pulses he measured are shown in Figure 2-1 **Error! Reference source not found..**

From these measurement results, Jordon [14] proposed to evaluate the Rise Time TR and some other relevant indexes namely, Steepness and Inversion index.

Rise time TR is the pulse length required to reach an energy level 3dB below the stationary level. This brought others' interest to look for other phenomenon to describe the energy building up process in the hall.

Steepness σ_{-5} , is the rate of change of intensity. I_0 is the stationary intensity of a noise pulse and I_{-5} is a the intensity at a level 5dB below the stationary level [15], its equation is shown in Eq. 2-7.

$$\sigma_{-5} = \frac{d}{dt} \left(10 \log \frac{I_{t(-5dB)}}{I_0} \right) \approx \frac{0.13}{RT(s)} \quad (dB/ms) \quad \text{Eq. 2-7}$$

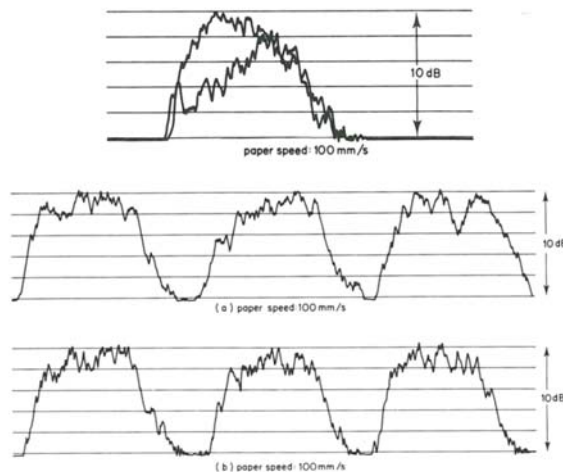


Figure 2-1 Examples of build-up curves measured by Jordon in Concert Studio(Copenhagen) and New York State Theatre.[14, p. 60]

Inversion index is the ratio of the average value of the rise time in the audience area to that on the stage area.

$$II \sim \frac{\text{average value of rise time in audience area}}{\text{average value of rise time on the stage area}} \quad \text{Eq. 2-8}$$

2.2.3 Sound pressure level

Sound level is the objective measure to determine the subjective sense of loudness. It, especially the A-weighted sound pressure level, is commonly used to evaluate environmental noise. [16]

2.2.4 Sound strength G , Loudness

Loudness is relative in size inside a single hall, thus, it is subjective and not comparable among different halls. Therefore, the G can be used to describe the normalized magnitude of the sound in different halls if they are measured with a calibrated system.

The G is measured by a calibrated omnidirectional sound source. It is the logarithmic ratio of the sound energy of the measured impulse onsite to that of the response measured at a 10m-free field. Its equation is as follows: [17], [18]

$$G = 10 \log \frac{\int_0^{\infty} p^2(t) dt}{\int_0^{\infty} p_{10}^2(t) dt} = L_{pE} - L_{pE,10} \text{ dB} \quad \text{Eq. 2-9}$$

where

$$L_{pE} = 10 \log \left[\frac{1}{T_0} \int_0^{\infty} \frac{p^2(t) dt}{p_0^2} \right] \text{ dB} \quad \text{Eq. 2-10}$$

And

$$L_{pE,10} = 10 \log \left[\frac{1}{T_0} \int_0^{\infty} \frac{p_{10}^2(t) dt}{p_0^2} \right] \text{ dB} \quad \text{Eq. 2-11}$$

$p(t)$ = instantaneous sound pressure of the impulse response
measured at the measurement point

$p_{10}(t)$ = instantaneous sound pressure of the impulse response
measured at 10m free field

$$p_0 = 20 \mu Pa$$

$$T_0 = 1s$$

L_{pE} = sound pressure exposure level $p(t)$

$L_{pE,10}$ = sound pressure exposure level $p_{10}(t)$

The measure of $L_{pE,10}$ requires a large anechoic chamber which is not easily available. Therefore, $L_{pE,10}$ can be measured at a short distance d , which is larger than 3m from the source and corrected by the following equation:

$$L_{pE,10} = L_{pE,d} + 20 \log \left(\frac{d}{10} \right) \text{dB} \quad \text{Eq. 2-12}$$

The energy-mean of the sound pressure exposure levels at every 12.5° around the sound source has to be calculated such that the directivity of the sound source is averaged.

$L_{pE,10}$ can also be measured using a reverberation room using equation 1.5:

$$L_{pE,10} = L_{pE} + 10 \log \left(\frac{A}{S_0} \right) - 37 \text{dB} \quad \text{Eq. 2-13}$$

$L_{pE,10}$ = spatial-average sound pressure exposure level measured
in the reverberation room

A = equivalent sound absorption area in square metres

$$S_0 = 1 \text{m}^2$$

2.2.5 Spaciousness and envelopment – IACC, ASW, LEV

Interaural cross correlation (IACC) is used to describe the difference of the sound arriving at the left and right ears of an audience sitting inside a hall. It is an important attribute in determining the perceived direction of a sound source, or the degree of subjective diffuseness of the sound field. [19], [20]

Binaural measurements were done by numerous researchers using a dummy head with built-in microphones at the entrance of ear canals. Their results correlate well with the subjective quality ‘spatial impression’ [4], [11], [21]. ISO standard 3382 has stated that the normalized inter-aural cross-correlation function for the first 50 ms of the impulse responses for the left and right ear canals, IACF, is defined as equation 2-14 while IACC, is given by equation 2-15 [13]

$$IACF_{t_1,t_2}(\tau) = \frac{\int_{t_1}^{t_2} p_1(t) \cdot p_r(t + \tau) dt}{\sqrt{\int_{t_1}^{t_2} p_1^2(t) dt \int_{t_1}^{t_2} p_r^2(t) dt}} \quad \text{Eq. 2-14}$$

$$IACC_{t_1,t_2} = \max|IACF_{t_1,t_2}| \text{ for } -1\text{ms} < \tau < +1\text{ms} \quad \text{Eq. 2-15}$$

$P_1(t)$ = impulse response measured at the entrance of the left ear canal

$P_r(t)$ = impulse response measured at the entrance of the right ear canal

The term ‘Spaciousness’ is made up of 2 parameters: apparent source width (ASW) and the degree of listener envelopment (LEV). [22] They are both related to the spatial impression caused by early reflection. ASW can be measured by lateral fraction (LF) and binaural quality index (BQI) where $BQI = [1 - IACC_{E3}]$. [4], [23]

The listener envelopment (LEV) is affected by the level of and the angular and temporal distributions of the late arriving energy. [24]

Gilbert Soulodre, Michael Lavoie, and Scott Norcross of the Communication Research Center in Ottawa, Canada, have made subjective measurements to quantify LEV. They proposed that the LEV can be calculated by the following equations 6.1 and 6.2:

$$LEV_{calc} = 0.5G_{late,mid} + 10\log[1 - IACC_{late,mid}]dB \quad \text{Eq. 2-16}$$

$$\text{where } G_{late,mid} = G_{mid,total} - 10\log\left(1 + \log\frac{C_{80,mid}}{10}\right) \quad \text{Eq. 2-17}$$

G_{late} = strength of the reverberant sound (measured after 80 ms);

G = overall sound strength

The subscript ‘mid’ refers to mid-frequencies, C80 is the clarity factor and $[1 - IACC_{late,mid}]$ is the binaural quality index (BQI). [25]

2.2.6 Intimacy- initial-time-delay-gap

The initial time delay gap is determined by finding the time interval between the direct sound and the reflection with the maximum amplitude arriving at the ears. [26], [27] This can be seen from the spectrogram of the recorded impulse response during measurements.

Bass ratio is determined by the mid and low frequency RT, 500 to 1000Hz and 125 to 250Hz respectively. Its equation is as follows:

$$BR = \frac{(RT_{125} + RT_{250})}{(RT_{500} + RT_{1000})} \quad \text{Eq. 2-18}$$

2.3 Subjective parameters

2.3.1 Pitch and brightness

Pitch and brightness are used to describe a melody or music played by instruments or sang by humans. The Pitch of a musical instrument is associated with the periodicity of the sound they produce. It is a perceptual measure which is assigned by human. The frequency spectrum of a musical note comprises of the pitch frequency as the fundamental frequency or its multiples as harmonics. [28]

Both the brightness and dullness of tone depend on the distribution of the total power between high and low frequencies.

2.3.2 Loudness

Loudness refers to the subjective feeling that how one perceives the intensity of sound. The equal loudness contour shows the sound pressure level of each frequency that sounds equally loud. The loudness level unit is Phons. [29] A loudness perception system is made up by 3 major parts: the weighting, the 1/3 octave band that is critical and the power law associated with the 'phon-level'. [30]

2.3.3 Liveness and fullness of tone

A reverberant room is called a 'live' room, or else, a 'dead' or a 'dry' room. 'Liveness' is related to the reverberation time at mid (500 to 1000 Hz) and high (2000Hz or above) frequencies. Therefore, a live room can also be lack of bass. A 'warm' room indicates that the room is with sufficient reverberation at low frequency. The fullness of tone is related to the reverberation time and early decay time of the space. The reflections that happen between the direct sound and later reflections fill up the gaps between different

notes played by the musician. The more number of reflections, the space is livelier or in other words, with a fuller tone. This term also emphasizes the ratio of the loudness of the reverberant sound to that of the early sound. [4]

2.3.4 Intimacy or presence

If the music played in a large hall gives the audience an impression that the music is played in a small hall, the hall can be said to have 'acoustical intimacy'. 'Presence' is a similar phrase that professions in recording and broadcasting industry used to describe an intimate hall. [2], [4]

2.3.5 Timbre

Timbre is a multidimensional attribute to describe the quality of a sound that distinguishes itself from the other mixed sounds of the same pitch and loudness.[31], [32]

2.3.6 Spaciousness

Spaciousness is the sense of envelopment and the apparent dimension of the source: whether the orchestra sounds wider than its real size and if the sound arrives in all directions at the audience. [2], [4]

2.3.7 Definition and Clarity

Definition can be sub-divided to horizontal and vertical definition. Horizontal definition applies to the tones played in succession while vertical definition is for tones played simultaneously.

Clarity is the ability to discrete the speech content or the melody from one another in a live room. [2], [4]

2.3.8 Warmth

Warmth is the fullness of bass tones relative to the mid-frequency tones. A room is dark if the bass sound in the room is too strong and not balanced with the high frequency tone. [2], [4]

2.3.9 Ensemble

Ensemble is the ability to assist the performers to play as a union and blend well with their fellows by releasing and projecting their notes or voice on top of playing and singing

accurately according to the music score. A good ensemble requires appropriate reflection on and to the stage for the performers and conductors to listen to each other. [2], [4]

2.4 Balcony

The locations of reflection, diffusion and absorption panels affect the reflection and energy diffusion in a hall. Particularly, the side walls of the hall and the side reflectors of the stage affect the early reflection of the hall. The acoustic symmetry of the stage and frontal area of the hall gives a smaller IACC values. [21]

Audience absorption is another important factor affecting the reverberance in a hall. Usually, all the hall measurements are done in unoccupied or studio situation. Berenak has proposed the absorption coefficient for audience and mentioned that the coefficient change in each hall is in a ratio of the area being seated rather than the number of seats being occupied[33]–[35]. Also, the difference in the audience absorption between the occupied state and unoccupied state has been studied by different researchers.[36]–[38] Covering the seats with a suitable cloth and using more absorptive material for the seats are the proper ways to simulate an occupied audience in real measurement and scale modelling respectively[36].

Haan and Fricke have shown that sound-diffusion in concert halls is a major acoustical parameter.[39], [40] The irregularities of the coffers, niches, projecting curved, or triangular surfaces and the likes on walls and ceiling, particularly in the upper parts of the hall diffuse the high frequency portions of the early reflected sound waves. This makes the sound appear livelier. [41]

While most of the architectural designs have been extensively studied in the past, the effects of balcony and overhang have received very limited attention.

Balconies are usually added in concert halls, opera houses and especially modern multi-purpose hall to increase the hall capacity while maintaining a relatively short distance between the stage and the audience.

Barron [42] has found that the overhangs reduce the late sound more than the early and that local reflections from back walls and soffits in the overhung section of the hall help maintain sound level. The overhangs create subjective effects of a reduction in the sense

of reverberation, a reduction in loudness and reduced perceived solid angle for arriving sound.

Furuya [43] has constructed a simple scale model with varying balcony depth and opening height to investigate the effects on changing the geometry to the acoustical properties at each the seats. Both the depth and the opening height were changed in the scale model. The balcony effects, BEs, of each parameter, were studied.

Kwon and Shimizu [44] analysed the energy loss under balcony while the sound energy comes from above via a vertical median plane. They aimed to look for preferred view angles against the balcony opening height. The results of scale model experiments in an anechoic room were compared with results from psycho-acoustical experiments associated with listener envelopment to determine the appropriate view angles. They used synthetic sound fields with constant lateral energy were maintained but variable vertical energy to determine the appropriate view angles. The minimum vertical angle of view was found to be 30 to 40 degrees from psycho-acoustical experiments.

Furuya and Fujimoto [45] used computer simulation to find out the relationship between the shape of a balcony in an auditorium and the respective acoustical properties under the balcony overhang. They calculated the impulse responses in models of auditoria with varying balcony depth and opening height. Their results show that the balcony reduces the total early reflection energy under the balcony. Their results also show that the ratio of the vertical component to total early reflection energy ERV is greatly reduced under the balcony in comparison with that in the main orchestra.

Through a regression expression, this energy ratio is found to be closely related to the balcony index of d/h through the regression expression, where d/h is the ratio of the balcony depth and opening height, which is geometrically defined by the positions of sound source, receiving point, and balcony edge. Applying the just noticeable difference of ERV to this relation, the maximum limit of d/h , within which the degree of auditory envelopment perceived under the overhang is equivalent to that in main orchestra (between 0.7 and 1.0).

Their results also reveal that once auditory envelopment became weak as the early reflection decreased while the lateral energy fraction is unchanged[46]. They suggest that this disturbance to auditory envelopment under the balcony is a result of the lack of early

reflections from the ceiling above the main orchestra bringing the peculiarity of directional distribution of early reflections.

Chiang et al. [47] suggested that flying balconies could be used to improve the sound qualities at the seats under deep balcony overhangs. Deep balcony overhangs reduces the acoustical energy as well as the sense of reverberation for the under-balcony seats.

They studied different design strategies including the flying balcony technique, optimizing the profile of the under-balcony space and utilizing ceiling and side reflectors near the platform. These methods are effective in enhancing early reflection.

According to the principle of acoustics, when a sound reaches a solid boundary, it will be diffracted, will pass over other barriers and propagate until it reaches another reflecting surface. Therefore, by observing the architectural design of halls and opera houses with balconies, one can suggest that a portion of the sound energy will be reflected back and diffracted from the balcony front to the stage and the hall main floor. Opinions of musicians and acousticians[6] also suggest such phenomenon. This would be a positive effect of the balcony to the performers on the stage and the audience on the main floor instead of just degrading the acoustical performance at seats under the overhangs.

Currently, scale models and ray-tracing based computer simulation are used for concert halls and opera houses design and modelling. The most commonly used one is the ray-tracing model. The situation with the presence of a balcony or similar structure makes the computation complicated. Scattering or diffraction at the balcony edges or the multiple scattering phenomenon by waves hitting the edge from reflections is not easy to model. Edwards and Kahn[48] reported that there is inaccuracy in such modelling. In their European horse shoe shaped opera houses modelling, simulation results show that sound focusing or the lack of reflected sound when the wall and balcony surfaces are too absorptive are problems for such halls. In real experience, these opera houses function well acoustically. Even modern ray-tracing based programs include an approximation for surface scattering and edge diffraction.[49]

According to Lam[49] and Hodgson[50], a sound hitting a wall will be scattered at angles other than the specular reflection angle because of the imperfectly smooth surfaces in practice, as well as the edge effects created by the thickness of the wall. They introduced

the diffuse-reflections into different tracing models, to approximate some of the scattering and diffracting properties of reflecting surfaces.

Chan and To[51] used computer simulation and ripple tank experiment to model the back scattering of the balconies. Their results indicate that the lower corner of the balcony front close to the sound source acts as a virtual source. Hence, they suggested that computer models incorporating such considerations can be constructed to evaluate the back-scattering effect in a concert hall and a horseshoe shaped opera house. Meanwhile, the cross-coupling effect between different panels should also be considered.

Full scale measurement can provide statistical data in the real situation for reference and comparison in modelling and simulation. Correlation and improvement can be developed by comparing real measurement results with modelling and simulation results. Factors being neglected in modelling and simulation can also be observed and recorded in real measurement.

No comprehensive analysis and measurement has been done in local halls. Although Beranek has included the concert hall in the Hong Kong Cultural Centre in his publication[6], no acoustical data can be found.

2.5 Impulse response Measurement method

Along with the development of different parameters, measurement method has also progressed for convenience and accuracy. From a cut-off music note to the interrupted noise method, Schroeder [52] has proposed the integrated tone-burst method. With a loudspeaker radiating a broadband noise covering the desired frequency bands, the response of the enclosed of each tone is then picked up by microphone and filtered and analysed. With a backward integration calculation, the signal decay in each frequency band can be found. Unlike a spark source or a music note, this measurement method with a standard noise signal not only increases the repeatability of the measurement, but also maintains a flat spectrum with sufficient power.

Schroeder later suggested to use pseudorandom noise generated by shift registers[53]. However, this requires digital processing to recover the desired single-impulse response. Schroeder and his team had been doing measurements using Maximum Length Sequence

(MLS) signal before publishing this MLS integrated-impulse method in 1979 [54]. They are the first to use this method and have achieved very well results.

2.5.1 Maximum Length Sequences, MLS

Maximum Length Sequences are periodic sequences of integers a_n . In the case of binary sequences, the integers are restricted to having two values only, say +1 and -1. They are generated by n-stage shift registers and the period length is $N = 2^n - 1$. Most importantly, their Fourier Transform (FDT) has the same magnitude for all frequency components (except the dc component). This is beneficial to measuring the decay of a hall. Their power spectrum is like that of a single impulse, which is independent of frequency.[54]

In other words, their periodic auto-correlation

$$r_m = \frac{1}{N} \sum_{k=1}^N a_k a_{k+m} \quad \text{Eq. 2-19}$$

is two-valued:

$$r_0 = 1$$

And

$$r_m = -\frac{1}{N} \text{ for } m \neq 0 \pmod{N}. \quad \text{Eq. 2-20}$$

The property immediately suggests that response measurements on linear systems can be made with a MLS with N constant-magnitude pulses per period, instead of a single pulse, that for equal energy, must have a $(N)^{\frac{1}{2}}$ times larger magnitude.

The sequence can be generated with any computer. With the advancement in computer power, this simple sequence can be generated and computed at once handily. As the magnitudes of all the Fourier-coefficients in the computation algorithms are equal, it suffices to store the phase angles as well.

The periodic characteristic of these signals improves the signal-to-noise ratio. It does not only maintain a sufficient signal-to-noise ratio in a quiet environment, it makes

measurement in a noisy, even actual performance, condition possible. With a designed period length and averaging of results, this method can maintain a very good SNR.

Different researchers have confirmed the repeatability and uniformity of a MLS signal in reverberation time and decay curve measurements[55]. Using MLS as source signal is already reproducible. To further limit the influence of the source to the measurements, an omni-directional loud speaker can maintain a more uniform sound power radiation into all directions. Lundeby et al.[56] suggested that if an omni-directional sound source is not available, the loud speaker should be turned on for at least 3 times for improving its uniformity.

2.5.2 Impulse source

Instead of a continuous source like MLS, simple impulse source can also be used to suit particular measurement constraints. Very simple impulse sources such as hand clapping, popping balloons and pistol shots, although are powerful sources of sound, are lack of repeatability and with variable directivity of the sound radiation. Researchers found that these sources are not sufficient especially in low frequencies.[57]–[60] Explosive source has maximum power at 1kHz and the power decreases in low frequencies, thus, a very high power source is required for a sufficient energy over the whole desired bandwidth. Summarac-Pavlovic et al. [59]suggested using a wooden clapper which produces a rather flat spectrum with a more uniform directivity.

A spark discharged in air will produce an acoustic wave. [61], [62] An electric discharge that creates a spark between two electrodes will give rise to an intense and broad-band acoustic pulse[62]. This pulse is strong enough to provide sufficient energy at high frequency up to at least 20kHz. A spark source with an exposed electrode will have a better directivity usually. Such high energy content at higher frequencies makes it suitable for use as sound source in scale down model measurements, where higher frequency is also measured.

2.5.3 Measurement locations

Measurement methods have progressed after the development of a measurement method for the impulse response using maximum-length sequence signals [63], [64]and swept sinusoidal signals[65], [66] The potential uncertainties in the measurement and calculation process [56], [67]and the effect of the unavoidable fluctuations of the sound

field [68] have also been examined for these methods. In 1997, some important quantities were summarized in the Annex of ISO3382. [13] In that annex, the definitions and methods of calculation of these parameters were presented. Practical problems concerning this standard were widely discussed in the symposium of room acoustics, RADS 2004 [68]–[73]. Some of the topics of discussion were summarized and published as papers in a special issue of Acoustical Science and Technology in 2005[17], [18], [74], [75].

As mentioned in the several papers cited above, as there is no definitive method for the selection of receiver locations, the method of locating the source and receivers is an important issue to be addressed. For example, a few points cannot fully represent the global characteristics of the sound field, while at the same time, the averaging of large groups of data will hide important information. [76]

In ISO 3382, the recommended number of measurement points and its selection guideline is for an appropriate coverage of a room. The minimum numbers of receiving positions and the selection guideline are described for low coverage of a room. For a normal coverage of the room, adding more receiver positions is a must for judging the evenness of the acoustical distribution. In addition, as Hidaka [74] and Bradley [17] suggested, more receiver positions than the number recommended in ISO 3382 might be needed for a more detailed picture of the hall distribution.

ISO 3382 [13] suggested that in a symmetrical hall, measurement points can be placed only on one side of the hall with the source located symmetrically about the centre line. Such source location should be at equal distance to the stage right and stage left. A source height of 1.5m is recommended so as to avoid low frequency modification of the source loudspeaker output. The directivity of the source should follow their recommendation, else should be repeated at least three steps and averaged. Depending on the size of the hall, the number of microphone positions should be at least as listed in Table 2-1 below. While breaking up the hall into separate areas, more locations should be added. The microphone should be placed at a height of 1.2m from the floor which represents the average height of a seated audience's ear level. Conditions on the stage which affect the source and the acoustic conditions should also be noted.

Table 2-1 Minimum number of receiver positions as a function of auditorium size [13]

Number of seats	Minimum number of microphone positions
500	6
1000	8
2000	10

Densely distributed measurement points are detailed enough to find spatial variations according to Bradley[17] [72] . In a more practical sense, reasonable values of the parameters can also be obtained even if mean values for a relatively small number of measurement points, such as 36 out of 1400, are used. [76]

2.6 Neural Network

2.6.1 Theory and how

Neural network analysis (NNA) is a paradigm of learning and automatic processing inspired by the biological model of the functioning of human brain: modelling a person's learning process. [77] It is a tool to solve complex problems by learning from precedents. It is comparable to multiple regression analysis with no assumptions needed. NNA has been discussed for decades while applications are developed to handle practical problems in recent 30 years. It has been applied in solving a large variety of problems, including non-linear problems which are not suitable in using classical analysis method.

NNA comprises of interconnecting groups of artificial neurons like a biological brain. These connections follow a highly-densed and parallel interconnecting scheme. The first layer is the input layer of the network, each neuron is an individual input. The middle layer is the 'hidden' layer while the last layer is the output layer having one neuron for each output. A neuron, also called processing element, is the basic unit of a neural network. It performs summation and activation function to determine the output of that neuron as shown in Figure 2-2. The number of neurons in the hidden layer depends on the number of training cases used; it is approximately the average of the inputs and outputs. A single hidden layer is usually sufficient, excessive hidden layers can result in 'over-training' and lead to large 'verification' errors. Insufficient neurons can result in

large ‘training’ and ‘verification’ errors. The inputs can be weighted, and then the node will be excited by the aggregation of the weighted inputs.

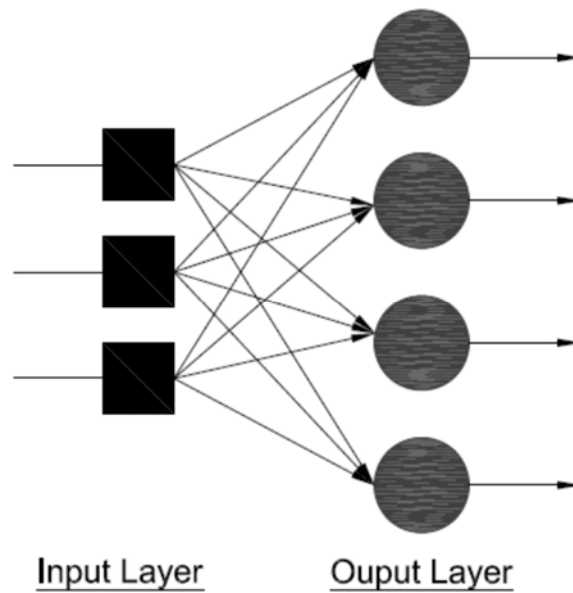


Figure 2-2 Structure of a single layer feedforward neural network.

An NNA propagates only in one direction is called a Feedforward network. Another form of network is a recurrent network with nodes connected with bi-directional arc without any layers.

An NNA learns the system behaviour and generalizes the information acquired from available examples, i.e. the training data. Starting from an initially randomized weighted network system, input data is propagated through the network to provide an estimate of the output value. The error between the output and the predicted value is used to adjust the network connection weightings to minimize the error in the predicted outputs. In this iterative procedure, the new weights are accepted if the resulting error is smaller than that recorded using the previous set of weights.

Several algorithms are commonly used to achieve the minimum error in the shortest time. There are also many alternative forms of neural networking systems and, indeed, many different ways in which they may be applied to a given problem. The suitability of an appropriate paradigm and strategy for application is very much dependent on the type of problem to be solved.

2.6.2 Application in Acoustics

Artificial neural network has been widely used in different fields especially for solving non-linear problems.

In room acoustics, Nannariello and Fricke [78] used the geometric variables of 65 halls with different shapes and sizes to ‘train’ a network for predicting the average strength factor, G . Seven sets of hall data were used to test the network. The volume V , the maximum length, L_{mx} , maximum width, W_{mx} , the tube ratio (proposed by Grade [79]), $D_{mean}/W_{mean} * H_{mean}$ were the 4 input parameters of the network.

Nannariello and Fricke [80] had also used 100 shoebox shaped enclosures of varying dimensions and surfaces to train and test another neural network for predicting G . This prediction result was compared with numerical simulations. Six geometric variables (volume of enclosure, maximum length, width, depth and height of enclosure, distance between source and receiver), three receiver position coordinates, the total floor area, source and receiver distance and the receiver position reverberation time were used as input to the network.

Besides, they used nine inputs to simulate the strength factor G , clarity $C80$ and Lateral energy fraction LF . Their results indicate that it is possible to use trained neural network to predict these parameters.[81]

With geometrical and acoustical data for 36 unoccupied concert halls, Nannariello and Fricke [20] successfully formed an neural network for simulating the early interaural cross-correlation coefficient ($IACC_{E3}$) for concert halls.

The results above show that neural network can be used as a tool to establish rules of thumb to be used in early stages of a hall design.

In outdoor acoustics, Yu and Kang [82] used ANN to establish a model to predict the soundscape quality evaluation of futures users in urban open spaces at the design stages. They used a three levels network for the prediction. Their results show that it is less feasible to have a generalized ANN to predict subjective sound level and acoustic comfort in urban open spaces. It is good to form a prediction network for an individual site. However, this application range is limited. Fortunately, forming model specifically for certain types of location/functions gave reliable and practical result.

2.7 Conclusion

The evolvement of performing arts calls for different acoustical requirements of performing halls across the centuries. The changing number of concert goers and theatre audience calls for different size and configuration of halls, like the needs of balconies for increasing the seating capacity. This ballooning needs of more halls brought the need of acoustic research in hall. Hall acoustics research started becoming solid in the 19th century when the Sabine equation was first developed.

Then, formulae for other objective parameters were developed by other researchers. Also, with the advancement of measuring technology, more and more halls and more and more hall parameters can be measured. Researchers have also correlated these objective parameters with the subjective parameters usually used by musicians in the measured halls. Relationships among some of these parameters have been found.

The most common method in hall measurement is measuring the impulse response at each measuring location and determine the different parameters through different calculation algorithms. However, extensive measurements throughout the hall are needed in order to understand the variations of acoustical properties inside a performance hall. In busy cities like Hong Kong, while hall resources are much tensed, a prediction model that only requires a small number of data input and having the possibility of predicting the acoustics at any location inside a performance hall is needed. In such cases, a black box solution like neural network analysis is a good option.

To increase the seating capacity of halls, balconies appear to be a good option. However, the effects of the balcony is not much discussed. The balcony increases the complexity of determining the acoustics in a hall as well. Scale model and 3D computer modelling are common ways to predict the acoustics in a hall before it is built. Thus, such methods are also used to study the effect of the presence and the size of the balcony.

Chapter 3 Methodology

This chapter details the methodology of this thesis, starting from the real hall measurements and scale model experiment, followed by the regression model and neural network analysis. Real hall measurements were done in various halls in Hong Kong. The measured performance halls are of different type and size. Large scale acoustical index measurements were done using room acoustic measurement software, DIRAC. The second part is the theoretical modelling and validation. The real hall data acquired in this large scale measurement were then analysed and compared with neural network analysis, 3D-simulations and 1/10 scale model experiment.

3.1 Real hall measurements

The performance halls in Hong Kong are owned by the Government, institutions, churches and different private owners. Most of the halls are dedicated for multi-purpose use. They vary in size, shape and design. In some of the halls, to cater the multipurpose use in the halls, acoustic shells are set up to convert from theatre setting to concert setting. Therefore, the measurement in this research includes both situations, with and without the acoustic shells for the evaluation of acoustical parameters.

Different acoustical parameters were measured in accordance with ISO 3382:1 (2009) [13] and the definitions of Beranek[6] and Hidaka et al.[19]. Integrated impulse response method[13] was used. Additional measurements around the balcony edge were done in Hall A for investigating the balcony diffraction and scattering.

Binaural measurements using Brüel & Kjær Type 4100 Head-and-Torso Simulator (HATS) were used to capture the sound fields inside the hall generated by a Brüel & Kjær Type 4296 omni-directional sound source located at 1 m inward from the edge of the stage on the stage centreline. The source was set at the height level of a standing human's mouth (1.6 m). The maximum length sequence procedure implemented by the DIRAC system [83] was used to obtain the binaural sound decay patterns. The measurement duration was set to be 5.5 sec at each measurement points. This value is at least twice the reverberation time of the hall which is sufficient for the DIRAC software to calculate an accurate result. The DIRAC software calculated the acoustical parameters C80, D50, RT, EDT and IACC in octave bands. The formulae for these parameters are presented in chapter 2 and can be found in BS EN ISO 3382[13] and some standard textbooks such as

Kutturff.[86] Thus, they are not presented here. During the measurements, the signal-to-noise ratios were all kept higher than 20 dB over the whole audio frequency range. The background noise level was around 30 dBA and the generated sound levels varied from 70 to 80 dBA during the measurements.

B&K sound level meters with 1/ inches transducer were used as receiving device in monoaural measurements throughout the halls and around the balcony edge. The spectrums of background noise in the venues were also measured using B&K Sound Analyser. Figure 3-1 shows the system setup for the measurements.

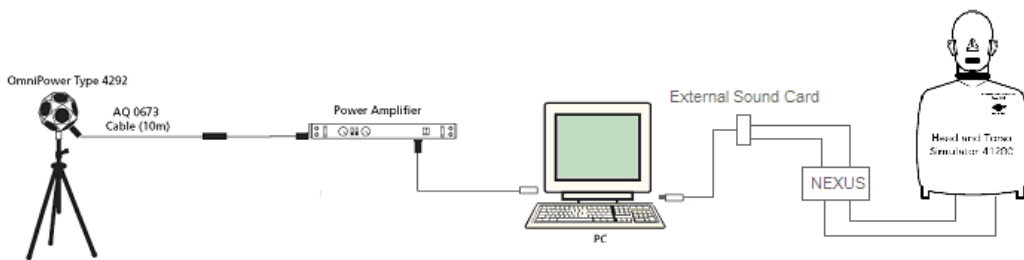


Figure 3-1 Dual Channel dummy head connection system

With reference to ISO 3382-1:2009[13], when the hall is symmetrical, the measurement points can only be placed on either side of the hall with appropriate quantity to represent the whole hall. The minimum number of microphone positions for a 1000 and 2000 seat hall are 8 and 10 respectively.

In these measurements, more microphone points were selected for obtaining more detailed distributions of the acoustical properties of the halls. Depending on the length of the seating row, at least 5 points, distributed averagely on every 3 to 5 rows, were marked as measurement positions.

A microphone array, surrounding the balcony edge was used for tracing the diffraction and scattering effect of the balcony. Acoustics properties were measured at each 15 degrees at 1.5m and 2m from the edge of the balcony. The physical dimension and design of the balcony edge governed the actual number of angular positions chosen.

3.2 Scale down model

Scale model experiments are commonly used for predicting acoustics performance in new performance design. It enables changes to be made to investigate the effects of material to be chosen and geometry to be built. In evaluating acoustics in an existing hall, scaling down the hall can allow changes to the geometry, which is impossible to carry out in real case. In this study, a 1:10 scale down model was constructed to study the effects of the balcony on energy and related parameters in a large performance hall. Intergraded-impulse source method was used to measure the acoustic properties in the experiment.

Owing to the limitation of the hall data and complexity of the other halls, only Hall A was chosen in the scale model experiment. It is believed that the results of Hall A model can provide sufficient insights into the sound propagation phenomena in halls.

3.2.1 Model

The geometry of the scale model was a simplified version of Hall A. Figure 3-2 shows the exterior of the scale model. The whole model was screwed and seated on a 2ft tall timbre frame. Raising the whole scale model allowed access to the inside from the bottom and the microphones could be plugged into the scale model without opening up the scale model repeatedly.



Figure 3-2 Exterior of the scale model from the side

As shown in the photo above (Fig. 3), the scale model was constructed with 18mm thick wood panels with smooth surfaces on both sides and raised by 2 feet from the floor so as to allow access from below.

The construction of the scale model was started from the audience floor, followed by the stage floor. This combined the floor to the base frame which provided a safe support to all vertical walls constructed. All the vertical walls were then sat onto the floors on each side and screwed together. Upon forming the perimeter of the stage, the ceiling was then rested on the walls. The sidewalls of the audience were done and the side galleries were then fitted in. Afterwards, the interfacing of the audience and stage was done. Gaps of all the adjoining panels were sealed with gypsum paste or silicon sealant. The construction continued with the building of the lower ceiling and the balcony floor. They were cantilevered and supported with an angled iron bar passing from the left to the right at the balcony edge position. The bar also formed the mounting of the balcony edge. The slanted cut wood pieces were then fixed at the right position to form the chamfered balcony edge. Three large pieces of wood were then lifted to the top of the model to form the upper ceiling of the audience area. Fabric of the scaled model was finished by closing the end of the back of the seating area on both floors separately. Gaps were sealed and double checked by visual inspection inside and outside the model, looking for light penetrating in or out. The model was further sealed with sealant from outside at any connecting edges and points.

The floor of the hall was smoothed while the ceiling was also simplified. The two gallery boxes on both sides of the hall were also omitted. As the back of the main stage of Hall A has a concrete wall as cyclorama, the back of the stage area was omitted in the scale model.

During the measurements, the temperature and relative humidity were measured before the start of each session of measurements. The average temperature was 20 degree Celsius while the average relative humidity was 80%.

3.2.2 Measurement Cases

To make possibility to compare with real hall measurements so as to investigate the effect of the balcony, four different settings were used in the scale model experiments. The four settings were denoted by case 1 to case 4. Case 1 was the basic case simulating the

proscenium setting of Hall A: pieces of dacron cloth were used as stage drapes. Case 2 was another case simulating the real hall condition with the sound canopy. Case 3 and case 4 were with same stage setting with case 1 and case 2 respectively. In these 2 cases, the balcony was taken down while the rear end of the ‘auditorium’ was completed with wood panels forming a side back wall with the existing one under the balcony in case 1 and 2.

Figure 3-3 shows the stage setting for case 1 and case 3. The scaled-down acoustic shell was fabricated with 18mm plywood with white finishing on both sides.

Figure 3-4 shows the stage setting for case 2 and case 4.



Figure 3-3 Interior of the scale model with a proscenium setting, view from the audience



Figure 3-4 Case 2 with balcony and with sound canopy



Figure 3-5 The balcony in the scale model in case 1 and case 2



Figure 3-6 View from the stage inside the scale model seeing the rear part of the scale model without the balcony structure

3.2.3 Source signal

An impulse source can be generated simply by a clapping hand or a pistol shot. However, these types of sources are not repeatable. . If many sets of measurements are required, a repeatable source is needed.

Pseudorandom noise is very repeatable. However, for a 1/10 scale model, a high frequency loudspeaker that can radiate sufficient amount of sound energy across the whole spectrum at all angles is required.

An electric spark source was used in this study. In general, is the setup is a step up circuit with capacitors, resistors, diodes and two probes. The circuit is supplied by 220V AC and converted to DC at the probes. The circuit provides the continuous charging and sparking to the source. Once the voltage accumulated across the gap is large enough to form an arc to overcome the resistance between the tips of the probes, voltage is discharge and then a spark is generated.

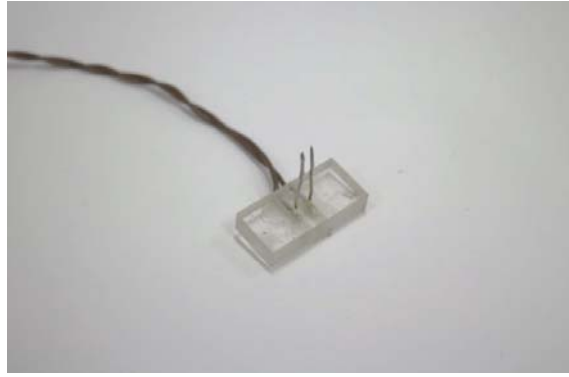


Figure 3-7 The probe of the electric spark

Figure 3-7 shows the probe of the electric spark used in this study. The sparking element consisted of 2 pins embedded in an acrylic block and connected to the circuit board. The separation between the tips was maintained at approx. 4.5mm. The tips were polished with sand paper to remove the debris remained from previous sparking before the start of each session of measurement. The sparking time gap was monitored to around 5-6 seconds to ensure there was sufficient time for the sound level to drop down to the background level. This could allow the impulse to be discrete. The directivity of the electric spark source was measured in the anechoic chamber and details will be presented in Chapter 4.



Figure 3-8 Spark source mounted at the source position.

3.2.4 Measurement locations

Only one source location was used in the scale model measurement. Figure 3-9 shows the source locations and receiver positions measured in the scale model.

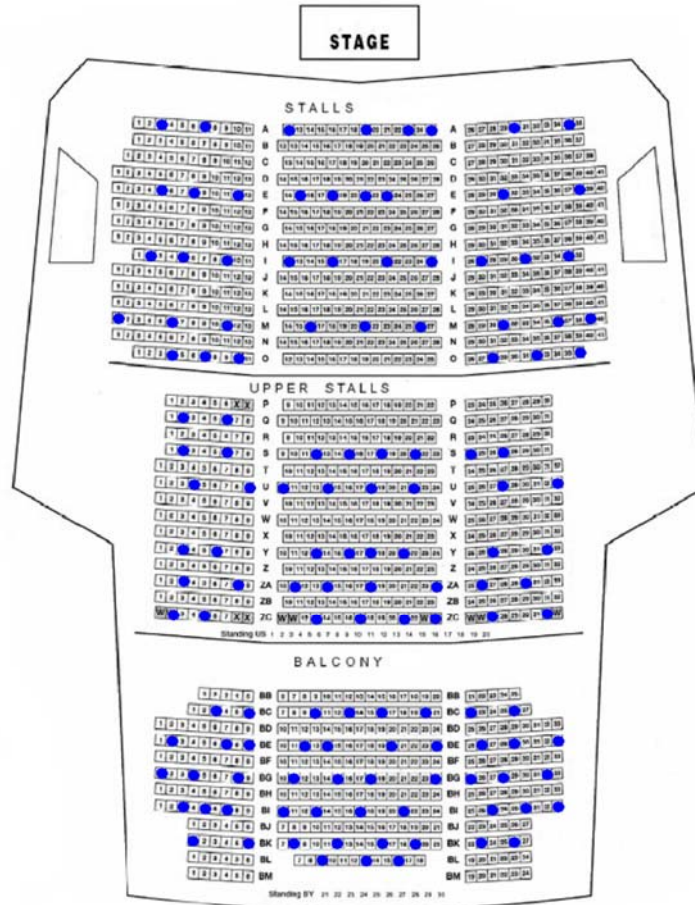


Figure 3-9 Points measured in scale model

Figure 3-10 shows the tailor-made measurement rack for the radial measurements around the balcony edge. Points measured were at 1.5m and 2m from the centre of the rack from -90 degrees to 225 degrees. 0 degree refers to the angle which the microphone was pointing towards the stage and horizontal to the ground. The microphone was rotated up from -90 degrees (vertically pointing downward at the specific distance) to 225 degrees point to the back of the balcony.



Figure 3-10 Microphones mounted on the tailor-made measurement rack at one of the balcony edge positions

3.2.5 Receiver and recording

High frequency LAN-XI data acquisition hardware, Pulse from B&K with 2 nos. of 1/8-inch B&K pressure-field microphone Type 4138 with Type 2670 preamplifier were used in recording the impulse measured at each receiver locations. Figure 3-11 shows the microphones mounted at 2 measurement positions in the stall area.

Figure 3-12 is the Pulse system used to record the impulse response at each receiver locations.



Figure 3-11 1/8 inch microphones at measurement position



Figure 3-12 High frequency LAN-XI data acquisition hardware, Pulse system used in scale model measurement

3.2.6 Analysis using Integrated-impulse method

The measured signals were processed using Matlab. Butterworth 3rd order filter was used to filter the signal into octave bands. Hilbert transform was applied to the signal before backward integration was carried out to form the decay curve for finding the reverberation times. The Hilbert transform of the signal is defined by:

$$F(t) = \frac{1}{\pi} \int_{-\infty}^{\infty} \frac{f(x)}{t-x} dx \quad \text{Eq. 3-1}$$

where $f(x)$ represents the respective filtered time signal

Theoretically, the integral is evaluated as a Cauchy principal value. Computationally one can write the Hilbert transform as the convolution:

$$F(t) = \frac{1}{\pi t} * f(t) \quad \text{Eq. 3-2}$$

which by the convolution theorem of Fourier transforms, may be evaluated as the product of the transform of $f(x)$ with $-j \cdot \text{sgn}(x)$, where:

$$\text{sgn}(x) = \begin{cases} -1 & x < 0 \\ 0 & x = 0 \\ 1 & x > 0 \end{cases}$$

The Hilbert transform can be considered as a filter which simply shifts the phases of all frequency components of its input by $-\pi/2$ radians.

A complex analytic signal $Y(t)$ consists of a real part and an imaginary part is constructed from a real-valued input signal $y(t)$:

$$Y(t) = y(t) + j h(t) \quad \text{Eq. 3-3}$$

where,

$Y(t)$ is the analytic signal constructed from $y(t)$ and its Hilbert transform

$y(t)$ is the input signal

$h(t)$ is the Hilbert Transform of the input signal

The imaginary part is a version of the original real sequence with a 90° phase shift. The real and imaginary parts can be expressed in polar coordinates as:

$$Y(t) = A(t)\exp[j\omega(t)] \quad \text{Eq. 3-4}$$

where,

$A(t)$ is the envelope or amplitude of the analytic signal

ω is the phase of the analytic signal while the derivative of ω is called the instantaneous frequency

The Hilbert transformed series $Y(t)$ has the same amplitude and frequency content as the original sequence and includes phase information that depends on the phase of the original. [85, Ch. 4]

The envelop $A(t)$ was then converted to decibel scale by the following equation

$$E(t) = 20\log_{10}A(t)\max(A(t)) \quad \text{Eq. 3-5}$$

By using the Schroeder Integration method, the decay profile, also known as the inversed time integration, was obtained.

In calculating the reverberation time and similar parameters, the decay curves were interpolated linearly as shown in in Eq. 3-6

$$L(t) = 10\log_{10} \left[\int_t^{\infty} h(\tau) d\tau \int_0^{\infty} h(\tau) d\tau \right] \quad \text{Eq. 3-6}$$

with the function

$$L = A \cdot t + B \quad \text{Eq. 3-7}$$

on their respective range and calculated from Eq. 3-8

$$RT = \frac{-60}{A} \quad \text{Eq. 3-8}$$

where A is a slope of the interpolated line (in dB/s). The correlation coefficients of the linear fit were also obtained to check the wellness of the linear fit.

In according to ISO 3382-2, the decay curves were then fitted linearly with the appropriate dynamic range so as to calculate the early decay time, EDT, and reverberation times, T10, T20, T30 and T60. The ranges are as follows:

- EDT (Early Decay Time): upper limit is 0dB and lower is -10dB. This parameter correlates well with perceived reverberation time. In practice though beginning for the sake of algorithms, people are using interval of -1dB and -10dB (i.e. in Norsonic analysers).
- T10: upper limit must start at -5dB to remove any fluctuations and then lower limit is taken to be -15dB, but it always must be at least 10dB above the noise floor. So in fact you need at least 25dB of dynamic range (or INR) to be able to calculate T10 (5+10+10).
- T20: upper limit at -5dB, lower at -25dB. Minimum dynamic range needed is 35dB
- T30: upper limit of -5dB, lower at -35dB, with minimum 45dB of dynamic range.
- T60: upper limit of -5dB, lower at -65dB, with minimum 75dB of dynamic range.

Since the calculation of T60 requires a very large dynamic range which is impractical, T60 was not used here.

3.3 Neural network analysis

A neural network requires a reliable database to function, the schemes used in the regression analysis were tested. They were brought forward and used in neural network analysis. Thus, general information from different halls may only be able to give indicative predictions.

The acoustic propagation inside a large hall with balconies is too complicated for analytical study. Thus, the artificial neural network approach appears very useful in finding out the functional relationships between various parameters though in rather implicit formats (for instance, Nannariello and Fricke[20], [78], [80], [81], [86] and Kang[82]) There are many different algorithms in existing literature as indicated in Genaro et al.[87] and for simplicity, a feed-forward network with one hidden layer was adopted in the present study. The transfer functions used in the hidden and output layers were of the tan-sigmoid and linear types respectively. No input weighting and bias were

applied and the number of neurons in the hidden layer was arbitrarily chosen to be twice the number of inputs. The Levenberg-Marquardt algorithm was adopted as the training algorithm. The computation was implemented using MATLAB and the default stop criteria of MATLAB was adopted for each simulation.[88]

The data used in the neural network analysis were Hall A and Hall B measurement data from the real hall measurements. Data from both the concert hall setting and proscenium setting of each hall were used and tested separately.

As both concert and proscenium setting of these two halls were measured and they could represent two different types of hall design, i.e. a shoebox hall with parallel walls and rectangle seating layout and a modern theatre with a fan shape hall front with fan-shaped seating area, data from Hall A was then used to test the workability of neural network and then validated with the data of Hall B for the network's workability on other shape of halls.

The measured data, together with the corresponding spherical co-ordinates, form the outputs of and inputs to the network respectively during the training stage. The acoustical parameters at all the measurement points are then simulated using the trained networks. Owing to the difference in the layouts of the halls investigated, the data from the two halls are analysed separately. There is then no need to separate the balcony and stall areas in the network analysis as the elevation angle (θ) should be sufficient for differentiating measurement points in the stall and the balcony sub-areas. It should be noted that the neural network simulation varies every time after the network is initialized.[88] Therefore, the simulated results for each scheme presented hereinafter are taken to be the arithmetic averages over many simulations. In the present study, 100 and 200 simulations are adopted for the study of the concert hall and proscenium setting respectively to ensure data convergence. The root-mean-square differences between simulations and measurements converge to within a tolerance comparable to that of measurement (not shown here). It was aimed to test whether neural network can be used for predicting hall parameters. Therefore, two halls with different shape is a sufficient start.

Four different training schemes were used in this study. The halls were firstly divided into several zones, front stall, mid-stall, under-balcony and balcony. In each zones, different numbers of measurement points were selected to form the four different analysis schemes. In each hall, scheme A is the simplest scheme which includes three measurement points spreading evenly in the middle region of each zone. Scheme B

includes measurement points on the nearest and the furthest row from the stage of each zone. Scheme C is the combination of scheme A and scheme B. The most complicated scheme is scheme D, it has the maximum number of points and is basically scheme C with a better span-wise selection. However, scheme D for Hall B is actually an undesirable option because of the relatively large number of training points required in the upper stall and the balcony area due to the relatively small balcony in Hall B.

3.4 Regression analysis

Having the extensive measurements in Hall A and Hall B done, the data was then analysed using regression approach in an attempt to find out an improved scheme for the prediction of various acoustical parameters using small number of measured data and regression inputs. A detailed regression analysis was done using the data of Hall A and was followed by a validation using the results of the Hall B. The same zone dividing strategies and measurement point's selection scheme used in neural network analysis were used in forming the analysis.

3.4.1 Point of reflection and path difference

Before further analysing the results, the following principle was used to find the point of reflection of the direct sound from the source to each particular receiver on the stall and hence, find the shortest travelling path (D) and path difference (δ) of the direct sound and the reflected sound.

Firstly, an analytical expression for the reflection point $\mathbf{X}_p = (x_p, y_p, z_p)$ on a 3D plane with the sound source located at the original $(0, 0, 0)$ and the receiver at $\mathbf{X}_r = (x_r, y_r, z_r)$ was sought. Figure 3-13 shows the schematics. $\mathbf{X}_i = (x_i, y_i, z_i)$ is the image of \mathbf{X}_r about the reflecting 3D plane. Thus, \mathbf{X}_i and then \mathbf{X}_p were found.

A 3D plane can be represented by $ax + by + cz = d$ and $d \neq 0$ for those planes which do not contain the Cartesian original. Without the loss of generality, the plane was set to cut the positive y-axis, such that $d > 0$. It is supposed that the reflection of the sound from the source takes place on this plane and the reflected sound reaches directly at \mathbf{X}_r . The perpendicular distance between this plane and \mathbf{X}_r must equal to the distance between this plane and \mathbf{X}_i and this distance is then related to d . It can be shown that the separation between the receiver point and the 3D plane is proportional to d_r , which is given by the expression:

$$ax_r + by_r + cz_r = d_r \quad \text{Eq. 3-9}$$

Similar phenomenon applies to the image as well and one then obtains

$$ax_p + by_p + cz_p = d \quad \text{Eq. 3-10}$$

and

$$ax_i + by_i + cz_i = d_i \quad \text{Eq. 3-11}$$

with the condition that $d - d_r = d_i - d \Rightarrow d_i = 2d - d_r$. One can also quickly realize, by similar-triangle principle, that

$$\frac{x_p}{x_i} = \frac{y_p}{y_i} = \frac{z_p}{z_i} = \frac{d}{d_i} \quad \text{Eq. 3-12}$$

Certainly, one can arrive at the same conclusion by solving the intersection between the reflecting plane and the line joining the original and \mathbf{X}_i .

The line joining the receiver and its image is perpendicular to the reflecting plane and thus

$$\frac{(x_i - x_r)}{a} = \frac{(y_i - y_r)}{b} = \frac{(z_i - z_r)}{c} = \alpha \quad \text{Eq. 3-13}$$

Combining this with the above equations :

$$a(\alpha a + x_r) + b(\alpha b + y_r) + c(\alpha c + z_r) = d_i \quad \text{Eq. 3-14}$$

$$\Rightarrow \alpha = \frac{-(ax_r + by_r + cz_r - d_i)}{(a^2 + b^2 + c^2)} \quad \text{Eq. 3-15}$$

$$= \frac{2(d - d_r)}{(a^2 + b^2 + c^2)} \quad \text{Eq. 3-16}$$

Thus, \mathbf{X}_i is solved and so does \mathbf{X}_p :

$$x_p = \frac{d}{d_i} x_i = \frac{d}{d_i} (\alpha a + x_r) = \frac{d}{2d - d_r} \left(\frac{2a(d - d_r)}{a^2 + b^2 + c^2} + x_r \right) \quad \text{Eq. 3-17}$$

$$y_p = \frac{d}{d_i} y_i = \frac{d}{d_i} (\alpha b + y_r) = \frac{d}{2d - d_r} \left(\frac{2b(d - d_r)}{a^2 + b^2 + c^2} + y_r \right) \quad \text{Eq. 3-18}$$

$$z_p = \frac{d}{d_i} z_i = \frac{d}{d_i} (\alpha c + z_r) = \frac{d}{2d - d_r} \left(\frac{2c(d - d_r)}{a^2 + b^2 + c^2} + z_r \right) \quad \text{Eq. 3-19}$$

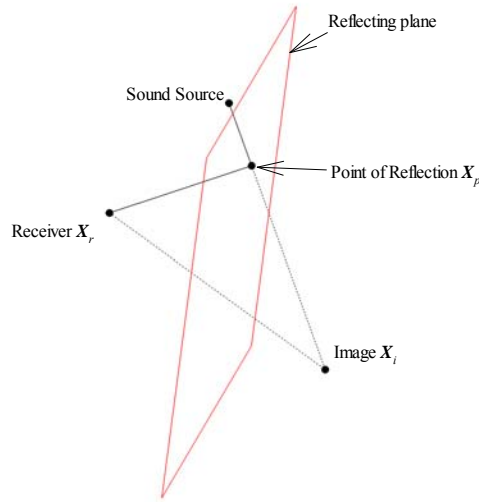


Figure 3-13 The schematic of the sound source, point of reflection, receiver and image

3.4.2 Regression inputs

The calculated direct distance and path difference and the other geometrical parameters were used to form the inputs in the regression analysis. Figure 3-14 shows the definitions of the geometrical parameters graphically. The azimuthal angle (ϕ) and elevation angle (θ) represent the angular position of a receiver point with respect to the hall centreline and the horizontal plane respectively.

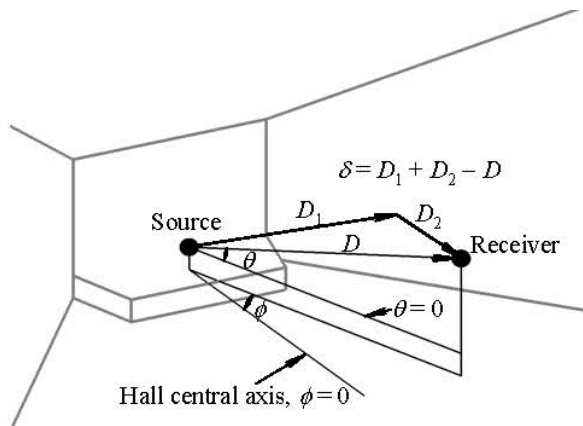


Figure 3-14 Definitions of the Geometrical parameters

The strengths of the signal was affected by the source-to-receiver distance (D) and the path difference (δ) between D and the distanced travelled buy the signals before reaching the two artificial ears of the HATS used in real hall measurements. The relationship and the use of these parameters will be further discussed in Chapter 6.

3.5 Conclusions

This chapter has detailed the methodology in collecting data and data analysis for this study. Four performance halls of different sizes and design had been measured in this study. Some of the halls are multi-purpose hall that both their concert and proscenium setting were measured. Measurement locations were selected randomly to maintain a thorough coverage of the hall. Binaural measurement were done in all halls while mono measurement were done at the balcony edge in Hall A. Measurement points in a radial arrangements were added to the balcony edge attempted to capture the sound propagation and scattering. Only 1.5m and 2 m radii were done in this study.

The results of these measurements not only formed a small hall database, they were also used for further analysis in the later part of this study.

A 1/10 scale model based on the geometry of Hall A has been done to investigate the effect of the balcony to the measured acoustic parameters in the hall. Both the concert setting and proscenium setting of the hall were scaled by erecting a sound canopy on the stage in the scale model. The balcony of the scale model was taken down and the measurement were repeated in the stall to under-balcony area. The balcony effect, the difference between measured values with and with the balcony with the same stage setting, were then determined.

The measured parameters with the geometric data of Hall A and B were used in neural network analysis for prediction. A single layer feedforward network was adopted in this study. Data of Hall A, a rectangular or shoe-box shaped hall, was first used to test whether the method can be used to predict the parameters. Such method was then tested with Hall B's data for validation and justified for its workability on other shape of halls like a fan-shaped hall like Hall B. Four different training schemes with different number of training data sets have been used in developing the neural networks.

Detailed regression analysis have been done using data of Hall A to find out the relationship among each measured and geometrical parameters. Four fitting schemes similar to those used in neural network analysis have been adopted. This analysis aim to develop a simple prediction model that only require a small number of measured values to predict the acoustics of the other locations in a hall. The usefulness of the models in fan-shaped hall has been proved using Hall B.

Chapter 4 Hall measurements

4.1 Introduction

Many performance halls and venues have been built in Hong Kong since the 60's in the last decades, there are more to be built in the West Kowloon Cultural District by the HKSAR Government. Meanwhile, there are some other private venues owned by institutes and churches. Yet, only the concert hall in Hong Kong Cultural Centre has been measured and published by Beranek[6], not much information can be found related to the hall properties in Hong Kong. This gives chance to start some hall measurements.

Different hall owners, from public and private sectors, are liaised throughout the years to arrange halls for measurements. Six different halls had been measured and four had been included in this study. This chapter starts with introducing the basic facts of the halls being measured, with their building information and size, followed by the measurement locations in each hall, and then with the binaural measurement results of each hall.

Around 1/10 of the seating capacity of the hall were measured. Brüel & Kjær Type 4100 Head-and-Torso Simulator (HATS) was used as receiver for the binaural measurements. Among the five halls, some of them are multi-purpose halls. Depending on the availability of the hall, the concert stage setting and proscenium setting were measured. Room acoustics measurement system, Dirac version 4.1 were used for the measurements. The data presented in this chapter were calculated using the same software.

The technical drawings and building recorded plans of hall A were obtained for determining the dimensions and distance of each measured point from the source. The direct distance, path difference and the associated azimuth as well as elevation angles were calculated for further analysis.

This short chapter acts as a start of the whole project, starting from collecting real hall data, presented in this chapter, for further analysis. Scale model experiment and computer simulations in the next few chapters use the data presented in this chapter.

4.2 The Halls

There are in total five large performance halls with balcony and one small size concert halls measured in this study. The halls measured are of different sizes and shape. They are owned by different public and private sectors. Table 4-1 summarises the brief

information for the halls. The halls are named from A to F for easy identification throughout this thesis.

Table 4-1 Summary of the halls measured

Hall	Setting measured	Shape	Balcony	No. of Seats Stall/Balcony/Total	Owner
A	Both	Rectangle	Yes	1032/340/1372	Public
B	Both	Rectangle/Fan	Yes	730/189/919	Public
C	Speech/Music	Rectangle	Yes	702/323/1025	Institute
D	Concert	Rectangle	Yes	183/82/265	Public

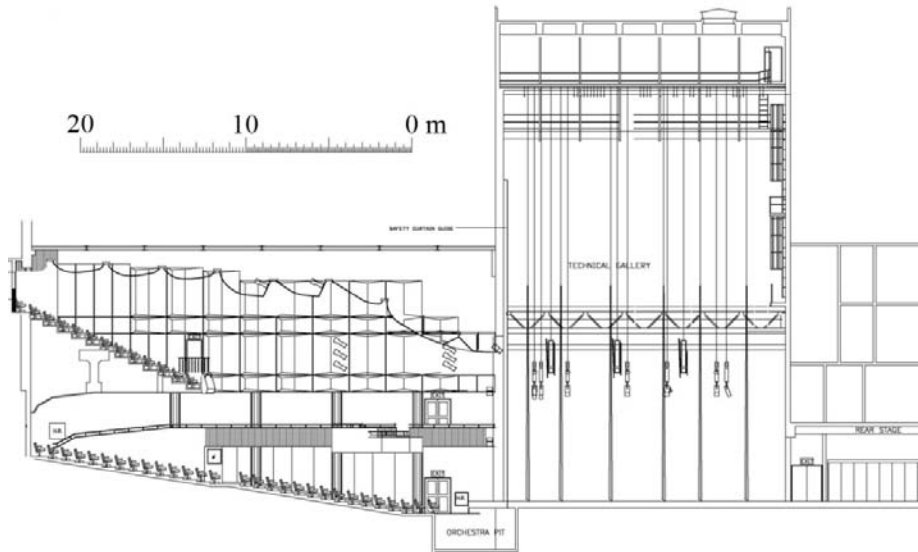
4.3 Hall details

4.3.1 Hall A

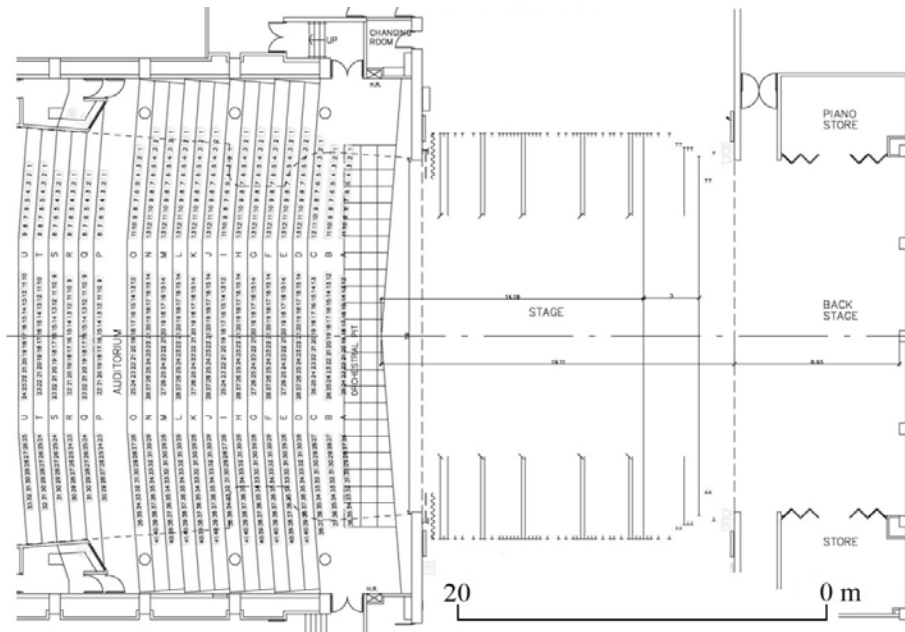
Hall A is of the typical design with a rectangular layout and a seating capacity of 1372 (stall: 589, upper stall: 443, balcony: 340) Figure 4-1 shows the interior of Hall A while Figure 4-2 illustrates the design and dimension of the hall. The walls of the hall, except those areas between the first audience row and the stage, are covered by soft materials and the floor by wood tiles. The balcony edge and parapet follow the curvature of the seating plan. Both the proscenium and concert hall settings of Hall A are included in the present study.



Figure 4-1 Interior of Hall A with concert setting



(a) Sectional view of Hall A



(b) Layout view of Hall A

Figure 4-2 Sectional and layout views of Hall A
 extracted from technical drawings of Hall A, available on the owner's website

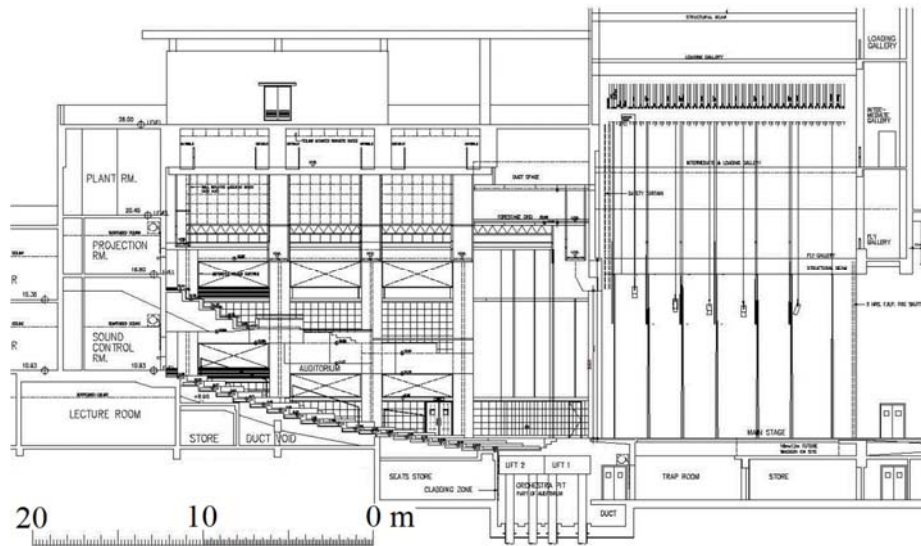
4.3.2 Hall B

Hall B is a smaller hall than Hall A with a fan-like seating layout and a seating capacity of 919 (stall: 527, upper stall: 203, balcony: 189). Figure 4-4(a) and (b) illustrates the design and dimension of the halls. Unlike Hall A, there are two technical balconies on the both sides of the stage opening as shown in Figure 4-3. They are of different levels and appear as small voids with timbre walls. On the side walls in the stall area and on the balcony, there are grids of acoustics boxes at low to midlevel and with motorised velour curtains covering the plastered walls at mid to high level. There are catwalks and lighting bars hoisted over the seating area. Nearly all the electrical and mechanical services installed at the ceiling are exposed. There are ceiling mounted acoustics boxes installed on top of them. The ceiling under the balcony is with false ceiling.

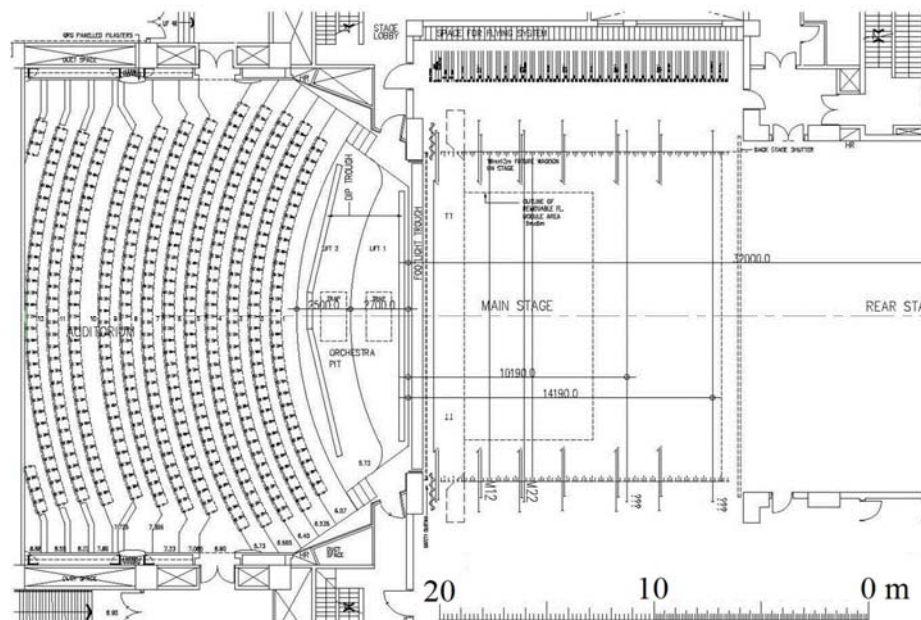
The walls of the hall except the technical balconies on two side are covered by soft materials and the floor by wood tiles. Its balcony edge is curved as shown in the layout plan. However, the balcony edge and parapet follow the curvature of the seating plan. Both the proscenium and concert hall settings of Hall B are included in the present study.



Figure 4-3 Interior of Hall B viewing from the stage



(a) Sectional view of Hall B



(b) Layout view of Hall B

*Figure 4-4 Sectional and layout views of Hall B
extracted from the technical drawings of Hall B, available on the owner's website*

4.3.3 Hall C

The hall is almost symmetrical on both sides. It has a balcony with 323 seats over the stall area with 702 seats. The seats on the balcony are arranged in 8 rows in the middle aisle and 9 rows on the left and right. Figure 4-5 shows the interior of the Hall C while Figure 4-6 show the sectional drawing and layout of Hall C. Instead of a smooth balcony edge,

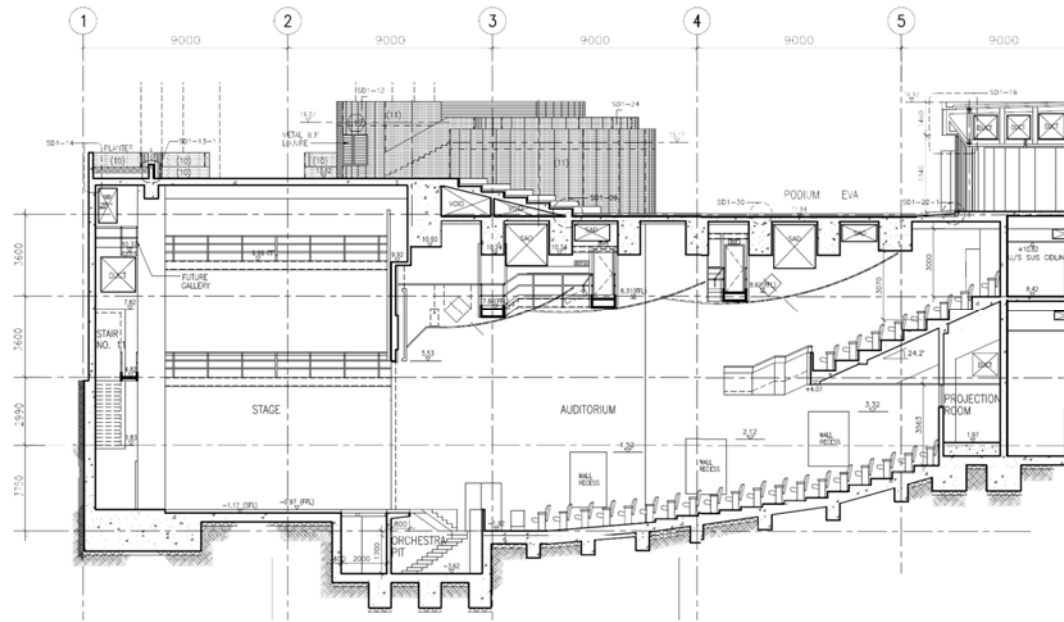
this balcony is designed with a zig-zag edge and it covers approximately 8 to 9 rows of seats in the stall. The two sides of the balcony extends to the side wall of the stage's proscenium. All the seats are fully upholstered with armrest. The stall and the balcony floor are covered with heavy carpets on concrete from the entrances to the stage edge. There is a platform in front of the stage which can be raised to enlarge the stage front, levelled to provide more seats and sunk to have an orchestral pit.

Both the side walls in the stall are fitted with wooden boards and heavily absorbing fabric panels while those on the balcony are plaster on concrete. The upper ceiling of the hall is slightly curved in three layers, slopping down from the back of the hall to the proscenium of the stage. The lower ceiling is mostly flat with steps at the interfacing with the balcony fronts at three levels on both sides. There are three number of wall recesses on both sides of the stall respectively.

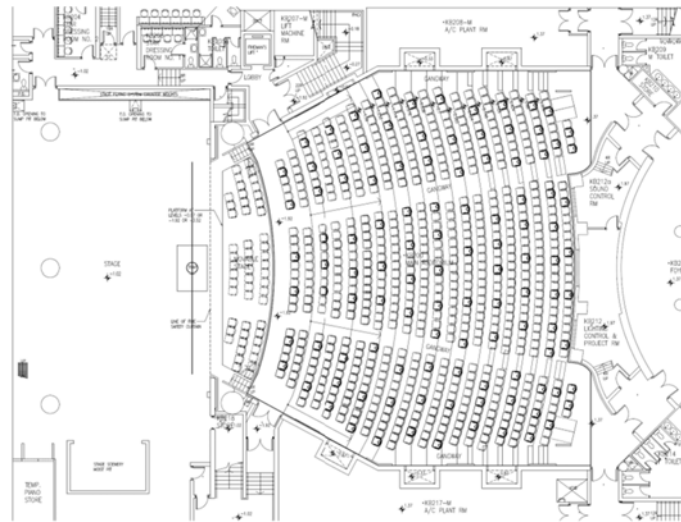
The stage is 10m deep from the setting line of proscenium, and 3.96m from setting line of proscenium to forestage edge on centreline. It has a width of 11m from centreline to stage left and 12m to the right. The proscenium opening can be adjusted from 14m wide and 6.5m tall to 10m wide and 5.5m tall. The stage floor is Maple wood. The actual stage house height is 13.8m tall.



Figure 4-5 Interior view of Hall C from the stage



(a) Sectional View of Hall C



(b) Layout view of Hall C

Figure 4-6(b) Sectional view and layout view of Hall C, from drawings from the hall owner

4.3.4 Hall D

Hall D is a small size recital hall in the music department of a local University. It is with a seating capacity of 269 (stall: 183, balcony 82). It is not symmetrical and rectangle in shape with a small balcony with only 4 rows. Its pipe organ is situated on the left of the stage. The side wall closer to the organ is fitted with specially designed metallic diffusers. There are acoustic panels on the back of the hall and the other sidewall of the hall. Fully

upholstered seats with armrests are fixed on wooden floors while the aisles and other part of the floor are carpeted. As shown in Figure 4-7, the balcony front is fenced by handrails which are acoustically transparent.



Figure 4-7 Interior of Hall D [89]

4.4 Measurement setup

To measure the binaural, monaural and the balcony edge, B&K Room acoustics software Dirac was used. Dirac is a piece of room acoustics software that measures and analyses impulse responses measured in a room. Internal MLS was used as the source signal and radiated out from the omni-directional sound source. The inputs and output of the system were connected to a laptop computer with an external sound card. Different type of receivers were used in binaural and mono-aural measurements.

4.4.1 Binaural measurement

Binaural measurements using Brüel & Kjær Type 4100 Head-and-Torso Simulator (HATS) were used to capture the sound fields inside the hall generated by a Brüel & Kjær Type 4296 omni-directional sound source located at 1 m inward from the edge of the stage on the stage centreline. The source was set at the height level of a standing human's mouth (1.6 m). The maximum length sequence procedure implemented by the DIRAC system [83] was used to obtain the binaural sound decay patterns. Each measurement lasted for 5.5 sec and it was found that a longer measurement duration of 10.9 sec did not result in significant differences in the data. The DIRAC software calculated the acoustical indices C80, D50, RT, EDT and IACC in octave bands. The formulae for these indices were presented in chapter 2 and can be found in BS EN ISO 3382[13] and some standard

textbooks such as Kutturff.[86] Thus, they are not presented here. During the measurements, the signal-to-noise ratios were all kept higher than 20 dB over the whole audio frequency range. The background noise level was around 30 dBA and the generated sound levels varied from 70 to 80 dBA during the measurements.

4.4.2 Mono-aural measurements around the balcony edge

In mono-aural measurements at each measurement locations and for points around the balcony edge, Brüel & Kjær sound level meter 2260, 2270 and 2250 were used as receivers. 2 channels were measured simultaneously to speed up the massive measurements. The microphone was mounted on a rotating microphone stand at 1.5m and 2m from the centre of rotation. To fit the shape of the balcony edge, points from -75 degrees to 135 degrees at 15 degrees each were measured. Figure 4-7 shows the measurement rack for the balcony edge.



Figure 4-8 Tailor-made measurement rack for the balcony edge of Hall A

4.5 Measurement points and survey results

The number of measurement points picked for binaural measurements differ in each hall due to the different size and shapes of the halls. The numbers of points measured are summarized in Table 4-2. Though the number of measurement locations is just about 10% of the total hall capacity, their distributions would be sufficient to reflect the acoustical properties of the halls. These points were repeated with monaural measurement in some of the halls where extra measurement timeslot were available. The points are classified into 3 zones, namely stall, upper stall and balcony. In Hall A, additional measurements around the balcony edge and at some high-level points were also carried out.

Table 4-2 Summary of number of binaural measurement points done in each hall

Hall	No. of Seats Stall/Balcony/Total	Points measured
A	1032/340/1372	182
B	730/189/919	84
C	702/323/1025	165
D	183/82/265	74

4.5.1 Hall A measurement points

Binaural measurements were carried out in Hall A with both the concert hall and proscenium setting. Additional measurements around the balcony edge and at the high level along the line from the source to the balcony edge were measured with the concert hall setting.

A total of 182 (stall: 73, upper stall: 56, balcony: 53) binaural measurements were carried out at the seats inside Hall A so as to have a full coverage of the hall. These points were measured in both concert and proscenium stage setting. The binaural measurement points are marked and shown in Figure 4-9. The location of balcony edge measurement rack and high level points are shown in Figure 4-10.

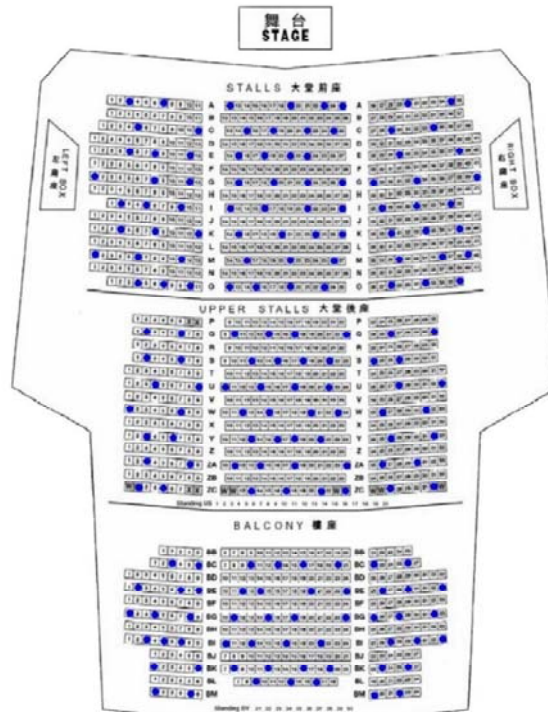


Figure 4-9 Binaural Measurement points (seats marked with blue dots) in Hall

There were 3 locations picked for balcony measurements, along the centreline of the hall, at 1/4 the full width of the hall, to the left and to the right. The high level points were set along the shortest distance from the omnidirectional sound source to the centre of the balcony rack on the balcony edge. The omnidirectional source was placed on the stage as shown in Figure 4-10. It was 1.5m tall, located along the centre line of the hall and 1m inward from the edge of the stage.

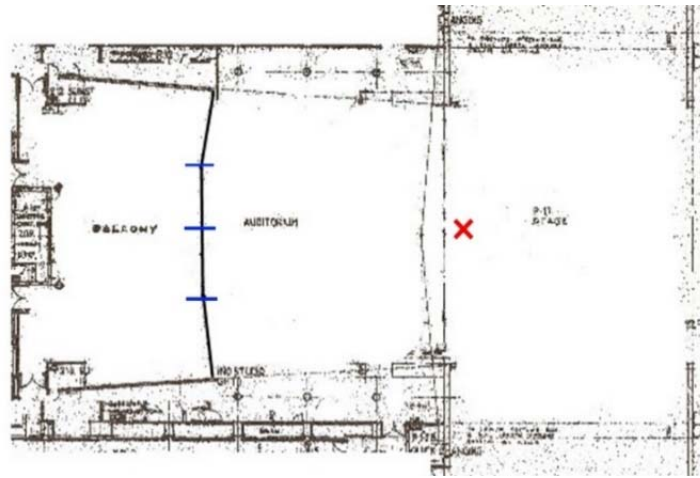


Figure 4-10 Locations of balcony measurement and high level points from the source to the balcony rack

4.5.2 Hall B measurement points

Hall B is a smaller hall with different shape and style. A total of 84 (stall : 48, upper stall : 18, balcony : 18) binaural measurements were carried out at the seats inside Hall B so as to have a full coverage of the hall. The binaural measurement points are marked and shown in Figure 4-11.

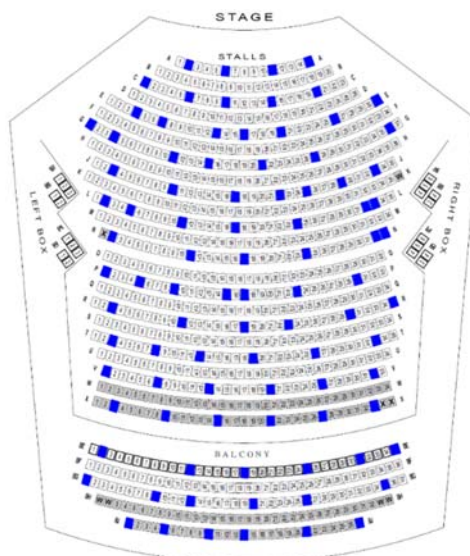


Figure 4-11 Measurement points (seats market with blue dots) in Hall B

Same as Hall A, the source in Hall B was also set at 1m inward from the edge of the stage along the centreline at 1.5m tall. However, in hall B the relative stage level is slightly higher than that in Hall A.

4.5.3 Hall C measurement points

Hall C has a size between Hall A and Hall B. A total number of around 158 points were measured (stall: 42, underbalcony: 60, balcony: 56). Figure 4-11 shows the measurement points marked on the layout plan.

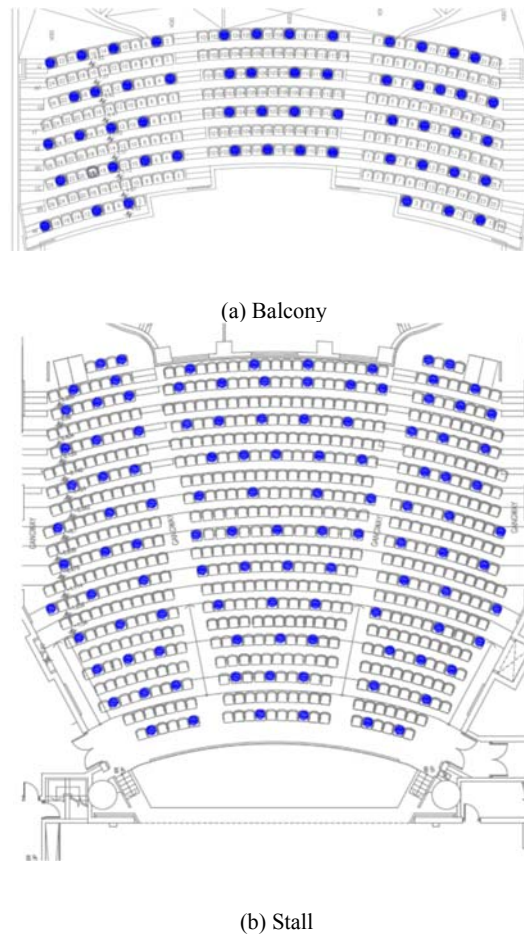


Figure 4-12 Measurement points (seats market with blue dots) in Hall C, (a) is balcony plan and (b) is stall area plan. Filled points are points measured.

4.6 Binaural Measurement Results

The head and torso simulator was used to pick up the impulse response in binaural measurements. The impulse responses were recorded and analysed using Room acoustics software Dirac version 4.0. In all the binaural data below, channel 1 refers to the left ear of the torso while channel 2 refers to the right ear.

4.6.1 Hall A Binaural Results

The impulse responses were measured and recorded using room acoustic software Dirac. The software calculated all the parameters in accordance to the ISO standard 3382 [13] for measuring room acoustics parameters in performance halls. The means and the standard deviations of the parameters measured in Hall A are summarized in the following tables.

4.6.1.1 Early decay time, EDT

Table 4-3 Mean and Stand deviation of averaged EDT (in sec) measured in Hall A with different settings. Numbers are averages of 2 channels, underlined and in italic are standard deviations while the other are means of each zone

	Hz Zone	125	250	500	1000	2000	4000	8000
Concert	Balcony	1.44	1.29	1.20	1.43	1.38	1.25	1.12
		<u>0.22</u>	<u>0.16</u>	<u>0.10</u>	<u>0.10</u>	<u>0.08</u>	<u>0.09</u>	<u>0.07</u>
	Stall	1.32	1.23	1.26	1.46	1.37	1.17	0.98
		<u>0.25</u>	<u>0.19</u>	<u>0.14</u>	<u>0.16</u>	<u>0.16</u>	<u>0.18</u>	<u>0.14</u>
	Mid Stall	1.55	1.43	1.34	1.60	1.51	1.36	1.12
		<u>0.20</u>	<u>0.13</u>	<u>0.11</u>	<u>0.08</u>	<u>0.08</u>	<u>0.08</u>	<u>0.07</u>
Under- balcony	1.53	1.28	1.29	1.51	1.48	1.33	1.15	
	<u>0.29</u>	<u>0.17</u>	<u>0.09</u>	<u>0.08</u>	<u>0.06</u>	<u>0.05</u>	<u>0.05</u>	
Proscenium	Balcony	1.16	1.02	0.96	1.08	1.02	0.93	0.88
		<u>0.27</u>	<u>0.14</u>	<u>0.07</u>	<u>0.05</u>	<u>0.11</u>	<u>0.10</u>	<u>0.07</u>
	Stall	1.17	1.12	1.09	1.19	1.08	1.02	0.86
		<u>0.29</u>	<u>0.22</u>	<u>0.12</u>	<u>0.16</u>	<u>0.20</u>	<u>0.20</u>	<u>0.19</u>
	Mid Stall	1.35	1.22	1.09	1.26	1.19	1.06	0.92
		<u>0.14</u>	<u>0.13</u>	<u>0.09</u>	<u>0.07</u>	<u>0.09</u>	<u>0.12</u>	<u>0.13</u>
Under- balcony	1.34	1.06	1.00	1.19	1.18	0.99	0.90	
	<u>0.33</u>	<u>0.15</u>	<u>0.08</u>	<u>0.07</u>	<u>0.07</u>	<u>0.09</u>	<u>0.08</u>	

Considering the standard deviations of the measured EDTs and T30s of each zones with different settings, the EDTs and T30s are quite uniform in the hall at each frequency band. From Table 4-3, it shows that the means of EDT in the concert setting in hall A are longer than that in the proscenium setting. The trends of means across the octaves in the two settings are with the pattern: longer at low frequencies (125Hz) and mid to high frequencies (500Hz and 1000Hz). Apart from lengthening the EDT throughout the hall in general, the concert setting enhances the early decay time more significantly at the mid-stall area, which are the seats before the balcony edge. This makes the change at the stall and the mid-stall area more obvious by having more early energy arriving at this area.

4.6.1.2 T30

Table 4-4 Mean and Stand deviation of averaged T30 (in sec) measured in Hall A with different settings. Numbers are averages of 2 channels, underlined and in italic are standard deviations while the other are means of each zone

	Hz Zone	125	250	500	1000	2000	4000	8000
Concert	Balcony	1.44	1.37	1.31	1.46	1.40	1.26	1.02
		<u>0.11</u>	<u>0.05</u>	<u>0.03</u>	<u>0.03</u>	<u>0.02</u>	<u>0.02</u>	<u>0.02</u>
	Stall	1.53	1.39	1.31	1.48	1.43	1.29	1.03
		<u>0.11</u>	<u>0.07</u>	<u>0.03</u>	<u>0.03</u>	<u>0.02</u>	<u>0.03</u>	<u>0.04</u>
	Mid Stall	1.52	1.40	1.32	1.47	1.44	1.30	1.05
		<u>0.09</u>	<u>0.06</u>	<u>0.02</u>	<u>0.02</u>	<u>0.01</u>	<u>0.01</u>	<u>0.02</u>
Under- balcony	1.53	1.39	1.32	1.48	1.44	1.30	1.03	
	<u>0.09</u>	<u>0.06</u>	<u>0.03</u>	<u>0.03</u>	<u>0.01</u>	<u>0.02</u>	<u>0.02</u>	
Proscenium	Balcony	1.52	1.43	1.14	1.21	1.17	1.08	0.92
		<u>0.16</u>	<u>0.08</u>	<u>0.03</u>	<u>0.02</u>	<u>0.02</u>	<u>0.02</u>	<u>0.02</u>
	Stall	1.46	1.47	1.13	1.21	1.20	1.10	0.93
		<u>0.27</u>	<u>0.09</u>	<u>0.04</u>	<u>0.03</u>	<u>0.04</u>	<u>0.04</u>	<u>0.02</u>
	Mid Stall	1.51	1.40	1.14	1.21	1.22	1.13	0.95
		<u>0.48</u>	<u>0.08</u>	<u>0.03</u>	<u>0.02</u>	<u>0.02</u>	<u>0.01</u>	<u>0.01</u>
Under- balcony	1.56	1.40	1.15	1.23	1.23	1.13	0.95	
	<u>0.52</u>	<u>0.10</u>	<u>0.03</u>	<u>0.02</u>	<u>0.02</u>	<u>0.02</u>	<u>0.01</u>	

Unlike EDT, there is not much difference in the measured T30 at low frequencies with different hall settings. As shown in Table 4-4, the T30 from 500 Hz to 2000Hz with the concert setting are longer than those with a proscenium setting by a min of 0.2 seconds. The T30 at 4000 Hz also has a difference of means of less than 0.2 seconds. The slightly longer EDT implies that the reverberant energy measured under the balcony is slightly stronger than those at all the other zones. The under balcony soffit helps compensate the total energy received at the seats under the balcony by giving slightly more late energy from reflections.

4.6.1.3 Clarity, C80 and Definition, D50

The values of C80 varies in both cases, zones and frequencies, especially in the proscenium setting. From Table 4-5, the values in the front stall area, i.e. the first few rows in the hall are much higher than the other parts of the hall. From 500Hz to 2000Hz, the values of the stall area are at least 2dB higher than those in the other areas in both settings. In the concert setting, the sound canopy on the stage has confined most of the energy within the stage area and projected to the audience. Most of the early and direct sound from the stage are reflected firstly to the first few rows and reflected from the slanted ceiling at the stage opening. This change in the architecture and reflecting surfaces increased the C80 significantly, that makes the hall favourable for music. However,

interestingly, the concert setting does not increase the C80s measured in the hall while the EDTs measured are longer

Table 4-5 Mean and Stand deviation of averaged C80 (in dB) measured in Hall A with different settings. Numbers are averages of 2 channels, underlined and in italic are standard deviations while the other are means of each zone

		Hz							
Zone		125	250	500	1000	2000	4000	8000	
Concert	balcony	0.54	1.08	0.42	0.36	-0.26	1.04	1.53	
		<u>1.63</u>	<u>1.38</u>	<u>0.87</u>	<u>0.62</u>	<u>0.66</u>	<u>0.90</u>	<u>1.03</u>	
	Stall	1.22	1.49	2.57	2.64	1.83	3.01	4.12	
		<u>1.96</u>	<u>2.32</u>	<u>2.07</u>	<u>2.11</u>	<u>2.51</u>	<u>2.36</u>	<u>2.03</u>	
	Mid Stall	-1.13	-0.24	0.16	0.34	0.01	1.53	2.32	
		<u>1.31</u>	<u>1.27</u>	<u>0.86</u>	<u>0.99</u>	<u>1.02</u>	<u>0.98</u>	<u>0.87</u>	
	Under-balcony	-0.87	0.02	0.14	0.25	-0.35	1.66	1.95	
		<u>1.81</u>	<u>1.72</u>	<u>0.97</u>	<u>0.66</u>	<u>1.09</u>	<u>1.64</u>	<u>1.21</u>	
Proscenium	Balcony	3.18	3.43	3.12	2.79	2.97	4.23	4.25	
		<u>2.08</u>	<u>1.57</u>	<u>0.78</u>	<u>0.41</u>	<u>0.77</u>	<u>1.02</u>	<u>0.78</u>	
	Stall	2.88	3.74	5.59	5.83	5.48	5.95	6.63	
		<u>2.55</u>	<u>2.63</u>	<u>2.07</u>	<u>1.80</u>	<u>2.34</u>	<u>2.34</u>	<u>1.70</u>	
	Mid Stall	-0.29	1.93	2.98	3.14	3.23	4.40	4.99	
		<u>1.18</u>	<u>1.23</u>	<u>0.83</u>	<u>1.00</u>	<u>1.19</u>	<u>1.19</u>	<u>1.12</u>	
	Under-balcony	0.34	2.85	2.90	3.11	3.16	5.36	4.75	
		<u>2.12</u>	<u>1.66</u>	<u>0.77</u>	<u>0.70</u>	<u>1.08</u>	<u>1.19</u>	<u>0.94</u>	

D50 is the ratio of the early energy to the total energy. Table 4-6 summarizes the means and standard deviations of D50 in each zone in Hall A with different settings. The D50 in a proscenium setting are generally higher than those in concert setting. Responding to the higher C80 in front stall area, the D50 in the front stall area are also much higher in all zones and setting, especially at 250Hz to 2000Hz. At low frequencies 125Hz, D50s on the balcony are almost as high as that in the stall area especially with the proscenium setting. Again, the concert setting does not increase the D50s measured in the hall with longer EDTs.

4.6.1.4 $G_{relative}$

From the standard deviation values in Table 4-7, the values of relative sound strength in dB ($G_{relative}$) in each frequency band in the stall area are more deviated than those in the other zones. As shown in Table 4-5 and Table 4-6, the C80 and D50 values show that the early energy is very strong in the front stall area. Therefore, while early energy is dominated in these seats in a wide hall, the sound pressure along the centreline and at the sides of the hall are very dependent on the distance from the point source used. The results

also show that more energy can be projected and reflected from the stage to all the audience in a concert hall setting. The sound canopy has minimized the difference of sound strength between the front stall and the balcony.

Table 4-6 Mean and Stand deviation of averaged D50 measured in Hall A with different settings. Numbers are averages of 2 channels, underlined and in italic are standard deviations while the other are means of each zone

Setting	Hz Zone	125	250	500	1000	2000	4000	8000
		Concert	Balcony	0.38	0.37	0.32	0.34	0.32
<u>0.11</u>	<u>0.10</u>			<u>0.05</u>	<u>0.04</u>	<u>0.05</u>	<u>0.07</u>	<u>0.07</u>
Stall	0.39		0.42	0.49	0.52	0.44	0.48	0.52
	<u>0.12</u>		<u>0.13</u>	<u>0.11</u>	<u>0.12</u>	<u>0.15</u>	<u>0.13</u>	<u>0.11</u>
Mid Stall	0.27		0.30	0.34	0.39	0.33	0.44	0.46
	<u>0.07</u>		<u>0.07</u>	<u>0.06</u>	<u>0.07</u>	<u>0.07</u>	<u>0.07</u>	<u>0.07</u>
Under-balcony	0.28		0.34	0.34	0.36	0.32	0.45	0.46
	<u>0.08</u>		<u>0.08</u>	<u>0.06</u>	<u>0.05</u>	<u>0.08</u>	<u>0.11</u>	<u>0.08</u>
Proscenium	Balcony	0.52	0.51	0.48	0.47	0.47	0.54	0.56
		<u>0.13</u>	<u>0.11</u>	<u>0.05</u>	<u>0.04</u>	<u>0.06</u>	<u>0.07</u>	<u>0.06</u>
	Stall	0.47	0.52	0.62	0.66	0.59	0.60	0.62
		<u>0.15</u>	<u>0.13</u>	<u>0.08</u>	<u>0.08</u>	<u>0.12</u>	<u>0.12</u>	<u>0.10</u>
	Mid Stall	0.33	0.42	0.49	0.53	0.51	0.58	0.60
		<u>0.08</u>	<u>0.10</u>	<u>0.07</u>	<u>0.06</u>	<u>0.08</u>	<u>0.07</u>	<u>0.05</u>
	Under-balcony	0.36	0.48	0.47	0.51	0.50	0.62	0.57
		<u>0.12</u>	<u>0.11</u>	<u>0.06</u>	<u>0.05</u>	<u>0.09</u>	<u>0.09</u>	<u>0.09</u>

Table 4-7 Mean and Stand deviation of averaged G-relative (in dB) measured in Hall A with different settings. Numbers are averages of 2 channels, underlined and in italic are standard deviations while the other are means of each zone

Setting	Hz Zone	125	250	500	1000	2000	4000	8000
		Concert	balcony	-248.99	-238.37	-239.32	-238.28	-232.65
<u>1.12</u>	<u>0.99</u>			<u>0.99</u>	<u>0.89</u>	<u>0.68</u>	<u>0.56</u>	<u>0.65</u>
Stall	-244.34		-234.06	-235.36	-234.67	-229.16	-223.75	-231.24
	<u>1.74</u>		<u>1.87</u>	<u>2.10</u>	<u>1.95</u>	<u>2.21</u>	<u>2.10</u>	<u>2.05</u>
Mid Stall	-246.63		-236.85	-238.14	-237.20	-231.46	-225.90	-234.02
	<u>0.55</u>		<u>0.42</u>	<u>0.59</u>	<u>0.69</u>	<u>0.77</u>	<u>0.78</u>	<u>0.60</u>
Under-balcony	-247.45		-237.51	-239.76	-238.76	-232.72	-227.03	-236.10
	<u>1.65</u>		<u>1.01</u>	<u>0.78</u>	<u>0.63</u>	<u>0.69</u>	<u>1.02</u>	<u>0.84</u>
Proscenium	Balcony	-248.57	-237.81	-238.57	-237.25	-232.03	-226.84	-236.15
		<u>1.08</u>	<u>1.00</u>	<u>0.88</u>	<u>0.80</u>	<u>0.62</u>	<u>0.70</u>	<u>0.51</u>
	Stall	-253.98	-244.37	-244.26	-243.04	-238.55	-233.68	-240.73
		<u>2.46</u>	<u>2.80</u>	<u>2.70</u>	<u>2.44</u>	<u>2.84</u>	<u>2.83</u>	<u>2.59</u>
	Mid Stall	-256.05	-246.72	-247.17	-245.44	-240.75	-235.44	-243.06
		<u>0.57</u>	<u>0.55</u>	<u>0.41</u>	<u>0.66</u>	<u>0.74</u>	<u>1.05</u>	<u>0.90</u>
	Under-balcony	-256.80	-247.17	-249.18	-247.43	-242.27	-236.15	-245.04
		<u>1.25</u>	<u>0.85</u>	<u>0.77</u>	<u>0.85</u>	<u>0.86</u>	<u>1.00</u>	<u>0.87</u>

4.6.2 Hall B Binaural Results

Hall B is a smaller hall in modern design with a fan shaped sitting area. The means and the standard deviations of the parameters measured in Hall B are summarized in the following tables.

4.6.2.1 EDT

Table 4-8 Mean and Stand deviation of averaged EDT (in sec) measured in Hall B with different settings. Numbers are averages of 2 channels, underlined and in italic are standard deviations while the other are means of each zone

Setting	Hz	125	250	500	1000	2000	4000	8000
	Zone							
Concert	Balcony	1.38	1.30	1.40	1.44	1.31	1.16	1.05
		<u>0.21</u>	<u>0.15</u>	<u>0.09</u>	<u>0.06</u>	<u>0.08</u>	<u>0.08</u>	<u>0.04</u>
	Stall	1.21	1.22	1.35	1.40	1.30	1.21	1.07
		<u>0.17</u>	<u>0.17</u>	<u>0.10</u>	<u>0.09</u>	<u>0.07</u>	<u>0.11</u>	<u>0.08</u>
	Mid Stall	1.27	1.29	1.42	1.43	1.28	1.17	1.01
		<u>0.17</u>	<u>0.14</u>	<u>0.06</u>	<u>0.08</u>	<u>0.05</u>	<u>0.06</u>	<u>0.04</u>
	Under-balcony	1.21	1.25	1.38	1.36	1.33	1.21	1.02
		<u>0.20</u>	<u>0.17</u>	<u>0.07</u>	<u>0.08</u>	<u>0.03</u>	<u>0.05</u>	<u>0.04</u>
Proscenium	Balcony	1.07	1.14	1.15	1.08	1.00	0.86	0.77
		<u>0.19</u>	<u>0.12</u>	<u>0.10</u>	<u>0.09</u>	<u>0.11</u>	<u>0.10</u>	<u>0.06</u>
	Stall	1.24	1.12	1.09	1.00	0.83	0.70	0.67
		<u>0.20</u>	<u>0.18</u>	<u>0.13</u>	<u>0.14</u>	<u>0.14</u>	<u>0.14</u>	<u>0.10</u>
	Mid Stall	1.44	1.13	1.18	0.99	0.89	0.75	0.67
		<u>0.24</u>	<u>0.10</u>	<u>0.09</u>	<u>0.07</u>	<u>0.11</u>	<u>0.10</u>	<u>0.06</u>
	Under-balcony	1.43	1.11	1.03	0.90	0.84	0.76	0.68
		<u>0.29</u>	<u>0.20</u>	<u>0.11</u>	<u>0.09</u>	<u>0.09</u>	<u>0.06</u>	<u>0.05</u>

Table 4-8 summarizes the EDTs measured in Hall B in both hall settings, the result was separated in different seating zones. The table shows that the EDTs in concert setting is longer than those in proscenium setting. With the sound canopy, the EDTs are higher in mid-frequencies. The sound canopy also helps project more early energy to the balcony area at low frequencies, i.e. the EDTs at low frequencies at the balcony are higher than those in proscenium setting.

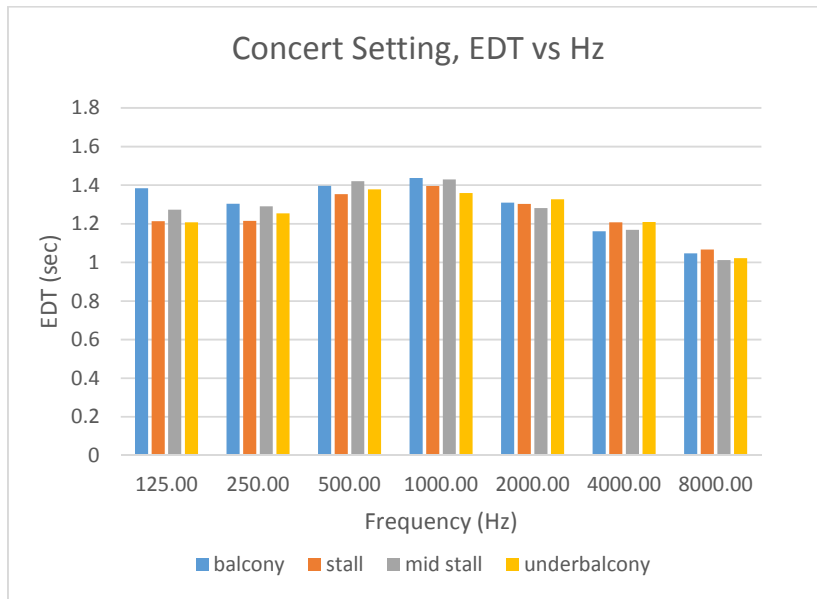


Figure 4-13 Spectrum of means of EDT in each seating zone of Hall B in concert setting

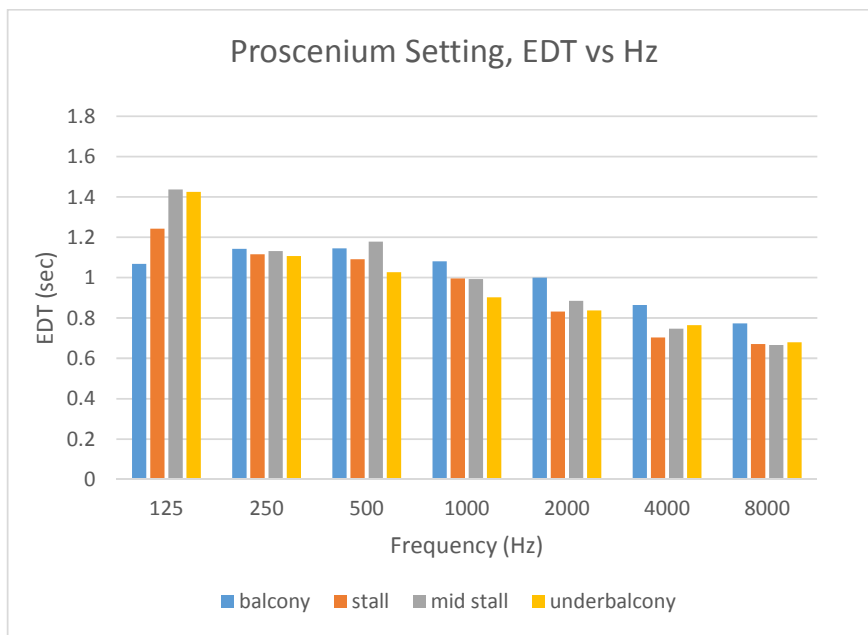


Figure 4-14 Spectrum of means of EDT in each seating zone of Hall B in proscenium setting

4.6.2.2 T30

Table 4-9 Mean and Stand deviation of averaged T30 (in sec) measured in Hall B with different settings. Numbers are averages of 2 channels, underlined and in italic are standard deviations while the other are means of each zone

Setting	Hz	125	250	500	1000	2000	4000	8000
	Zone							
Concert	Balcony	1.33	1.38	1.48	1.53	1.45	1.30	1.12
		<u>0.08</u>	<u>0.06</u>	<u>0.02</u>	<u>0.02</u>	<u>0.02</u>	<u>0.01</u>	<u>0.02</u>
	Stall	1.36	1.39	1.47	1.52	1.44	1.29	1.11
		<u>0.07</u>	<u>0.05</u>	<u>0.02</u>	<u>0.02</u>	<u>0.01</u>	<u>0.01</u>	<u>0.01</u>
	Mid Stall	1.39	1.37	1.46	1.52	1.45	1.32	1.13
		<u>0.09</u>	<u>0.04</u>	<u>0.03</u>	<u>0.01</u>	<u>0.01</u>	<u>0.01</u>	<u>0.01</u>
	Under-balcony	1.37	1.37	1.45	1.50	1.44	1.31	1.13
		<u>0.08</u>	<u>0.05</u>	<u>0.03</u>	<u>0.02</u>	<u>0.01</u>	<u>0.01</u>	<u>0.01</u>
Proscenium	Balcony	1.84	1.69	1.44	1.32	1.19	0.99	0.84
		<u>0.23</u>	<u>0.08</u>	<u>0.03</u>	<u>0.02</u>	<u>0.02</u>	<u>0.03</u>	<u>0.02</u>
	Stall	1.93	1.68	1.42	1.31	1.17	0.99	0.82
		<u>0.16</u>	<u>0.07</u>	<u>0.03</u>	<u>0.03</u>	<u>0.03</u>	<u>0.02</u>	<u>0.02</u>
	Mid Stall	1.89	1.65	1.42	1.32	1.19	1.01	0.82
		<u>0.20</u>	<u>0.07</u>	<u>0.04</u>	<u>0.03</u>	<u>0.02</u>	<u>0.02</u>	<u>0.01</u>
	Under-balcony	1.85	1.62	1.43	1.28	1.15	0.99	0.83
		<u>0.17</u>	<u>0.08</u>	<u>0.05</u>	<u>0.04</u>	<u>0.03</u>	<u>0.03</u>	<u>0.03</u>

Table 4-9 summarizes the mean and standard deviation of the T30 measured in Hall B. T30s here have different magnitudes are different between the two settings. However, with the sound canopy, the T30s changes in the same pattern across the spectrum, decreasing with the increasing frequency. The sound canopy has lengthened the decay time at middle to higher frequencies while shortened that at low frequencies. The T30 is the longest at low frequency and is the shortest at high frequencies in a proscenium setting. It attains a maximum in middle range in a concert hall setting. The variation among different zones in each frequency band is uniform.

4.6.2.3 C80 and D50

Table 4-10 summarizes the means and standard deviation of the measured C80 in Hall B with both stage settings. The C80s of concert setting are around 2dB less than those of the proscenium setting. All of them increase with frequencies in all seating zones. Without the sound canopy, the C80 in the front stall area is the largest from 500 Hz to 8000Hz. The values for mid-stall are relatively lower than all other zones in most frequencies in both settings.

Table 4-11 shows that the values of D50 are slightly high without the sound canopy. The increases in the stall area are very significant. It is the largest among all zones at 125Hz

in concert hall setting. The values in the stall area at all other frequencies are also increased by at least 0.1 and become the largest among all zones.

Table 4-10 Mean and Stand deviation of averaged C80 (in dB) measured in Hall B with different settings. Numbers are averages of 2 channels, underlined and in italic are standard deviations while the other are means of each zone

Setting	Hz	125	250	500	1000	2000	4000	8000
	Zone							
Concert	Balcony	-1.25	1.42	0.45	1.46	2.00	3.47	3.03
		<u>1.55</u>	<u>1.45</u>	<u>1.13</u>	<u>0.75</u>	<u>0.99</u>	<u>1.18</u>	<u>0.87</u>
	Stall	1.23	0.69	1.04	2.27	1.78	2.55	2.49
		<u>1.79</u>	<u>2.13</u>	<u>1.61</u>	<u>0.64</u>	<u>1.11</u>	<u>1.60</u>	<u>1.27</u>
	Mid Stall	-0.35	-0.50	0.14	2.24	1.90	2.54	3.02
		<u>1.36</u>	<u>1.65</u>	<u>0.69</u>	<u>0.79</u>	<u>0.87</u>	<u>0.95</u>	<u>1.07</u>
Under-balcony	0.11	0.50	1.31	3.13	2.21	3.53	3.39	
	<u>2.16</u>	<u>1.41</u>	<u>0.62</u>	<u>0.99</u>	<u>0.86</u>	<u>1.03</u>	<u>0.94</u>	
Proscenium	Balcony	3.05	2.89	2.94	3.78	4.18	5.03	5.35
		<u>1.70</u>	<u>1.74</u>	<u>0.96</u>	<u>0.59</u>	<u>1.11</u>	<u>1.16</u>	<u>0.78</u>
	Stall	2.80	3.27	4.44	5.39	6.54	7.63	7.25
		<u>1.62</u>	<u>1.66</u>	<u>1.45</u>	<u>1.21</u>	<u>1.42</u>	<u>1.85</u>	<u>1.37</u>
	Mid Stall	0.28	2.63	2.85	4.63	5.37	6.46	6.61
		<u>1.97</u>	<u>1.60</u>	<u>0.96</u>	<u>0.62</u>	<u>0.88</u>	<u>0.93</u>	<u>0.85</u>
Under-balcony	1.64	4.03	4.37	5.29	6.17	6.81	6.79	
	<u>1.45</u>	<u>2.06</u>	<u>0.82</u>	<u>1.02</u>	<u>1.01</u>	<u>1.05</u>	<u>0.91</u>	

Table 4-11 Mean and Stand deviation of averaged D50 measured in Hall B with different settings. Numbers are averages of 2 channels, underlined and in italic are standard deviations while the other are means of each zone

Setting	Hz	125	250	500	1000	2000	4000	8000
	Zone							
Concert	Balcony	0.30	0.43	0.37	0.44	0.45	0.55	0.50
		<u>0.08</u>	<u>0.08</u>	<u>0.06</u>	<u>0.05</u>	<u>0.06</u>	<u>0.08</u>	<u>0.06</u>
	Stall	0.42	0.36	0.40	0.51	0.46	0.52	0.48
		<u>0.10</u>	<u>0.14</u>	<u>0.10</u>	<u>0.04</u>	<u>0.08</u>	<u>0.10</u>	<u>0.09</u>
	Mid Stall	0.30	0.26	0.35	0.51	0.47	0.51	0.51
		<u>0.07</u>	<u>0.07</u>	<u>0.05</u>	<u>0.04</u>	<u>0.05</u>	<u>0.07</u>	<u>0.07</u>
Under-balcony	0.26	0.33	0.41	0.54	0.49	0.56	0.52	
	<u>0.09</u>	<u>0.07</u>	<u>0.03</u>	<u>0.06</u>	<u>0.06</u>	<u>0.07</u>	<u>0.07</u>	
Proscenium	Balcony	0.45	0.51	0.44	0.48	0.52	0.57	0.59
		<u>0.10</u>	<u>0.12</u>	<u>0.05</u>	<u>0.03</u>	<u>0.06</u>	<u>0.07</u>	<u>0.05</u>
	Stall	0.52	0.52	0.59	0.60	0.63	0.67	0.66
		<u>0.12</u>	<u>0.10</u>	<u>0.10</u>	<u>0.09</u>	<u>0.11</u>	<u>0.11</u>	<u>0.09</u>
	Mid Stall	0.35	0.46	0.46	0.52	0.58	0.62	0.63
		<u>0.11</u>	<u>0.10</u>	<u>0.05</u>	<u>0.05</u>	<u>0.07</u>	<u>0.07</u>	<u>0.06</u>
Under-balcony	0.43	0.55	0.54	0.53	0.60	0.66	0.65	
	<u>0.09</u>	<u>0.11</u>	<u>0.03</u>	<u>0.03</u>	<u>0.10</u>	<u>0.09</u>	<u>0.08</u>	

4.6.2.4 G_{relative}

Table 4-12 Mean and Stand deviation of averaged G -relative (in dB) measured in Hall B with different settings. Numbers are averages of 2 channels, underlined and in italic are standard deviations while the other are means of each zone

Setting	Hz	125	250	500	1000	2000	4000	8000
	Zone							
Concert	Balcony	-226.61	-215.54	-216.62	-215.37	-209.78	-203.82	-213.66
		<u>1.17</u>	<u>0.94</u>	<u>0.68</u>	<u>0.37</u>	<u>0.44</u>	<u>0.61</u>	<u>0.43</u>
	Stall	-226.43	-215.19	-215.66	-215.07	-209.73	-203.84	-212.75
		<u>4.68</u>	<u>4.51</u>	<u>4.17</u>	<u>4.39</u>	<u>4.44</u>	<u>4.34</u>	<u>4.37</u>
	Mid Stall	-226.16	-214.70	-215.22	-213.99	-208.54	-202.78	-211.87
		<u>0.84</u>	<u>0.72</u>	<u>0.43</u>	<u>0.38</u>	<u>0.41</u>	<u>0.59</u>	<u>0.69</u>
	Under-balcony	-225.94	-214.87	-216.65	-215.36	-210.61	-204.56	-214.41
		<u>1.63</u>	<u>1.41</u>	<u>0.85</u>	<u>0.71</u>	<u>0.69</u>	<u>0.73</u>	<u>0.86</u>
Proscenium	Balcony	-247.48	-238.46	-239.63	-238.68	-233.79	-229.29	-238.52
		<u>1.86</u>	<u>1.14</u>	<u>0.80</u>	<u>0.47</u>	<u>0.54</u>	<u>0.78</u>	<u>0.61</u>
	Stall	-246.10	-235.38	-235.62	-235.48	-229.83	-225.25	-233.73
		<u>1.29</u>	<u>1.27</u>	<u>1.30</u>	<u>1.02</u>	<u>1.38</u>	<u>1.70</u>	<u>1.40</u>
	Mid Stall	-248.99	-237.19	-238.07	-237.34	-232.20	-227.58	-236.34
		<u>0.64</u>	<u>0.64</u>	<u>0.47</u>	<u>0.53</u>	<u>0.94</u>	<u>1.13</u>	<u>1.20</u>
	Under-balcony	-248.08	-236.51	-238.80	-239.03	-233.85	-229.43	-238.73
		<u>1.94</u>	<u>1.84</u>	<u>0.63</u>	<u>0.83</u>	<u>1.00</u>	<u>1.05</u>	<u>0.89</u>

It can be observed from Table 4-12 that the averaged sound strength in each frequency band in Hall B in a proscenium setting ranges from approximating -245 to -210dB. This is significantly lower than that in a concert setting in each frequency band which ranges from -225 to -190dB. The sound strengths are rather uniform in the concert setting, however, at the balcony in the proscenium setting, the averaged sound strength is relatively smaller than those in the other zones.

4.6.3 Hall C Binaural Results

The means and the standard deviations of the parameters measured in Hall C are summarized in the following tables. Hall C is designed for a conference purpose, to convert it into a concert setting, a demountable standing sound canopy will be used.

4.6.3.1 EDT

The sound canopy in Hall C does not bring as much change to the hall as the fully enclosed sound canopy in Hall A and B. With the sound canopy in the concert setting, only a small increase of around 0.1 second can be found from Table 4-13. The result from the table also show that the canopy decreases the early time at 125Hz especially in the zones not under the balcony. When we look at the changes to the stall area, with the additional

canopy, the EDTs are increased in all frequencies. However, the effect to the other zones is very small.

Table 4-13 Mean and Stand deviation of averaged EDT (in sec) measured in Hall C with different settings. Numbers are averages of 2 channels, underlined and in italic are standard deviations while the other are means of each zone

Setting	Hz	125	250	500	1000	2000	4000	8000
	Zone							
Concert	Balcony	0.98	0.79	0.74	0.78	0.71	0.67	0.70
		<u>0.24</u>	<u>0.16</u>	<u>0.11</u>	<u>0.12</u>	<u>0.12</u>	<u>0.19</u>	<u>0.15</u>
	Stall	1.06	1.00	0.89	0.75	0.84	0.77	0.71
		<u>0.11</u>	<u>0.02</u>	<u>0.11</u>	<u>0.22</u>	<u>0.07</u>	<u>0.02</u>	<u>0.10</u>
	Mid Stall	1.07	1.01	0.92	0.85	0.77	0.71	0.76
		<u>0.15</u>	<u>0.19</u>	<u>0.11</u>	<u>0.08</u>	<u>0.08</u>	<u>0.07</u>	<u>0.06</u>
	Under-balcony	1.18	0.88	0.80	0.70	0.67	0.61	0.65
		<u>0.20</u>	<u>0.16</u>	<u>0.10</u>	<u>0.10</u>	<u>0.11</u>	<u>0.09</u>	<u>0.10</u>
Proscenium	Balcony	1.12	0.87	0.79	0.69	0.59	0.54	0.54
		<u>0.26</u>	<u>0.25</u>	<u>0.17</u>	<u>0.14</u>	<u>0.13</u>	<u>0.12</u>	<u>0.12</u>
	Stall	1.16	0.82	0.73	0.80	0.59	0.64	0.64
		<u>0.02</u>	<u>0.23</u>	<u>0.08</u>	<u>0.03</u>	<u>0.07</u>	<u>0.04</u>	<u>0.02</u>
	Mid Stall	1.20	1.01	0.95	0.79	0.76	0.67	0.67
		<u>0.24</u>	<u>0.12</u>	<u>0.12</u>	<u>0.15</u>	<u>0.10</u>	<u>0.08</u>	<u>0.09</u>
	Under-balcony	1.23	0.96	0.83	0.65	0.64	0.58	0.55
		<u>0.18</u>	<u>0.17</u>	<u>0.12</u>	<u>0.11</u>	<u>0.09</u>	<u>0.09</u>	<u>0.10</u>

Table 4-14 Mean and Stand deviation of averaged T30 (in sec) measured in Hall C with different settings. Numbers are averages of 2 channels, underlined and in italic are standard deviations while the other are means of each zone

Setting	Hz	125	250	500	1000	2000	4000	8000
	Zone							
Concert	Balcony	1.22	1.13	0.97	0.89	0.81	0.76	0.73
		<u>0.16</u>	<u>0.05</u>	<u>0.04</u>	<u>0.02</u>	<u>0.02</u>	<u>0.03</u>	<u>0.03</u>
	Stall	1.25	1.18	0.98	0.89	0.81	0.75	0.74
		<u>0.12</u>	<u>0.05</u>	<u>0.02</u>	<u>0.01</u>	<u>0.03</u>	<u>0.01</u>	<u>0.01</u>
	Mid Stall	1.30	1.13	0.95	0.87	0.82	0.76	0.74
		<u>0.09</u>	<u>0.03</u>	<u>0.04</u>	<u>0.02</u>	<u>0.02</u>	<u>0.02</u>	<u>0.01</u>
	Under-balcony	1.28	1.13	0.95	0.85	0.80	0.77	0.74
		<u>0.11</u>	<u>0.07</u>	<u>0.04</u>	<u>0.03</u>	<u>0.02</u>	<u>0.02</u>	<u>0.02</u>
Proscenium	Balcony	1.39	1.28	1.02	0.85	0.76	0.68	0.63
		<u>0.13</u>	<u>0.08</u>	<u>0.04</u>	<u>0.02</u>	<u>0.02</u>	<u>0.02</u>	<u>0.01</u>
	Stall	1.38	1.35	0.98	0.83	0.76	0.69	0.64
		<u>0.10</u>	<u>0.03</u>	<u>0.01</u>	<u>0.02</u>	<u>0.02</u>	<u>0.01</u>	<u>0.01</u>
	Mid Stall	1.30	1.23	1.01	0.86	0.77	0.69	0.63
		<u>0.09</u>	<u>0.07</u>	<u>0.04</u>	<u>0.01</u>	<u>0.01</u>	<u>0.01</u>	<u>0.01</u>
	Under-balcony	1.35	1.25	1.01	0.85	0.78	0.71	0.64
		<u>0.13</u>	<u>0.08</u>	<u>0.03</u>	<u>0.02</u>	<u>0.01</u>	<u>0.01</u>	<u>0.01</u>

4.6.3.2 T30

From the standard deviation in **Error! Reference source not found.**, the result shows that the T30s in the hall are uniform from 500Hz to 8000Hz. The largest deviation is 0.04 which is less than the just noticeable difference(JND) of 5% suggested in ISO 3382[13]. In low frequencies 125 and 250 Hz, the deviation is much larger. The contour plot of T30 at low frequencies are not very uniform and in accordance to the results in **Error! Reference source not found.** The sound canopy in the hall has also only lengthened the T30 in higher frequencies slightly without prolonging that at low frequencies. While increasing the middle to higher frequencies and lowering that in lower frequencies, the sound canopy has evened out the reverberation time and minimized the difference between different seating zones.

4.6.3.3 C80 and D50

Table 4-15 summarizes the mean and the standard deviation of the measured C80 in Hall C in both settings. The sound canopy changes the C80 at the balcony and the front stall area more than those at the mid-stall and under the balcony. In general, in a proscenium setting, the C80s are higher than those in a concert setting.

Table 4-16 summarizes the mean and the standard deviation of the measured D50 in Hall C in both settings. The D50s in proscenium setting are higher than those in concert setting. In a concert setting, the D50s at the front stall area are usually higher than those in the other zones. However, in a proscenium setting, the front stall area has smaller definitions than all other zones.

4.6.3.4 G_{relative}

Table 4-17 shows a simple statistical summary of the measured relative sound strength in Hall C. When comparing the results in each frequency band of the two settings, one can find that the sound strength with the sound canopy are higher than that without the sound canopy. In each frequency band, the means of the sound strength values at the balcony become smaller when the sound canopy is in place.

Table 4-15 Mean and Stand deviation of averaged C80 (in dB) measured in Hall C with different settings. Numbers are averages of 2 channels, underlined and in italic are standard deviations while the other are means of each zone

Setting	Hz Zone	125	250	500	1000	2000	4000	8000
Concert	Balcony	3.15	6.05	6.16	6.11	7.14	7.99	6.89
		<u>2.31</u>	<u>1.50</u>	<u>1.25</u>	<u>1.26</u>	<u>1.01</u>	<u>1.40</u>	<u>1.59</u>
	Stall	4.56	2.49	7.71	7.02	6.34	6.92	7.90
		<u>0.87</u>	<u>2.28</u>	<u>0.10</u>	<u>2.56</u>	<u>0.69</u>	<u>1.56</u>	<u>1.21</u>
	Mid Stall	2.75	4.34	4.97	5.22	5.65	6.62	5.41
		<u>2.22</u>	<u>1.62</u>	<u>0.84</u>	<u>1.01</u>	<u>1.33</u>	<u>1.05</u>	<u>1.49</u>
	Underbalcony	1.74	4.02	5.15	6.26	6.69	7.53	6.79
		<u>1.77</u>	<u>2.06</u>	<u>1.33</u>	<u>1.15</u>	<u>1.26</u>	<u>1.18</u>	<u>1.31</u>
Proscenium	Balcony	3.65	6.06	6.97	8.51	9.49	10.57	10.08
		<u>2.28</u>	<u>2.41</u>	<u>1.34</u>	<u>1.17</u>	<u>1.21</u>	<u>1.87</u>	<u>1.62</u>
	Stall	1.11	6.29	6.67	6.25	8.25	7.97	7.93
		<u>3.78</u>	<u>1.53</u>	<u>0.11</u>	<u>0.01</u>	<u>0.78</u>	<u>0.29</u>	<u>0.17</u>
	Mid Stall	2.62	4.54	5.64	8.16	7.35	8.13	8.65
		<u>2.08</u>	<u>1.20</u>	<u>0.83</u>	<u>1.19</u>	<u>1.41</u>	<u>1.52</u>	<u>1.35</u>
	Underbalcony	1.92	4.43	6.28	8.86	8.34	9.53	9.39
		<u>1.98</u>	<u>1.62</u>	<u>1.25</u>	<u>1.12</u>	<u>1.29</u>	<u>1.79</u>	<u>1.54</u>

Table 4-16 Mean and Stand deviation of averaged D50 measured in Hall C with different settings. Numbers are averages of 2 channels, underlined and in italic are standard deviations while the other are means of each zone

Setting	Hz Zone	125	250	500	1000	2000	4000	8000
Concert	Balcony	0.45	0.65	0.65	0.66	0.71	0.75	0.69
		<u>0.12</u>	<u>0.08</u>	<u>0.06</u>	<u>0.06</u>	<u>0.04</u>	<u>0.06</u>	<u>0.07</u>
	Stall	0.66	0.43	0.79	0.74	0.71	0.72	0.77
		<u>0.03</u>	<u>0.07</u>	<u>0.04</u>	<u>0.10</u>	<u>0.02</u>	<u>0.07</u>	<u>0.05</u>
	Mid Stall	0.49	0.61	0.60	0.62	0.62	0.68	0.64
		<u>0.12</u>	<u>0.08</u>	<u>0.06</u>	<u>0.05</u>	<u>0.05</u>	<u>0.06</u>	<u>0.04</u>
	Underbalcony	0.42	0.52	0.60	0.64	0.66	0.71	0.67
		<u>0.11</u>	<u>0.11</u>	<u>0.07</u>	<u>0.05</u>	<u>0.07</u>	<u>0.06</u>	<u>0.06</u>
Proscenium	Balcony	0.56	0.67	0.70	0.78	0.81	0.83	0.81
		<u>0.13</u>	<u>0.12</u>	<u>0.07</u>	<u>0.06</u>	<u>0.05</u>	<u>0.05</u>	<u>0.06</u>
	Stall	0.42	0.66	0.69	0.66	0.76	0.74	0.74
		<u>0.18</u>	<u>0.01</u>	<u>0.00</u>	<u>0.01</u>	<u>0.03</u>	<u>0.02</u>	<u>0.01</u>
	Mid Stall	0.52	0.65	0.68	0.78	0.72	0.76	0.78
		<u>0.15</u>	<u>0.07</u>	<u>0.03</u>	<u>0.05</u>	<u>0.08</u>	<u>0.08</u>	<u>0.06</u>
	Underbalcony	0.46	0.57	0.68	0.78	0.74	0.79	0.78
		<u>0.13</u>	<u>0.11</u>	<u>0.06</u>	<u>0.05</u>	<u>0.07</u>	<u>0.07</u>	<u>0.06</u>

Table 4-17 Mean and Stand deviation of averaged G-relative (in dB) measured in Hall C with different settings. Numbers are averages of 2 channels, underlined and in italic are standard deviations while the other are means of each zone

Setting	Hz Zone	125	250	500	1000	2000	4000	8000
Concert	Balcony	-251.15	-240.59	-241.66	-241.60	-235.44	-229.27	-238.81
		<u><i>2.61</i></u>	<u><i>2.14</i></u>	<u><i>1.56</i></u>	<u><i>1.66</i></u>	<u><i>1.51</i></u>	<u><i>1.44</i></u>	<u><i>2.05</i></u>
	Stall	-240.12	-233.58	-231.94	-232.05	-228.39	-223.46	-229.91
		<u><i>0.74</i></u>	<u><i>0.74</i></u>	<u><i>0.01</i></u>	<u><i>1.41</i></u>	<u><i>0.15</i></u>	<u><i>1.03</i></u>	<u><i>0.45</i></u>
	Mid Stall	-246.32	-235.50	-236.96	-236.27	-231.26	-226.17	-219.40
		<u><i>0.97</i></u>	<u><i>0.56</i></u>	<u><i>0.63</i></u>	<u><i>1.02</i></u>	<u><i>0.96</i></u>	<u><i>0.75</i></u>	<u><i>48.94</i></u>
	Under- balcony	-248.34	-237.16	-238.13	-237.00	-232.51	-227.65	-236.41
		<u><i>1.45</i></u>	<u><i>0.96</i></u>	<u><i>0.75</i></u>	<u><i>0.91</i></u>	<u><i>1.04</i></u>	<u><i>1.22</i></u>	<u><i>1.00</i></u>
Proscenium	Balcony	-252.24	-241.77	-242.77	-241.72	-236.15	-230.18	-239.62
		<u><i>2.43</i></u>	<u><i>2.25</i></u>	<u><i>1.52</i></u>	<u><i>1.77</i></u>	<u><i>1.41</i></u>	<u><i>1.84</i></u>	<u><i>1.56</i></u>
	Stall	-255.43	-244.25	-243.80	-243.37	-238.24	-232.73	-242.58
		<u><i>0.92</i></u>	<u><i>0.42</i></u>	<u><i>0.28</i></u>	<u><i>0.25</i></u>	<u><i>0.03</i></u>	<u><i>0.23</i></u>	<u><i>0.30</i></u>
	Mid Stall	-255.79	-245.60	-247.91	-246.20	-241.83	-236.58	-244.54
		<u><i>1.11</i></u>	<u><i>0.59</i></u>	<u><i>0.44</i></u>	<u><i>1.05</i></u>	<u><i>0.88</i></u>	<u><i>1.16</i></u>	<u><i>1.10</i></u>
	Under- balcony	-258.24	-247.97	-249.47	-247.38	-243.34	-237.69	-246.57
		<u><i>1.60</i></u>	<u><i>1.02</i></u>	<u><i>0.80</i></u>	<u><i>0.89</i></u>	<u><i>1.04</i></u>	<u><i>1.44</i></u>	<u><i>1.38</i></u>

4.6.4 Hall D Binaural Results

Hall D is a small concert/ recital hall, there is only one row of seats that are under the balcony. The small balcony appears like a canopy above the seats rather than a real balcony. Still, the data are zoned into four zones as in other halls. The means and the standard deviations of the parameters are summarized in the following tables.

4.6.4.1 EDT

Table 4-18 presents the simple statistics of the measured EDT in Hall C. The early decay times in the mid stall and those under the balcony are very similar, as the hall is small, the last row of the stall area is slightly covered by the shallow balcony above, this row of seats are exposed to similar reflections as the few rows of seats in front of them i.e. the mid-stall. The EDTs on the balcony are the longest at all frequencies. The EDTs are longer in low frequencies than in mid to high frequencies.

Table 4-18 Mean and Stand deviation of averaged EDT (in seconds) measured in Hall D. Numbers are averages of 2 channels, underlined and in italic are standard deviations while the other are means of each zone

Setting	Hz Zone	125	250	500	1000	2000	4000	8000
		Concert	Stall	1.46	1.19	1.18	1.25	1.23
<u>0.23</u>	<u>0.11</u>			<u>0.08</u>	<u>0.06</u>	<u>0.06</u>	<u>0.08</u>	<u>0.05</u>
Mid Stall	1.42		1.29	1.20	1.23	1.16	1.04	0.86
	<u>0.21</u>		<u>0.15</u>	<u>0.08</u>	<u>0.08</u>	<u>0.11</u>	<u>0.09</u>	<u>0.07</u>
Under- balcony	1.43		1.24	1.10	1.10	1.19	1.10	0.92
	<u>0.17</u>		<u>0.13</u>	<u>0.08</u>	<u>0.08</u>	<u>0.05</u>	<u>0.05</u>	<u>0.03</u>
Balcony	1.50	1.19	1.13	1.13	1.18	1.10	0.91	
	<u>0.32</u>	<u>0.17</u>	<u>0.07</u>	<u>0.10</u>	<u>0.05</u>	<u>0.05</u>	<u>0.05</u>	

4.6.4.2 T30

Table 4-19 Mean and Stand deviation of averaged T30 (in seconds) measured in Hall D. Numbers are averages of 2 channels, underlined and in italic are standard deviations while the other are means of each zone

Setting	Hz Zone	125	250	500	1000	2000	4000	8000
		Concert	Stall	1.24	0.92	0.91	0.96	0.94
<u>0.21</u>	<u>0.10</u>			<u>0.06</u>	<u>0.06</u>	<u>0.04</u>	<u>0.04</u>	<u>0.05</u>
Mid Stall	1.11		1.02	0.92	0.94	0.94	0.89	0.73
	<u>0.14</u>		<u>0.18</u>	<u>0.07</u>	<u>0.05</u>	<u>0.03</u>	<u>0.05</u>	<u>0.06</u>
Under- balcony	1.07		1.03	0.92	0.93	0.93	0.89	0.71
	<u>0.12</u>		<u>0.14</u>	<u>0.03</u>	<u>0.04</u>	<u>0.03</u>	<u>0.03</u>	<u>0.02</u>
Balcony	1.07	0.98	0.92	0.93	0.93	0.90	0.73	
	<u>0.15</u>	<u>0.09</u>	<u>0.03</u>	<u>0.03</u>	<u>0.03</u>	<u>0.03</u>	<u>0.05</u>	

Table 4-19 presents the simple statistics of the measured Reverberation time, T30, in Hall C. The T30s in this hall in each sub-divided zone are having a similar pattern as the early decay time. At the mid- frequencies, the spectrum from 500 to 4000 Hz is nearly flat. With a very small standard deviation in each zone of data as shown in Table 4-19, we can say the reverberation time across this range is almost the same. At 125 Hz, the reverberation time T30 is the longest among all.

4.6.4.3 C80

Table 4-20 Mean and Stand deviation of averaged C80 (in dB) measured in Hall D. Numbers are averages of 2 channels, underlined and in italic are standard deviations while the other are means of each zone

Setting	Hz	125	250	500	1000	2000	4000	8000
	Zone							
Concert	Stall	-0.10	0.41	1.08	0.95	1.09	2.38	2.19
		<u>1.47</u>	<u>0.97</u>	<u>0.85</u>	<u>0.74</u>	<u>0.85</u>	<u>1.49</u>	<u>0.94</u>
	Mid Stall	0.75	1.40	2.95	3.19	3.58	4.01	4.71
		<u>1.46</u>	<u>1.43</u>	<u>1.07</u>	<u>0.93</u>	<u>1.44</u>	<u>1.21</u>	<u>0.87</u>
	Under-balcony	1.13	1.68	2.56	2.81	1.94	2.28	3.32
		<u>0.88</u>	<u>0.64</u>	<u>0.49</u>	<u>0.41</u>	<u>0.91</u>	<u>0.89</u>	<u>0.69</u>
	Balcony	1.51	1.89	2.40	2.41	1.91	2.43	3.21
		<u>0.78</u>	<u>0.92</u>	<u>0.27</u>	<u>0.30</u>	<u>0.72</u>	<u>0.91</u>	<u>0.99</u>

Table 4-20 presents the simple statistics of the measured Clarity, C80, in Hall C. The clarity, C80s on the balcony are relatively small compared to those on the stall floor. This may be caused by the glass balustrade on the balcony edge. To fulfil a safety requirement, the balustrade is too tall relative to the hall geometry and may have blocked the direct sound from propagating directly from the stage to the seats on the balcony. The seats at the later part of the stall, the mid-stall and under the balcony, have a slightly lower clarity than the front stall at 500Hz and 1000Hz. However, the C80s at this area are at least 1dB less than those in the front stall at higher frequencies.

4.6.4.4 D50

Table 4-21 presents the simple statistics of the measured Definition, D50. The D50 has a similar pattern across the spectrum like C80. These two parameters, together, state that the energy to the front stall area is much stronger than other parts of the hall. This is very good as a recital or practice hall.

Table 4-21 Mean and Stand deviation of averaged D50 measured in Hall D. Numbers are averages of 2 channels, underlined and in italic are standard deviations while the other are means of each zone

Setting	Hz Zone	125	250	500	1000	2000	4000	8000
Concert	Stall	0.34	0.34	0.39	0.41	0.41	0.49	0.45
		<u>0.09</u>	<u>0.06</u>	<u>0.05</u>	<u>0.05</u>	<u>0.06</u>	<u>0.10</u>	<u>0.06</u>
	Mid Stall	0.39	0.45	0.54	0.56	0.58	0.60	0.61
		<u>0.09</u>	<u>0.10</u>	<u>0.09</u>	<u>0.07</u>	<u>0.09</u>	<u>0.07</u>	<u>0.07</u>
	Under- balcony	0.38	0.43	0.49	0.52	0.46	0.48	0.52
		<u>0.11</u>	<u>0.05</u>	<u>0.06</u>	<u>0.03</u>	<u>0.08</u>	<u>0.07</u>	<u>0.07</u>
Balcony	0.45	0.44	0.50	0.49	0.46	0.49	0.50	
	<u>0.06</u>	<u>0.06</u>	<u>0.04</u>	<u>0.04</u>	<u>0.04</u>	<u>0.07</u>	<u>0.07</u>	

4.6.4.5 G_{relative}

Table 4-22 Mean and Stand deviation of averaged Sound Strength, G_{rel} (in dB) measured in Hall D. Numbers are averages of 2 channels, underlined and in italic are standard deviations while the other are means of each zone

Setting	Hz Zone	125	250	500	1000	2000	4000	8000
Concert	Stall	-240.95	-232.63	-234.57	-234.95	-228.94	-223.06	-231.81
		<u>1.18</u>	<u>0.97</u>	<u>0.98</u>	<u>0.65</u>	<u>0.76</u>	<u>1.11</u>	<u>0.92</u>
	Mid Stall	-239.20	-230.59	-232.04	-231.98	-225.93	-220.72	-228.07
		<u>1.17</u>	<u>1.61</u>	<u>1.47</u>	<u>1.27</u>	<u>1.63</u>	<u>1.44</u>	<u>1.19</u>
	Under- balcony	-241.00	-231.42	-233.44	-233.38	-228.03	-222.68	-230.13
		<u>0.67</u>	<u>0.96</u>	<u>0.93</u>	<u>0.65</u>	<u>0.91</u>	<u>0.87</u>	<u>0.68</u>
Balcony	-240.80	-232.24	-234.34	-234.25	-228.54	-223.11	-230.75	
	<u>0.80</u>	<u>0.76</u>	<u>0.54</u>	<u>0.54</u>	<u>0.65</u>	<u>0.61</u>	<u>0.51</u>	

Table 4-22 presents the simple statistics of the measured relative sound strength, G_{rel} . The energy at the front stall area is the strongest in the hall. The values of G_{rel} in the other parts of the hall are very similar at all frequencies. The perceived sound at each seat around the hall will be very uniform.

4.7 Balcony Edge Mono Measurement

4.7.1 Balcony edge points, high level points in Hall A

A total number of 90 points were measured around the balcony edge. They fell along the circumferences of 1.5m and 2m from the edge of the balcony. Figure 4-7 and Figure 4-9 shows the measurement rack around the balcony and the measurement locations respectively.

4.7.2 Results

In Hall A, additional measurement was done around the balcony edge to try to look at how the sound propagates around the balcony and the possibility to trace the effects of the balcony to the seats in details. Three locations naming point 1 to point 3 were picked to perform a radial measurement around the balcony edge. Table 4-23 and

Table 4-24 summarized the means with standard deviation of different hall parameters measured at the balcony edge in Hall A.

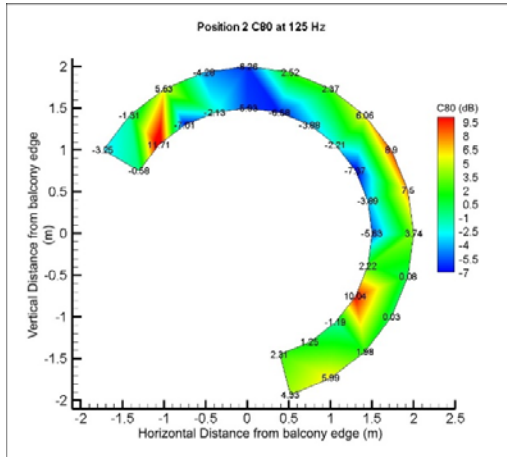
The values of the measured parameters at each point are interpolated and plotted into contours at each frequency in Figure 4-15 (a-h). The horizontal and vertical axes represent the horizontal and vertical distances of the measurement points from the top of the balcony edge respectively. The contour pattern can be divided to 2 parts, from -75 degrees to around -15 degree, from -15 degree to around 195 degree. The measured values in these 3 zones are quite different. The first zone is very close to the front face of the balcony that would receive much more reflections than Zone 2 behind the balcony. Zone 2 is the zone where the sound wave ‘bend’ across the balcony. The distribution there is very uniform. The last part is within the seating around the seats on the balcony, some points may give similar results as those measured at balcony seats.

Table 4-23 Mean and Standard deviation of EDT and T30 (in sec) measured in Hall A at the balcony edge. Numbers are averages of all angles while underlined and in italic are standard deviations

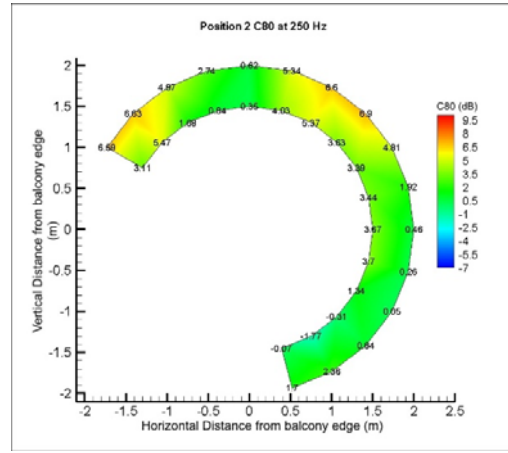
Parameter	Point	Radius	Frequency (Hz)						
			125	250	500	1000	2000	4000	8000
EDT	2	1.5	1.53	1.53	1.46	1.58	1.67	1.59	1.31
			<u>0.18</u>	<u>0.13</u>	<u>0.12</u>	<u>0.06</u>	<u>0.04</u>	<u>0.05</u>	<u>0.03</u>
		2	1.59	1.54	1.44	1.59	1.65	1.59	1.31
			<u>0.18</u>	<u>0.11</u>	<u>0.14</u>	<u>0.08</u>	<u>0.06</u>	<u>0.06</u>	<u>0.03</u>
	3	1.5	1.51	1.60	1.39	1.59	1.72	1.62	1.32
			<u>0.19</u>	<u>0.15</u>	<u>0.09</u>	<u>0.06</u>	<u>0.07</u>	<u>0.05</u>	<u>0.04</u>
		2	1.54	1.55	1.39	1.57	1.68	1.61	1.34
			<u>0.23</u>	<u>0.11</u>	<u>0.11</u>	<u>0.06</u>	<u>0.06</u>	<u>0.06</u>	<u>0.04</u>
	4	1.5	1.60	1.49	1.49	1.57	1.64	1.57	1.29
			<u>0.21</u>	<u>0.10</u>	<u>0.09</u>	<u>0.06</u>	<u>0.06</u>	<u>0.07</u>	<u>0.05</u>
		2	1.69	1.53	1.46	1.61	1.66	1.58	1.28
			<u>0.15</u>	<u>0.20</u>	<u>0.12</u>	<u>0.06</u>	<u>0.07</u>	<u>0.06</u>	<u>0.05</u>
T30	2	1.5	1.65	1.42	1.37	1.55	1.55	1.46	1.15
			<u>0.11</u>	<u>0.12</u>	<u>0.08</u>	<u>0.14</u>	<u>0.05</u>	<u>0.06</u>	<u>0.01</u>
		2	1.67	1.47	1.37	1.50	1.55	1.47	1.14
			<u>0.11</u>	<u>0.05</u>	<u>0.03</u>	<u>0.03</u>	<u>0.03</u>	<u>0.02</u>	<u>0.02</u>
	3	1.5	1.64	1.50	1.36	1.51	1.54	1.48	1.15
			<u>0.10</u>	<u>0.04</u>	<u>0.03</u>	<u>0.02</u>	<u>0.02</u>	<u>0.02</u>	<u>0.05</u>
		2	1.74	1.51	1.37	1.51	1.54	1.47	1.10
			<u>0.10</u>	<u>0.05</u>	<u>0.05</u>	<u>0.03</u>	<u>0.04</u>	<u>0.10</u>	<u>0.10</u>
	4	1.5	1.66	1.49	1.34	1.51	1.56	1.46	1.16
			<u>0.10</u>	<u>0.09</u>	<u>0.04</u>	<u>0.04</u>	<u>0.03</u>	<u>0.06</u>	<u>0.05</u>
		2	1.67	1.49	1.36	1.49	1.53	1.45	1.14
			<u>0.10</u>	<u>0.04</u>	<u>0.02</u>	<u>0.03</u>	<u>0.02</u>	<u>0.07</u>	<u>0.05</u>

Table 4-24 Mean and Stand deviation of C80 (in dB), D50 and G_{rel} (in dB) measured in Hall A at the balcony edge. Numbers are averages of all angles while underlined and in italic are standard deviations

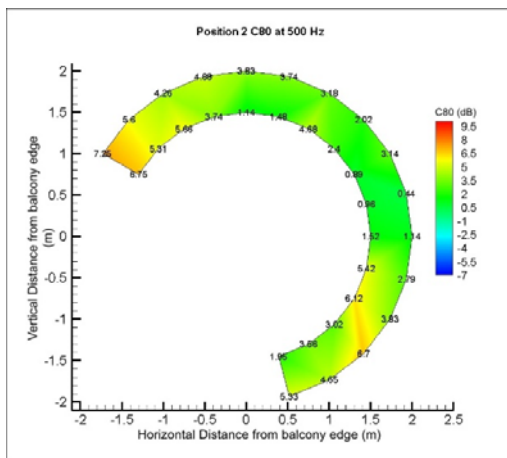
Parameter	point	radius	Frequency (Hz)						
			125	250	500	1000	2000	4000	8000
C80	2	1.5	-0.08	-0.58	0.22	-1.65	-2.09	-1.21	-0.52
			<u>1.37</u>	<u>1.20</u>	<u>0.93</u>	<u>0.67</u>	<u>0.52</u>	<u>0.43</u>	<u>0.43</u>
		2	-0.26	-0.02	0.21	-1.68	-2.20	-1.18	-0.45
			<u>1.59</u>	<u>1.16</u>	<u>0.66</u>	<u>0.62</u>	<u>0.65</u>	<u>0.49</u>	<u>0.62</u>
	3	1.5	-1.42	-0.88	1.01	-1.73	-1.95	-2.59	-0.07
			<u>1.68</u>	<u>1.04</u>	<u>0.49</u>	<u>0.93</u>	<u>0.81</u>	<u>1.06</u>	<u>1.36</u>
		2	-1.67	-0.23	0.65	-1.80	-1.90	-2.32	-0.49
			<u>1.04</u>	<u>1.31</u>	<u>0.80</u>	<u>0.66</u>	<u>0.98</u>	<u>1.04</u>	<u>1.70</u>
	4	1.5	0.01	0.07	-0.16	-1.66	-1.01	-1.15	0.51
			<u>0.99</u>	<u>0.90</u>	<u>0.95</u>	<u>0.51</u>	<u>1.42</u>	<u>1.24</u>	<u>0.97</u>
		2	-0.43	0.49	0.08	-1.59	-1.21	-1.01	0.42
			<u>0.87</u>	<u>1.01</u>	<u>0.62</u>	<u>0.72</u>	<u>1.36</u>	<u>1.21</u>	<u>1.26</u>
D50	2	1.5	0.32	0.35	0.37	0.26	0.26	0.31	0.32
			<u>0.07</u>	<u>0.08</u>	<u>0.05</u>	<u>0.04</u>	<u>0.03</u>	<u>0.02</u>	<u>0.04</u>
		2	0.35	0.39	0.38	0.26	0.25	0.30	0.32
			<u>0.06</u>	<u>0.05</u>	<u>0.04</u>	<u>0.03</u>	<u>0.03</u>	<u>0.04</u>	<u>0.05</u>
	3	1.5	0.21	0.34	0.38	0.27	0.28	0.24	0.38
			<u>0.05</u>	<u>0.08</u>	<u>0.07</u>	<u>0.05</u>	<u>0.04</u>	<u>0.05</u>	<u>0.07</u>
		2	0.26	0.36	0.38	0.26	0.28	0.25	0.36
			<u>0.06</u>	<u>0.07</u>	<u>0.05</u>	<u>0.03</u>	<u>0.05</u>	<u>0.05</u>	<u>0.07</u>
	4	1.5	0.33	0.34	0.37	0.25	0.31	0.29	0.38
			<u>0.09</u>	<u>0.07</u>	<u>0.05</u>	<u>0.03</u>	<u>0.09</u>	<u>0.06</u>	<u>0.04</u>
		2	0.34	0.38	0.38	0.25	0.29	0.31	0.38
			<u>0.06</u>	<u>0.04</u>	<u>0.03</u>	<u>0.04</u>	<u>0.08</u>	<u>0.06</u>	<u>0.06</u>
G _{rel}	2	1.5	-237.38	-228.48	-230.02	-229.93	-227.89	-228.89	-236.00
			<u>1.36</u>	<u>1.46</u>	<u>1.39</u>	<u>1.20</u>	<u>1.25</u>	<u>1.34</u>	<u>1.31</u>
		2	-236.89	-227.54	-229.39	-229.76	-227.92	-228.72	-235.25
			<u>0.94</u>	<u>0.65</u>	<u>0.47</u>	<u>0.57</u>	<u>0.50</u>	<u>0.50</u>	<u>0.46</u>
	3	1.5	-236.50	-228.68	-229.33	-229.89	-227.95	-229.52	-235.70
			<u>0.57</u>	<u>0.64</u>	<u>0.59</u>	<u>0.60</u>	<u>0.37</u>	<u>0.85</u>	<u>1.57</u>
		2	-236.67	-227.89	-229.08	-229.83	-228.26	-229.67	-235.48
			<u>0.82</u>	<u>0.53</u>	<u>0.60</u>	<u>0.59</u>	<u>0.42</u>	<u>1.15</u>	<u>1.46</u>
	4	1.5	-237.36	-228.32	-229.85	-229.88	-227.44	-228.75	-235.23
			<u>0.77</u>	<u>0.62</u>	<u>0.52</u>	<u>0.48</u>	<u>1.17</u>	<u>1.28</u>	<u>1.09</u>
		2	-237.08	-227.71	-229.51	-230.00	-227.91	-228.98	-234.99
			<u>1.03</u>	<u>0.65</u>	<u>0.58</u>	<u>0.55</u>	<u>1.28</u>	<u>1.20</u>	<u>1.30</u>



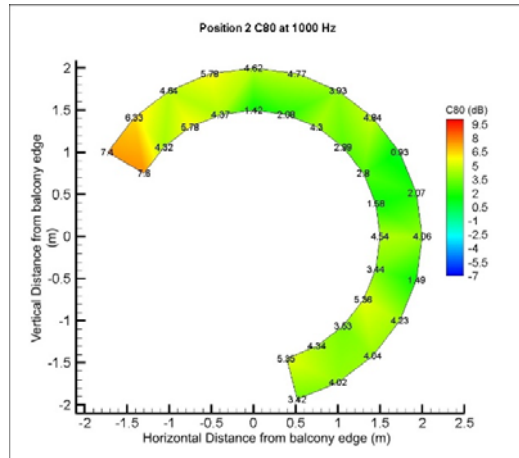
(a) 125Hz



(b) 250Hz

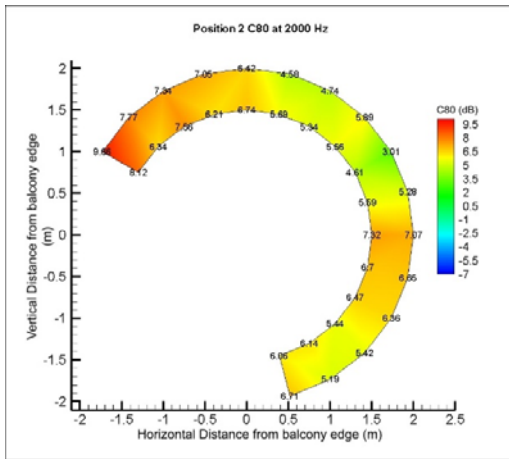


(c) 500Hz

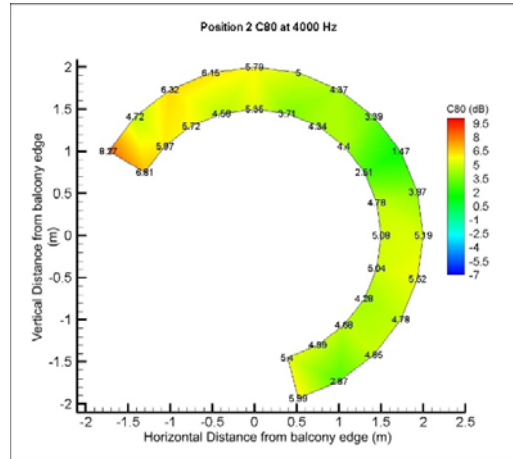


(d) 1000Hz

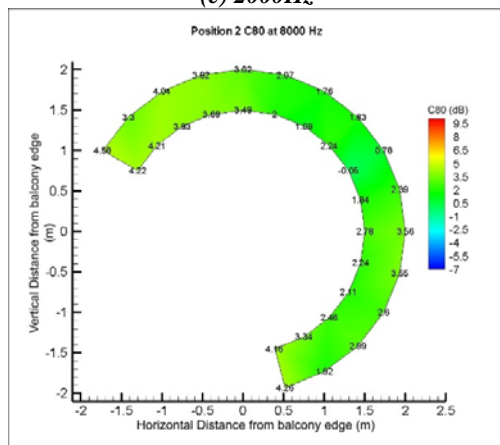
Figure 4-15 (a-d) Contour plots of measured C80 around the balcony edge at point 2 in Hall A



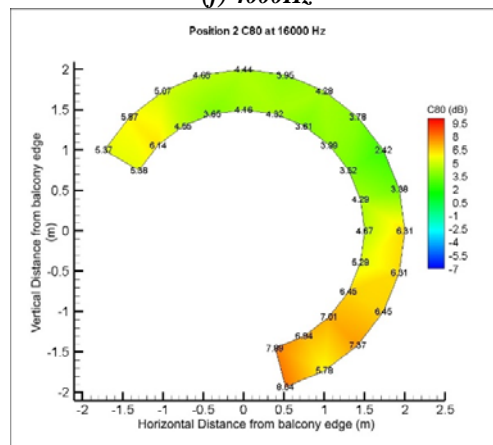
(e) 2000Hz



(f) 4000Hz



(g) 8000Hz



(h) 16000Hz

Figure 4-15(e-h) Contour plots of measured C80 around the balcony edge at point 2 in Hall A

4.8 Analysis and discussion

The stage setting would affect the sound propagation thus the acoustic properties of different seats in the hall. The design of the halls would also affect the measured results. Hall A is the only hall with a shoe box design in this study while hall B and Hall C are more similar to a fan-shaped modern design. For simplicity in comparing the difference between the two kinds of design, Hall B was used as the example here.

These two halls are well designed that the measured range of T30 and EDT are similar in both halls. However, their forms of variation across the frequency are not the same. Those measured in Hall A, despite the stage setting, decrease from low frequency to 500Hz, then increase suddenly at 1000Hz and then decrease gently toward high frequency end. Those measured in Hall B have different patterns with different stage settings. With the proscenium setting, T30 decreases with a constant slope from low frequencies to high frequencies. Those measured with the sound canopy on the stage increase to maximum at 1000Hz and then decrease. The sound canopy may help reflecting energy at mid frequencies such that the measured values at these frequencies are higher and the variation of the averages appears to be a convex curve instead of a straight line across the frequencies.

The measured EDTs show similar trend in the measured results. The interquartile ranges of the EDT measured with the sound canopy on the stage in Hall A are much larger than those without the sound canopy. This suggests that the sound canopy should have reflected more early energy to part of the audience only. Those seats that are not covered by the sound canopy will have a similar amount of early energy as with a proscenium stage setting. The sharp decrease of EDT across frequencies is also observed in Hall B under proscenium setting.

The range of values of T30 and EDT measured in these two halls are very similar, therefore the patterns of their early energy ratios are expected to be very similar, too. As the EDT and T30 are having a sloped decrease with frequency in Hall B with a proscenium setting, the associated clarity C80 increases with frequency.

The EDTs measured in the four halls A to D are shorter than those recommended by Beranek according to their usage. [4] In Table 4-3, the means of the measured EDT in Hall A at 500Hz and 1000 Hz with concert setting range from 1.2s to 1.3s and 1.4s to 1.6s

respectively. The measured EDTs are much shorter than the recommended designed values of Beranek. [4] The ranges of EDTs at 1000Hz approximately matches the lower limit of the recommended values of an opera hall. However, the measured ranges in Hall A with the proscenium setting hardly fall into the recommended range of an opera house with around 0.4sec shorter.

The measured ranges of EDTs at 500Hz of Hall B are around 0.1 seconds higher than those of Hall A while those at 1000Hz are around 0.1sec smaller in values in both settings as shown in Table 4-8. With a concert setting, the mean of EDTs at 500 Hz is around 1s with that at 1000Hz around 1.4s. With a proscenium setting, the means are around 1.1s and around 1s respectively. These are shorter than Beranek's recommended range for symphony halls, chamber music or opera houses.

The measured EDTs of Hall C summarized in Table 4-13 are all shorter than the recommended values. This is expected as the hall was originally designed for a conference purpose. The recital hall, Hall D has EDTs ranging from 1.1s to 1.18s and 1.25s at 500Hz and 1000Hz respectively as shown in Table 4-18. As a recital hall, which is usually used for chamber music, these values are considered to be low comparing with the recommendations of Beranek.

The measured reverberation time in the four halls, as shown in Table 4-4, 4-9, 4-14 and 4-19 respectively, are also shorter than the recommended values according to their usage. The measured mean T30s in Hall A are around 1.3s and around 1.46s to 1.48s at 500Hz and 1000 Hz respectively with the concert setting. Those with a proscenium setting range from 1.13s to 1.15s and 1.21s to 1.23s at 500Hz and 1000Hz respectively. Only the values at 1000Hz with concert setting can barely fall into the recommended range for an opera house.

The T30s measured in Hall B are longer than those in Hall A. All the measured means with a concert hall setting are within the recommended range of an opera house. The mean T30s are 1.46s to 1.48s at 500 Hz and 1.5s to 1.55s at 1000Hz respectively. As a theatre itself, these reverberation times are sufficient for providing a suitable reverberation for the hall when the hall is with a concert hall setting. Only the mean T30s at 500 Hz are with around 1.4s. Those at 1000Hz were 1.28s to 1.32s which are shorter than the recommended values.

Hall C's measured T30s are far shorter than any recommended values. All the mean T30s measured are shorter than 1s which are only suitable for a speech purpose as it is designed to be an auditorium. Hall D is also with T30s less than 1s. This is not ideal for a performance hall, however, would be suitable for a practice hall which requires less reverberation.

Generally speaking, the measured C80s in Table 4-5, 4-10, 4-15 and 4-20 in Hall A to D are larger than the recommended values. Hall A has means of C80 of a chamber hall with its concert hall setting. The mean C80s are 0.14dB to 2.57dB, 0.25dB to 2.64dB and -0.35dB to 1.83dB respectively at 500, 1000 and 2000Hz. The measured values with a proscenium stage setting are much larger. They increase to 2.9dB and 2.79dB with wider ranges up to more than 5dB at 500Hz and 1000 Hz. The values at 2000Hz are measured with a similar range at these frequencies.

Hall B with a concert setting are also measured with means of C80s matching the recommended values for chamber music. Most of the means lies between 0.1dB to 2dB while those of the C80s under the balcony at 1000Hz are around 3.31dB. The values measured with the proscenium setting are far beyond the suggested range. The mean C80s at 500Hz ranges from 2.9dB to 4.4dB which is even beyond the range for an opera hall which requires better clarity. The values at 1000 Hz and 2000 Hz are also beyond the suggested ranges.

With reference to the measured C80 values of Hall C as summarized in Table 4-15, Hall C is very good for speech while its measured C80s are with very large values, ranging from around 5dB up to approximately 9.5dB at 500 to 2000Hz. The measured values in Hall D lie around the suggested range for chamber music to opera. With the relatively short T30s measured, Hall D is with a design suitable for small recital music especially for rehearsals and practices which requires more clarity.

4.9 Conclusions

Four performance halls of different sizes and design have been measured in this study. Among these four halls, if they are convertible from concert setting to proscenium setting, or vice versa, both settings were measured. The range of the measured values from each hall and each stage setting are rather small, suggesting that the halls are having a rather uniform acoustics. The difference between each zones in the same hall can be observed. Yet, the effect of the balcony cannot be observed from these statistical data, further analysis should be done.

The difference between different hall designs is also observed. With a fan-shaped hall, the sound canopy in Hall B helps converge the sound energy to the audience, increasing the early decay time and reverberation time at mid to high frequencies. The non-parallel sidewalls make it less straight-forward in finding the first reflection's path difference for further analysis in Chapter 6.

More detailed building information with drawings of Hall A were obtained after this measurements. With these sufficient information and the relatively simple geometry, Hall A were selected for in-depth study throughout this project. Hall B were also used in neural network analysis in the next chapter.

The results of these extensive measurements create a data bank for further analysis. These survey type measurement is important for developing a database for local research or reference.

In Hall A, measurement points in a radial arrangements were added to the balcony edge in an attempt to capture the sound propagation and scattering. Only 1.5m and 2 m radii measurements were done in this study. Some observations can be found from the current set of results. However, in order to have a more in-depth investigation, the recorded waves have to be studied while more measurements with different radii should be done.

Chapter 5 Neural network

5.1 Introduction

Most of the mentioned acoustical parameters, such as RT, C80, D50 and etc. vary from location to location within a large performance hall. In general, some of the parameters like IACCs, are binaural. Extensive measurements of these parameters inside a performance hall are very time consuming. Also, it is not easy to vacate the venues for measurements easily. The most extensive measurements done were the binaural measurements of Barron and Lee[90] and the monaural measurements of Akama et al[76]. Since the acoustical properties are functions of spatial locations[76], [90] and binaural differences are expected while it is impractical to carry out numerous measurements inside a hall for its evaluation, a neural network analysis is used in the present study to examine the effectiveness of predictions using limited number of measurements.

Hall A and Hall B measured in the previous chapter are included in this chapter. Hall A is a relatively classic shoebox-typed performance hall while Hall B is a modern hall with a fan-shaped design. It is hoped that a simple framework for evaluating the acoustical properties of performance halls can be established.

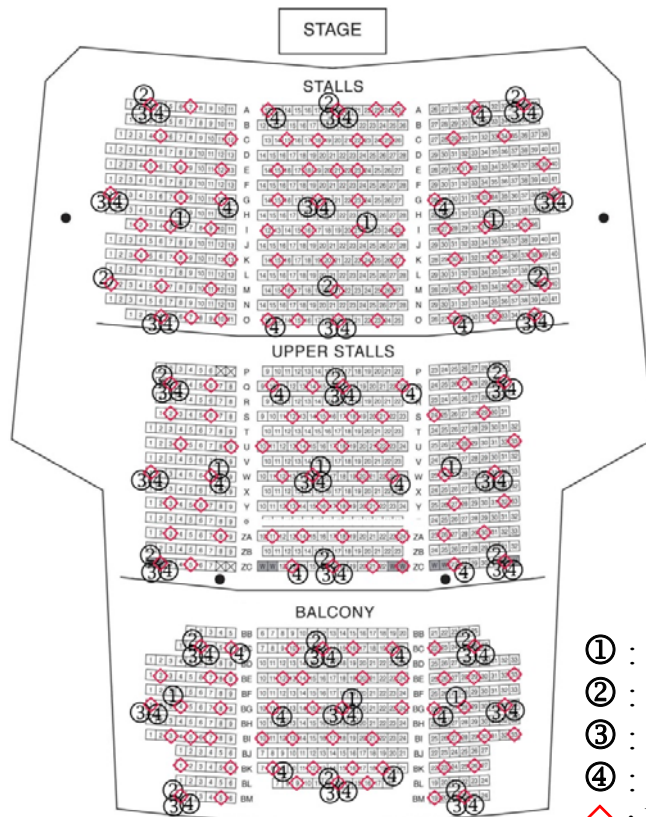
5.2 Neural Network Analysis

The acoustic propagation inside a large hall with balconies is too complicated for analytical study. Thus, the artificial neural network approach appears very useful in finding out the functional relationships between various parameters though in rather implicit formats (for instance, Nannariello and Fricke[20], [78], [80], [81], [86] and Kang[82]). Researches from Genaro et al [87] indicated that there are many different algorithms in existing literature. For simplicity, a feed-forward network with one hidden layer was adopted in the present study. A tan-sigmoid and linear types transfer functions were used in the hidden and output layers respectively. The inputs to the network were neither weighted nor biased. The number of neurons in the hidden layer was chosen arbitrarily to be twice the number of inputs. The training algorithm was chosen to be Levenberg-Marquardt. The computation was implemented using MATLAB and the default stop criteria of MATLAB was adopted for each simulation.[88] The difference between using one or two hidden layers in predicting clarity, C_{80} for the concert setting

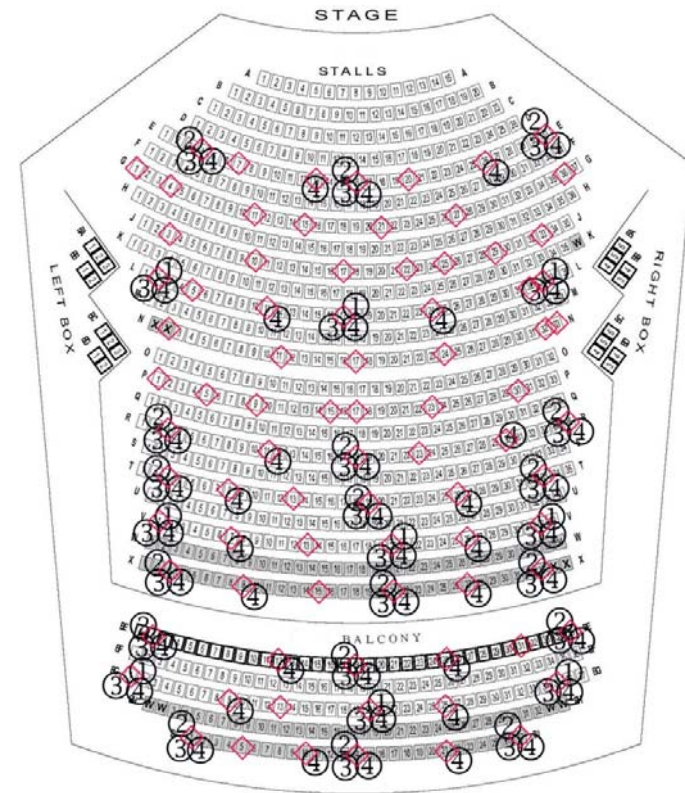
of Hall A was generally small, but the computation time using two hidden layers was substantially longer. It is believed that the situations for the other parameters would be the same. Hence, the two hidden layers scheme was not chosen for the present study.

The effectiveness of neural network predictions by four different training schemes (denoted as S-A, S-B, S-C and S-D) will be discussed. The outputs and inputs to the network during the training stage consist of the measured data from Chapter 4 and the corresponding spherical coordinates respectively. The trained network is then used to simulate the acoustical parameters at all the measurement points under each scheme. While the layout of Hall A and Hall B are different, the measurement data from these two halls were analysed separately. The balcony and stall areas in the network analysis were done at the same time while the elevation angle θ was sufficient for differentiating measurement points in the stall and the balcony sub-areas. One should note that the neural network simulation results varied every time after the network was initialized. [88, Ch. 5]. Hence, the simulation for each scheme were done and averaged before presenting here. To ensure the data convergence, 100 and 200 simulations are adopted for the study of the concert hall and proscenium setting respectively in the present study. The root-mean-square differences between simulations and measurements converge to within a tolerance comparable to that of measurement.

Figure 5-1 shows the selected measurement points of the four schemes. Scheme A is the simplest scheme which includes three measurement points spreading evenly in the middle region of each zone. Scheme B includes measurement points on the nearest and the furthest row from the stage of each zone. Scheme C is the combination of scheme A and scheme B. The most complicated scheme is scheme D, it has the maximum number of points and is basically scheme C with a better span-wise selection. However, scheme D for is undesirable option for Hall B because of the relatively large number of training points required in the upper stall and the balcony areas while the balcony of Hall B is relatively small.



Hall A



Hall B

- ① : Scheme S-A
- ② : Scheme S-B
- ③ : Scheme S-C
- ④ : Scheme S-D
- ◇ : Measurement Points

Figure 5-1 Measurement point distributions in performance halls and the four training schemes adopted

5.3 Results and Discussion

The HATs simulator was used in measuring different acoustical parameters in the halls. The left and the right ear of the simulator were connected as Channel 1 (CH1) and Channel 2 (CH2) respectively for all parameters, except for IACC. A Student-t test was performed to check if there were significant differences between the two channels before performing the neural network analysis. Table 5-1 summarises the t-test results. The t-test results was obtained at 95% confidence level. For a two-tail test with a degree of freedom of 181, the critical t -value is 2.26, over which the null hypothesis of “vanishing mean difference” would be rejected. The corresponding critical t -value for a degree of freedom of 83 is 2.28.

Under the concert hall setting with the acoustic shell on the stage, it is noticed that Hall A was not symmetrical especially in the middle frequency band and at high frequencies. The hall was more symmetrical in the proscenium stage case in terms of acoustical properties, and it was the worst at higher frequencies basically.

Table 5-1 Results of paired comparison t-test for vanishing differences (95% confidence level)

Hall	Stage Setting	Parameter	Octave Band Centre Frequency (Hz)						
			125	250	500	1000	2000	4000	8000
A	Concert	C ₈₀	0.06	4.03	12.3	9.16	3.99	2.59	2.93
		D ₅₀	0.95	4.28	9.88	7.39	2.18	0.98	0.81
		EDT	0.00	2.47	6.71	3.09	0.05	3.43	4.00
		RT	0.54	0.27	2.71	1.24	1.88	2.82	4.06
		BR	1.13				--	--	--
	Proscenium	C ₈₀	0.15	0.31	1.00	0.09	1.28	2.16	3.49
		D ₅₀	1.18	0.13	1.06	1.22	1.78	2.60	3.64
		EDT	1.60	0.80	0.38	0.95	0.17	0.70	3.14
		RT	0.22	2.01	0.56	0.27	0.30	0.56	2.09
		BR	0.86				--	--	--
B	Concert	C ₈₀	1.27	0.16	2.10	0.42	0.33	0.77	0.54
		D ₅₀	1.11	0.57	1.80	0.77	0.96	0.38	1.55
		EDT	0.54	0.57	0.79	0.90	0.72	0.47	1.90
		RT	1.55	0.36	0.28	1.19	0.30	0.06	4.83
		BR	1.42				--	--	--
	Proscenium	C ₈₀	0.79	2.00	0.62	1.89	0.03	1.61	1.49
		D ₅₀	0.48	2.66	0.58	2.32	0.35	1.27	2.26
		EDT	0.49	0.27	0.78	2.69	0.88	0.58	0.29
		RT	0.91	0.45	0.92	2.14	1.53	2.03	0.40
		BR	0.70				--	--	--

Table 5-2 Simple statistics of the acoustical parameters of Hall A

Stage Setting	Parameter	Octave Band Centre Frequency (Hz)*							
		125	250	500	1000	2000	4000	8000	
Concert	C _{80,L} (dB)	0.13 (1.97)	0.84 (1.94)	1.34 (1.67)	1.36 (1.70)	0.55 (1.95)	2.06 (2.02)	2.75 (2.03)	
	C _{80,R} (dB)	0.13 (2.03)	0.64 (1.94)	0.55 (1.87)	0.64 (1.81)	0.17 (1.94)	1.68 (2.17)	2.27 (2.15)	
	D _{50,L}	0.34 (0.12)	0.37 (0.11)	0.40 (0.11)	0.42 (0.11)	0.36 (0.12)	0.44 (0.12)	0.47 (0.11)	
	D _{50,R}	0.34 (0.12)	0.36 (0.11)	0.36 (0.11)	0.38 (0.12)	0.35 (0.12)	0.44 (0.13)	0.46 (0.12)	
	EDT _L (s)	1.44 (0.27)	1.28 (0.19)	1.24 (0.13)	1.47 (0.15)	1.42 (0.13)	1.25 (0.15)	1.07 (0.14)	
	EDT _R (s)	1.44 (0.26)	1.29 (0.18)	1.28 (0.13)	1.49 (0.12)	1.42 (0.13)	1.28 (0.15)	1.11 (0.12)	
	RT _L (s)	1.51 (0.12)	1.37 (0.08)	1.30 (0.04)	1.48 (0.04)	1.43 (0.03)	1.28 (0.04)	1.02 (0.03)	
	RT _R (s)	1.51 (0.13)	1.37 (0.08)	1.31 (0.05)	1.47 (0.04)	1.43 (0.03)	1.29 (0.03)	1.03 (0.03)	
	IACC _{0,+}	0.97 (0.02)	0.93 (0.02)	0.76 (0.07)	0.62 (0.12)	0.46 (0.13)	0.36 (0.15)	0.29 (0.11)	
	IACC _{0,80}	0.98 (0.02)	0.96 (0.03)	0.83 (0.10)	0.71 (0.17)	0.57 (0.21)	0.52 (0.19)	0.41 (0.17)	
	IACC _{80,+}	0.97 (0.01)	0.92 (0.03)	0.72 (0.06)	0.58 (0.06)	0.44 (0.06)	0.33 (0.07)	0.27 (0.05)	
	BR		1.03 (0.06)			--	--	--	
	Proscenium	C _{80,L} (dB)	1.86 (2.65)	3.20 (2.04)	3.83 (1.87)	3.82 (1.81)	3.89 (2.05)	5.31 (2.09)	5.51 (1.99)
		C _{80,R} (dB)	1.85 (2.62)	3.17 (2.19)	3.72 (1.94)	3.83 (1.99)	3.71 (2.10)	4.90 (2.18)	4.87 (1.95)
		D _{50,L}	0.43 (0.15)	0.50 (0.13)	0.52 (0.10)	0.55 (0.11)	0.53 (0.12)	0.60 (0.12)	0.61 (0.12)
D _{50,R}		0.44 (0.15)	0.49 (0.12)	0.52 (0.10)	0.54 (0.11)	0.51 (0.11)	0.57 (0.12)	0.56 (0.12)	
EDT _L (s)		1.23 (0.30)	1.08 (0.19)	1.03 (0.13)	1.17 (0.12)	1.11 (0.18)	0.98 (0.18)	0.86 (0.18)	
EDT _R (s)		1.25 (0.31)	1.09 (0.21)	1.02 (0.14)	1.16 (0.16)	1.10 (0.16)	0.99 (0.17)	0.91 (0.14)	
RT _L (s)		1.50 (0.25)	1.36 (0.13)	1.13 (0.06)	1.22 (0.04)	1.20 (0.05)	1.11 (0.04)	0.93 (0.03)	
RT _R (s)		1.50 (0.26)	1.34 (0.14)	1.13 (0.06)	1.22 (0.03)	1.20 (0.04)	1.11 (0.04)	0.94 (0.04)	
IACC _{0,+}		0.90 (0.06)	0.74 (0.10)	0.36 (0.14)	0.31 (0.16)	0.31 (0.13)	0.32 (0.14)	0.21 (0.10)	
IACC _{0,80}		0.93 (0.08)	0.83 (0.13)	0.57 (0.20)	0.51 (0.19)	0.52 (0.18)	0.50 (0.17)	0.36 (0.17)	
IACC _{80,+}		0.88 (0.06)	0.68 (0.10)	0.23 (0.11)	0.17 (0.07)	0.19 (0.08)	0.18 (0.07)	0.10 (0.03)	
BR			1.21 (0.15)			--	--	--	

*Numbers not in parentheses represent mean values and those inside parentheses standard deviations.

Table 5-3. Simple statistics of the acoustical parameters of Hall B

Stage Setting	Parameter	Octave Band Centre Frequency (Hz)*						
		125	250	500	1000	2000	4000	8000
Concert	C _{80,L} (dB)	0.25	0.62	0.93	2.25	1.92	3.02	2.93
		(2.08)	(1.87)	(1.50)	(1.00)	(1.01)	(1.32)	(1.27)
	C _{80,R} (dB)	0.12	0.64	0.72	2.29	1.96	2.92	2.84
		(2.02)	(1.97)	(1.21)	(1.04)	(1.22)	(1.65)	(1.44)
	D _{50,L}	0.34	0.36	0.39	0.50	0.46	0.53	0.49
		(0.11)	(0.12)	(0.09)	(0.06)	(0.07)	(0.08)	(0.08)
	D _{50,R}	0.34	0.35	0.38	0.50	0.47	0.53	0.51
		(0.12)	(0.12)	(0.08)	(0.07)	(0.08)	(0.11)	(0.10)
	EDT _L (s)	1.26	1.26	1.38	1.41	1.30	1.19	1.03
		(0.21)	(0.18)	(0.12)	(0.10)	(0.08)	(0.11)	(0.09)
	EDT _R (s)	1.26	1.25	1.37	1.40	1.31	1.20	1.06
		(0.21)	(0.18)	(0.10)	(0.11)	(0.08)	(0.13)	(0.09)
	RT _L (s)	1.26	1.26	1.38	1.41	1.30	1.19	1.03
		(0.21)	(0.18)	(0.12)	(0.10)	(0.08)	(0.11)	(0.09)
	RT _R (s)	1.35	1.38	1.46	1.51	1.44	1.29	1.12
(0.10)		(0.08)	(0.04)	(0.03)	(0.02)	(0.03)	(0.02)	
IACC _{0,+}	0.90	0.80	0.42	0.32	0.19	0.20	0.14	
	(0.04)	(0.07)	(0.11)	(0.10)	(0.06)	(0.09)	(0.05)	
IACC _{0,80}	0.93	0.86	0.61	0.53	0.41	0.37	0.28	
	(0.06)	(0.10)	(0.13)	(0.13)	(0.11)	(0.13)	(0.09)	
IACC _{80,+}	0.89	0.77	0.33	0.15	0.09	0.09	0.07	
	(0.05)	(0.07)	(0.12)	(0.07)	(0.02)	(0.03)	(0.02)	
BR		0.83	(0.28)		--	--	--	
Proscenium	C _{80,L} (dB)	2.66	3.64	4.26	5.36	6.20	7.38	7.20
		(2.25)	(2.59)	(2.04)	(1.67)	(2.18)	(2.63)	(2.12)
	C _{80,R} (dB)	2.58	3.89	4.33	5.12	6.20	7.07	6.84
		(2.32)	(2.40)	(1.96)	(1.78)	(2.34)	(2.76)	(2.32)
	D _{50,L}	0.47	0.53	0.55	0.58	0.62	0.66	0.66
		(0.13)	0.14	0.12	0.11	0.12	0.12	0.11
	D _{50,R}	0.47	0.55	0.55	0.56	0.61	0.65	0.64
		(0.13)	(0.13)	(0.12)	(0.12)	(0.13)	(0.12)	(0.11)
	EDT _L (s)	1.24	1.09	1.08	0.96	0.87	0.73	0.68
		(0.27)	(0.21)	(0.17)	(0.16)	(0.19)	(0.20)	(0.16)
	EDT _R (s)	1.25	1.09	1.09	1.00	0.85	0.74	0.69
		(0.28)	(0.23)	(0.15)	(0.13)	(0.19)	(0.18)	(0.15)
	RT _L (s)	1.81	1.52	1.35	1.25	1.15	0.99	0.82
		(0.24)	(0.18)	(0.11)	(0.07)	(0.05)	(0.03)	(0.03)
	RT _R (s)	1.79	1.53	1.33	1.27	1.16	0.98	0.82
(0.26)		(0.18)	(0.09)	(0.06)	(0.04)	(0.04)	(0.03)	
IACC _{0,+}	0.91	0.81	0.47	0.39	0.36	0.37	0.26	
	(0.04)	(0.07)	(0.11)	(0.11)	(0.15)	(0.15)	(0.13)	
IACC _{0,80}	0.93	0.87	0.61	0.52	0.49	0.50	0.38	
	(0.05)	(0.11)	(0.14)	(0.13)	(0.17)	(0.16)	(0.15)	
IACC _{80,+}	0.90	0.75	0.32	0.25	0.23	0.24	0.15	
	(0.04)	(0.07)	(0.10)	(0.10)	(0.11)	(0.13)	(0.06)	
BR		1.28	(0.12)		--	--	--	

*Numbers not in parentheses represent mean values and those inside parentheses standard deviations.

The corresponding symmetry of Hall B was acceptable. As it was not symmetrical most of the time, the measured data from the left and right channel from the HATS, except the BR, are analysed separately in the present study. The BR data is averaged between the two left and right channels of the HATS microphone. The source strength G in the balcony is found well correlated with distance d when they are handled separately within the hall data. Such that, the G is not included in the neural network study while it is not necessary. Except G , all other acoustical parameters do not show significant dependence on distance d alone in this present study. To facilitate foregoing discussions, a summary of the simple statistics of the measured acoustical parameters was presented in Table 5-2 and Table 5-3 to provide a general overview of all the acoustical parameters. Suffices L and R denote the left and right side of the HATS respectively in the foregoing discussions.

5.3.1 Hall A

5.3.1.1 Concert setting

The BR is the averaged single value rating for each location inside the hall and thus it is discussed in the first place. Actually the variation of BR within the hall under the concert hall setting was quite small as indicated in Table 5-2. **Error! Reference source not found.** The root-mean-square difference between the neural network predictions and the 182 measurements for training schemes S-A, S-B, S-C and S-D are 0.07, 0.06, 0.06 and 0.06 respectively. These differences are accounting around 5% all BRS while most are around unity in most of the location. It appears that S-A is a simple scheme with acceptable prediction deviation that is suitable for evaluating the BR of the halls.

The IACCs are frequency-dependent. Figure 5-2 compares the measured values and the simulated $IACC_{0,80}$ (also denoted as $IACC_E$)[91] using the four training schemes. The measured $IACC_{0,80}$ is decreasing with frequency but its range is increasing independent of the scheme adopted. The differences between simulations and measurements were also increasing with frequency. From Figure 5-2, it can be seen that S-D gives the best performance while S-A result is the worst. The performances of S-B and S-C are comparable, but S-C appears to perform slightly better. Such performance of the four schemes is expected because of the number of data points input to the neural network training. However, the aim of the present study is to examine the possibility of using a small number of data points for the acoustical assessment of a performance hall and it will be discussed in detail later. One can observe that the simulated $IACC_{0,80}$ values are

all positive and are all smaller than one despite the lack of physical consideration in the neural network algorithm. However, if some number of simulations would produce data out of this range and the number of simulations for data average is insufficient, such acceptable result cannot be simulated.

Figure 5-3 illustrates the differences between the simulated early decay time from the left ear of the HATs, EDT_L and the corresponding measured data. Table 5-2 and Figure 5-4 shows that the EDT values have wide ranges, from 0.2 to above 1 especially in mid frequencies. The performances of S-B, S-C and S-D are comparable in here, while S-B is slightly better especially at low frequencies. S-A simulated EDT_L s with a relatively narrow range. This could be the result of the narrower data input range to the neural network simulation in S-A than in the other schemes.

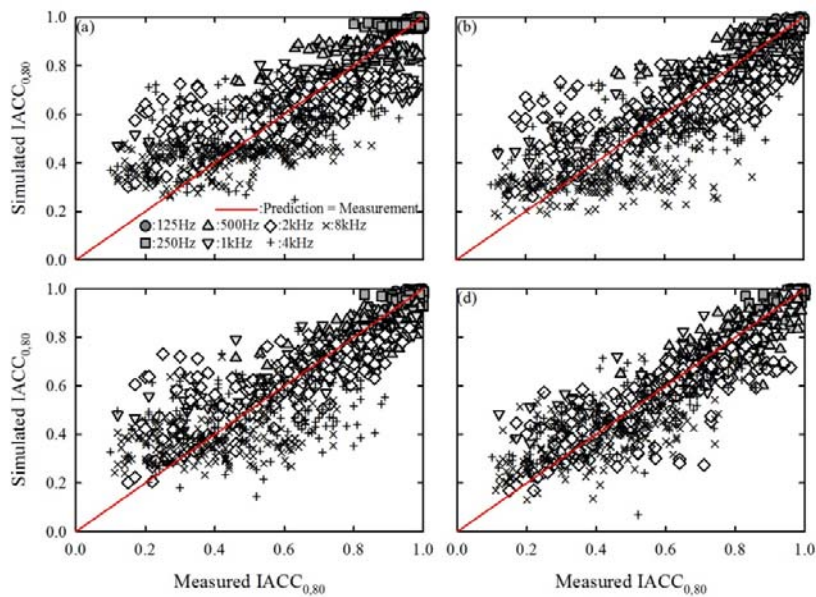


Figure 5-2 Comparison between simulated $IACC_{0,80}$ and measurements for Hall A under concert setting.

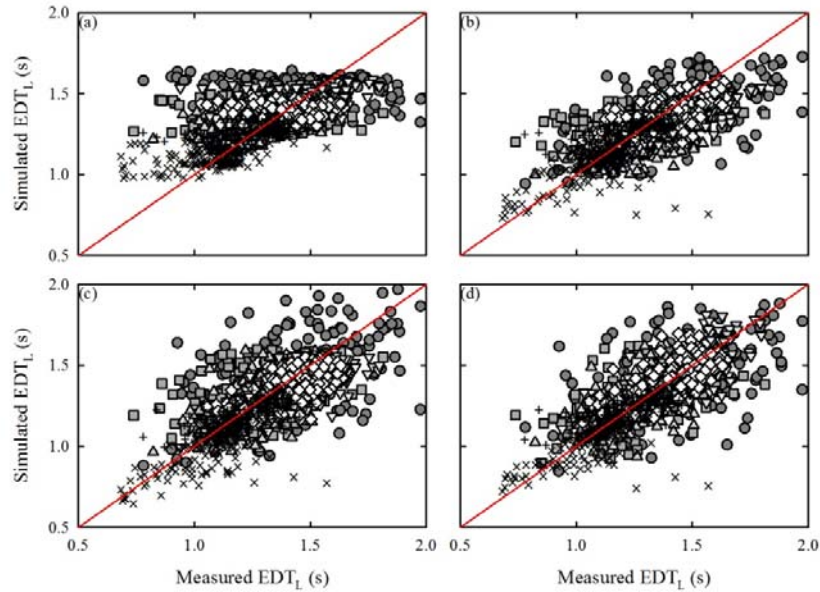


Figure 5-3 Comparison between simulated EDT_L and measured EDT for Hall A under concert setting.

It should be noted that the behaviours of the EDTs from the right ear of the HATs are reasonably similar to those of from the left ear. The RT values are relatively uniform within a concert hall as suggested by Barron[42] and the measured results shown in Table 5-2 are uniform as well, and thus are not discussed. Under such uniformity, similarity in the performances of the four training scheme is rather anticipated for RT.

The clarity C_{80} is in decibel scale and ranges from negative to positive values. The measured data in the halls are varying over a wide range and thus have large standard deviations as indicated in Table 5-2. The simulated values are relatively different from the measured values. This is probably because of the large variation of this parameter which tends to reduce the neural network simulation accuracy. However, such differences do not show any definite trend of variation with frequency. While S-A has the least number of inputs, it gives the worst simulations under such a large fluctuating C_{80} range. The definition D_{50} is not very meaningful for concert activity and thus the corresponding results are not presented.

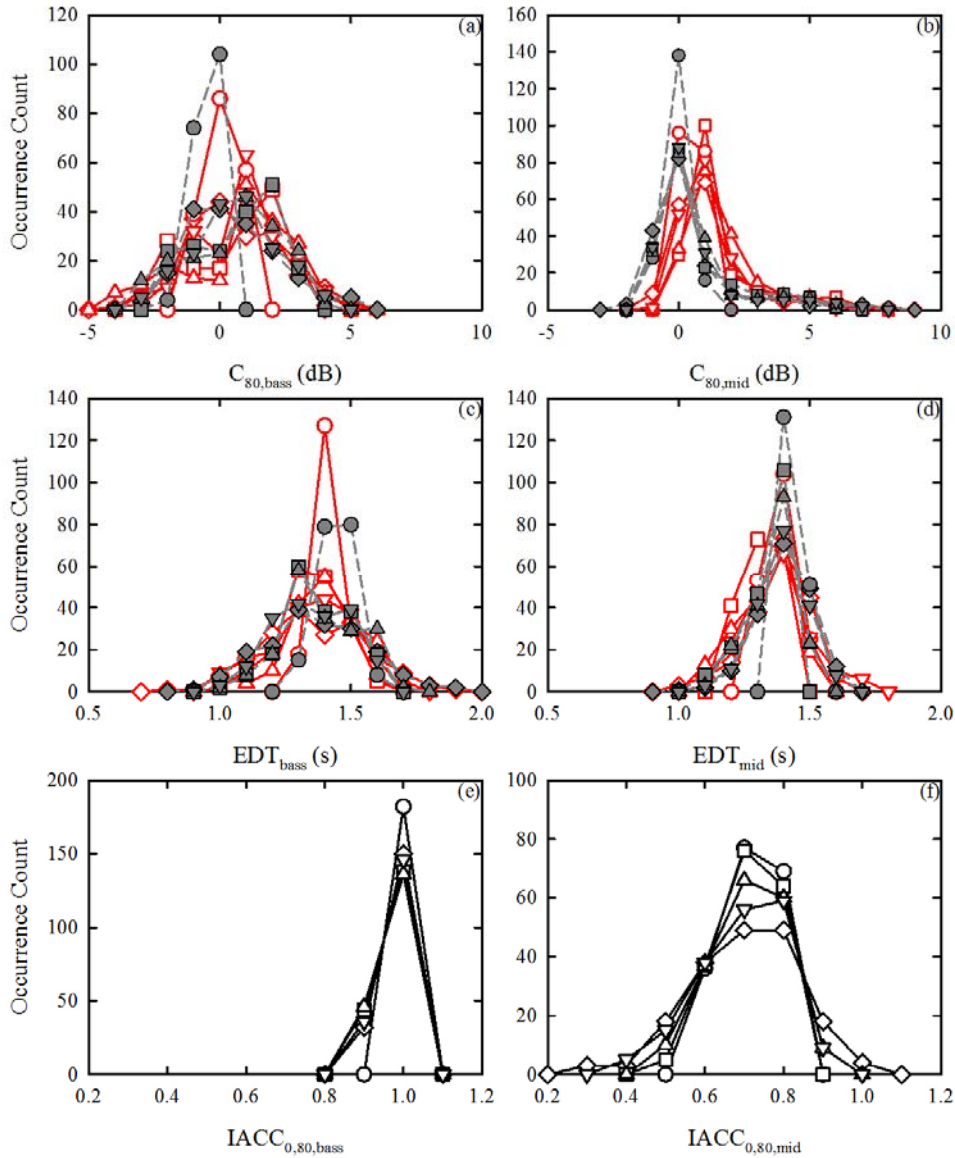


Figure 5-4 Statistical distributions of acoustical parameters under concert setting of Hall A.

(a) $C_{80,bass}$; (b) $C_{80,mid}$; (c) EDT_{bass} ; (d) EDT_{mid} ; (e) $IACC_{0,80,bass}$; (f) $IACC_{0,80,mid}$. \diamond : measurement;

\circ : S-A; \square : S-B; \triangle : S-C; ∇ : S-D. Closed symbols: right of HATS; open symbols: left of HATS

(except for $IACC_{0,80}$).

To examine the overall difference of the neural network simulated results and the measurement results, three different statistical tests are done. They are tested firstly by using first the root-mean-square differences, then the consideration of statistical distributions and lastly by a Student t -test analysis for point-to-point discrepancy checking. The following analysis is mainly focused on the reverberance parameters C_{80} and EDT, and the early hall spaciousness $IACC_{0,80}$, as D_{50} may not be so relevant for concert hall situation and the RTs are relatively uniform within the hall under the concert hall setting.

Table 5-4 illustrates the root-mean-square differences between simulated results and measurements for all the acoustical parameters included in the present study. The convergence tolerance for C_{80} is of $O(10^{-2})$ while those of the other parameters of $O(10^{-3})$. S-D gives the smallest differences in general. S-A remains performing the worst except at octave band at 250Hz octave or above. At these octave band frequencies, the overall root-mean-square differences resulted from the application of S-A, except for C_{80} , are acceptable practically when compared to those obtained from S-B, S-C and even S-D. The performance of S-B is similar to that of S-C, but the former is a bit better in handling the reverberance-related parameters such as D_{50} , EDT and C_{80} as well as the mid-frequency hall spaciousness ($1-IACC_{E3}$)[20], [92]. Though S-D performs the best in terms of the least overall differences between simulations and measurements, it is still yet an attractive scheme while it requires a large number of measurement points for training the neural network but relatively small improvements over S-B and S-C (comparable to measurement uncertainty). The neural network simulation results obtained using the schemes S-C and S-D by considering each seating area separately do not show better predictions and thus are not presented. It is also meaningful to look into the ability of the neural network algorithm in predicting the statistical distributions of the acoustical parameters inside the performance hall. Figure 5-4a and Figure 5-4b illustrate the measured and simulated distributions of C_{80} under the concert setting within the bass frequency ($C_{80,bass}$) and mid-frequency ranges ($C_{80,mid}$) respectively. The bin widths of the distributions are set to 1 dB. 125Hz and 250Hz are put into the bass frequency category, while the mid-frequency are octave band frequencies from 500 Hz to 2000Hz.[42] The clarities are averaged logarithmically. The $C_{80,bass}$ at both the right and left ear cannot be predicted using all the four schemes. The schemes are performing better

in estimating the mid-frequency values. The performance of S-C and S-D are comparable when $C_{80, \text{midS}}$ is concerned.

EDT are having a similar simulation results as those of the C_{80} as shown in Figure 5-4c and Figure 5-4d. The bin width for the EDT distribution is 0.1 sec. At bass frequencies 125Hz and 250Hz, only S-D can give reasonable prediction of the distribution as illustrated in Figure 5-4e. Similar to $C_{80, \text{mid}}$, S-B and S-C give comparable results, while S-A is a failure. Both S-C and S-D are acceptable for the mid-frequency EDT distribution predictions. In principle, S-B, S-C and S-D predict the modes of the distributions of bass and mid-frequency EDTs very well.

As the IACC values are within 0 and 1, the bin width of the $IACC_{0,80}$ distribution is chosen to be 0.1. At bass frequencies, $IACC_{0,80}$ (that is, $IACC_{E3, \text{bass}}$) fluctuates within a very narrow range of 0.15 (between 0.85 and 1.0), such that all the four schemes result in similar predicted distributions (Figure 5-5e). At mid frequencies, prediction of $IACC_{0,80}$ is performing better while there is more number of training data provided to the scheme as shown in Figure 5-5. However, the mode of distribution is predicted with good accuracy no matter which scheme is used. Once again, S-C and S-D are giving similar prediction accuracy.

Table 5-5 summarizes the paired t -test statistics with the point-to-point compared null hypothesis set to be “vanishing mean difference between simulation and measurement”. Again, the 95% confidence level is adopted. Those failed tests are highlighted in bold letters in Table 5-5 (with test statistics higher than 2.26). The negative test statistics indicate that the tendency for the mean of the simulation being smaller than that of the measurement. The decrease in root-mean-square difference and a similar statistical distributed set of do not necessarily increase the chance of a point-by-point “vanishing difference”. However, the smaller the standard deviation that the parameter has will in fact increase the chance of null hypothesis rejection because of small variances of the two tested distributions, even though the simulated values are acceptably close to the measurements. The RT is an example for such phenomenon. In general, the neural network simulation performs better when the number of training data increases, however, it is found that the simulation of the mid-frequency hall spaciousness $IACC_{0,80}$ does not require large number of training data. Contrastingly, the reverbrance parameters (C_{80} and EDT) need larger number of training data before the “vanishing difference” condition can be achieved.

Table 5-4. Root-mean-square differences between simulations and measurements for Hall A

Scheme	Parameter	Octave Band Centre Frequency (Hz)*						
		125	250	500	1000	2000	4000	8000
S-A	C _{80,L} (dB)	1.95/2.57	2.12/2.50	1.79/1.66	1.47/1.44	1.84/1.78	2.01/1.90	1.93/1.68
	C _{80,R} (dB)	2.14/2.46	2.31/2.29	2.16/2.01	1.63/1.54	1.78/1.60	2.07/2.21	2.24/1.75
	D _{50,L}	0.12/0.16	0.13/0.14	0.10/0.09	0.09/0.09	0.12/0.10	0.12/0.12	0.11/0.13
	D _{50,R}	0.13/0.17	0.13/0.14	0.12/0.11	0.09/0.08	0.10/0.10	0.13/0.12	0.12/0.11
	EDT _L (s)	0.29/0.30	0.22/0.25	0.13/0.14	0.15/0.16	0.13/0.18	0.14/0.18	0.14/0.21
	EDT _R (s)	0.32/0.33	0.19/0.23	0.14/0.13	0.14/0.15	0.13/0.14	0.14/0.18	0.12/0.15
	RT _L (s)	0.15/0.26	0.08/0.15	0.04/0.06	0.05/0.04	0.03/0.04	0.03/0.04	0.03/0.03
	RT _R (s)	0.16/0.27	0.08/0.16	0.05/0.06	0.04/0.04	0.03/0.04	0.03/0.03	0.04/0.03
	IACC _{0,+}	0.01/0.05	0.02/0.09	0.06/0.14	0.09/0.11	0.12/0.12	0.13/0.14	0.11/0.10
	IACC _{0,80}	0.02/0.07	0.04/0.13	0.09/0.18	0.13/0.12	0.16/0.14	0.17/0.16	0.16/0.16
	IACC _{80,+}	0.01/0.05	0.02/0.11	0.05/0.13	0.06/0.07	0.06/0.07	0.06/0.07	0.06/0.03
	BR			0.07/0.13		--	--	--
	S-B	C _{80,L} (dB)	1.77/1.83	2.10/2.16	1.19/1.11	0.98/0.95	1.57/1.28	1.54/1.68
C _{80,R} (dB)		1.86/1.90	1.73/2.11	1.14/1.27	0.87/0.94	1.48/1.54	1.51/1.82	1.36/1.36
D _{50,L}		0.11/0.12	0.08/0.12	0.07/0.07	0.08/0.06	0.09/0.09	0.12/0.12	0.10/0.11
D _{50,R}		0.12/0.13	0.09/0.12	0.07/0.08	0.05/0.07	0.07/0.10	0.10/0.13	0.09/0.11
EDT _L (s)		0.23/0.28	0.17/0.18	0.13/0.13	0.14/0.11	0.10/0.17	0.13/0.16	0.12/0.17
EDT _R (s)		0.23/0.31	0.17/0.19	0.12/0.13	0.12/0.13	0.12/0.16	0.12/0.16	0.09/0.14
RT _L (s)		0.12/0.27	0.08/0.14	0.04/0.07	0.04/0.05	0.03/0.04	0.03/0.03	0.03/0.02
RT _R (s)		0.16/0.27	0.09/0.16	0.05/0.06	0.04/0.04	0.03/0.03	0.03/0.02	0.03/0.03
IACC _{0,+}		0.01/0.04	0.03/0.10	0.08/0.17	0.09/0.10	0.10/0.10	0.14/0.13	0.10/0.09
IACC _{0,80}		0.02/0.06	0.03/0.10	0.10/0.19	0.11/0.11	0.15/0.11	0.18/0.14	0.18/0.14
IACC _{80,+}		0.01/0.04	0.03/0.12	0.07/0.15	0.06/0.07	0.05/0.06	0.06/0.06	0.05/0.03
BR				0.06/0.12		--	--	--
S-C		C _{80,L} (dB)	1.76/1.84	2.14/2.48	1.17/0.98	1.17/1.24	1.32/1.33	1.54/1.47
	C _{80,R} (dB)	1.81/1.85	1.90/2.18	1.17/1.19	0.96/0.95	1.01/1.55	1.55/1.84	1.56/1.56
	D _{50,L}	0.10/0.12	0.08/0.12	0.06/0.06	0.07/0.08	0.10/0.09	0.11/0.10	0.11/0.10
	D _{50,R}	0.10/0.12	0.10/0.13	0.07/0.07	0.05/0.07	0.08/0.09	0.10/0.12	0.08/0.11
	EDT _L (s)	0.26/0.29	0.19/0.20	0.14/0.13	0.14/0.14	0.11/0.16	0.13/0.15	0.13/0.18
	EDT _R (s)	0.25/0.29	0.17/0.21	0.10/0.12	0.10/0.13	0.10/0.17	0.12/0.17	0.09/0.15
	RT _L (s)	0.14/0.24	0.10/0.15	0.04/0.06	0.04/0.04	0.03/0.03	0.04/0.03	0.03/0.03
	RT _R (s)	0.14/0.33	0.09/0.16	0.05/0.06	0.04/0.03	0.03/0.03	0.03/0.03	0.03/0.03
	IACC _{0,+}	0.01/0.04	0.03/0.10	0.06/0.13	0.08/0.09	0.09/0.11	0.14/0.11	0.11/0.07
	IACC _{0,80}	0.02/0.05	0.04/0.10	0.08/0.15	0.10/0.13	0.14/0.13	0.18/0.13	0.15/0.10
	IACC _{80,+}	0.01/0.05	0.03/0.11	0.05/0.12	0.06/0.07	0.05/0.06	0.06/0.06	0.06/0.03
	BR			0.06/0.13		--	--	--
	S-D	C _{80,L} (dB)	1.52/1.72	1.50/2.09	1.11/0.94	0.98/0.92	1.27/1.04	1.25/1.18
C _{80,R} (dB)		1.59/1.87	1.54/2.00	1.27/1.03	0.71/0.91	0.88/1.19	1.08/1.46	1.19/1.31
D _{50,L}		0.10/0.12	0.08/0.11	0.06/0.06	0.07/0.06	0.09/0.07	0.09/0.08	0.08/0.08
D _{50,R}		0.10/0.12	0.08/0.11	0.06/0.06	0.05/0.06	0.07/0.08	0.08/0.09	0.08/0.09
EDT _L (s)		0.24/0.24	0.16/0.16	0.13/0.12	0.11/0.09	0.10/0.16	0.12/0.15	0.12/0.18
EDT _R (s)		0.25/0.26	0.15/0.17	0.11/0.13	0.10/0.12	0.10/0.12	0.09/0.16	0.08/0.15
RT _L (s)		0.14/0.24	0.08/0.13	0.04/0.06	0.04/0.04	0.03/0.03	0.03/0.03	0.03/0.03
RT _R (s)		0.13/0.29	0.08/0.16	0.04/0.06	0.05/0.03	0.03/0.03	0.03/0.03	0.03/0.03
IACC _{0,+}		0.01/0.03	0.02/0.08	0.05/0.11	0.06/0.09	0.08/0.08	0.11/0.10	0.09/0.07
IACC _{0,80}		0.01/0.04	0.03/0.09	0.07/0.14	0.08/0.10	0.12/0.11	0.13/0.13	0.13/0.11
IACC _{80,+}		0.01/0.05	0.02/0.09	0.06/0.11	0.05/0.07	0.04/0.07	0.05/0.05	0.04/0.03
BR				0.06/0.12		--	--	--

*concert / proscenium

Table 5-5 Paired t-test statistics for vanishing differences between simulations and measurements under concert setting of Hall A (95% confidence level)

Scheme	Parameter	Octave Band Centre Frequency (Hz)						
		125	250	500	1000	2000	4000	8000
S-A	C _{80,L} (dB)	-1.28	-4.66	-4.68	-5.93	-5.13	-3.71	-6.55
	C _{80,R} (dB)	-4.36	-7.88	-6.16	-1.75	-3.57	-6.55	-6.74
	D _{50,L}	-6.18	-4.72	-2.16	-7.67	-3.74	-1.15	-1.64
	D _{50,R}	-8.86	-4.69	-6.37	-5.07	-3.96	-5.26	-6.38
	EDT _L (s)	2.56	4.82	5.33	-0.46	-1.85	1.70	4.35
	EDT _R (s)	5.66	1.99	4.20	5.81	-0.71	1.52	0.31
	RT _L (s)	-7.67	-0.61	4.46	3.24	6.06	-0.05	0.05
	RT _R (s)	-8.55	2.47	-2.07	4.58	-4.92	2.98	-0.94
	IACC _{0,+}	-1.43	6.03	1.14	-0.76	5.57	1.48	0.75
	IACC _{0,80}	-0.66	5.32	3.15	-1.89	2.65	1.51	0.94
	IACC _{80,+}	-0.66	2.73	1.96	7.24	6.82	0.10	6.26
	BR			-6.02		--	--	--
	S-B	C _{80,L} (dB)	4.05	-1.82	7.64	1.68	6.14	2.71
C _{80,R} (dB)		1.63	1.57	2.93	0.04	2.66	-1.11	-6.15
D _{50,L}		0.77	-3.18	-0.29	-7.80	-2.16	2.16	0.17
D _{50,R}		2.51	2.00	0.18	-2.17	0.86	0.99	1.03
EDT _L (s)		-2.78	2.10	-7.91	-10.3	-3.05	3.19	-1.92
EDT _R (s)		-1.85	2.60	-5.68	-11.5	-4.09	0.78	-1.16
RT _L (s)		-0.85	2.38	0.56	-3.33	-0.71	-0.37	7.32
RT _R (s)		7.59	3.32	-1.22	-4.03	2.45	3.31	-2.59
IACC _{0,+}		2.00	-7.23	-0.23	1.96	2.78	5.39	-1.75
IACC _{0,80}		0.49	-6.94	0.84	-0.37	0.79	-0.71	-5.55
IACC _{80,+}		1.99	-6.79	0.77	8.52	1.99	2.31	2.74
BR				4.16		--	--	--
S-C		C _{80,L} (dB)	0.09	1.84	5.16	7.79	2.20	2.77
	C _{80,R} (dB)	-0.64	1.17	0.66	3.53	-2.30	0.98	1.67
	D _{50,L}	-2.21	-1.53	-2.45	-1.95	-4.34	-0.48	1.65
	D _{50,R}	-0.05	1.02	-1.26	-0.79	-6.50	-1.71	0.36
	EDT _L (s)	2.22	2.35	-0.86	-9.57	-6.46	-3.72	-5.88
	EDT _R (s)	0.91	1.76	0.39	-8.87	-7.65	-5.40	-7.12
	RT _L (s)	3.68	-2.06	-2.15	-3.29	-1.93	-1.22	-0.38
	RT _R (s)	2.06	1.51	-3.13	3.37	-0.67	-2.20	-1.59
	IACC _{0,+}	1.00	-4.73	-0.12	4.26	4.21	2.85	1.70
	IACC _{0,80}	-3.50	-4.36	-0.91	-0.40	1.96	-2.81	-0.72
	IACC _{80,+}	1.91	-1.16	1.67	8.87	1.20	3.14	4.03
	BR			3.47		--	--	--
	S-D	C _{80,L} (dB)	2.94	-1.83	3.22	1.17	-2.58	3.60
C _{80,R} (dB)		0.38	2.16	3.26	0.53	-1.71	-2.81	1.26
D _{50,L}		2.64	-1.43	0.65	2.98	-2.13	3.09	3.23
D _{50,R}		2.56	0.47	2.85	2.69	-3.38	1.55	3.25
EDT _L (s)		-0.81	0.33	1.48	-1.28	-0.30	-0.95	-2.79
EDT _R (s)		-2.42	1.00	0.54	-1.15	-1.24	-2.88	2.73
RT _L (s)		2.02	0.07	-3.06	-4.19	-0.97	-0.02	-0.57
RT _R (s)		-0.29	0.71	-0.52	-1.66	-1.09	-1.66	-1.47
IACC _{0,+}		3.87	-2.42	-1.62	-0.82	-2.91	3.36	2.73
IACC _{0,80}		0.67	-2.12	-0.98	1.20	-3.54	-0.97	-1.21
IACC _{80,+}		4.11	-1.53	-1.79	1.68	-3.21	-0.21	1.81
BR				2.00		--	--	--

5.3.1.2 Proscenium setting

The proscenium setting, without the acoustic shell on the stage, is mainly used during opera and dancing performance. Table 5-2 shows the spatial variations of the acoustical parameters under this condition, it can be observed that the variations here are larger than that under the concert setting. This is probably because of the weaker reverberation under the proscenium condition. As many of the essential features of the data variations have been illustrated in Section 4.A1, this section focuses on the differences between simulations and measurements.

Table 5-4 presents the root-mean-square differences between simulations and measurements results of the four training schemes adopted in the present study under the proscenium setting condition. The four schemes in proscenium setting performs similarly to those observed under the concert hall setting, but the root-mean-square differences under this setting are in general slightly higher than those obtained under the concert hall setting probably due to the larger spatial variations of the parameters with the proscenium stage. Under the less reverberant proscenium setting, the parameters at low frequencies varies more and this significantly affects the IACCs adversely as the correlations between the left and right hand signals are deteriorated. Thus, this resulted in higher percentage of increase in the root-mean-square differences over the IACCs values at bass frequencies under the concert hall setting than at higher frequencies. Again, as the elevation angle θ has represented the geometrical location satisfactorily, the separation of different hall areas in the neural network analysis does not result in better simulations.

The statistical distributions for the prediction of C_{80} , EDT and $IACC_{0,80}$ in the bass frequency and mid-frequency ranges under the proscenium setting are illustrated in Figure 5-5. The plots can compare the effectiveness of prediction using the four schemes. The same bin widths as those for Figure 5-4 are adopted. For the sake of completeness, the bass frequency data are included here for discussion even they are not so relevant for the activities on proscenium stage. One can observe that S-A fails to predict the distributions of the C_{80} s in bass frequency range Figure 5-5(a). Even a large number of training data is used, S-D cannot give a closer prediction but yet satisfactory. S-C predicts the most accurate values at the bass frequency range for C_{80} values. At mid frequencies, the mode of the $C_{80, \text{mid}}$ is correctly predicted by all schemes as shown in Figure 5-5(b). It appears that S-C is again the best in terms of both distribution shape and spread range.

For the bass frequency EDTs, S-B, S-C and S-D give similar simulations while S-A is again a failure in Figure 5-5(c). Similar to the case of $C_{80,bass}$, the performance of S-D is slightly lagging behind those of S-B and S-C in predicting the distribution of EDT_{bass} . The results shown in Figure 5-5d suggest that all four schemes are having a comparable performance in the prediction of the statistical distribution of EDT_{mid} , but none of them has predicted the right kurtosis of the measured distribution. As in the case of $C_{80,mid}$, sharper distributions are simulated by the neural network.

S-C and S-D performed the best in predicting the $IACC_{0,80}$ distributions at bass frequencies while all schemes can predict accurately the mode of the measured distribution as shown in Figure 5-5e. However, as shown in Figure 5-5f, only S-D can predict a distribution that is similar to that of the measured mid-frequency early hall spaciousness $IACC_{0,80}$.

Concerning the point-to-point comparison, it can be seen from Table 5-6 again that the increase in the number of training data can improve the scheme performance. S-A is not good even for the bass ratio. Together with the results shown in Table 5-4 and Figure 5-5 the prediction from S-D for the $IACC_{0,80}$ is exciting, but S-C is not bad at all when the $IACC_{0,80}$, C_{80} and EDT are considered together. This makes S-C an important alternative as it requires only 60% of training data as S-D does.

In conclusion, S-C and S-D are acceptable schemes for the acoustical parameter predictions for both the concert hall and proscenium settings of Hall A. The reverberance parameters appears to be more difficult to be predicted than the spaciousness parameters in general. The weaker reverberation under the proscenium setting results in less uniform spatial acoustical parameter distribution, resulting in the less significant point-to-point deviation between simulations and measurements statistically. However, the actual differences can be larger under the proscenium setting than under the concert hall setting.

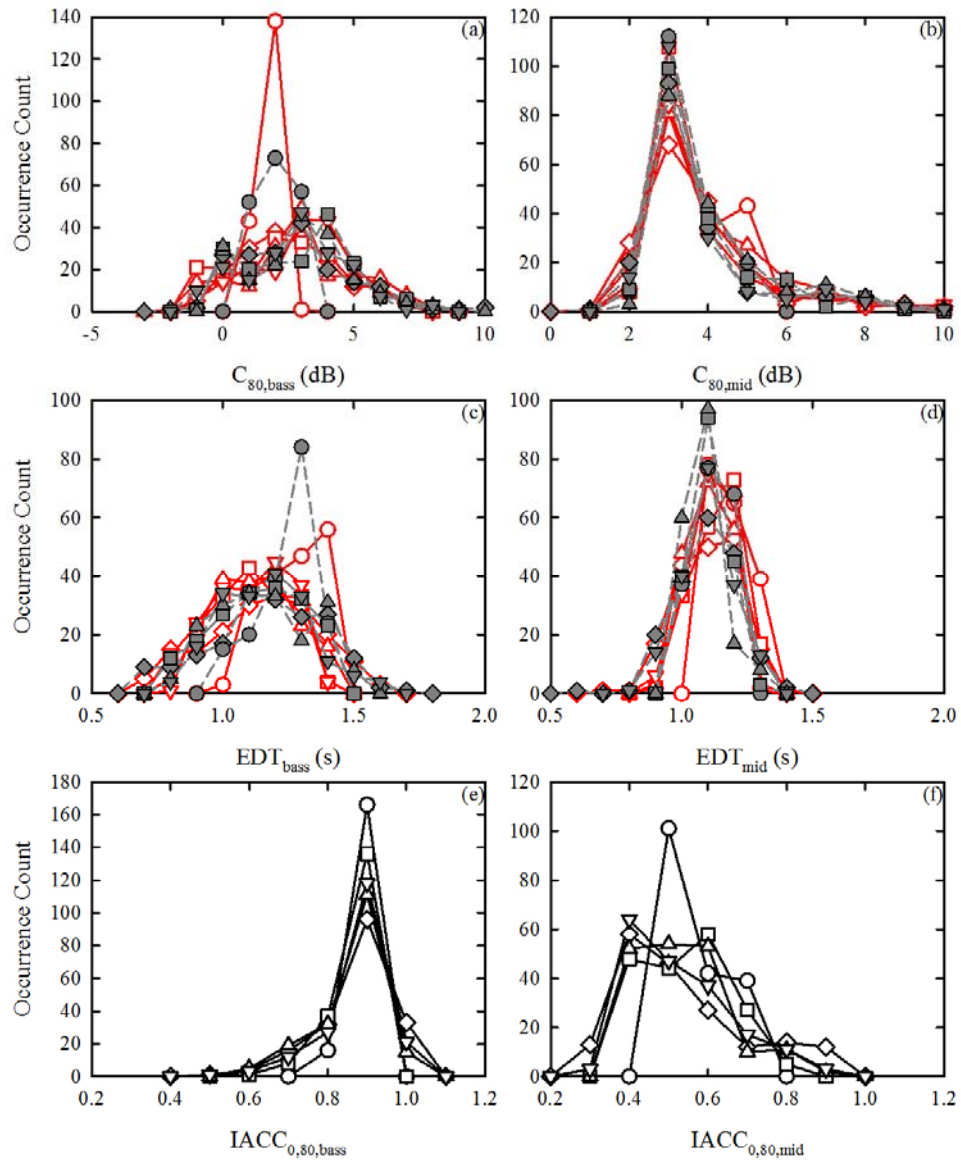


Figure 5-5 Statistical distributions of acoustical parameters under proscenium setting of Hall A.
 (a) $C_{80,bass}$; (b) $C_{80,mid}$; (c) EDT_{bass} ; (d) EDT_{mid} ; (e) $IACC_{0,80,bass}$; (f) $IACC_{0,80,mid}$. Legends : same as those for Figure 5-4

Table 5-6 Paired t-test statistics for vanishing differences between simulations and measurements under proscenium setting of Hall A (95% confidence level)

Scheme	Parameter	Octave Band Centre Frequency (Hz)						
		125	250	500	1000	2000	4000	8000
S-A	C _{80,L} (dB)	-3.63	-5.84	-4.19	-3.35	-2.13	-0.73	0.59
	C _{80,R} (dB)	-2.47	-4.57	-5.03	-2.40	-1.38	-4.92	-2.89
	D _{50,L}	-5.62	-3.50	-4.61	-4.36	-1.06	1.82	2.95
	D _{50,R}	-6.97	-5.24	-7.01	-3.14	-1.54	-2.31	0.94
	EDT _L (s)	3.41	10.7	4.34	12.3	4.73	4.28	5.96
	EDT _R (s)	2.29	5.36	1.94	2.26	2.50	4.14	3.94
	RT _L (s)	-5.69	4.05	2.83	-0.78	2.06	4.02	0.97
	RT _R (s)	-5.02	-2.77	-2.29	6.37	-0.32	-5.35	2.79
	IACC _{0,+}	0.89	-1.57	0.38	0.15	-1.82	2.44	5.72
	IACC _{0,80}	0.06	5.40	4.99	-0.22	1.42	3.79	5.56
	IACC _{80,+}	0.42	-7.71	-4.90	0.01	-1.37	-2.04	-3.83
BR			-5.26		--	--	--	
S-B	C _{80,L} (dB)	1.16	-3.67	-3.31	-1.17	-0.61	3.28	3.80
	C _{80,R} (dB)	1.50	2.14	-3.12	-0.56	3.09	0.02	0.77
	D _{50,L}	1.29	-0.08	-1.23	0.21	2.81	3.60	4.10
	D _{50,R}	3.59	5.97	2.59	2.86	4.02	4.46	4.03
	EDT _L (s)	-2.42	-5.03	3.25	3.81	3.41	-0.06	-1.98
	EDT _R (s)	-3.20	1.17	0.36	-0.81	2.34	1.43	-2.60
	RT _L (s)	-3.39	-0.75	-4.99	3.20	-1.32	-4.88	1.54
	RT _R (s)	-0.82	-1.45	0.03	-5.12	0.53	1.84	3.14
	IACC _{0,+}	1.92	-7.52	-1.03	7.45	1.74	3.39	1.33
	IACC _{0,80}	1.59	-3.19	-1.29	3.87	2.20	-0.37	-3.05
	IACC _{80,+}	2.02	-7.51	6.17	1.92	-0.94	1.17	2.14
BR			-1.66		--	--	--	
S-C	C _{80,L} (dB)	0.17	2.21	-1.17	3.58	0.57	1.60	4.26
	C _{80,R} (dB)	0.00	2.56	1.85	3.44	0.94	4.22	5.34
	D _{50,L}	-0.86	1.61	-1.90	3.86	1.02	1.68	1.49
	D _{50,R}	2.16	4.19	-1.00	2.65	1.15	3.50	5.89
	EDT _L (s)	0.61	-4.65	0.96	-2.71	1.12	-1.45	-3.47
	EDT _R (s)	0.14	-1.42	-2.00	-2.82	1.77	-1.43	-2.42
	RT _L (s)	2.26	-0.29	1.21	3.00	0.83	-2.36	-2.36
	RT _R (s)	3.02	-0.69	0.84	-0.05	1.11	0.27	5.43
	IACC _{0,+}	-3.75	-3.58	-1.22	2.76	2.55	2.09	3.14
	IACC _{0,80}	-4.03	-1.44	1.65	-1.89	-0.13	1.59	2.64
	IACC _{80,+}	-0.18	-5.63	4.25	1.63	-0.59	0.92	2.89
BR			1.00		--	--	--	
S-D	C _{80,L} (dB)	2.84	2.47	1.75	1.39	-2.77	-1.66	1.61
	C _{80,R} (dB)	2.35	-0.32	2.66	-0.27	-5.16	-0.95	4.04
	D _{50,L}	3.59	2.65	1.59	1.66	-2.29	-1.16	0.85
	D _{50,R}	4.61	3.51	1.83	2.17	-4.25	-1.53	4.06
	EDT _L (s)	-1.53	-2.27	-1.04	-0.87	3.48	-1.31	-4.14
	EDT _R (s)	-2.06	1.94	-0.30	0.37	1.08	-0.20	0.05
	RT _L (s)	-1.58	-1.66	2.78	-0.44	-1.79	-2.74	-4.07
	RT _R (s)	0.48	-0.46	0.09	-1.87	0.37	2.42	3.78
	IACC _{0,+}	1.45	-0.88	1.79	1.32	-2.72	-1.49	-0.25
	IACC _{0,80}	-0.56	-0.43	0.41	-2.12	-1.91	-2.23	0.06
	IACC _{80,+}	1.95	-1.80	0.42	3.33	-0.11	2.32	-0.66
BR			-0.04		--	--	--	

5.3.2 Hall B

Hall B has a totally different design from Hall A. Hall B has a smaller seating capacity from Hall A while its seating layout and stage curvature are also different from those of Hall A. The acoustic shell is in a convex shape towards the audience with its curvature following that of its seating plan. In general, this matching curvature of the shell with the hall geometry resulted in a higher uniformity of reverberance related acoustical parameters like EDT and reverberation time. Table 5-3 shows that such speciality in the layout does not affect the spaciousness parameters. As stated in the previous session, the main focus in this section is to observe the performances of four neural networking schemes inside this much smaller performance hall which having a totally different layout as in Hall A. The present investigation does not intend to compare the difference between the acoustical properties of Hall A and Hall B. Hereinafter, upper stall in Hall B refers to the area under the balcony (starting from Row S). The measurement points and the training points for Hall B are shown in Figure 5-1. One should note that the first three rows of seats were removed during the hall measurement and thus not measured or included in current study.

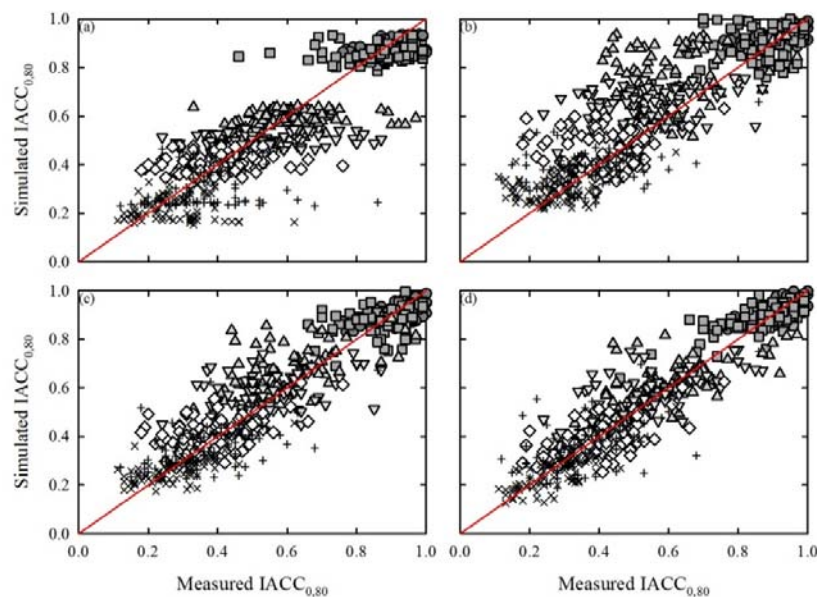


Figure 5-6 Comparison between simulated $IACC_{0,80}$ and measurements for Hall B under concert setting.

5.3.2.1 Concert setting

The measured $IACC_{0,80}$ for Hall B is compared with the predicted numbers in Figure 5-6. Expectedly, the performance of the prediction scheme can be improved by an increase

in the number of training data input to the prediction scheme, but one can observe from Figure 5-6 that the increase of training data from S-C to S-D does not give significant difference in their performance. Apparently, the schemes, except S-B, perform better in Hall B than in Hall A. Similar result pattern can be observed in other measured and predicted parameters including C_{80} , D_{50} , EDTs and RTs. Thus, the corresponding data are not presented.

Table 5-7 presents the root-mean-square differences between simulations and measurements for Hall B. In general, the increased number of training data here give the same effect in predicting the reverberance and spaciousness parameters: the performance for the reverberance parameters can be improved while that for the latter ones remain not affected. In spaciousness parameters prediction, S-A just performs slightly better than S-B. This performance pattern can be briefly observed in the analysis for Hall A in Table 5-4. All the four schemes give similar accuracy on the overall predictions of Bass Ratio. The predictions using S-C give similar degree of accuracy as S-D. Considering the number of training points used in the two schemes, S-C should be a more attractive option.

The statistical distributions of predicted C_{80} , EDT and $IACC_{0,80}$ within the bass and mid frequency range for Hall B under the concert setting are illustrated in Figure 5-7. The distribution of the measured data are also included for comparison. The scheme with the least number of training data, S-A fails again in $C_{80,bass}$ while the other 3 schemes give similar performances as shown in Figure 5-7a. However, in predicting C_{80} at mid frequencies, the all the four schemes gave similar performance, while the distributions of data obtained using S-C and S-D are closer to those obtained from the measured data as shown in Figure 5-7b. It can be observed that there is similar phenomenon for the EDTs in Figure 5-7c and d, but S-A is not as bad though it produces distributions with kurtosis considerably higher than those of the measurements, especially for the mid frequency EDT. Like in Hall A, the early hall spaciousness $IACC_{0,80,bass}$ at low frequencies have a narrow range. S-B, S-C and S-D give very similar prediction results and all the schemes can predict the mode of the statistical distribution accurately.

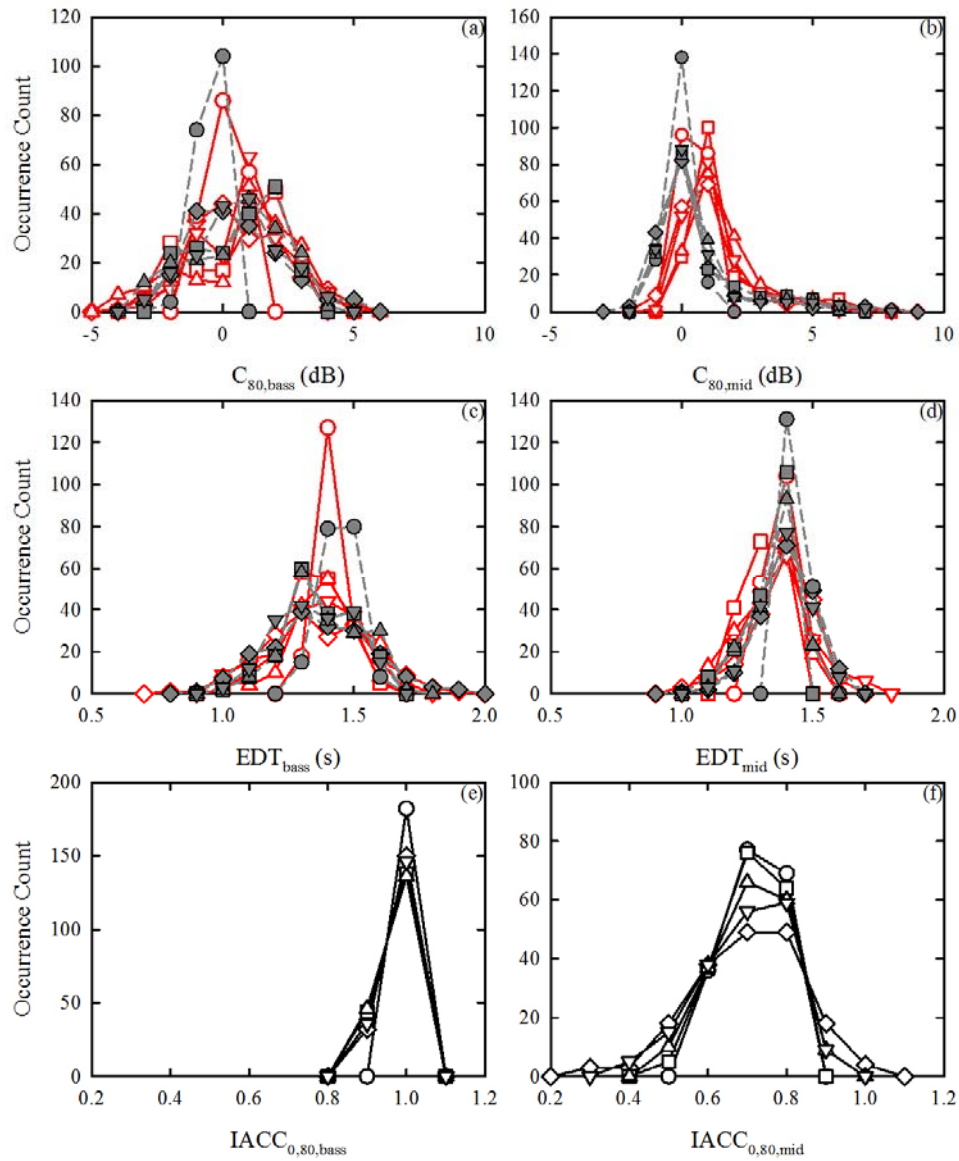


Figure 5-7 Statistical distributions of acoustical parameters under concert setting of Hall B. (a) $C80_{bass}$; (b) $C80_{mid}$; (c) EDT_{bass} ; (d) EDT_{mid} ; (e) $IACC_{0,80,bass}$; (f) $IACC_{0,80,mid}$. Legends same as those for Figure 5-4

Table 5-7 Root-mean-square differences between simulations and measurements for Hall B

Scheme	Parameter	Octave Band Centre Frequency (Hz)*						
		125	250	500	1000	2000	4000	8000
S-A	C _{80,L} (dB)	2.35/1.84	1.85/2.32	1.53/1.40	0.95/1.04	0.98/1.45	1.52/1.55	1.36/1.33
	C _{80,R} (dB)	3.23/2.38	1.99/1.98	1.26/1.39	1.10/1.16	1.27/1.46	1.84/1.87	1.88/1.46
	D _{50,L}	0.12/0.13	0.13/0.13	0.10/0.09	0.06/0.08	0.07/0.09	0.08/0.10	0.08/0.08
	D _{50,R}	0.13/0.13	0.13/0.13	0.08/0.09	0.07/0.09	0.08/0.09	0.11/0.11	0.11/0.09
	EDT _L (s)	0.20/0.24	0.19/0.22	0.14/0.17	0.09/0.13	0.08/0.12	0.13/0.11	0.08/0.10
	EDT _R (s)	0.19/0.27	0.17/0.21	0.12/0.16	0.14/0.11	0.08/0.12	0.12/0.13	0.09/0.09
	RT _L (s)	0.11/0.26	0.09/0.18	0.05/0.11	0.04/0.10	0.03/0.04	0.02/0.03	0.02/0.03
	RT _R (s)	0.12/0.26	0.09/0.17	0.04/0.10	0.06/0.06	0.02/0.04	0.03/0.03	0.02/0.02
	IACC _{0,+}	0.04/0.04	0.07/0.07	0.13/0.10	0.10/0.10	0.06/0.12	0.08/0.12	0.06/0.09
	IACC _{0,80}	0.07/0.07	0.10/0.11	0.12/0.13	0.13/0.12	0.11/0.15	0.15/0.15	0.11/0.13
	IACC _{80,+}	0.05/0.04	0.07/0.07	0.12/0.11	0.07/0.09	0.02/0.08	0.03/0.11	0.02/0.05
BR			0.05/0.04		--	--	--	
S-B	C _{80,L} (dB)	1.75/2.10	1.94/1.89	1.28/1.06	0.91/0.94	0.96/1.17	1.32/1.35	1.15/1.25
	C _{80,R} (dB)	1.67/1.88	1.65/1.55	1.20/0.95	1.02/0.86	1.07/1.20	1.48/1.29	1.37/1.35
	D _{50,L}	0.10/0.17	0.10/0.11	0.06/0.08	0.05/0.06	0.06/0.09	0.08/0.09	0.08/0.08
	D _{50,R}	0.10/0.13	0.10/0.11	0.07/0.08	0.06/0.07	0.08/0.10	0.10/0.10	0.09/0.10
	EDT _L (s)	0.20/0.27	0.23/0.15	0.10/0.14	0.09/0.11	0.09/0.12	0.09/0.16	0.07/0.12
	EDT _R (s)	0.18/0.31	0.18/0.19	0.10/0.13	0.11/0.10	0.07/0.10	0.12/0.11	0.08/0.09
	RT _L (s)	0.10/0.27	0.11/0.19	0.06/0.11	0.04/0.08	0.03/0.04	0.02/0.03	0.01/0.03
	RT _R (s)	0.10/0.29	0.08/0.16	0.04/0.12	0.04/0.07	0.02/0.04	0.03/0.03	0.02/0.02
	IACC _{0,+}	0.05/0.03	0.09/0.08	0.19/0.09	0.14/0.08	0.09/0.12	0.10/0.11	0.06/0.07
	IACC _{0,80}	0.05/0.05	0.10/0.11	0.21/0.14	0.18/0.12	0.13/0.12	0.12/0.12	0.10/0.10
	IACC _{80,+}	0.07/0.05	0.11/0.08	0.22/0.09	0.09/0.07	0.02/0.08	0.03/0.11	0.02/0.05
BR			0.05/0.05		--	--	--	
S-C	C _{80,L} (dB)	1.86/1.71	1.74/1.70	0.94/0.91	0.68/0.75	0.76/1.06	1.09/1.34	0.92/1.18
	C _{80,R} (dB)	1.79/1.94	1.70/1.49	0.85/0.89	1.00/0.64	1.12/1.11	1.59/1.15	1.43/1.19
	D _{50,L}	0.11/0.12	0.09/0.12	0.06/0.06	0.04/0.05	0.06/0.09	0.08/0.09	0.06/0.07
	D _{50,R}	0.10/0.11	0.08/0.11	0.05/0.06	0.06/0.05	0.07/0.08	0.10/0.08	0.09/0.07
	EDT _L (s)	0.21/0.23	0.21/0.14	0.10/0.13	0.09/0.10	0.07/0.09	0.10/0.13	0.06/0.10
	EDT _R (s)	0.18/0.24	0.18/0.16	0.09/0.13	0.09/0.09	0.07/0.09	0.12/0.11	0.06/0.08
	RT _L (s)	0.09/0.27	0.11/0.17	0.05/0.10	0.04/0.08	0.03/0.04	0.02/0.03	0.01/0.03
	RT _R (s)	0.10/0.27	0.09/0.15	0.04/0.10	0.05/0.06	0.02/0.04	0.02/0.03	0.02/0.02
	IACC _{0,+}	0.04/0.03	0.06/0.06	0.14/0.06	0.10/0.06	0.06/0.09	0.09/0.09	0.04/0.06
	IACC _{0,80}	0.05/0.05	0.08/0.09	0.12/0.10	0.12/0.09	0.10/0.10	0.11/0.11	0.07/0.09
	IACC _{80,+}	0.05/0.04	0.07/0.07	0.15/0.09	0.07/0.06	0.02/0.07	0.03/0.10	0.02/0.05
BR			0.04/0.04		--	--	--	
S-D	C _{80,L} (dB)	1.51/1.48	1.24/1.41	1.19/0.70	0.57/0.72	0.71/0.88	0.87/1.04	0.86/1.06
	C _{80,R} (dB)	1.43/1.42	1.37/1.33	0.97/0.77	0.92/0.63	1.05/0.87	1.43/0.94	1.31/0.96
	D _{50,L}	0.08/0.11	0.08/0.09	0.05/0.05	0.04/0.05	0.05/0.07	0.06/0.08	0.05/0.05
	D _{50,R}	0.07/0.11	0.07/0.08	0.05/0.05	0.06/0.04	0.07/0.06	0.09/0.07	0.10/0.05
	EDT _L (s)	0.18/0.19	0.19/0.12	0.11/0.11	0.09/0.08	0.06/0.08	0.09/0.11	0.07/0.07
	EDT _R (s)	0.15/0.23	0.16/0.15	0.08/0.13	0.10/0.08	0.05/0.08	0.10/0.09	0.06/0.07
	RT _L (s)	0.08/0.25	0.08/0.16	0.04/0.10	0.04/0.08	0.02/0.03	0.02/0.03	0.01/0.02
	RT _R (s)	0.10/0.27	0.07/0.14	0.04/0.10	0.03/0.06	0.02/0.03	0.02/0.02	0.02/0.02
	IACC _{0,+}	0.04/0.03	0.05/0.06	0.10/0.06	0.09/0.05	0.06/0.08	0.08/0.07	0.04/0.05
	IACC _{0,80}	0.04/0.04	0.07/0.09	0.10/0.10	0.11/0.07	0.09/0.08	0.11/0.07	0.06/0.07
	IACC _{80,+}	0.04/0.03	0.06/0.06	0.11/0.08	0.06/0.05	0.02/0.06	0.03/0.10	0.02/0.04
BR			0.04/0.04		--	--	--	

*concert / proscenium

Table 5-8. Paired t-test statistics for vanishing differences between simulations and measurements under concert setting of Hall B (95% confidence level)

Scheme	Parameter	Octave Band Centre Frequency (Hz)						
		125	250	500	1000	2000	4000	8000
S-A	C _{80,L} (dB)	-5.82	0.69	-1.64	-3.18	2.73	4.27	5.22
	C _{80,R} (dB)	-12.03	-1.54	-0.42	-4.15	2.13	4.39	3.85
	D _{50,L}	-5.99	-3.27	-5.07	0.45	1.80	2.76	2.62
	D _{50,R}	-7.88	-2.62	-2.79	0.67	0.91	1.71	0.59
	EDT _L (s)	-0.93	-1.07	0.20	-0.69	-1.05	-6.57	-3.51
	EDT _R (s)	-0.83	0.12	4.70	6.01	0.26	0.00	-2.15
	RT _L (s)	-2.30	-6.53	3.28	2.57	-1.09	0.34	1.41
	RT _R (s)	0.11	-1.69	-1.72	-6.46	-1.22	-3.71	-0.10
	IACC _{0,+}	-1.84	0.35	-2.48	-1.98	2.64	-1.01	-4.78
	IACC _{0,80}	-7.06	-0.69	-1.64	-2.10	0.39	-4.12	-3.90
	IACC _{80,+}	-0.84	1.62	0.59	-2.06	0.81	-0.75	0.45
	BR			-3.20		--	--	--
S-B	C _{80,L} (dB)	-2.45	-5.78	3.04	4.93	-0.08	-2.91	-1.28
	C _{80,R} (dB)	-1.24	-1.98	5.78	1.41	0.53	-0.45	-3.71
	D _{50,L}	-4.57	-1.97	2.66	4.72	2.30	1.91	1.52
	D _{50,R}	-4.22	-6.42	5.51	4.52	0.21	0.66	-1.63
	EDT _L (s)	-2.46	3.16	1.40	-1.08	-3.05	0.81	1.71
	EDT _R (s)	-1.85	-3.32	-0.71	-2.22	-0.95	-0.48	0.54
	RT _L (s)	-3.49	-7.95	5.12	-1.98	4.17	-2.19	-0.72
	RT _R (s)	-3.06	-2.77	-3.97	-3.79	-3.58	5.39	3.87
	IACC _{0,+}	5.39	6.50	8.46	8.93	4.85	3.09	3.97
	IACC _{0,80}	1.55	2.40	8.18	7.59	3.71	1.09	3.03
	IACC _{80,+}	5.62	8.57	10.41	7.91	-0.06	2.39	1.81
	BR			-4.74		--	--	--
S-C	C _{80,L} (dB)	-5.22	-2.38	-0.24	1.74	0.45	1.89	-1.04
	C _{80,R} (dB)	-5.85	-2.95	2.69	1.35	-0.09	1.44	0.63
	D _{50,L}	-2.99	-3.62	1.31	2.22	1.94	2.50	2.32
	D _{50,R}	-4.99	-4.55	1.75	1.50	0.45	1.63	-0.16
	EDT _L (s)	-3.31	-1.54	1.08	0.11	-1.63	-3.00	0.24
	EDT _R (s)	-0.57	-2.52	0.55	4.40	-0.91	-1.26	-0.23
	RT _L (s)	-1.13	-7.57	3.65	0.38	2.73	-1.46	0.39
	RT _R (s)	-0.59	-2.26	-2.37	-5.40	-3.32	1.73	2.03
	IACC _{0,+}	2.50	3.32	7.47	5.21	3.52	2.42	1.23
	IACC _{0,80}	-2.98	1.15	5.03	2.53	1.72	-1.15	-0.52
	IACC _{80,+}	3.77	4.18	7.38	4.19	0.15	1.85	2.06
	BR			-2.87		--	--	--
S-D	C _{80,L} (dB)	-0.90	0.46	-0.31	2.33	0.31	0.36	-0.48
	C _{80,R} (dB)	-3.07	-2.02	0.51	2.76	0.43	1.09	1.82
	D _{50,L}	-0.40	1.14	-1.09	3.90	0.42	0.37	0.56
	D _{50,R}	-1.62	-0.56	1.34	2.23	-0.64	0.88	-2.43
	EDT _L (s)	-3.28	-0.38	1.25	-2.99	-0.77	-1.04	3.47
	EDT _R (s)	-0.51	-2.40	-0.38	2.56	-0.88	-0.24	0.71
	RT _L (s)	2.50	-2.31	1.97	0.01	-0.87	-0.60	0.60
	RT _R (s)	-2.66	0.27	-0.18	-1.42	0.02	2.62	-1.01
	IACC _{0,+}	3.44	2.49	2.53	4.90	-0.65	0.66	0.95
	IACC _{0,80}	0.10	2.30	1.30	3.22	-1.21	0.04	-2.77
	IACC _{80,+}	3.10	0.09	1.48	-0.32	1.52	0.39	2.34
	BR			-1.27		--	--	--

S-B and S-A do not perform well in predicting the $IACC_{0,80}$ at low frequencies. S-B literally fail and S-A is the second worst. The performances of S-C and S-D are similar; however, the shape of the statistical distribution can be predicted by neither of the schemes, despite the large number of training data points used in S-D.

Table 5-7 and Table 5-8 show the point-by-point differences between the predicted and measured values. It can be seen that the performance of S-B is the worst, while S-A and S-C give comparable performance. Generally, S-D is considered to be the best scheme, but, its ability to predict the mid-frequency reverberance parameters are yet comparable with S-C. S-D is barely better than S-C in the prediction of hall spaciousness. From Table 5-6 and Figure 5-7, one can see that S-A and S-B are less desirable, while S-C and S-D are giving comparable performance. S-C requires fewer training points required which makes it slightly more preferable for the present application. This is in-line with the results obtained in Hall A.

5.3.2.2 Proscenium setting

Without the acoustic shell in the proscenium setting, as shown Table 5-3, the spatial variations of the acoustical properties inside Hall B become larger. The weaker reverberation enhances the clarities and definition, but reduces the spaciousness feeling. In term of the root-mean-square difference between prediction and measurement, S-D performs the best as illustrated in Table 5-7 while a better performance requires a larger number of training points. Though this is rather expected, one can notice that the differences between S-C and S-D are very small.

All the schemes except S-A can predict the statistical distributions of the C_{80} at bass to mid frequencies as shown in Figure 5-8a and Figure 5-8b. It appears that S-C and S-D performed slightly better for $C_{80,bass}$ and $C_{80,mid}$ respectively. The EDT_{bass} distributions predicted by using S-A and S-B are not satisfactory, while S-C and S-D give similar prediction results and can produce a similar statistical distributions following those of the measured data as seen in Figure 5-8c. In the mid frequency range in Figure 5-8d, S-A performed the worst again. The predicted EDT_{mid} using S-B has a proper distribution skewness but with larger kurtosis. Again, S-C and S-D give more accurate predictions and their performances are similar. Results shown in Figure 5-8e and Figure 5-8f indicate that the distribution mode can be predicted by all the four schemes accurately. Similar

IACC_{0,80} statistical distribution can be predicted even with a small number of training points, the results of S-A at bass frequencies are also acceptable.

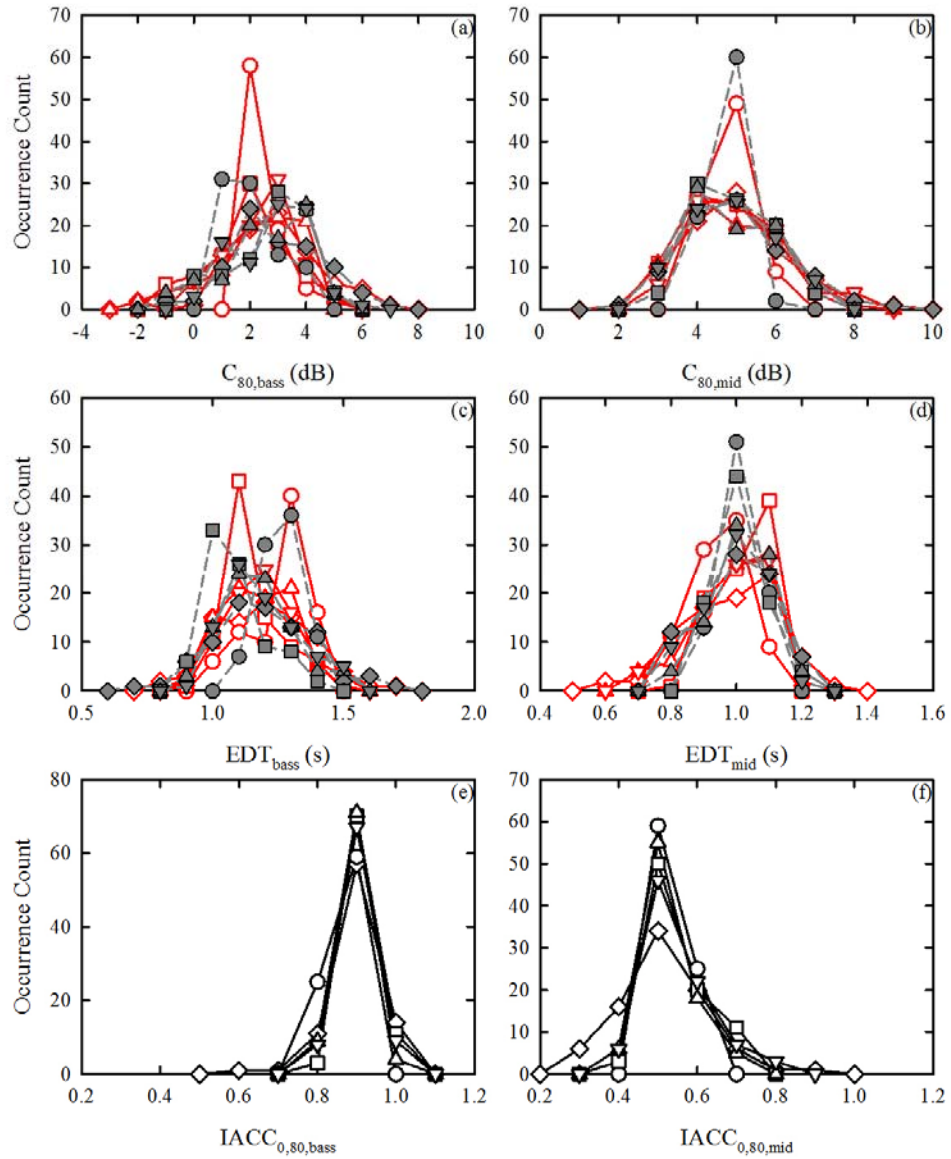


Figure 5-8 Statistical distributions of acoustical parameters under proscenium setting of Hall B. (a) $C_{80,bass}$; (b) $C_{80,mid}$; (c) EDT_{bass} ; (d) EDT_{mid} ; (e) $IACC_{0,80,bass}$; (f) $IACC_{0,80,mid}$. Legends : same as those for Figure 5-4

Table 5-9. Paired t-test statistics for vanishing differences between simulations and measurements under proscenium setting of Hall B(95% confidence level)

Scheme	Parameter	Octave Band Centre Frequency (Hz)						
		125	250	500	1000	2000	4000	8000
S-A	C _{80,L} (dB)	-1.72	-2.03	0.95	-2.16	-0.14	0.62	0.25
	C _{80,R} (dB)	-7.03	-1.78	-1.10	-3.79	0.58	-3.25	-3.27
	D _{50,L}	-0.67	-3.18	-1.24	-2.68	1.83	1.34	-1.19
	D _{50,R}	-4.51	-3.24	-2.08	-3.09	0.07	-0.54	-1.20
	EDT _L (s)	1.53	3.37	-4.92	-1.31	-1.57	-0.21	0.53
	EDT _R (s)	1.39	3.53	2.67	-0.04	-0.17	4.40	3.94
	RT _L (s)	-1.68	0.99	-2.54	-7.07	0.95	-4.15	-0.95
	RT _R (s)	2.49	1.09	0.63	1.88	2.56	-2.25	-3.81
	IACC _{0,+}	-6.47	-0.40	3.02	-2.98	-0.26	-1.44	0.67
	IACC _{0,80}	-9.40	-1.54	1.48	-0.52	1.11	-0.26	-0.89
	IACC _{80,+}	-0.94	2.93	6.42	-1.21	-0.60	0.36	-1.72
	BR			-2.10		--	--	--
	S-B	C _{80,L} (dB)	-4.28	-4.22	-4.19	1.27	-3.59	-0.73
C _{80,R} (dB)		-0.37	-1.10	-0.77	3.10	-1.69	0.57	2.08
D _{50,L}		-5.10	-3.67	-7.11	3.84	-0.89	-1.62	0.74
D _{50,R}		-2.14	-5.00	-4.61	2.84	-0.24	2.16	0.06
EDT _L (s)		-3.67	0.65	2.07	0.46	5.80	5.05	0.38
EDT _R (s)		-5.42	-3.41	-1.00	0.41	2.95	3.21	-0.37
RT _L (s)		-3.58	-2.21	-1.82	-0.79	0.92	-0.64	-0.22
RT _R (s)		1.27	0.75	-6.71	-3.01	0.16	-2.02	0.21
IACC _{0,+}		3.98	3.13	2.70	3.29	2.78	2.73	1.56
IACC _{0,80}		1.49	2.54	1.56	2.08	2.12	2.52	1.32
IACC _{80,+}		6.54	4.29	3.27	1.65	0.73	-0.64	1.12
BR				-6.26		--	--	--
S-C		C _{80,L} (dB)	-2.13	-3.33	-1.29	-0.10	-0.55	-0.79
	C _{80,R} (dB)	-1.19	-2.79	-2.38	-0.62	-1.06	-0.85	0.33
	D _{50,L}	-3.83	-5.02	-5.43	1.99	0.88	-0.02	1.11
	D _{50,R}	-3.47	-4.56	-4.58	-1.64	-0.51	0.44	-0.34
	EDT _L (s)	-3.22	2.12	-0.21	-0.12	0.95	3.11	-0.97
	EDT _R (s)	-3.16	0.98	0.62	1.16	3.46	4.49	1.19
	RT _L (s)	-2.68	-0.73	-1.86	-3.23	1.09	-3.38	-1.59
	RT _R (s)	1.73	1.08	-3.79	-0.60	1.08	-2.96	-2.96
	IACC _{0,+}	0.73	2.07	2.89	0.60	2.58	1.53	2.29
	IACC _{0,80}	-2.08	0.56	0.61	0.55	1.19	1.47	0.03
	IACC _{80,+}	3.44	3.76	4.87	1.25	0.64	0.37	-0.68
	BR			-3.08		--	--	--
	S-D	C _{80,L} (dB)	-2.27	-2.74	-0.84	0.78	2.56	2.74
C _{80,R} (dB)		-1.13	-0.60	-0.59	-1.76	-0.62	0.03	-0.99
D _{50,L}		-2.50	-2.91	-1.92	0.95	1.34	2.56	1.07
D _{50,R}		-3.06	-2.68	-1.77	-2.21	0.39	-0.16	-0.47
EDT _L (s)		-1.63	-0.11	-0.76	-0.44	-1.66	-0.81	-0.32
EDT _R (s)		-2.12	1.49	0.39	-0.66	-0.26	-0.13	-0.36
RT _L (s)		1.36	0.61	1.26	-0.56	0.58	-1.83	0.34
RT _R (s)		2.57	-0.07	-0.71	-0.75	0.64	-0.38	-0.33
IACC _{0,+}		1.86	1.86	4.14	2.56	3.01	0.96	0.09
IACC _{0,80}		-0.10	1.72	3.37	2.50	2.94	3.27	2.25
IACC _{80,+}		2.24	1.66	2.63	-0.87	-0.37	-1.78	-0.49
BR				-1.18		--	--	--

The Point-by-point paired- t test results in Table 5-9 present the deviations of the neural network simulations from the measurement results in a more detail way. It is again observable that reverbrance-related parameters with more training data are easier to be predicted with a higher accuracy. However, S-D, with the largest number of training data inputs, is not producing early hall spaciousness accurate that can only marginally pass the paired- t test. On the other hand, S-C has reasonable estimations of these $IACC_{0,80s}$. This can be concluded from Table 5-7, Table 5-9 and Figure 5-8. Meanwhile, it can also predict the mid-frequency reverbrance parameters acceptably; yet, its results for the 500 Hz D_{50} are marginally acceptable. In addition, with reference to the overall root-mean-square difference results shown in Table 5-7. S-C is a more preferable scheme for Hall B under the proscenium setting. The schemes S-A and S-B do not have a very good performance in the paired t -test, but that of the $IACC_{0,80,mid}$ are still acceptable, this confirmed once again that the neural network prediction for the hall spaciousness does not require large amount of training data.

5.4 Conclusions

Two multi-purpose performance halls with balcony have been measured binaurally in a detailed way. They are of different design and seating capacity. They are with 1372-seat in rectangular shape and 919-seat in fan shape layout respectively. In each of the hall, the seating area was divided into three specific sub-areas, including the stall, the upper stall and balcony in the present study. The measurements points were approximately 10% of the total seating locations throughout the hall. The effectiveness of using neural network in the prediction of the acoustical properties inside these halls was examined in terms of point-by-point deviations from measurements and overall statistical distributions of acoustical parameters. This neural network was trained with four different training schemes which have different numbers of training input. All schemes consisted of three training data sets selecting point from each specific zone in the hall. The first scheme used points from the near and far ends and the centre point of each zone. The second one took 3 sets of data from the closet and further rows from the stage of each zone. The third one was a combination of scheme one and scheme two while the last one was a more detailed set of the third scheme with a finer span-wise resolution. To maintain the simplicity of the inputs, the inputs to the neural network algorithm are the spherical coordinates of the measurement points. This study had included both the concert hall and proscenium setting

of the halls concerned. A relatively simple neural network prediction algorithm was adopted.

The present result is independent of the stage setting and hall design. A small number of training data input with points only from the middle region or from the boundaries of each specific hall area fails to produce acceptable results. The more reverberant the hall is, such as in a concert hall setting instead of proscenium setting, the results were varying less spatially. Hence, the difference between the performance of the four neural network training scheme is less differentiable. In general, the more input data is given to train the neural network, the better the performance, in terms of the overall root-mean-square deviation from measurements, statistical distribution matching and point-to-point statistical deviations, can be achieved.

Scheme three with nine uniformly distributed data points within each zone appears to be the best choice in both all hall design and setting, while the differences of its predictions from measurements are acceptable. Further increasing the number of training data, even to 70% more in scheme four, can only yield insignificant improvement on the prediction accuracy. The result also shows that it only requires a smaller amount of training data in predicting the hall spaciousness parameters than predicting the reverberance parameters, regardless of the hall design and setting.

In the present study, the two performance halls selected are very different in designs and layouts; therefore, it is believed that the present findings are relevant to other multi-purpose performance halls. A simple framework for the evaluation of performance hall acoustics is established, at least for halls with similar level of reverbrance.

Chapter 6 The influence of geometrical parameters on early interaural cross-correlation coefficients, $IACC_{E3}$

6.1 Introduction

Studies focused on the development of psycho-acoustical indices that can quantify hall performance have been rigorously conducted in the past few decades. Apart from the commonly used Reverberation Time and Early Decay Time, the energy-based indices Clarity and Definition have been proposed to cater for a balance between clarity and reverberation.[12], [93] Ando and Imamura[91] and Barron and Marshall[94] found that the interaural cross-correlation coefficients (IACC) have good relationships with the perceived spatial impression, while Hidaka et al.[92] suggested to use them as a measure of acoustical quality. There are also studies investigating into the relationships between various developed indices, for instance, Okano et al.,[95] Carvalho[96] and Tang.[97] These indices include IACC, coefficient lateral fraction (LFE), apparent source width (ASW) and Rasti rapid speech transmission index (RASTI), D50, C80, centre time (T_s) and reverberation times.

The prediction of objective performance indices is also a hot topic. However, owing to the complexity of a performance hall, analytical formulae are hardly available. There are formulae for the prediction of energy-based indices, but it is done with an assumption of exponential sound decay in the halls.[90], [98] The ray-tracing algorithm[99] follows the development of rays and is able to provide information for the estimation of basically all performance hall indices when used together with the image-source method. However, the modelling of surfaces and the complex internal hall geometry has been a big challenge. Nannariello and Frickle[20] investigated the application of neural networks for predictions. However, the neural network requires a reliable database to function. Thus, general information from different halls may only be able to give indicative predictions.

In this chapter, the binaural hall measurement results from the last chapter were analysed using the regression approach. An improved scheme for the prediction of the mid-frequency early interaural cross correlation, $IACC_{E3}$ using small number of measured data and regression inputs were found. The binaural quality index ($1 - IACC_{E3}$) relates closely

with the mid-frequency hall spaciousness.[20], [22] In this chapter, a detailed regression analysis done using data obtained from hall A surveyed in the previous chapter is firstly presented in the first place. It is followed by a validation using the results of the Hall B surveyed.

6.2 The Surveyed Hall and Measurements

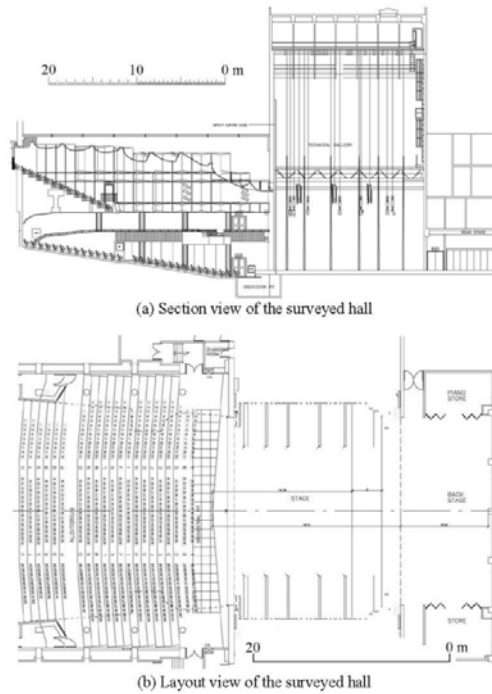


Figure 6-1 Layout and dimensions of Hall A



(a) Proscenium Stage



(b) Concert Setting (with Acoustic shells on stage)

Figure 6-2 Two different settings of Hall A

Hall A was chosen for the illustration of the present regression analysis approach. Its internal shape is rectangular with a total seating capacity of 1372 (stall: 589, upper stall: 443, balcony: 340). Figure 6-1 illustrates the layout and dimensions of this hall. It is a multi-purpose hall with two basic settings: proscenium and concert (Figure 6-2). This design is typical among all the auditoriums in Hong Kong. Hall B was chosen to validate the model built from Hall A's data. Hall B is a younger hall in Hong Kong which is of a fan-like internal shape with a modern design. Its seating capacity is smaller than that in Hall A.

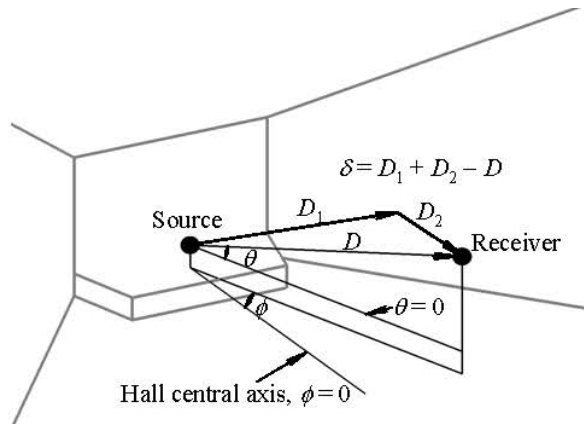


Figure 6-3 Definitions of the Geometrical parameters

In this study, it was targeted to predict the early IACC from the correlations between the binaural signals measured, therefore, only the first reflection measured was considered for the calculation of the geometric parameters. The azimuthal angle ϕ , the elevation angle θ , the source-to-receiver distance D and the path difference δ was founded to be affecting the correlations. Figure 6-3 shows the definitions of these geometrical parameters graphically. Both the azimuthal angle and elevation angle define the angular position of a receiver point relative to the centreline of the hall and the horizontal respectively. While the travelling distance D affects the strength of the signal received at each measured point, the path difference δ represents the differences in the direct source-receiver distances and actual distance that the sound energy travelled and undergone the first reflection at the hall boundary opposite to the direct sound arrival direction before reaching the measured location. In order to make the coefficients non-dimensional, the overall longitudinal length of the hall, L_{\max} , was used to normalize D , while δ is made non-dimensional using D . Whereas the angular parameters θ and ϕ are normalized by 30° and 90° respectively. The abovementioned normalization of D , θ and ϕ does not affect the regression statistics. However, the normalisation of δ by a spatially varying D rather than a constant gave a better result in the regression.

6.3 Regression Analyses

6.3.1 IACC_{E3} and distance

Multi-variant regression analysis does not usually give rise to physically sound formulae for prediction purposes. However, it is quite commonly done for topics where analytical

solution is nearly impossible to establish.[100], [101] Figure 6-4 shows the variations of $IACC_{E3}$ with distance from source, D , in Hall A with the concert and proscenium setting. One can see that no matter a linear fit, a quadratic fit nor a cubic fit would result with weak correlation. These variations were obviously not linear which was expected. The quadratic fit of D was slightly better than the linear fit as shown in Figure 6-4a and b. The cubic fit was very close to the quadratic one in both cases and thus that for the proscenium setting was not presented in Figure 6-4a . Under concert hall setting, the three fittings were weakly correlated with very similar standard errors. Though the $IACC_{E3}$ was not the sole function of D , Figure 6-4 illustrated that it tended to decrease with increasing D . The variations of $IACC_{E3}$ and D under the concert hall setting were weak.

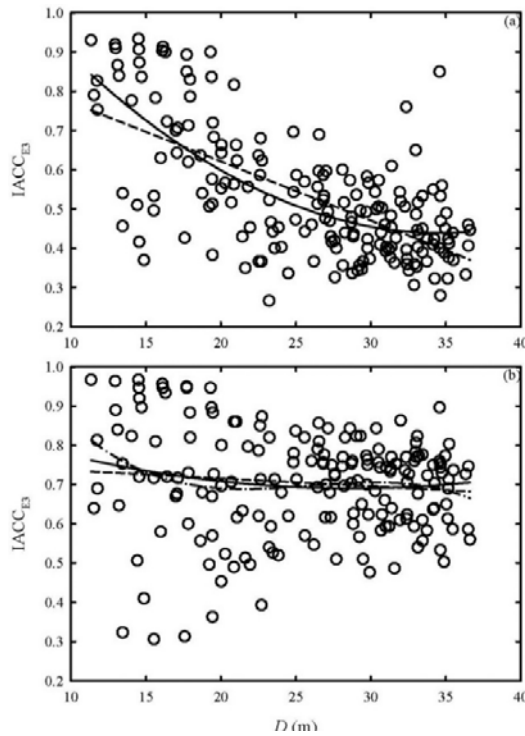


Figure 6-4 Variation of $IACC_{E3}$ with distance from source D in Hall A (a) Proscenium stage; (b) concert setting.

○ : Measured data; — : linear fit; - - - : quadratic fit; - · - : cubic fit.

6.3.2 Regression fitting

There are many nonlinear functional forms for curve fitting, for simplicity as well as practicality, only the polynomial one is adopted here. Cross terms formed by the products of the different geometrical parameters are not considered. A procedure was developed to generate the regression models in this study systematically. One major objective is to keep minimise the number of regression inputs. A quadratic form of D was firstly adopted as hinted by Figure 6-4 (discussed further in section 6.3.2C). The most effective

parameter among ϕ , θ and δ was then included with the order of the corresponding polynomial increased until a drop of prediction efficiency was observed. The next effective parameter was then added to the model and this cycle continued until all the four geometrical parameters were tested. The prediction efficiency was reflected by a higher standard error or lower adjusted R^2 . This procedure should guarantee that a regression model of the lowest possible standard error is generated. As there are two hall settings and each of them results in different acoustical properties of the hall, the corresponding results are analysed separately.

A. Proscenium Stage Setting

Table 6-1 Regression Analysis at 95% confidence level for the proscenium stage case of Hall A with all 182 data included

Model	Regression Inputs*	Correlation Coefficient, R^2	Adjusted R^2	Standard Error, ϵ	F	$F_{critical}$	Significance
PA01	D, D^2	0.4575	0.4515	0.1213	75.47	3.05	0.000
PA02	$D, D^2, \phi $	0.7297	0.7251	0.0859	106.18	2.66	0.000
PA03	D, D^2, θ	0.4730	0.4641	0.1199	53.26	2.66	0.000
PA04	D, D^2, δ	0.6148	0.6083	0.1025	94.71	2.66	0.000
PA05	$D, D^2, \phi , \phi^2 $	0.7336	0.7276	0.0855	121.84	2.42	0.000
PA06	$D, D^2, P(\phi , 3)$	0.7383	0.7309	0.0850	99.32	2.27	0.000
PA07	$D, D^2, P(\phi , 4)$	0.7389	0.7299	0.0851	82.52	2.15	0.000
PA08	$D, D^2, P(\phi , 3), \theta$	0.7657	0.7576	0.0806	92.30	2.15	0.000
PA09	$D, D^2, P(\phi , 3), \delta$	0.7434	0.7346	0.0843	84.49	2.15	0.000
PA10	$D, D^2, P(\phi , 3), P(\theta, 2)$	0.7903	0.7818	0.0765	93.66	2.06	0.000
PA11	$D, D^2, P(\phi , 3), P(\theta, 3)$	0.7959	0.7865	0.0757	84.34	1.99	0.000
PA12	$D, D^2, P(\phi , 3), P(\theta, 4)$	0.8116	0.8017	0.0729	82.30	1.93	0.000
PA13	$D, D^2, P(\phi , 3), P(\theta, 5)$	0.8183	0.8077	0.0718	77.01	1.89	0.000
PA14	$D, D^2, P(\phi , 3), P(\theta, 6)$	0.8208	0.8092	0.0715	70.80	1.85	0.000
PA15	$D, D^2, P(\phi , 3), P(\theta, 7)$	0.8216	0.8089	0.0716	64.85	1.81	0.000
PA16	$D, D^2, P(\phi , 3), P(\theta, 6), \delta$	0.8210	0.8083	0.0717	64.58	1.81	0.000
PA17	$D, D^2, P(\phi , 3), P(\theta, 6), P(\delta, 2)$	0.8210	0.8072	0.0719	59.28	1.78	0.000
PA18	$D, D^2, \phi , P(\theta, 2)$	0.7857	0.7796	0.0769	129.02	2.27	0.000

* $P(x, n)$: Polynomial in x of order n .

Proscenium stage is usually set for conducting musicals or when the hall is used as an auditorium. This hall is marginally symmetrical in terms of acoustical properties presented in Chapter 4. Table 6-1 summarizes the regression statistics of different combinations of geometrical parameters with IACC_{E3}, numbered from PA01 to PA18. Under this scheme, measurement scheme A, all 182 sets of measurement data were included in the modelling. The analysis starts from PA01 that is with the quadratic form of D . The regression with $|\phi|$ are having significantly better results than those with ϕ and thus only those with the former are presented. This is probably due to the marginal acoustical symmetry of the proscenium setting of the hall as explained in Chapter 4. From the results, it is observed that ϕ is more influential than θ and δ .

The inputs size is large here: all the 182 measurement data sets are used in the regression analysis. Seeing the correlation coefficients and error terms of the better performed Model PA08 than Model PA09, one can see that the implicit inclusion of θ in δ is not as

effective as the direct inclusion of θ once ϕ is included in the regression model. This indicates that path difference, δ is the least important parameter among the four geometrical parameters studied in this investigation. If a large enough database is available for analysis, δ can be used to fine tune the regression model performance. The other models also demonstrate the unimportance of δ : the best performing model PA14, only consists of a linear combination of a sixth order polynomial of θ and a third order polynomial of $|\phi|$ but not δ .

In fact, the standard errors of Model PA05 to PA18 are all less the root-mean-square differences by the neural network prediction schemes in Chapter 5. However, while the measurement data used here only covers around 13% of the total seating capacity of the hall, it is not effective to predict the IACC_{E3} distribution in this hall. The regression analysis done here is to give a rough idea on the best model that can be achieved by regression analysis. Model PA18 is not generated using the present proposed procedure, but is included here for later discussion.

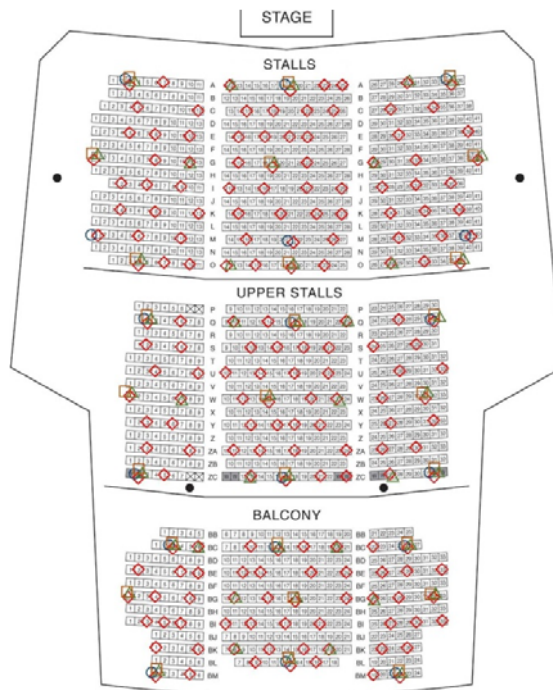


Figure 6-5 Measurement Schemes adopted in Hall A

◇ : Scheme A; ○ : Scheme B; □ : Scheme C; △ : Scheme D

There can be many ways to select measurement points, the 182 measurement points were selected randomly during measurements and further selected to form Scheme A, B, C and D as mentioned in previous chapter. However, one of the schemes, Scheme A, with only 9 points is not suitable for regression analysis as such measurement scheme will result in extrapolation of regression formula during prediction, which will certainly bring large errors. In the rest of this Section 6.3.2, the performances of the other three measurement schemes adopted in previous chapter are investigated. Figure 6-5 shows these schemes again, namely hereinafter as Schemes B, C and D. Scheme B has 18 measurement points on the near and far boundaries of each sub-area in the hall. Scheme C has 27 measurement points, which are made of up the 18 measurement points in Scheme B and additional points in the middle of each sub-zone. Scheme D, which includes 45 measurement points, is formed by adding two rows of measurement points on the two sides of the middle longitudinal row of measurement points in Scheme C.

Table 6-2 Regression Analysis at 95% confidence level for the proscenium case of Hall A (Scheme B)

Model	Regression Inputs*	Correlation Coefficient, R^2	Adjusted R^2	Standard Error, ε	F	$F_{critical}$	Significance
PB01	D, D^2	0.1182	0.0006	0.1966	1.01	3.68	0.389
PB02	D, D^2, ϕ	0.1251	-0.0624	0.2027	0.67	3.34	0.586
PB03	D, D^2, θ	0.1408	-0.0432	0.2009	0.76	3.34	0.533
PB04	D, D^2, δ	0.5016	0.3948	0.1531	4.70	3.34	0.018
PB05	$D, D^2, \phi $	0.7090	0.6466	0.1169	11.37	3.34	0.000
PB06	$D, D^2, \phi , \phi^2 $	0.7177	0.6308	0.1195	8.26	3.18	0.002
PB07	D, D^2, ϕ , θ	0.8043	0.7441	0.0995	13.36	3.18	0.000
PB08	D, D^2, ϕ , δ	0.7134	0.6253	0.1204	8.09	3.18	0.002
PB09	$D, D^2, \phi , P(\theta, 2)$	0.8213	0.7468	0.0990	11.03	3.11	0.000
PB10	$D, D^2, \phi , P(\theta, 3)$	0.8270	0.7327	0.1017	8.77	3.09	0.001
PB11	$D, D^2, \phi , P(\theta, 2), \delta$	0.8285	0.7349	0.1013	8.86	3.09	0.001
PB12	$D, D^2, \phi , P(\theta, 2), P(\delta, 2)$	0.8332	0.7164	0.1047	7.13	3.14	0.003
PB13	$D, D^2, \phi , P(\theta, 2), P(\delta, 3)$	0.8333	0.6852	0.1104	5.63	3.23	0.009

* $P(x, n)$: Polynomial in x of order n .

Table 6-2 summarizes the regression statistics of Hall A with a proscenium stage under Scheme B. With only 18 data sets, the number of plausible regression models is reduced to 13 and the standard errors are considerably larger than those in Table 6-1. Although Model PB04 only consists of distance, D and path difference, δ , it still gives a marginally satisfactory performance as δ carries the information of ϕ and θ . However, again, δ is not necessary in the analysis once both θ and $|\phi|$ are included in the regression model. Under this small number of data sets which tend to restrict the number of inputs to a regression model, without δ , Models PB07 and PB09 are the best two for the prediction of IACC_{E3}. Even though, PB09 is slightly better than the PB07. The corresponding standard errors are similar to those root-mean-square differences presented in the neural network analysis in Chapter 5.

Table 6-3 Regression Analysis at 95% confidence level for the proscenium stage case of Hall A (Scheme C)

Model	Regression Inputs*	Correlation Coefficient, R^2	Adjusted R^2	Standard Error, ε	F	$F_{critical}$	Significance
PC01	D, D^2	0.1818	0.1136	0.1605	2.67	3.40	0.090
PC02	D, D^2, ϕ	0.1908	0.0853	0.1631	1.81	3.03	0.174
PC03	D, D^2, θ	0.1990	0.0945	0.1622	1.90	3.03	0.157
PC04	D, D^2, δ	0.3049	0.2143	0.1511	3.36	3.03	0.036
PC05	$D, D^2, \phi $	0.6922	0.6521	0.1006	17.24	3.03	0.000
PC06	$D, D^2, \phi , \phi^2 $	0.6922	0.6363	0.1028	12.37	2.82	0.000
PC07	D, D^2, ϕ , θ	0.7574	0.7133	0.0913	17.17	2.82	0.000
PC08	D, D^2, ϕ , δ	0.6928	0.6369	0.1027	12.04	2.82	0.000
PC09	$D, D^2, \phi , P(\theta, 2)$	0.7760	0.7226	0.0899	14.55	2.68	0.000
PC10	$D, D^2, \phi , P(\theta, 3)$	0.7764	0.7093	0.0919	11.57	2.60	0.000
PC11	$D, D^2, \phi , P(\theta, 2), \delta$	0.7764	0.7093	0.0919	11.57	2.60	0.000
PC12	$D, D^2, \phi , P(\theta, 2), P(\delta, 2)$	0.7769	0.6947	0.0942	9.45	2.54	0.000
PC13	$D, D^2, \phi , P(\theta, 2), P(\delta, 3)$	0.7813	0.6842	0.0958	8.04	2.51	0.000

* $P(x, n)$: Polynomial in x of order n .

The results obtained using Scheme C are quite similar to that using Scheme B, though the number of data sets has been increased from 18 to 27 (Table 6-3). Model PC09, which consists of the same inputs as Model PB09, still give the best prediction performance. Model PC07 is the second best. Using θ instead of δ , the standard errors are slightly reduced. Though more sets of data, 45 sets, are included in Scheme D, the number of plausible regression models remains unchanged as shown in Table 6-4. Again, the implications from Table 6-4 are very similar to those from Table 6-2 and Table 6-3. Model PD09, which is the counterpart of Models PB09 and PC09, performs the best. Therefore, one can conclude that in the surveyed Hall A with a proscenium stage setting, when the number of data sets available for regression modelling is small, regression model made up of a linear combination of a constant, a quadratic polynomial in D , a linear term with $|\phi|$ and a quadratic polynomial in θ is the best for the prediction of IACC_{E3}.

Table 6-4 Regression Analysis at 95% confidence level for the proscenium stage case of Hall A (Scheme D)

Model	Regression Inputs*	Correlation Coefficient, R^2	Adjusted R^2	Standard Error, ε	F	$F_{critical}$	Significance
PD01	D, D^2	0.2873	0.2534	0.1329	8.47	3.21	0.001
PD02	D, D^2, ϕ	0.3030	0.2519	0.1330	5.94	2.83	0.002
PD03	D, D^2, θ	0.3205	0.2708	0.1314	6.45	2.83	0.001
PD04	D, D^2, δ	0.5563	0.5238	0.1061	17.13	2.83	0.000
PD05	$D, D^2, \phi $	0.6825	0.6593	0.0898	29.38	2.83	0.000
PD06	$D, D^2, \phi , \phi^2 $	0.6882	0.6571	0.0908	22.08	2.61	0.000
PD07	D, D^2, ϕ , θ	0.7598	0.7358	0.0791	31.63	2.61	0.000
PD08	D, D^2, ϕ , δ	0.6825	0.6508	0.0909	21.50	2.61	0.000
PD09	$D, D^2, \phi , P(\theta, 2)$	0.7871	0.7598	0.0754	28.84	2.46	0.000
PD10	$D, D^2, \phi , P(\theta, 3)$	0.7883	0.7549	0.0762	23.59	2.35	0.000
PD11	$D, D^2, \phi , P(\theta, 2), \delta$	0.7873	0.7537	0.0763	23.44	2.35	0.000
PD12	$D, D^2, \phi , P(\theta, 2), P(\delta, 2)$	0.7875	0.7472	0.0773	19.58	2.27	0.000
PD13	$D, D^2, \phi , P(\theta, 2), P(\delta, 3)$	0.7935	0.7476	0.0773	17.29	2.21	0.000

* $P(x, n)$: Polynomial in x of order n .

The standard errors presented in Table 6-1 to Table 6-4 show the errors of the regression model prediction with reference to the data set in each scheme. In order to further understand the effectiveness of using these models to predict the IACC_{E3} distribution in

the hall, the IACC_{E3} of the 182 measurement points in Scheme A are predicted by the Models PA14, PA18, PB09, PC09 and PD09. Model PA18 is counterpart of Models PB09, PC09 and PD09 in Scheme A. It is included here for the sake of comparison.

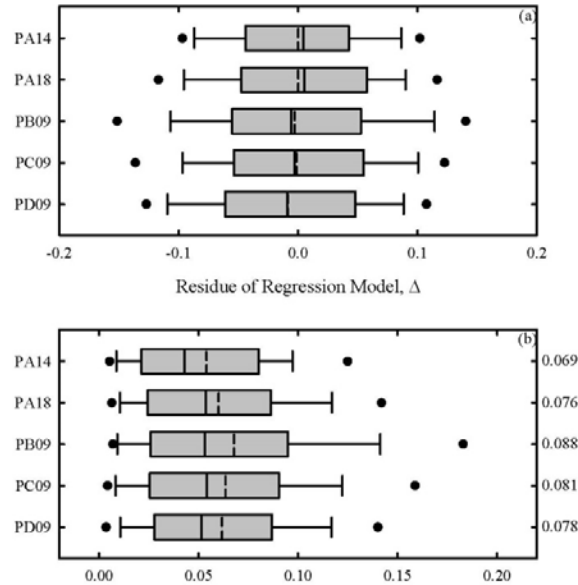


Figure 6-6 Regression model residue distributions of Hall A under proscenium stage setting (a) Δ ; (b) $|\Delta|$.

• : 5th and 95th percentiles; error bars : 10th and 90th percentiles; box edges : 25th and 75th percentiles; vertical lines within boxes : median; vertical dashed lines : mean values

Box plots in Figure 6-6a and Figure 6-6b illustrate the corresponding distributions of the regression residues, Δ . This residue is the prediction errors at the abovementioned 182 locations, and those of $|\Delta|$ respectively. As shown in Figure 6-6a, the distributions of Δ are symmetrical and the mean of Δ is nearly zero. However, it is more practical to analyse the distributions of $|\Delta|$ as it is always the absolute deviation which is more important. One can see from Figure 6-6b that the performances of Models PA18 and PD09 are very similar. In fact, Model PD09 gives a slightly lower $|\Delta|$ median than Model PA18. The numbers on the left-hand-side axis of Figure 6-6b show the standard deviations of Δ , which is also the root-mean-square deviation between predictions and measurements. All these regression models appear to out-perform the neural network simulations in Chapter 5. The residue distributions show that Scheme C can be a good choice for a trade-off between prediction accuracy and time and manpower resource for full scale measurement. It should also be noted that though the Models PA18, PB09, PC09 and PD09 are obtained from different measurement schemes, they have the same inputs and the coefficients

inside the models are reasonably close to each other in terms of degrees of variables, as seen from Table 6-5. One can say they are basically the same model. The models in Table 6-5 which begin with a ‘C’ are for the concert setting and will be discussed in Section 6.3.2B. It is noted that the coefficients in the regression formulae are only valid for Hall A. It is expected that they vary from hall to hall.

Table 6-5 Coefficients of the regression models for Hall A

Model	Regression formula
PA18	$IACC_{E3} = 3.0932 - 6.4414D + 4.0528D^2 - 0.7924 \phi + 0.7952\theta - 2.0660\theta^2$
PB09	$IACC_{E3} = 2.6506 - 5.1556D + 3.2831D^2 - 1.1264 \phi + 0.5021\theta - 1.8102\theta^2$
PC09	$IACC_{E3} = 2.5608 - 5.0434D + 3.2274D^2 - 0.9094 \phi + 0.5076\theta - 1.6331\theta^2$
PD09	$IACC_{E3} = 2.7028 - 5.4238D + 3.4401D^2 - 0.8701 \phi + 0.5743\theta - 1.7504\theta^2$
CA11	$IACC_{E3} = 0.9611 - 0.3347D + 0.1290D^2 + 0.7475\phi - 3.9590\phi^2 - 6.9810\phi^3 + 11.1280\phi^4 + 26.5727\phi^5 - 0.1203\theta$
CB11	$IACC_{E3} = 0.9976 - 0.4602D + 0.2829D^2 + 0.9617\phi - 4.3798\phi^2 - 15.2082\phi^3 + 13.1168\phi^4 + 57.5141\phi^5 - 0.2351\theta$
CC11	$IACC_{E3} = 1.1097 - 0.7803D + 0.4697D^2 + 0.7019\phi - 3.8395\phi^2 - 8.3954\phi^3 + 9.9697\phi^4 + 31.6655\phi^5 - 0.1586\theta$
CD22	$IACC_{E3} = 0.8544 - 0.0520D - 0.0317D^2 + 0.6513\phi - 4.3352\phi^2 - 6.2659\phi^3 + 12.9996\phi^4 + 23.3590\phi^5 - 0.1725\theta$

B. Concert Hall Setting

Table 6-6 Regression Analysis at 95% confidence level for the concert hall setting of Hall A

(Scheme A)

Model	Regression Inputs*	Correlation Coefficient, R^2	Adjusted R^2	Standard Error, ϵ	F	$F_{critical}$	Significance
CA01	D, D^2	0.0168	0.0058	0.1342	1.53	19.49	0.220
CA02	D, D^2, ϕ	0.3466	0.3356	0.1098	31.47	8.54	0.000
CA03	D, D^2, θ	0.0222	0.0057	0.1343	1.35	8.54	0.261
CA04	D, D^2, δ	0.2086	0.1953	0.1209	15.64	8.54	0.000
CA05	$D, D^2, P(\phi, 2)$	0.7410	0.7351	0.0693	126.57	5.65	0.000
CA06	$D, D^2, P(\delta, 2)$	0.2143	0.1965	0.1207	12.07	5.65	0.000
CA07	$D, D^2, P(\phi, 3)$	0.7578	0.7509	0.0672	110.12	4.39	0.000
CA08	$D, D^2, P(\phi, 4)$	0.7912	0.7841	0.0626	110.54	3.69	0.000
CA09	$D, D^2, P(\phi, 5)$	0.8060	0.7982	0.0605	103.24	3.26	0.000
CA10	$D, D^2, P(\phi, 6)$	0.8065	0.7976	0.0606	90.15	2.96	0.000
CA11	$D, D^2, P(\phi, 5), \theta$	0.8255	0.8174	0.0575	102.30	2.96	0.000
CA12	$D, D^2, P(\phi, 5), \delta$	0.8060	0.7970	0.0607	89.83	2.96	0.000
CA13	$D, D^2, P(\phi, 5), \theta, \delta$	0.8255	0.8164	0.0577	90.44	2.74	0.000
CA14	$D, D^2, P(\phi, 5), P(\theta, 2)$	0.8331	0.8244	0.0564	95.38	2.74	0.000
CA15	$D, D^2, P(\phi, 5), P(\theta, 3)$	0.8340	0.8243	0.0565	85.90	2.57	0.000
CA16	$D, D^2, P(\phi, 5), P(\theta, 2), \delta$	0.8337	0.8239	0.0565	85.70	2.57	0.000
CA17	$D, D^2, P(\phi, 5), P(\theta, 2), P(\delta, 2)$	0.8337	0.8229	0.0567	77.48	2.44	0.000
CA18	$D, D^2, P(\phi, 5), P(\theta, 2), P(\delta, 3)$	0.8349	0.8232	0.0566	71.23	2.33	0.000
CA19	$D, D^2, P(\phi, 5), P(\theta, 2), P(\delta, 4)$	0.8416	0.8293	0.0556	68.64	2.24	0.000
CA20	$D, D^2, P(\phi, 5), P(\theta, 2), P(\delta, 5)$	0.8478	0.8350	0.0547	66.44	2.16	0.000
CA21	$D, D^2, P(\phi, 5), P(\theta, 2), P(\delta, 6)$	0.8489	0.8352	0.0547	62.17	2.10	0.000
CA22	$D, D^2, P(\phi, 5), P(\theta, 2), P(\delta, 7)$	0.8515	0.8371	0.0544	59.14	2.05	0.000
CA23	$D, D^2, P(\phi, 5), P(\theta, 2), P(\delta, 8)$	0.8520	0.8367	0.0544	55.34	1.69	0.000

* $P(x, n)$: Polynomial in x of order n .

The acoustic shell has shorten the depth of the stage and covers the rear side, the ceiling and the two openings to the left and right rear stage area (Figure 6-2b). It is used as a concert hall setting for musical events and singing performances. However, the measurement result from the Chapter 5 says that the hall is not acoustically symmetrical in the presence of this shell. Utilizing the same procedure adopted in the analysis of the proscenium stage setting results, the plausible regression models for predicting IACC_{E3} in a concert setting are developed.

As the hall is acoustically non-symmetrical, $|\phi|$ is not included in the regression analysis. The results obtained using measurement Scheme A are tabulated in Table 6-6. The best performing regression model is CA22, which consists of high order polynomials in ϕ and δ . However, including the δ only slightly improves the standard error. δ is again only important when ϕ is not included in the regression modelling. Actually, the standard error has no further significant improvement in models after CA11. Compared to the results obtained with the proscenium stage, the higher order of the ϕ polynomial within the regression model with the acoustic shell tends to imply that the IACC_{E3} is more correlated with ϕ when the hall is in this setting. The multiple reflections by the acoustic cells within the stage strengthen the sound radiation and gives a more organized radiation directivity. The asymmetrical sound field inside the hall may be the result of a small misalignment of the cell assembly with the stage.

Table 6-7 Regression Analysis at 95% confidence level for the concert hall setting of Hall A (Scheme B)

Model	Regression Inputs*	Correlation Coefficient, R^2	Adjusted R^2	Standard Error, ε	F	$F_{critical}$	Significance
CB01	D, D^2	0.0581	-0.0675	0.1547	0.46	3.68	0.639
CB02	D, D^2, ϕ	0.2710	0.1148	0.1409	1.74	3.34	0.206
CB03	D, D^2, θ	0.0627	-0.1382	0.1597	0.31	3.34	0.816
CB04	D, D^2, δ	0.2874	0.1347	0.1393	1.88	3.34	0.179
CB05	$D, D^2, P(\phi, 2)$	0.7399	0.6599	0.0873	9.25	3.18	0.001
CB06	$D, D^2, P(\delta, 2)$	0.3136	0.1024	0.1418	1.48	3.18	0.263
CB07	$D, D^2, P(\phi, 3)$	0.7492	0.6447	0.0892	7.17	3.11	0.003
CB08	$D, D^2, P(\phi, 4)$	0.7836	0.6655	0.0866	6.64	3.09	0.004
CB09	$D, D^2, P(\phi, 5)$	0.8612	0.7640	0.0727	8.86	3.14	0.001
CB10	$D, D^2, P(\phi, 6)$	0.8622	0.7396	0.0764	7.04	3.23	0.004
CB11	$D, D^2, P(\phi, 5), \theta$	0.9309	0.8694	0.0541	15.15	3.23	0.000
CB12	$D, D^2, P(\phi, 5), \delta$	0.8612	0.7379	0.0766	6.98	3.23	0.004
CB13	$D, D^2, P(\phi, 5), \theta, \delta$	0.9314	0.8542	0.0572	12.06	3.39	0.001
CB14	$D, D^2, P(\phi, 5), P(\theta, 2)$	0.9376	0.8674	0.0545	13.35	3.39	0.000
CB15	$D, D^2, P(\phi, 5), P(\theta, 3)$	0.9376	0.8486	0.0583	10.53	3.64	0.002
CB16	$D, D^2, P(\phi, 5), P(\theta, 2), \delta$	0.9377	0.8486	0.0583	10.53	3.64	0.002
CB17	$D, D^2, P(\phi, 5), P(\theta, 2), P(\delta, 2)$	0.9377	0.8235	0.0629	8.21	4.03	0.009

* $P(x, n)$: Polynomial in x of order n .

With a small number of sets of measurement data in Scheme B, the regression model is only meaningful after ϕ^2 is included as shown in Table 6-7. Model CB11 gives the best prediction while δ has not been a useful prediction parameter. As the quantity of the available data sets is much reduced, the number of inputs to the regression models is limited. Similar observations can be made from Table 6-8 which illustrates the regression statistics obtained under Scheme C, except that δ is only marginally satisfactory to be considered as an input when ϕ is not included. The best performing model is CC11, which is basically the counterpart of Model CB11. However, it will be shown later that the coefficients within these two models are quite different. They are not the same.

Table 6-8 Regression Analysis at 95% confidence level for the concert hall setting of Hall A (Scheme C)

Model	Regression Inputs*	Correlation Coefficient, R^2	Adjusted R^2	Standard Error, ε	F	$F_{critical}$	Significance
CC01	D, D^2	0.0431	-0.0366	0.1508	0.54	3.40	0.589
CC02	D, D^2, ϕ	0.3033	0.2124	0.1314	3.34	3.03	0.037
CC03	D, D^2, θ	0.0451	-0.0795	0.1539	0.36	3.03	0.781
CC04	D, D^2, δ	0.3019	0.2108	0.1316	3.12	3.03	0.038
CC05	$D, D^2, P(\phi, 2)$	0.7972	0.7604	0.0725	21.63	2.82	0.000
CC06	$D, D^2, P(\delta, 2)$	0.3028	0.1974	0.1327	2.60	2.82	0.064
CC07	$D, D^2, P(\phi, 3)$	0.8075	0.7616	0.0723	17.61	2.68	0.000
CC08	$D, D^2, P(\phi, 4)$	0.8237	0.7709	0.0709	15.58	2.60	0.000
CC09	$D, D^2, P(\phi, 5)$	0.8453	0.7883	0.0681	14.83	2.54	0.000
CC10	$D, D^2, P(\phi, 6)$	0.8489	0.7818	0.0692	12.64	2.51	0.000
CC11	$D, D^2, P(\phi, 5), \theta$	0.8779	0.8234	0.0622	16.18	2.51	0.000
CC12	$D, D^2, P(\phi, 5), \delta$	0.8481	0.7806	0.0694	12.56	2.51	0.000
CC13	$D, D^2, P(\phi, 5), \theta, \delta$	0.8813	0.8185	0.0631	14.03	2.49	0.000
CC14	$D, D^2, P(\phi, 5), P(\theta, 2)$	0.8807	0.8175	0.0633	13.94	2.49	0.000
CC15	$D, D^2, P(\phi, 5), P(\theta, 2), \delta$	0.8871	0.8044	0.0655	10.72	2.49	0.000

* $P(x, n)$: Polynomial in x of order n .

Table 6-9 Regression Analysis at 95% confidence level for the concert hall setting of Hall A (Scheme D)

Model	Regression Inputs*	Correlation Coefficient, R^2	Adjusted R^2	Standard Error, ε	F	$F_{critical}$	Significance
CD01	D, D^2	0.0012	-0.0463	0.1418	0.03	3.22	0.975
CD02	D, D^2, ϕ	0.3571	0.3100	0.1151	7.59	2.83	0.000
CD03	D, D^2, θ	0.0084	-0.0644	0.1430	0.12	2.83	0.950
CD04	D, D^2, δ	0.2369	0.1811	0.1254	4.24	2.83	0.011
CD05	$D, D^2, P(\phi, 2)$	0.7257	0.6982	0.0761	24.45	2.61	0.000
CD06	$D, D^2, P(\delta, 2)$	0.2888	0.2177	0.1226	4.06	2.61	0.007
CD07	$D, D^2, P(\phi, 3)$	0.7352	0.7013	0.0758	21.66	2.46	0.000
CD08	$D, D^2, P(\phi, 4)$	0.7857	0.7518	0.0691	23.22	2.35	0.000
CD09	$D, D^2, P(\phi, 5)$	0.7964	0.7579	0.0682	20.68	2.27	0.000
CD10	$D, D^2, P(\phi, 6)$	0.8105	0.7684	0.0667	19.25	2.21	0.000
CD11	$D, D^2, P(\phi, 7)$	0.8329	0.7899	0.0635	19.38	2.16	0.000
CD12	$D, D^2, P(\phi, 8)$	0.8329	0.7919	0.0632	17.75	2.12	0.000
CD13	$D, D^2, P(\phi, 9)$	0.8409	0.7879	0.0638	15.86	2.09	0.000
CD14	$D, D^2, P(\phi, 8), \theta$	0.8802	0.8402	0.0554	21.72	2.09	0.000
CD15	$D, D^2, P(\phi, 8), \delta$	0.8393	0.7857	0.0641	15.66	2.09	0.000
CD16	$D, D^2, P(\phi, 8), \theta, \delta$	0.8802	0.8353	0.0562	19.60	2.07	0.000
CD17	$D, D^2, P(\phi, 8), P(\theta, 2)$	0.8831	0.8392	0.0556	20.14	2.07	0.000
CD18	$D, D^2, P(\phi, 8), P(\theta, 3)$	0.8831	0.8341	0.0565	18.02	2.05	0.000
CD19	$D, D^2, P(\phi, 8), P(\theta, 2), \delta$	0.8838	0.8350	0.0563	18.13	2.05	0.000
CD20	$D, D^2, P(\phi, 8), P(\theta, 2), P(\delta, 2)$	0.9010	0.8547	0.0528	19.49	2.04	0.000
CD21	$D, D^2, P(\phi, 8), P(\theta, 2), P(\delta, 3)$	0.9010	0.8498	0.0537	17.59	2.03	0.000
CD22	$D, D^2, P(\phi, 5), \theta$	0.8410	0.8056	0.0611	23.79	2.21	0.000

* $P(x, n)$: Polynomial in x of order n .

The inclusion of more data sets under Scheme D makes δ a reasonable parameter to be included in the regression modelling as illustrated in Table 6-9. However, it is still the least important one compared to the two geometric angles. The best performing model CD20 consists of a polynomial in ϕ of order higher than that of CA22, probably due to the data sets available for analysis. Model CD22 is the counterpart of Models CA11, CB11 and CC11. It is presented in Table 6-9 for reference only. In fact, regression models with $P(\phi, 5)$ cannot give a standard error lower than that of CD20. Comparing the present results with those predicted by neural network in Chapter 5, it is found that these regression models which contain ϕ^2 can perform better than the neural network prediction.

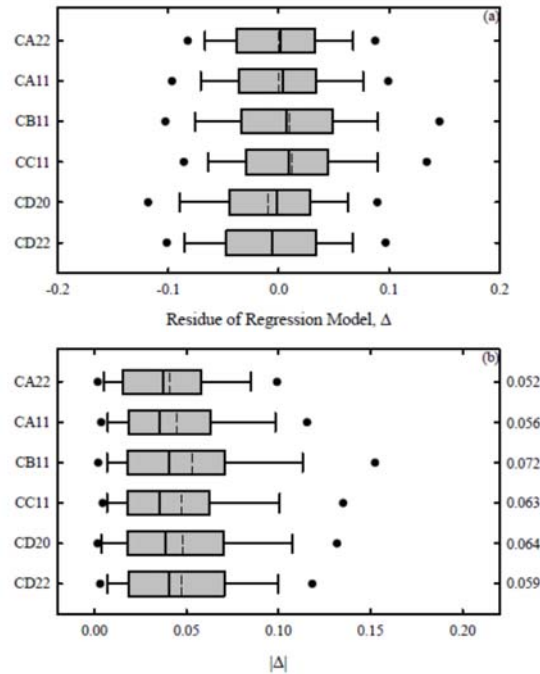


Figure 6-7 Regression model residue distributions of Hall A under concert hall setting.. (a) Δ ; (b) $|\Delta|$. Legends : same as those for Fig. 6.

Figure 6-7 shows the distributions of Δ and $|\Delta|$ under the concert setting. As Models CA11 and CD22 are extremely similar to Schemes B and C's best performing models CB11 and CC11, the results of Models CA11 and CD22 are included here for comparison. Comparing the results of Model CA11 with those of the best performing models under Scheme A Model CA22, CA11 results in a wider band between the 10th and the 90th percentiles of the residues as shown in Figure 6-7a. This brings and increases to the higher root-mean-square residue of Model CA11 than Model CA22 presented in Figure 6-7b. Pairing up Models CD20 and CD22 for comparison, the width between the 25th and 75th residue percentiles of the CD22 is shorter and the corresponding median of residue is also lower as shown in Figure 6-7a. The root-mean-square residue of CD20 is slightly larger than that of CD22, presented in Figure 6-7b. This implies that there are a small proportion of Model CD20 predictions which deviates relatively large from the measurements. The shorter width between the $|\Delta|$ error bars of Model CD22 in Figure 6-7b further proves that this is the case. However, the difference between Models CD20 and CD22 predictions is not significant, suggesting that the CD22 is an acceptable choice of prediction model although its standard error is not as low as CD20. It should also be noted all the models presented in Figure 6-7 are performing significantly better than the

neural network model in Chapter 5 in term of deviations between predictions and measurements when all the 182 data are considered together.

The regression models CA11, CB11, CC11 and CD22 are presented in Table 6-5. Again, even the signs of the coefficients, not including that of D^2 of Model CD22, are the same, these models are similar. However, the sign of D^2 coefficient of Model CD22 suggests that the $IACC_{E3}$ decreases monotonically with D , which is not conflicting with those suggested by the other regression models in the present range of D , except at values near to its upper boundary where the negative coefficient of θ helps reducing the $IACC_{E3}$. It can be concluded that Scheme C appears very satisfactory for $IACC_{E3}$ distribution prediction for a balance between manpower and prediction accuracy.

C. Model Validation

The results of Hall B of from the previous chapter are used here for model validation. Hall B is a fan-shaped performance hall with a smaller seating capacity. There are 84 measurement data sets. The layout and dimensions of Hall B can be found in in the previous chapters and therefore they are not presented here. Unlike Hall A, Hall B is basically acoustically symmetrical under both the proscenium stage and concert hall settings. Scheme C results are adopted here as it is shown in the previous sections that it is a better measurement approach in balancing the measurement resources and prediction accuracy. Meanwhile, the results obtained using Scheme D are largely similar with the Scheme C results. It can be noted that this validation targets at validating the forms of the models. As mentioned before, the various coefficients in the models are expected to be functions of hall details, absorption and many other design parameters, and varying substantially from hall to hall, hence, they are not of major concern in this validation.

Table 6-10 Regress Analysis at 95% confidence level for Hall B under Scheme C

Hall Setting	Model	Regression Inputs*	Correlation Coefficient, R^2	Adjusted R^2	Standard Error, ε	F	$F_{critical}$	Significance
Proscenium	BC01P	D, D^2, ϕ	0.1319	0.0187	0.0978	1.17	2.83	0.345
	BC02P	$D, D^2, \phi $	0.5890	0.5354	0.0673	10.99	2.83	0.000
	BC03P	$D, D^2, P(\phi , 2)$	0.6640	0.6029	0.0622	10.87	2.61	0.000
	BC04P	D, D^2, ϕ , θ	0.6138	0.5436	0.0667	8.74	2.61	0.000
	BC05P	$D, D^2, P(\phi , 3)$	0.6641	0.5842	0.0637	8.31	2.46	0.000
	BC06P	$D, D^2, P(\phi , 2), \theta$	0.6800	0.6038	0.0622	8.92	2.46	0.000
	BC07P	$D, D^2, P(\phi , 2), P(\theta, 2)$	0.7408	0.6631	0.0573	9.53	2.35	0.000
	BC08P	$D, D^2, P(\phi , 2), P(\theta, 3)$	0.7615	0.6734	0.0564	8.67	2.27	0.000
	BC09P	$D, D^2, P(\phi , 2), P(\theta, 4)$	0.8520	0.7862	0.0457	12.95	2.21	0.000
	BC10P	$D, D^2, P(\phi , 2), P(\theta, 5)$	0.8521	0.7738	0.0470	10.88	2.15	0.000
	BC11P	$D, D^2, \phi , P(\theta, 2)$	0.6531	0.5706	0.0647	7.91	2.46	0.000
	BC12P	$D, D^2, \phi , P(\theta, 3)$	0.6839	0.5890	0.0633	7.21	2.35	0.000
	BC13P	$D, D^2, \phi , P(\theta, 4)$	0.6986	0.5876	0.0634	6.29	2.27	0.001
Concert	BC01C	D, D^2, ϕ	0.0218	-0.1058	0.1149	0.17	2.83	0.915
	BC02C	$D, D^2, \phi $	0.6517	0.6063	0.0685	14.35	2.83	0.000
	BC03C	$D, D^2, P(\phi , 2)$	0.6586	0.5965	0.0694	10.61	2.61	0.000
	BC04C	D, D^2, ϕ , θ	0.6628	0.6015	0.0690	10.81	2.61	0.000
	BC11C	$D, D^2, \phi , P(\theta, 2)$	0.7145	0.6466	0.0649	10.51	2.46	0.000
	BC12C	$D, D^2, \phi , P(\theta, 3)$	0.7275	0.6458	0.0650	8.90	2.35	0.000
	BC14C	$D, D^2, P(\phi, 3), \theta$	0.5647	0.4341	0.0822	4.32	2.35	0.006
	BC15C	$D, D^2, P(\phi, 4), \theta$	0.6103	0.4667	0.0798	4.25	2.27	0.006
	BC16C	$D, D^2, P(\phi, 5), \theta$	0.6147	0.4435	0.0815	3.59	2.21	0.012

* $P(x, n)$: Polynomial in x of order n .

The IACC_{E3} in Hall B has been predicted using the same model generation approach adopted in the Hall A analysis. The performances of the more important regression models were illustrated in Table 6-10. While hall B is acoustically symmetrical, $|\phi|$ is better than just ϕ regardless of the hall setting. Combining with the results of the Hall A under the proscenium stage setting, the magnitude of the azimuthal angle appears to be more important than its actual values and any polynomials in ϕ for acoustically symmetrical halls (which should be the common design).

In terms of standard error using the 27 measurement points of Scheme C, Hall B with the proscenium stage setting has BC09P as the best performing model is BC09P. The Models BC11P and BC12P give very similar performance. Model BC11P is the counterpart of PC09 (for Hall A). However, when all the measurement data in Hall B are included, the root-mean-square residue $|\Delta|$ of Model BC11P (and also BC12P) is better than that of BC09P. This will be further discussed later. Under the concert hall setting, as counterparts of BC11P, Model BC11C performs the best in terms of standard error. However, models with polynomial in ϕ , such as Model BC15C which is the counterpart of CD22 (for Hall A), do not perform so well in this acoustically symmetrical hall. Apart from the relatively larger standard error, the significance of the regression is also marginal.

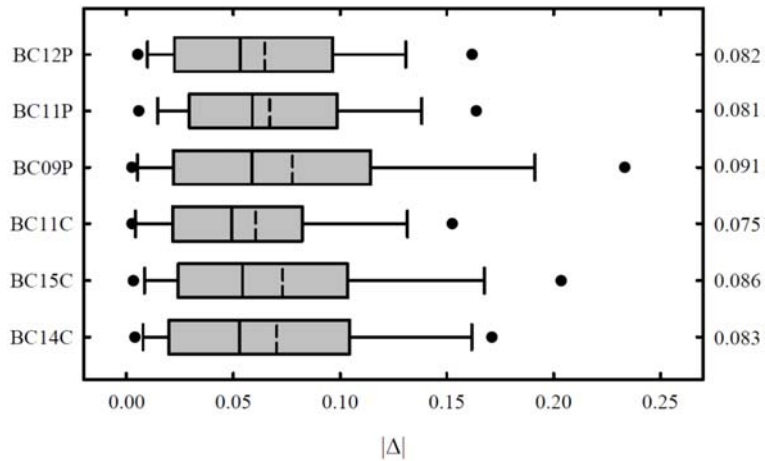


Figure 6-8 $|\Delta|$ distributions of Hall B

Legends : same as those for Figure 6-6

Figure 6-8 shows the $|\Delta|$ distributions of Models BC09P, BC11P, BC12P, BC11C, BC14C and BC15C, and the corresponding standard deviations of Δ . All 84 data sets in Hall B are included. Again, all these models, even those involving polynomials in ϕ , out-perform the neural network approach in the previous chapter in the prediction of $IACC_{E3}$ in terms of the standard deviation of residue.

Model BC09P results in the lowest standard error for the Scheme C data and can predict relatively accurately at many surveyed locations in Hall B, however, it gives a larger range of prediction error with a median of $|\Delta|$ which is very similar to that of Model BC11P and a root-mean-square residue Δ even lower than that of Model BC11P. Therefore, Models BC11P and BC12P are good alternatives. For Hall B, Model BC11C performs the best in terms of both the standard error and $|\Delta|$ distribution under concert hall setting. Combining with the results of Hall A, it can be concluded that models with a structure similar to that of Model BC11P and BC11C, are suitable for predicting $IACC_{E3}$ in an acoustically symmetrical hall. The structures of Model PC10, as well as its similar Models BC12P and BC12C, also fit this purpose. The difference between PC09 and PC10 is insignificant.

From the performances of Models BC11C and BC15C and the results of Hall A, it can be seen that polynomials in ϕ may be more useful when the hall is acoustically asymmetrical. However, this is not a common hall design. It is conjectured the degree of the acoustical asymmetry determines the order of the polynomial of the best prediction model. For Hall B, the best regression model which involves polynomial of ϕ appears to be Model BC14C.

It consists of a fourth order polynomial in ϕ . Those models, regardless of the order of polynomial, ie. second and sixth order ϕ polynomials, are not performing as good as the fourth order one. The results of this validation seem to suggest that the order of such a polynomial may vary from hall to hall. However, the present results indicate that such change may not be substantial as there is only a one order difference between an asymmetrical concert setting Hall A and a symmetrical Hall B. This is left to further investigation. It is also expected that the degree of asymmetry should be low in real halls.

D. Application Remarks

The regression models in this study start with a quadratic formula in D. This is done because of the availability of data obtained from an earlier intensive measurement inside the hall. However, it is not possible and practical to obtain such data in all halls especially those still at the design stage. In fact, the results obtained with a linear D are quite close to those presented. Hotehama et al.[102] and Sakurai et al.[103], found that the early IACCs decrease with increasing distance from the sound source unless at locations relatively close to solid boundaries inside halls with aspect ratios similar to the present study. Therefore, any simple function that decreases monotonically with increasing D should be useful in the formation of the regression model. Thus, the very simple quadratic formula in D is a reasonable choice. An example is illustrated by a successfully model validation using data from Hall B where no prior correlation between D and IACC_{E3} has to be done. It is also important to know that though the symmetry of the sound field inside the surveyed hall is known beforehand, it is never a parameter to consider in the formation of the regression models. Instead, the performance of ϕ and $|\phi|$ can be tested in the first place.

It is observed that the path difference δ is only useful when ϕ is not included in the modelling and is basically of no use when both ϕ and θ are taken into account. This may be due to the fact that only one hall with a shoebox design is investigated in this study. As δ contains information of the physical nearfield hall layout which can affect the acoustics of a hall,[20], [104] it may be useful when data of many halls of different designs are analysed together. It is left to further investigation.

6.4 Conclusions

In this study, the previous binaural measurement results obtained in two multi-purpose performance halls from the previous chapter are analysed in an attempt to establish a systematic framework for predicting the early interaural cross-correlation coefficients through simple regression models with as little geometrical hall parameters and measurements as possible. The geometrical parameters, including the source-to-receiver distance, the elevation and azimuthal angles of the receiver relative to the source and the path difference between the direct sound and the first reflection, are investigated. For simplicity, the regression models generated are formed by linear combinations of polynomials of these parameters without any inclusion of cross-products of different parameters. A procedure is also proposed for the generation of regression models in this study.

Both proscenium stage and concert hall settings are included in the present study. For both settings, a scheme, out of four schemes tested, where the measurement points are roughly arranged in three 3-by-3 matrices. Each spans over a sub-area of the whole hall. This arrangement appears to be effective with a balance between the need of measurement resources and accuracy of regression prediction. The regression models generated give much better predictions than the neural network approach in Chapter 5 once the source-to-receiver distance, azimuthal and elevation angle are included. However, the best performing regression models for symmetrical and asymmetrical halls under this measurement scheme are different. For the symmetrical cases, a model consisting of quadratic polynomials in source-to-receiver distance and elevation angle and a linear function of the azimuthal angle magnitude would be the best choice for both the proscenium stage setting and the concert hall setting. The best regression model for the asymmetrical concert setting is made up of a linear function of elevation angle, a polynomial in azimuthal angle and a quadratic function of source-to-receiver distance. However, such model is still able to give acceptable performance when the concert hall is acoustically symmetrical. Since asymmetrical hall design yet common in Hong Kong and lack of measurement data, further validation is required.

It is believed with the presence of the acoustic shell on the stage, the stronger and probably more organized sound radiation in an acoustically asymmetrical concert hall has largely increased the influence of azimuthal angle on the early sound and its binaural correlation. The path difference and the azimuthal with elevation angles are supplementary to each

other in the regression models. Once the angles are included, the path difference become not important.

It should be noted that this study never aims to develop a universal regression formula with fixed coefficients for general application. It is believed that the measurement scheme used in this study, which is suitable for studies in both rectangular and fan-shaped halls, together with the present proposed regression model generation procedures and the geometrical parameters should be able to perform $IACC_{E3}$ prediction in halls with simple layouts. The results of this study show that a simple model for predicting $IACC_{E3}$ to within engineering tolerance in acoustically symmetrical halls is feasible.

Chapter 7 The effect of balcony design

7.1 Introduction

While real hall measurements can only provide data of the current as-built condition, scale model and 3D simulation are alternatives to study the outcomes of any changes on the hall's construction. In present study, a 1/10 scale model experiment and a 3D simulation were done to study the impact of the balcony design in a hall.

A 1/10 scaled-down model of Hall A was constructed to investigate the effect of the balcony on the acoustical qualities at different locations throughout the hall. The balcony could be removed and measurements were done under both the concert hall and proscenium setting. These formed four different cases for measurements. Around two-third of the measurement points in Chapter 4 were used in the scale model again for measurement. A spark source was used and the impulse responses were recorded by B&K 1/8 inches high frequency microphones and recorded by a 3-channel B&K high frequency Pulse system. The results were exported and processed using Matlab. Integrated impulse response method was used to evaluate the impulse decay curve and the associated parameters.

The 3D simulation using Odeon investigated the effect of the change of the balcony size on the acoustical parameters in the hall. It includes all the points measured in Chapter 4. The hall geometry used in these two models here is Hall A, which is surveyed and analysed in the previous chapters.

7.2 The scale model and measurement setup

The scale model was constructed on-site in a lecture theatre of the University. The theatre was a carpeted room, with centralized air-conditioning, located on the ground floor of the building. It was not an isolated room and there was only a double fire door directly opening to the outside. The floor area, where the model was sited, was separated from the outdoor with the dressing room behind the stage. The entrance foyer provided another buffer and isolation to the outside. At the other end of the hall, the two sides of the hall were fitted with slotted acoustic panels while the back of the hall was mounted with upholstered panels. The room was furnished with panel-type false ceilings concealing the air ducts and the other building services. Part of the false ceiling was constructed with steps to match the sloped seating area. The model was constructed on a two-foot-tall

timbre frame. The sectional drawing of the scale model after removing the balcony structure is shown in Figure 7-1. As shown in Figure 7-5, the model also beard the side stages and the top of the main stages. As the cyclorama of the hall was a hard concrete wall in Hall A, therefore, the space behind the main stage and cyclorama was omitted in the scaled-down model. The ceiling reflectors of the main stage was omitted. In cases with the concert hall setting, the acoustic shell was constructed on the stage as shown in Figure 7-2. The scaled-down shell was resting on the stage with the slanted ceiling extending to the edge of stage front. As shown in Figure 7-3, the shell was removed and black nylon clothes were hanged from on the stage in the proscenium stage setting.

The balcony stage was removed in two of the measurement cases. The whole balcony structure was removed and replaced by a ‘back wall’ as shown in Figure 7-2 and Figure 7-3. The seats under the balcony were then exposed to the topmost ceiling inside the scale model while the internal volume of the whole model was increased.

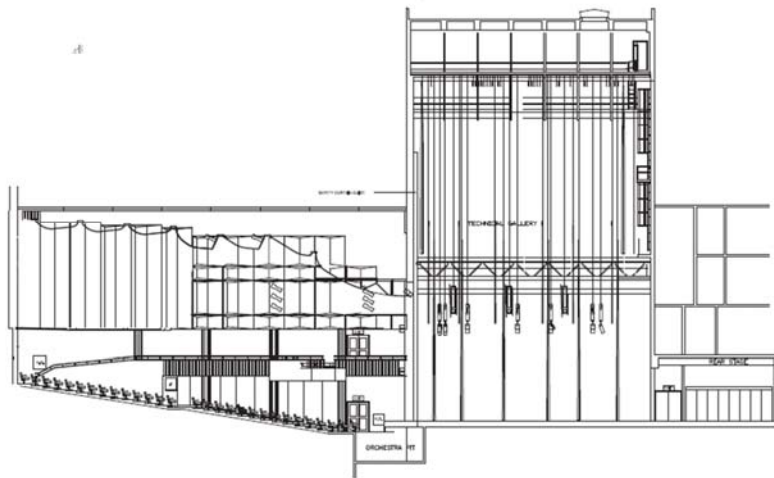


Figure 7-1 Sectional drawing of the scale model with the balcony removed



Figure 7-2 View from the seating area to the stage in the scale model with the acoustic shell



Figure 7-3 View from the seating area to the stage in the scale model without the acoustic shell, ie proscenium setting

The measurement was done in four different cases, naming from Case 1 to Case 4. Table 7-1 concludes the settings of the four measurement cases. The measurements were started with Case 1 and Case 2 with the balcony in the model. The balcony was then taken down for Case 3 and Case 4. In Case 1 and Case 3, the stage in the model was in a proscenium setting as shown in Figure 7-3. To convert from Case 1 to Case 2 and from Case 3 to Case 4, the acoustic shell added as shown in Figure 7-2.

Table 7-1 Model setting for 4 scale model measurement cases.

Case	Balcony	Stage setting
1	With	Proscenium
2	With	Concert
3	Without	Proscenium
4	without	Concert

Figure 7-4 shows the location of the spark source in the scale model while the blue lines on the drawings indicate the balcony edge measuring location. Figure 7-5 shows the exterior of the scale model without the balcony, ie for case 3 and case 4. Figure 7-6 shows the reduced number of measurements points used in the scale model. All these points were repeated in case 1 and case 2. After the balcony was removed, in case 3 and case 4, the points on the balcony were excluded.

Figure 7-4 shows the location of the balcony edge measurement locations in the scale model. These locations corresponded to those measurement locations in real hall measurements as presented in Chapter 4. There were 116 and 85 points measured with and without the balcony respectively. Alternate points were omitted out of the 183 points measured in Chapter 4 while the points at the perimeter and middle of each zone defined in Chapter 5 and Chapter 6 were still retained. When the balcony was removed, the points on the balcony were omitted.

The balcony edge measurement was also done in case 1 and case 2 where the balcony were present. Instead of using a rotating rack as in Chapter 4, a tailor-made circular rack was used. To measure the impulse response at each 15°, the two 1/8-inches microphones were secured onto the rack at 90 or 180 degrees apart. Thus two different angles at the same measurement point at the balcony edge were measured at the same time. These balcony edge measurement locations are marked in blue line in Figure 7-4. The three locations are along the centreline of the stage, around 1/4 to the left and to the right along the balcony edge.

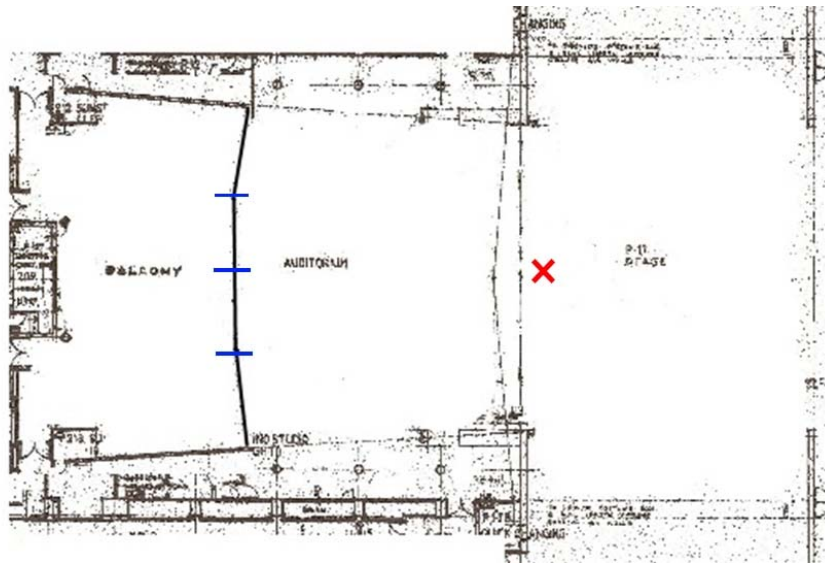


Figure 7-4 Location of spark source (marked as a red cross) and balcony edge measuring racks mark in blue line.



Figure 7-5 The exterior view of the scale model after the conversion

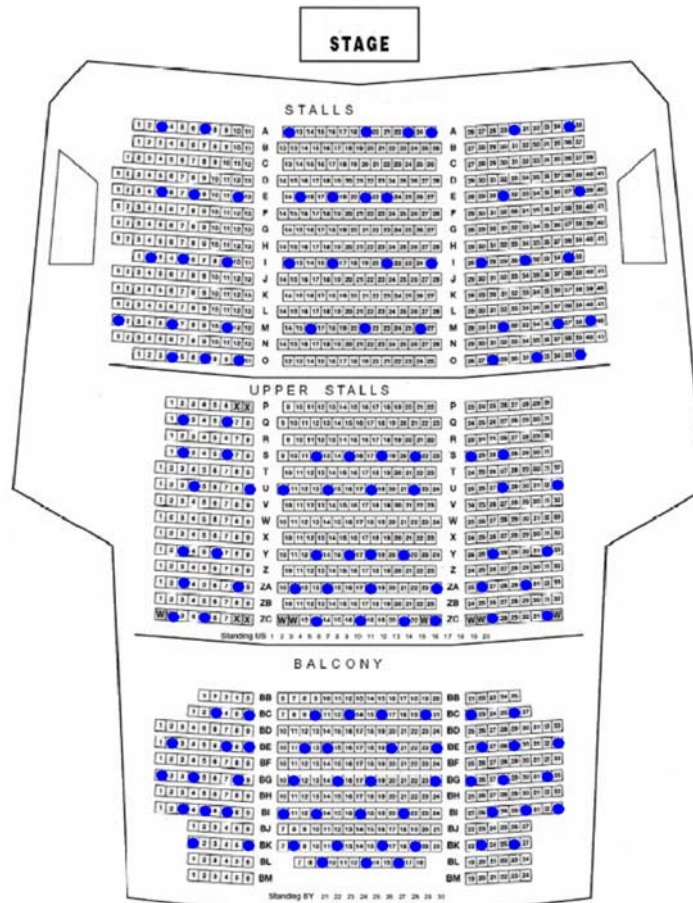


Figure 7-6 Measurement points in the scale model are marked with blue dots

7.3 Spark source

The spark source used in the scaled-model measurement was a tailor-made source with 36 parallel-connected $470\mu\text{F}$ capacitors generating a very high voltage at the tips of the two metal pins. The capacitors were charged each time and discharged to spark continuously for each set of measurements. The tips of the pins were polished and the separation was adjusted from time to time to maintain a long enough time separation between each spark. The source was inserted from the bottom of the stage and mounted at 16cm above the floor surface of the stage, which was the scaled down height as the source height used in Chapter 4.

To ensure the uniformity of the spark source, the directivity pattern of the spark source was measured in the anechoic chamber with 4 different radii (1m, 1.5m, 2m and 3m) and

5 different angles (from 0 degree to 180 degree). Figure 7-7 shows the plotted directivity of the spark source used. From the plots, the sound pressure levels measured at each distance at different angle are very uniform. This shows that the spark source had a very good uniformity in all directions. Figure 7-8 is the pressure spectrum of the impulse measured in the anechoic chamber at 90 degree position 2m from the spark source. The line at low frequency probably is the noise of the setup itself while the plot shows that our desired frequency range is enough with a SNR larger than 30dB.

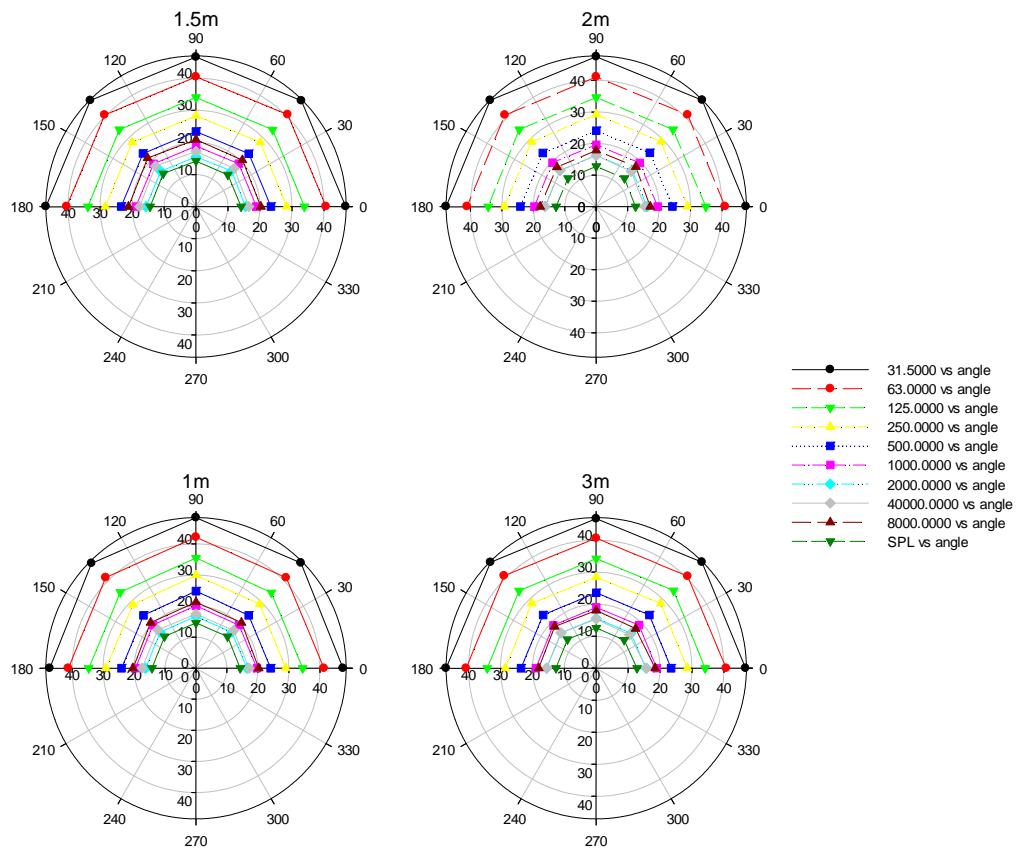


Figure 7-7 Directivity plots of the spark source measured in anechoic chamber, at 1m, 1.5m 2m and 3m from the source

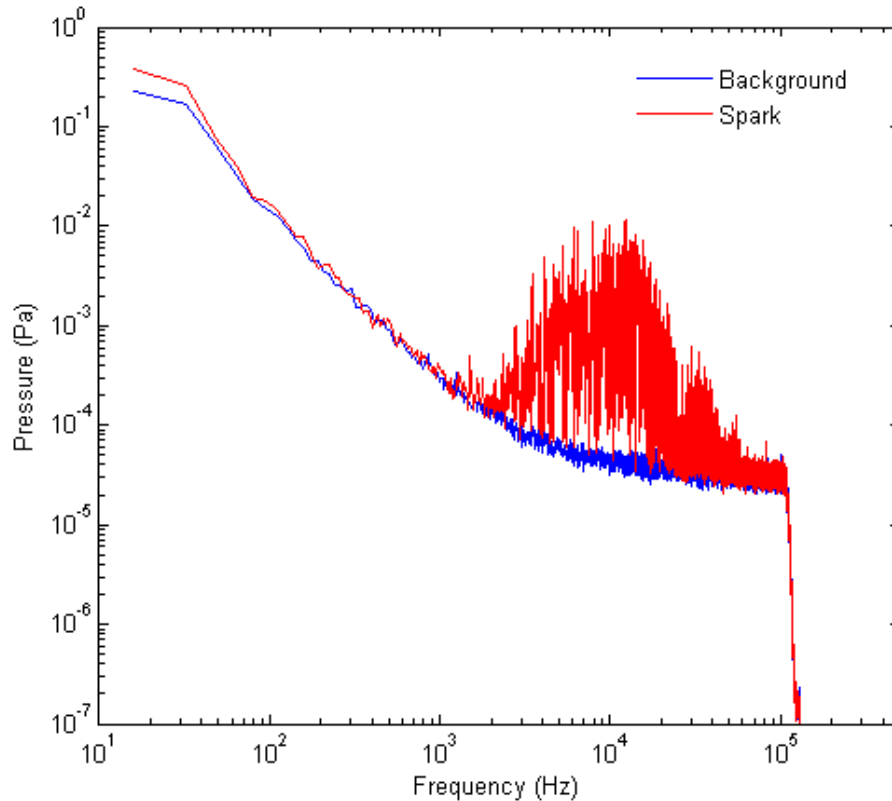
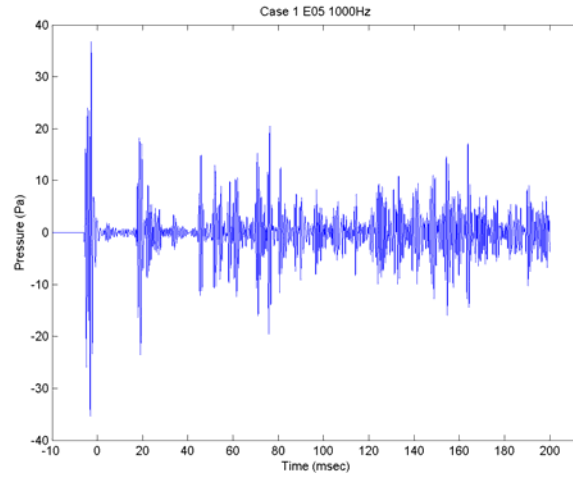


Figure 7-8 Measured pressure spectrum at 2m at 90 degree of the spark source and its background pressure spectrum

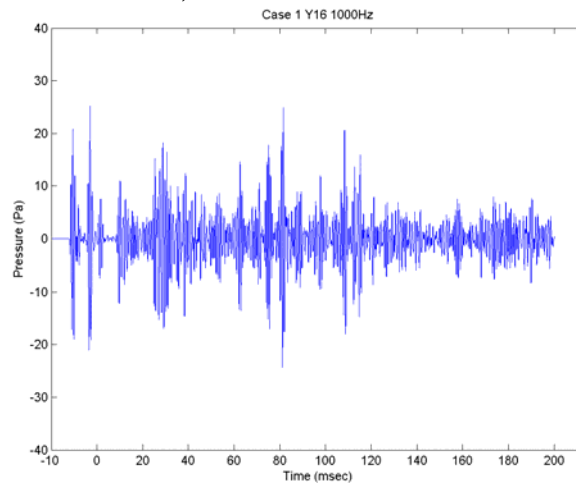
7.4 Results

Impulse responses were recorded with a sampling frequency of 262144Hz using a high-frequency pulse measurement system. Each set of recording contained data of two measurement points. There were at least three isolated decays recorded in each track. The recorded pressure-time series were firstly separated into isolated impulses and then processed. Afterwards, the signals were filtered into desired frequency bands and smoothed using Hilbert transform in Matlab. The resulted time series was calculated using integrated impulse response method to obtain the decay curve and the desired parameters.

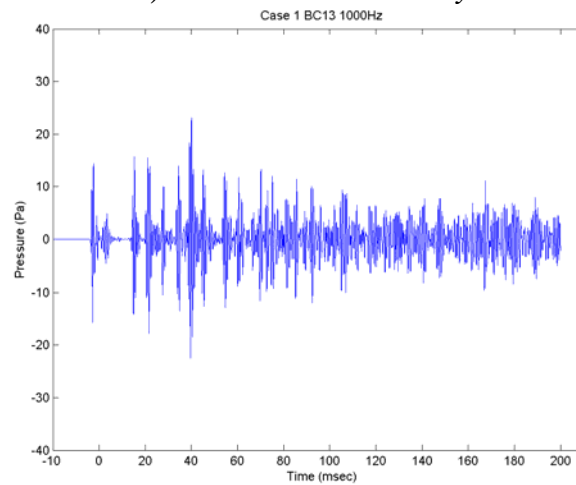
Figure 7-9a to c shows samples of isolated impulses measured at various seats in the 3 main areas in the scaled-model with concert hall setting. The spark source was strong enough to produce very sharp impulses at various locations. It is very obvious that the measured impulses were weaker at the balcony, the early energy was higher at other locations. Figure 7-10a to c shows the sample impulses measured at various seats in the three main areas in the scale mode with proscenium setting.



a) Seat E05 in stall area

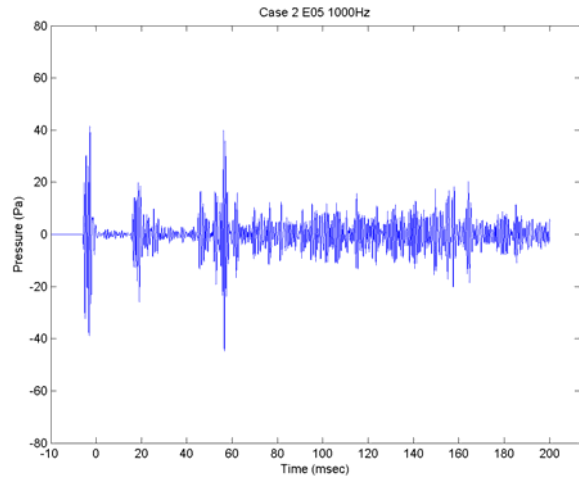


b) Seat Y16 under the balcony

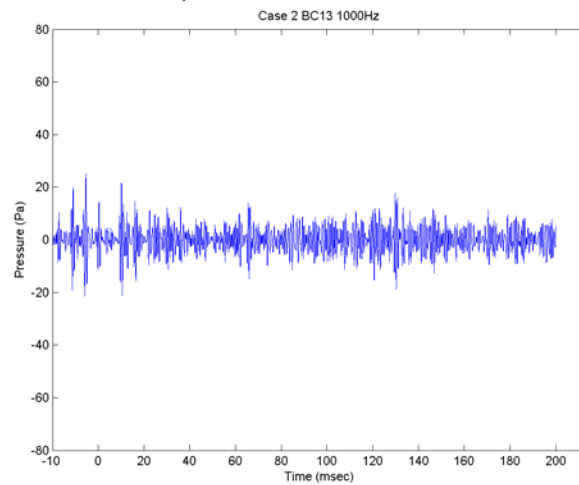


c) seat BC13 on the balcony

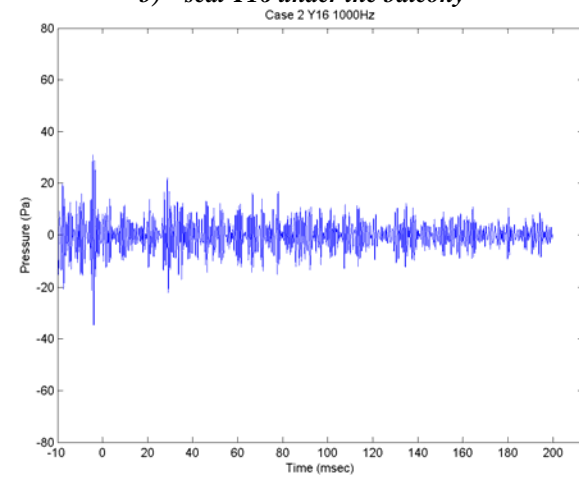
Figure 7-9 Measured impulse at 1000Hz in case 1, a) shows the impulse at seat E05 in the stall area, b) at seat Y16 under the balcony and c) at seat BC13 on the balcony



a) seat E05 in stall area



b) seat Y16 under the balcony



c) seat BC13 on the balcony

Figure 7-10 Measured impulse at 1000Hz in case 2,
a) shows the impulse at seat E05 in the stall area, b) at seat Y16 under the balcony and c) at seat BC13 on the balcony

The following sections present the simple statistics of the results measured. The internal environment of the scale model was very reverberant, therefore, with a very strong pulse produced by the spark source, the decays obtained were long enough to calculate the T60 in additional T30 for evaluating the reverberation time.

7.4.1 Student t-test/ difference between with and without balcony

The measured parameters in each comparing cases, with respect to the balcony condition, (Case 1 vs Case 3 and Case 2 vs Case 4) have to be different such that the effect can be observed. Therefore, student two-tailed t-tests were performed to check whether the parameters calculated in different cases are the same. The null hypothesis was set to be the two data sets were equal, at the 95% confident interval. $H = 1$ indicates a rejection of the null hypothesis at the 5% significance level. This test was done using Matlab. Calculated results of below-mentioned parameters were tested in individual frequency bands. Except in 63Hz and 8000Hz, most of the sets of results give $H=1$, which means the data are not the same. At most of the frequencies except 8000Hz, the measured parameters are significantly different. The t-test results for the concert hall setting is slightly different from that of the proscenium setting, all the concerned parameters except C80 are significantly different while C80s' are significantly different at 125Hz to 4000Hz. One can conclude that the results of the different cases are not the same and can look at the differences between cases with and with the balcony in details.

7.4.2 Proscenium setting

7.4.2.1 Early decay time and Reverberation time

The EDTs were measured at all measurement points in the scale model in each case. They were firstly divided into stall and balcony with an overall value giving a general concept of the measured condition and then the stall area was divided into front stall, mid-stall and balcony. The hall was also divided into the same 4 subzones as in Chapter 4 to 6. The measured EDT ranges up to 6 to 7 sec at low frequencies with a proscenium setting with and without the balcony. The standard deviations at low frequencies like 63Hz are up to 10% of the EDT values. At all the other frequencies, the EDT are uniform and within ± 1 JND, ie 5%. Figure 7-11 and Figure 7-12 show the spectra of the EDT measured in the scale model with and without the balcony in the proscenium setting. In both cases, the measured data are of a similar trend in all subzones: having EDT as long as around 6sec at 63Hz, with a small drop at 125Hz, and rise again before falling back to around 1sec at

8000Hz. The variation of measured data is the largest at 63Hz and the variation decreases when frequency increases.

In case 1, a proscenium stage with the balcony, the average value under the balcony is smaller than the others measured at the stall, mid stall or on the balcony, especially at 250Hz. The variation of mean values from 63Hz to 125Hz and 250Hz is smaller under the balcony than in the other zones. In general, the seats on the balcony are having a longer averaged EDT than seats in the other zones. In case 3, as shown in Figure 7-12, the EDT are longer without the balcony with the same proscenium stage setting. The values at 63Hz are the highest among all frequencies in both Case 1 and Case 3.

Reverberation time T30 was calculated based on the time for the impulse to decay from -5dB to -30dB from the peak of the impulse. The measured signal was backward integrated and then the decay slope was found within this frame to determine the reverberation time. Figure 7-13 and Figure 7-14 plot the spectra of the measured T30s in the scale model with a concert stage setting with and without the balcony respectively. The measured T30s are having a similar increasing and decreasing pattern across the octave frequency bands as for the cases of EDT. In Case 1, a normal proscenium hall, the values at 63Hz at all four zones are more diverse than those at the other frequencies, this diversity decreases with the increasing frequency generally. Unlike EDT, T30 is maximum at 250Hz in all zones in this case and again reaches its minimum at 8000Hz. Those seats under the balcony are having slightly smaller mean T30s than in the other zones. The variation of T30s from 125 Hz onwards as less than 5% of the mean values and thus not audible while the JND of T30s are 5%. However, as seen in Figure 7-13, the values at 63Hz are around 10% of the mean values. Figure 7-14 shows that the T30 measured at seats in the stall area without the balcony has larger outliers than those measured with the balcony. The means of the measured T30s without the balcony are also larger than those with the balcony. Very likely, with the balcony removed, the internal volume of the scale model increases and this tends to lengthen the reverberation times at all frequencies. This change in volume and increased ceiling height may also bring more diverse T30 at low frequencies like 63Hz and 125Hz.

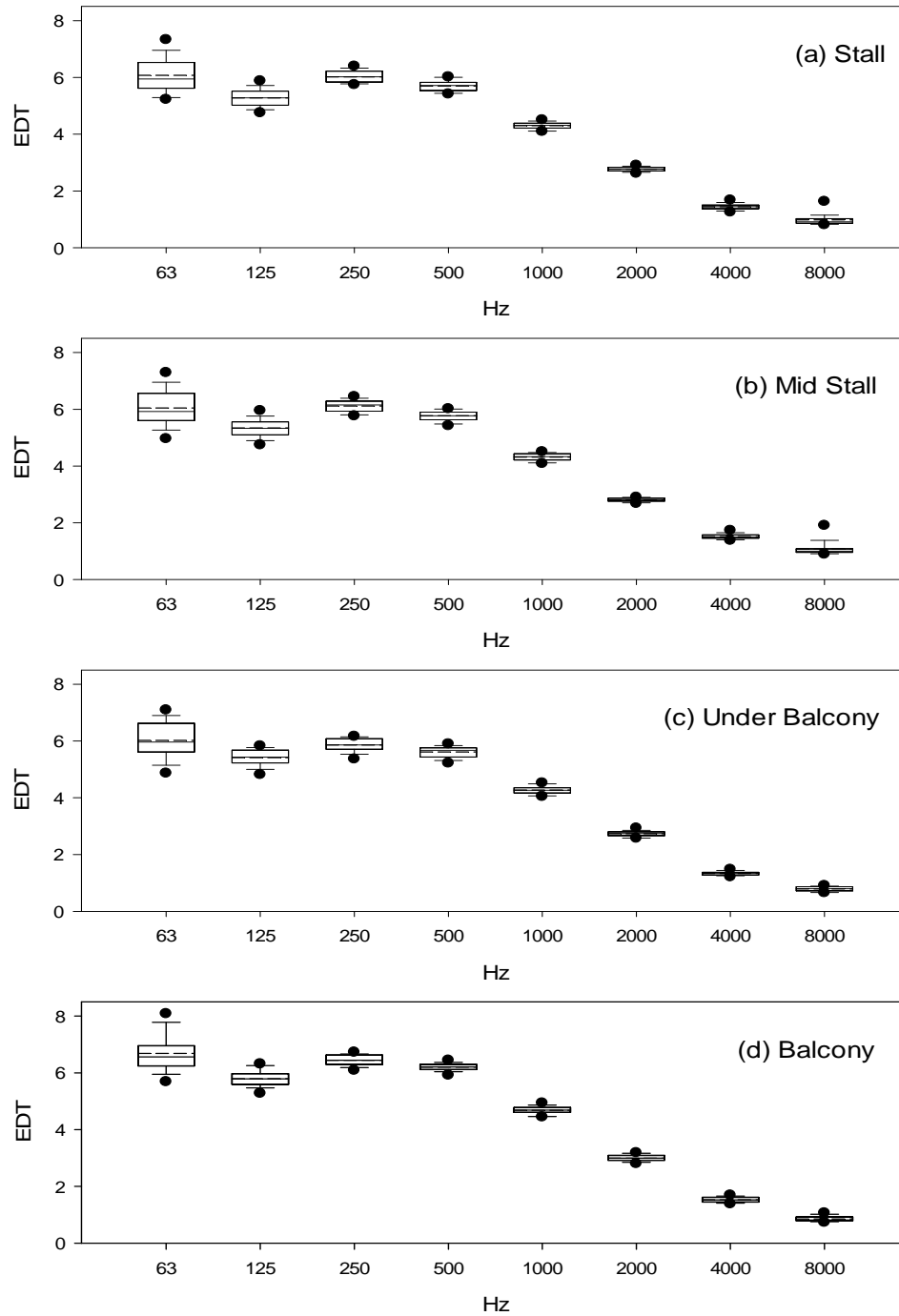


Figure 7-11 Measured EDT (in sec) spectrum of the scaled-model with balcony and a proscenium stage setting (Case 1)
 • : 5th and 95th percentiles; error bars : 10th and 90th percentiles; box edges : 25th and 75th percentiles; horizontal lines within boxes : median; horizontal dashed lines : mean values

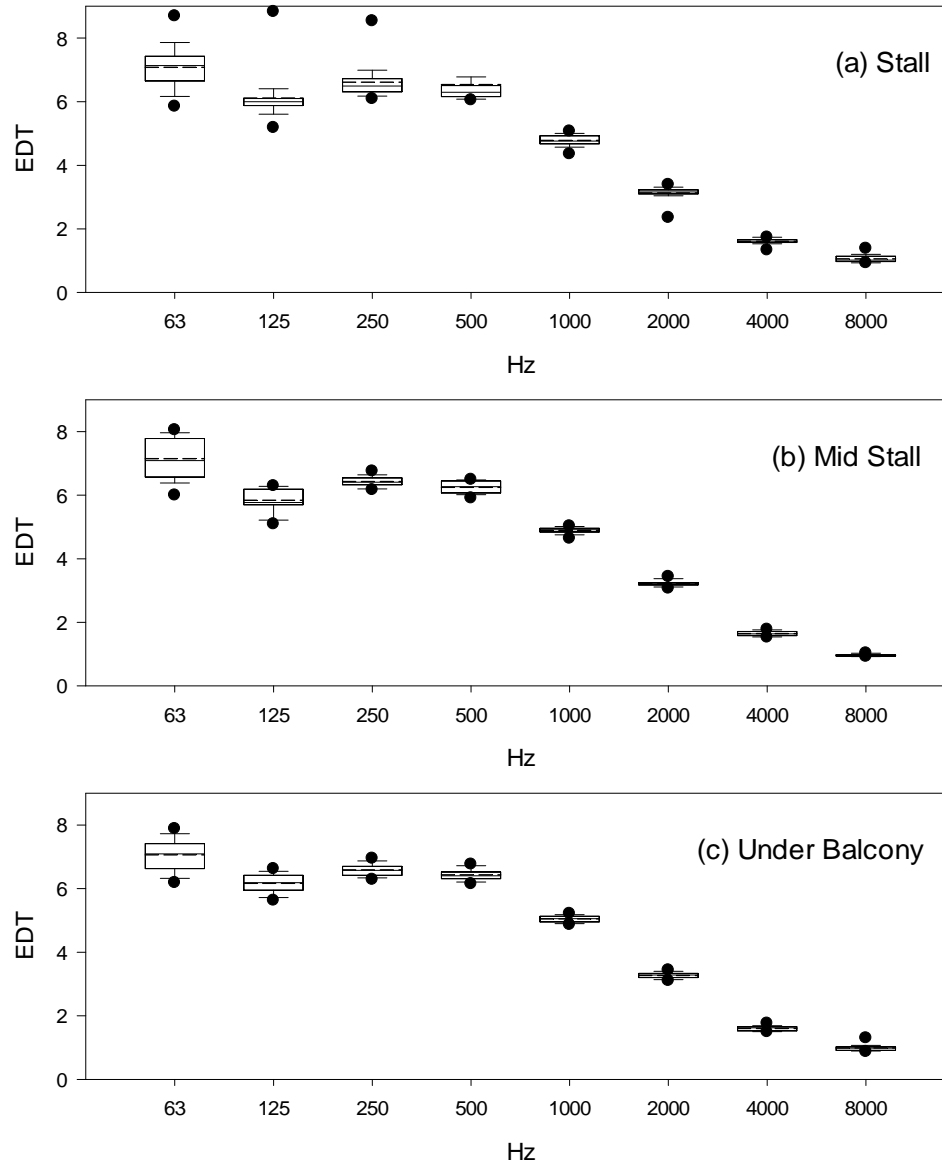


Figure 7-12 Measured EDT (in sec) spectrum of the scaled-model without balcony with a proscenium stage setting (Case 3)

• : 5th and 95th percentiles; error bars : 10th and 90th percentiles; box edges : 25th and 75th percentiles; horizontal lines within boxes : median; horizontal dashed lines : mean values

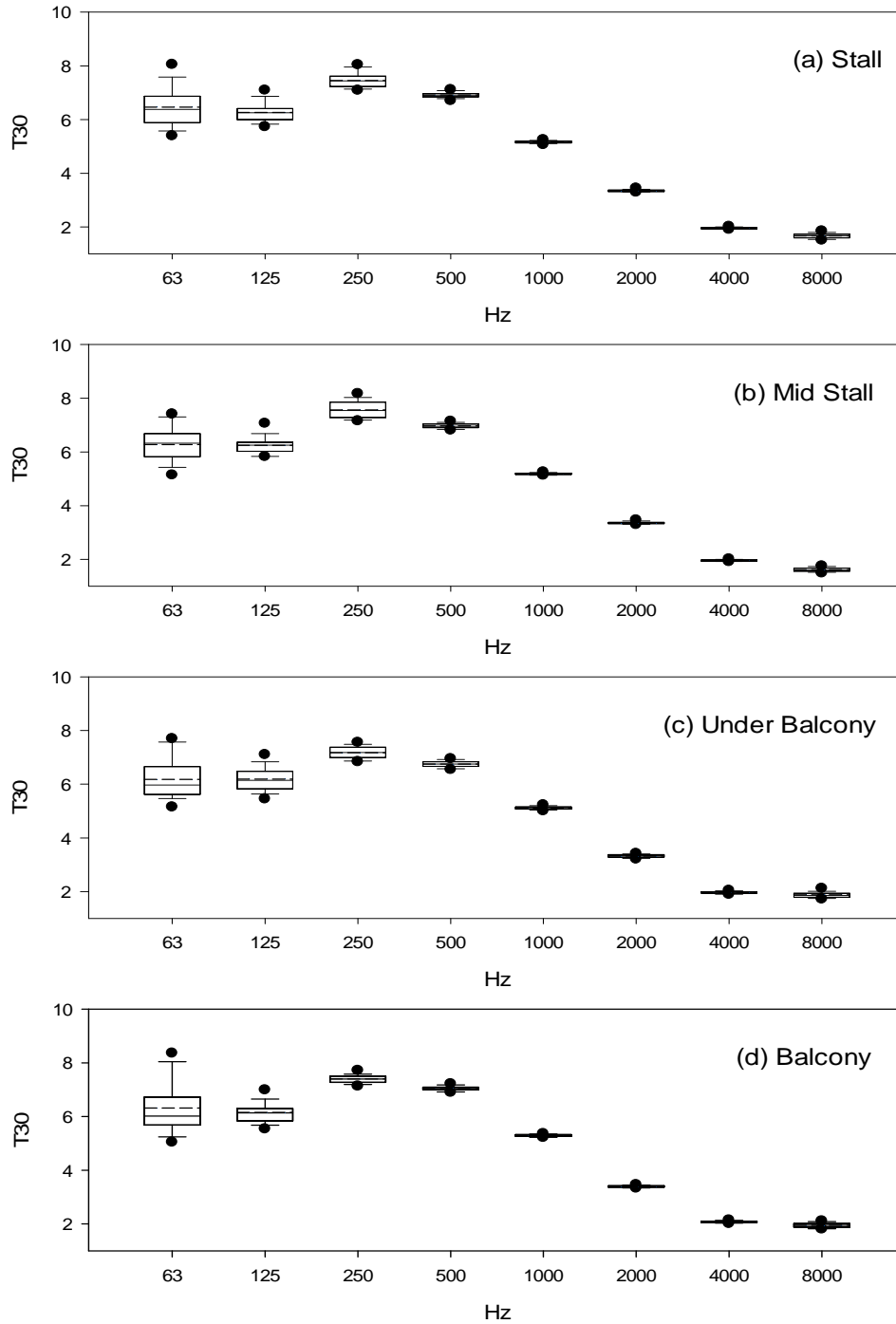


Figure 7-13 Measured T30 (in sec) spectrum of the scaled-model with balcony and a proscenium stage setting (Case 1)

• : 5th and 95th percentiles; error bars : 10th and 90th percentiles; box edges : 25th and 75th percentiles; horizontal lines within boxes : median; horizontal dashed lines : mean values

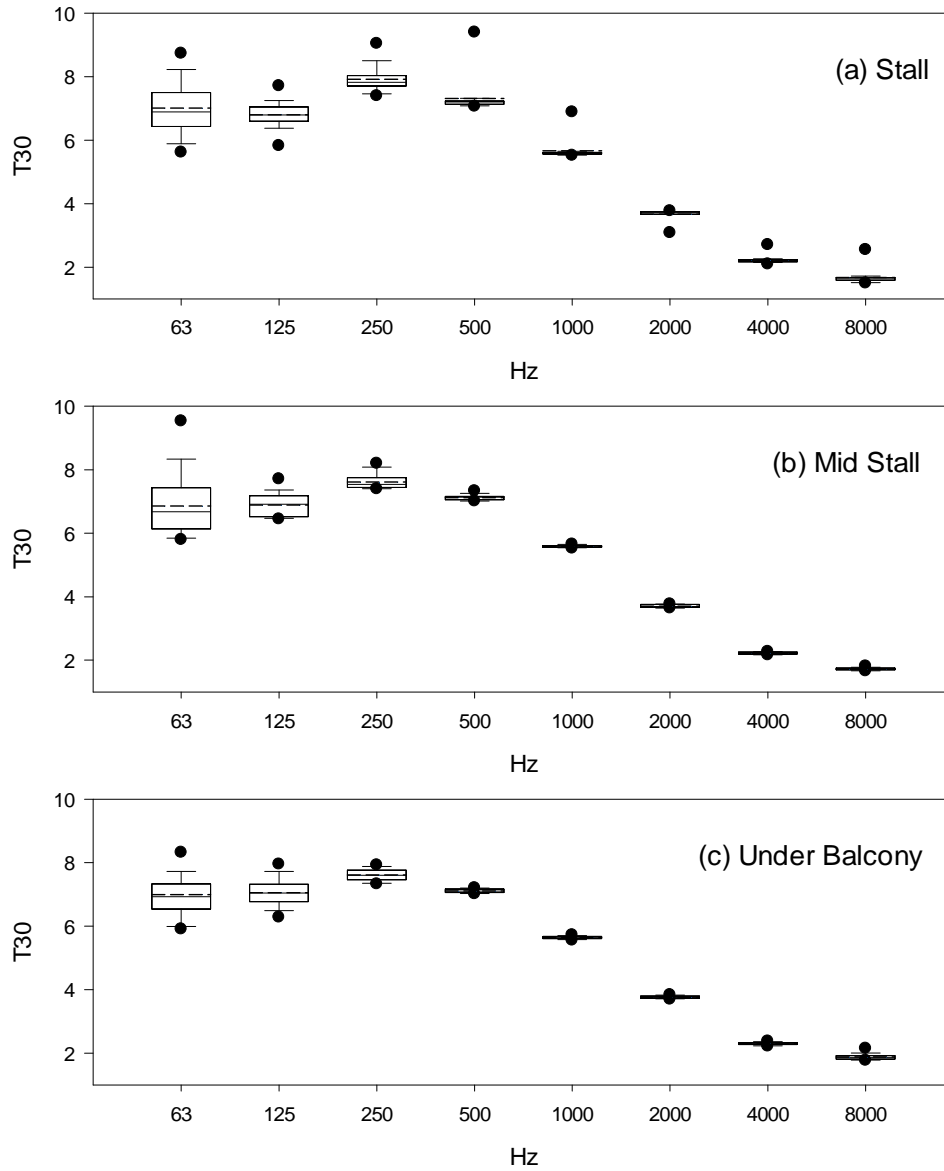


Figure 7-14 Measured T30 (in sec) spectrum of the scaled-model without balcony with a proscenium stage setting (Case 3)
 • : 5th and 95th percentiles; error bars : 10th and 90th percentiles; box edges : 25th and 75th percentiles; horizontal lines within boxes : median; horizontal dashed lines : mean values

7.4.2.2 Energy ratios, Clarity and Definition

Clarity is the ratio of the early energy to late energy. Increasing the early energy will increase the clarity while lengthening the reverberation time will increase the amount of late energy thus decreasing clarity. The most commonly used clarity is C80, which takes the early energy received in the first 80 milliseconds into account. Accounting the first 80 milliseconds is commonly used for music while 50msec is used for speech.

Figure 7-15 and Figure 7-16 plot the spectra of the measured C80 in the scale model with a proscenium stage setting with and without the balcony. In the stall, mid-stall and under balcony area, the C80s drops slightly from 63Hz and the rise up starting from 250Hz and attain maxima at 8000Hz. The variations within each frequency band are more constant on the balcony while the variation is the largest at 63 Hz in areas down in the stall, mid-stall and under the balcony. The values are the most diverse at 63Hz. The range of values measured at 63Hz within the stall and mid-stall area can be up to 10dB, which are far more larger than the JND suggested by ISO3382 [13]. The variation at 8000Hz measured under the balcony is also relatively large. Among different frequencies, the values at 8000Hz are the largest.

The C80s measured with the balcony are larger than those measured without the balcony. The values measured at the stall area without the balcony appear to have a deeper valley at 250Hz in Figure 7-16 while those at 63Hz are having a much larger variation than those with the balcony in Figure 7-15. This may be due to the removal of the balcony has increased the distances from these seats to the balcony edge which is one of their major reflecting surface, and thus the reflections arrive at very different times. After the removal of the balcony, the range of the measured values at 63Hz within the mid-stall and that at 8000Hz under the balcony diminish.

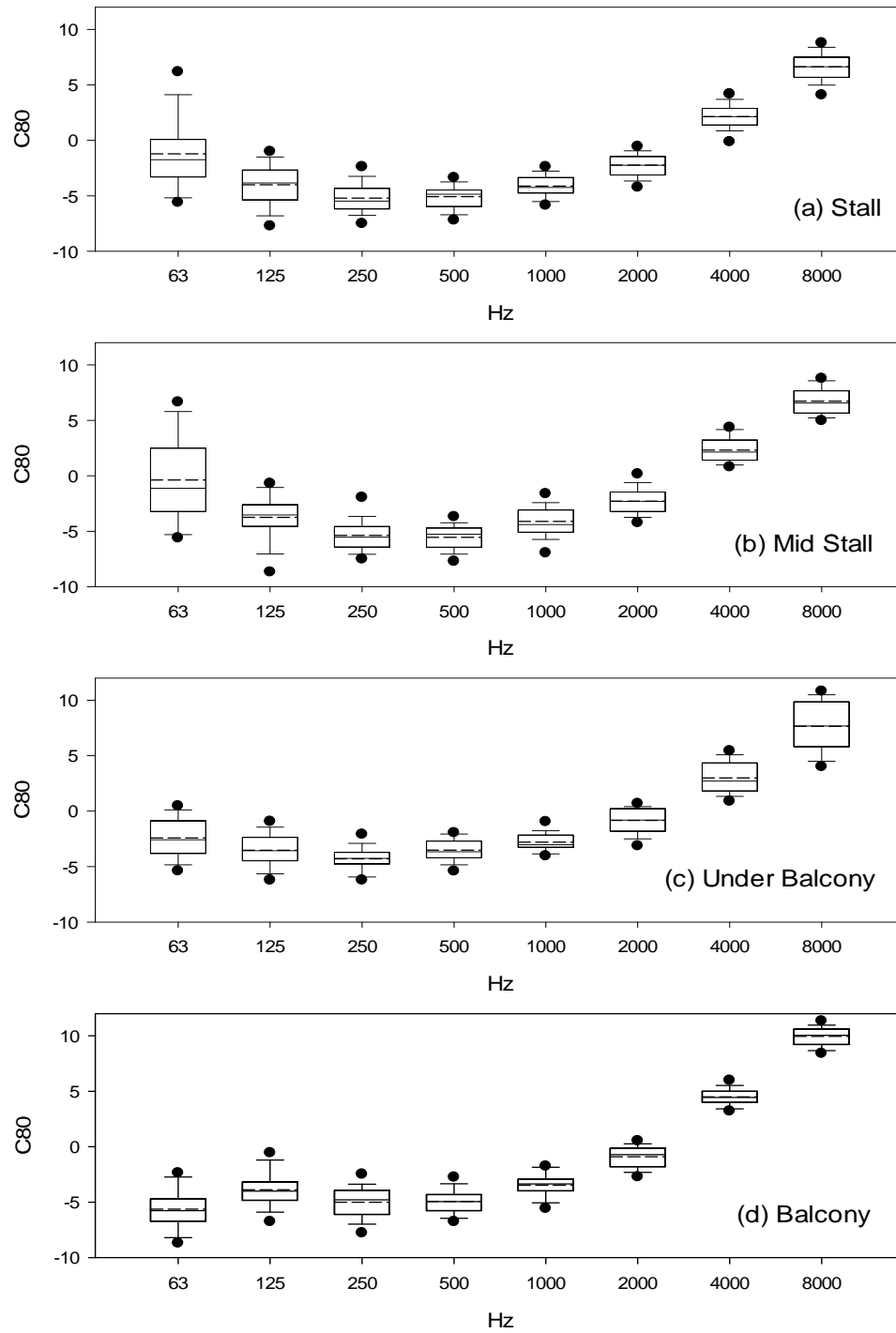


Figure 7-15 Measured C80 (in dB) spectrum of the scaled-model without balcony with a proscenium stage setting (Case 1)

• : 5th and 95th percentiles; error bars : 10th and 90th percentiles; box edges : 25th and 75th percentiles; horizontal lines within boxes : median; horizontal dashed lines : mean values

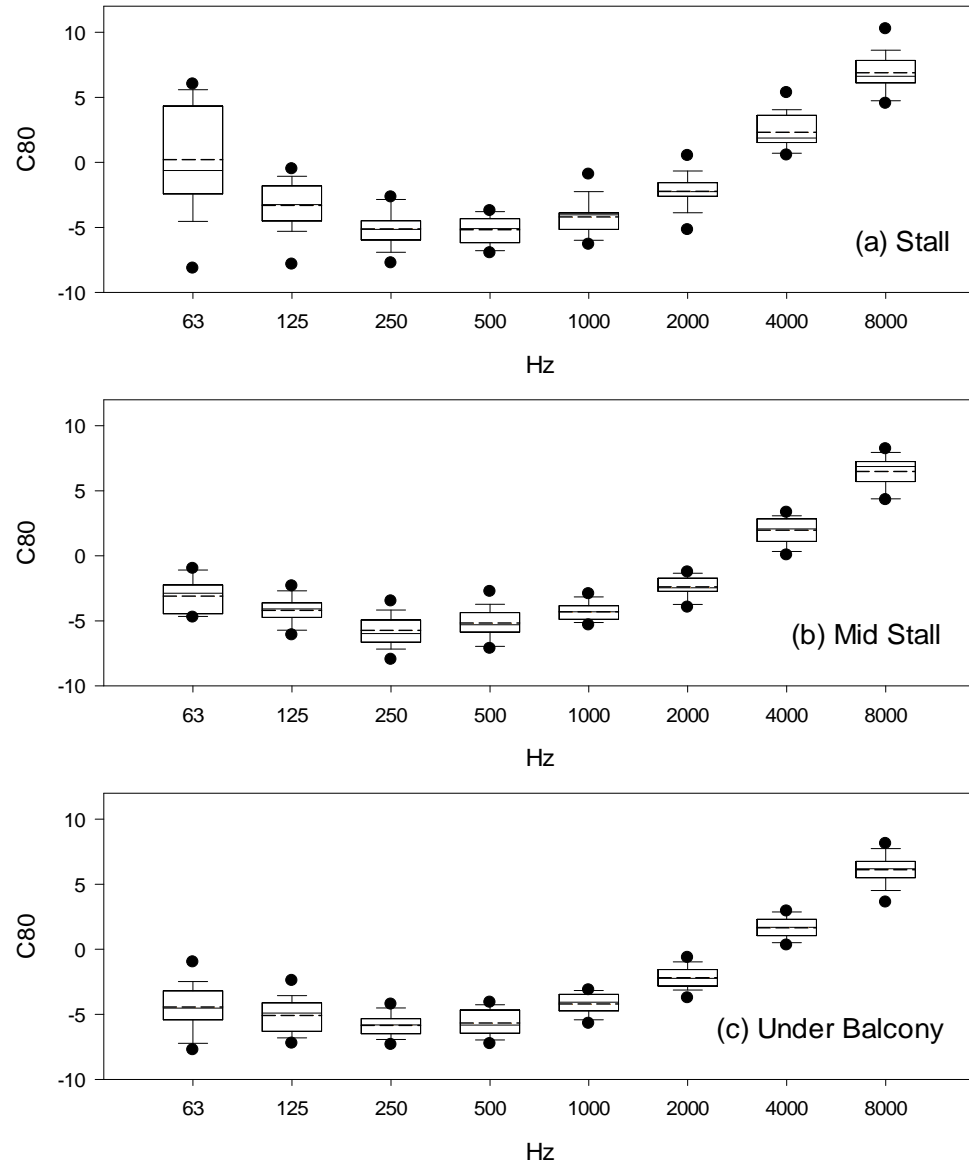


Figure 7-16 Measured C80 (in dB) spectrum of the scaled-model without balcony with a proscenium stage setting (Case 3)

- : 5th and 95th percentiles; error bars : 10th and 90th percentiles; box edges : 25th and 75th percentiles; horizontal lines within boxes : median; horizontal dashed lines : mean values

The plots of the measured D50 spectra in Figure 7-17 and Figure 7-18 appear to have a similar pattern as the plot of C80. The D50s measured with and without the balcony are all decreasing from 63Hz to 250Hz and then increases to maximum at 8000Hz. The variation of the C80s measured at 63Hz in the stall area significantly higher. From only having outliners at 0.8dB, the data change to having a diverged ranges from 0.3 to values larger than 0.8. However, in the mid stall area, the variation at 63Hz decreased to a range similar to other frequencies, which are within the JND recommended. The situation under the balcony is slightly different here, the whisker boxes at 4000Hz and 8000Hz minimize once the balcony is removed.

The frequency variations of C80 and D50 are similar. The range and the mean of measured D50 increases at 63Hz in the stall area while the variation and mean decrease in the mid-stall area after the removal of the balcony. This also reduces the range of values at 8000Hz in the mid-stall. The range of values and mean at 4000Hz to 8000Hz at seats under the balcony are also reduced. The overall ranges of the measured values in Case 1 and Case 3 are approximately the same.

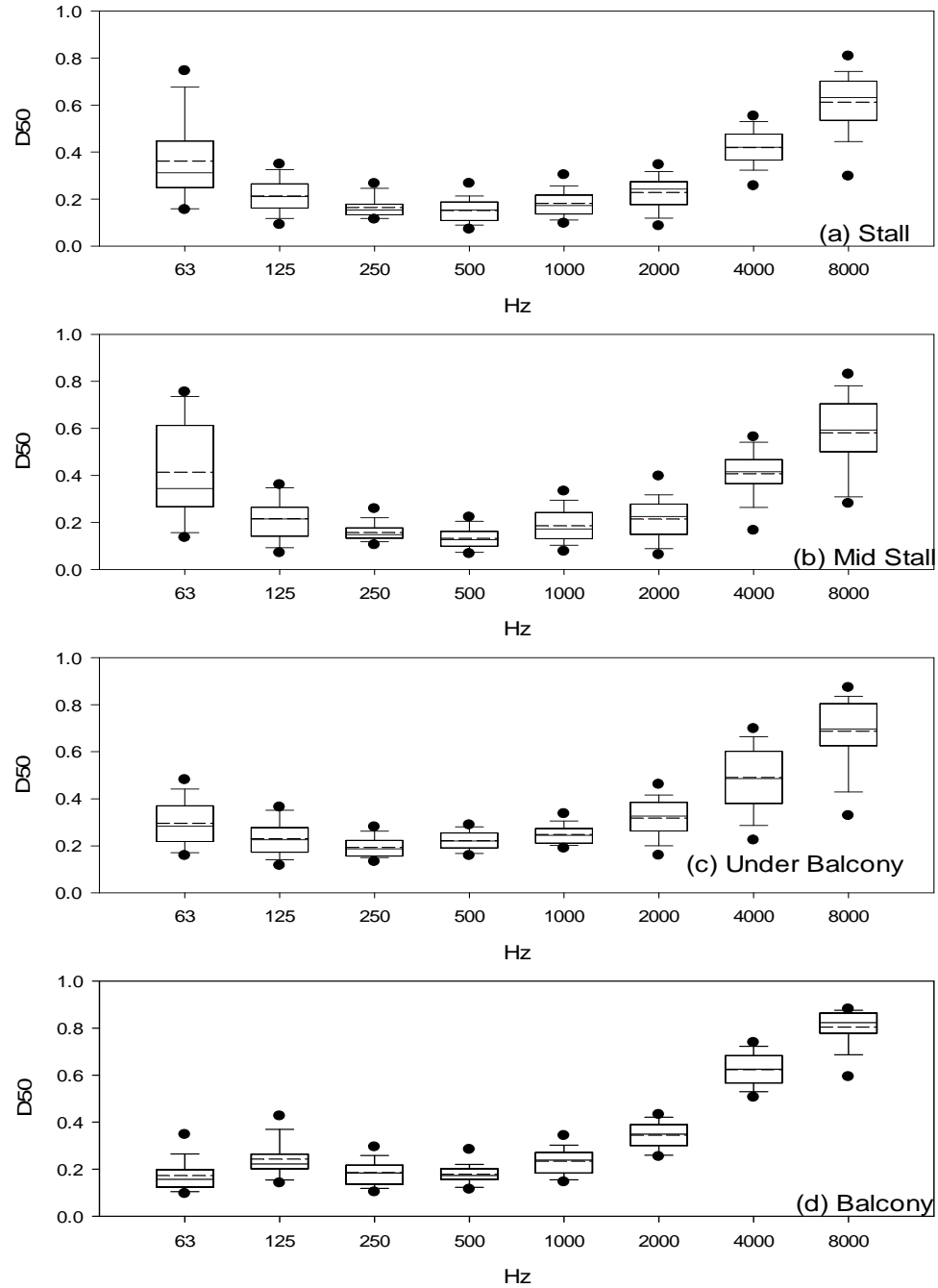


Figure 7-17 Measured D50 spectrum of the scaled-model without balcony with a proscenium stage setting (Case 1)

• : 5th and 95th percentiles; error bars : 10th and 90th percentiles; box edges : 25th and 75th percentiles; horizontal lines within boxes : median; horizontal dashed lines : mean values

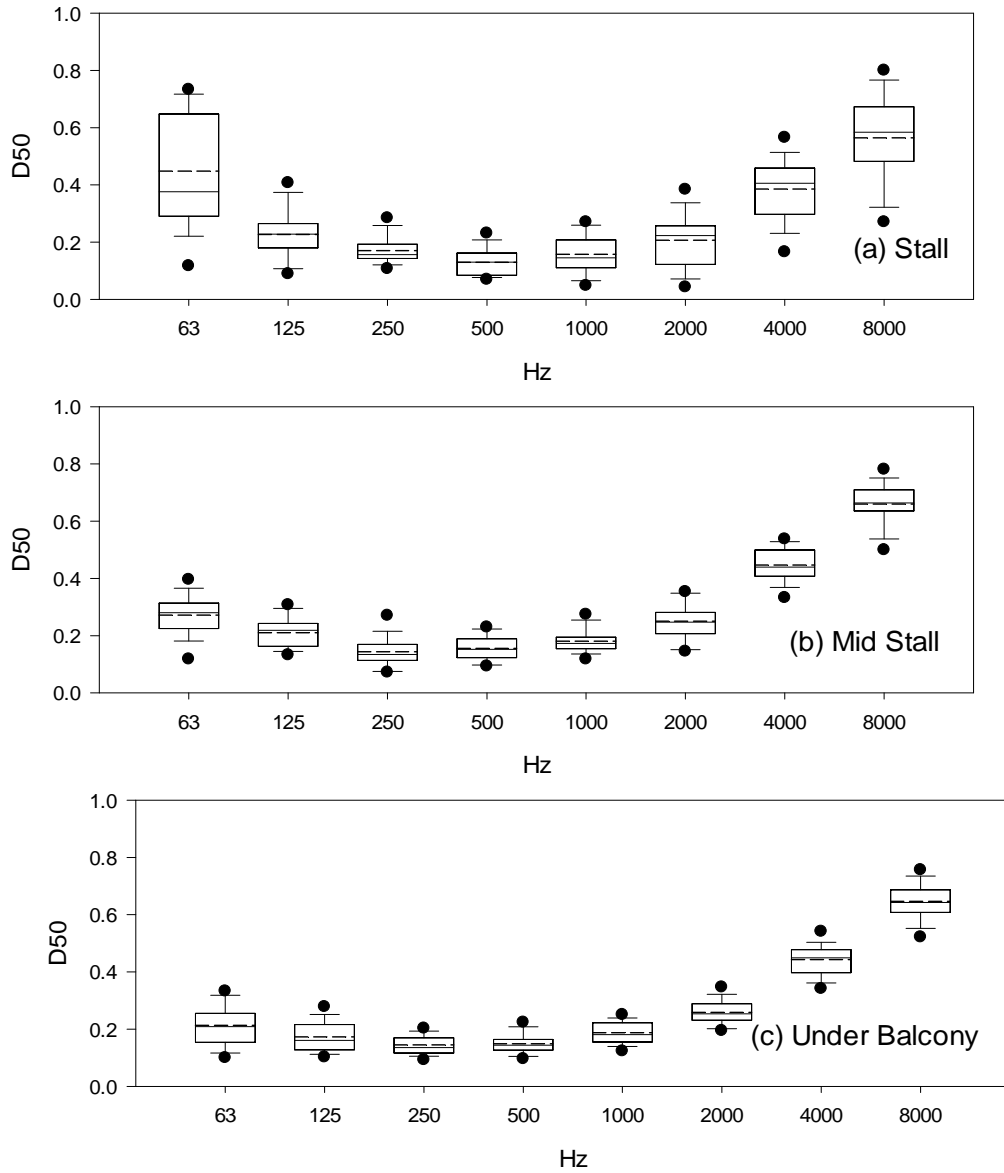


Figure 7-18 Measured D50 spectrum of the scaled-model without balcony with a proscenium stage setting (Case 3)

• : 5th and 95th percentiles; error bars : 10th and 90th percentiles; box edges : 25th and 75th percentiles; horizontal lines within boxes : median; horizontal dashed lines : mean values

7.4.3 Concert setting

7.4.3.1 Early decay time and Reverberation time

Figure 7-19 and Figure 7-20 plots the spectra of the measured EDT in the scale model with a concert stage setting, with the sound canopy, with and without the balcony. The sound canopy on the stage results in a distribution of EDT relatively similar to that in the proscenium setting.

The values decrease slightly at 125Hz and then increase at 250Hz. At mid- frequencies up to 2000Hz are decreasing again with the frequencies. These values are far much longer than values measured at real hall measurements in Chapter 4 and in usual circumstances. This is probably resulted from the untreated surface inside the scale model that has made the measured EDT longer than usual. Except the fabric used to simulate the proscenium setting on the stage, there are not any absorption materials added to the interior of the scale model. Therefore, with all the hard and smooth surface of the wood panels forming the scale model, the decay inside the scale model should be very long. The smooth and hard surfaces inside the scale model, as well as the tall ceiling, have contributed to this results. At higher frequencies, 4000 and 8000 Hz, the frequencies measured in real scale are 40000Hz and 80000Hz. Air absorption at these real frequencies should be strong, thus, the measured EDT at these frequencies are likely to be much shorter than those at lower frequencies. This pattern also appears in the results of reverberation time, T30 and T60. One can observe from Figure 7-21 and Figure 7-22 that the means of T30 are decreasing from 63Hz to 125Hz and significantly increase before decreasing with increasing frequency. The means of the measured T30s at 63Hz and 125Hz are around 8 sec, those at 500 Hz are increased to around 9 secs while those measured at 1000Hz are around 6sec. The means decrease, starting from 1000Hz.

From the tabulated data, the standard deviations at low frequencies like 63Hz are up to 10% of the EDT values. At all the other frequencies, the EDTs are uniform and within ± 1 JND, i.e. 5%. T60s are not as uniform as the two other decay time related parameters. In both Case 1 and Case 3, the mean reverberation times, T60s, are longer in the front stall than in the mid stall area.

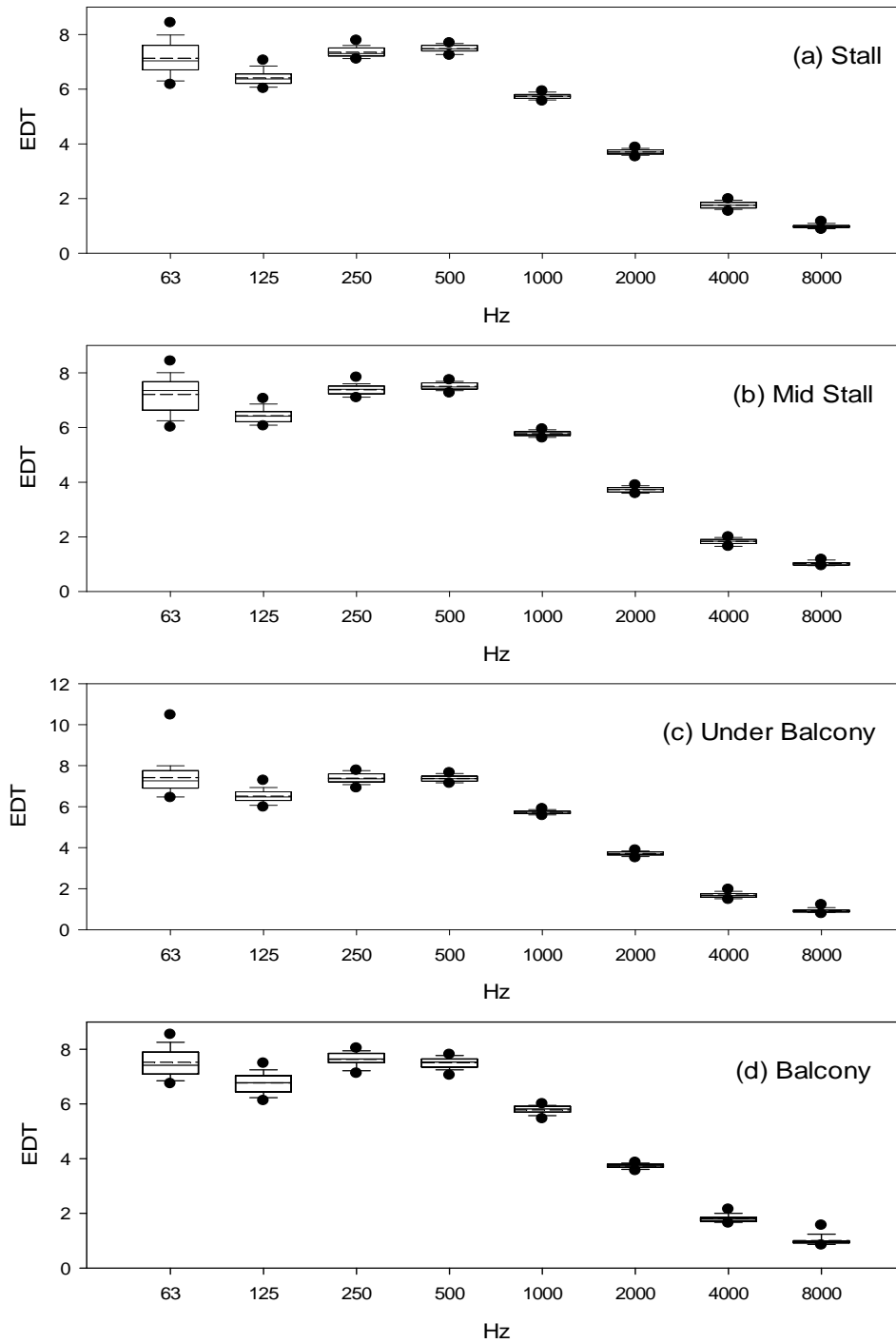


Figure 7-19 Measured EDT (in sec) spectrum of the scaled-model without balcony with a proscenium stage setting (Case 2)
 • : 5th and 95th percentiles; error bars : 10th and 90th percentiles; box edges : 25th and 75th percentiles; horizontal lines within boxes : median; horizontal dashed lines : mean values

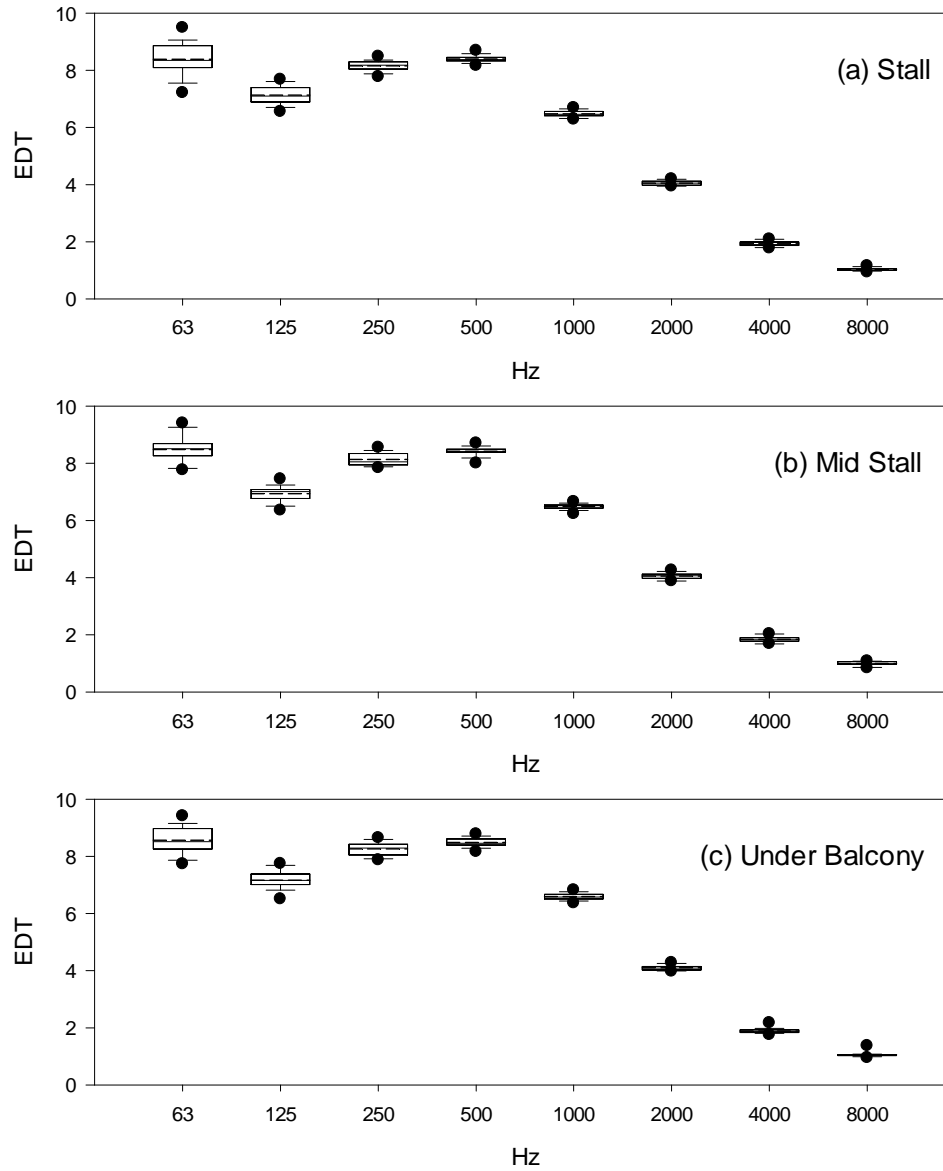


Figure 7-20 Measured EDT (in sec) spectrum of the scaled-model without balcony with a proscenium stage setting (Case 4)
 • : 5th and 95th percentiles; error bars : 10th and 90th percentiles; box edges : 25th and 75th percentiles; horizontal lines within boxes : median; horizontal dashed lines : mean values

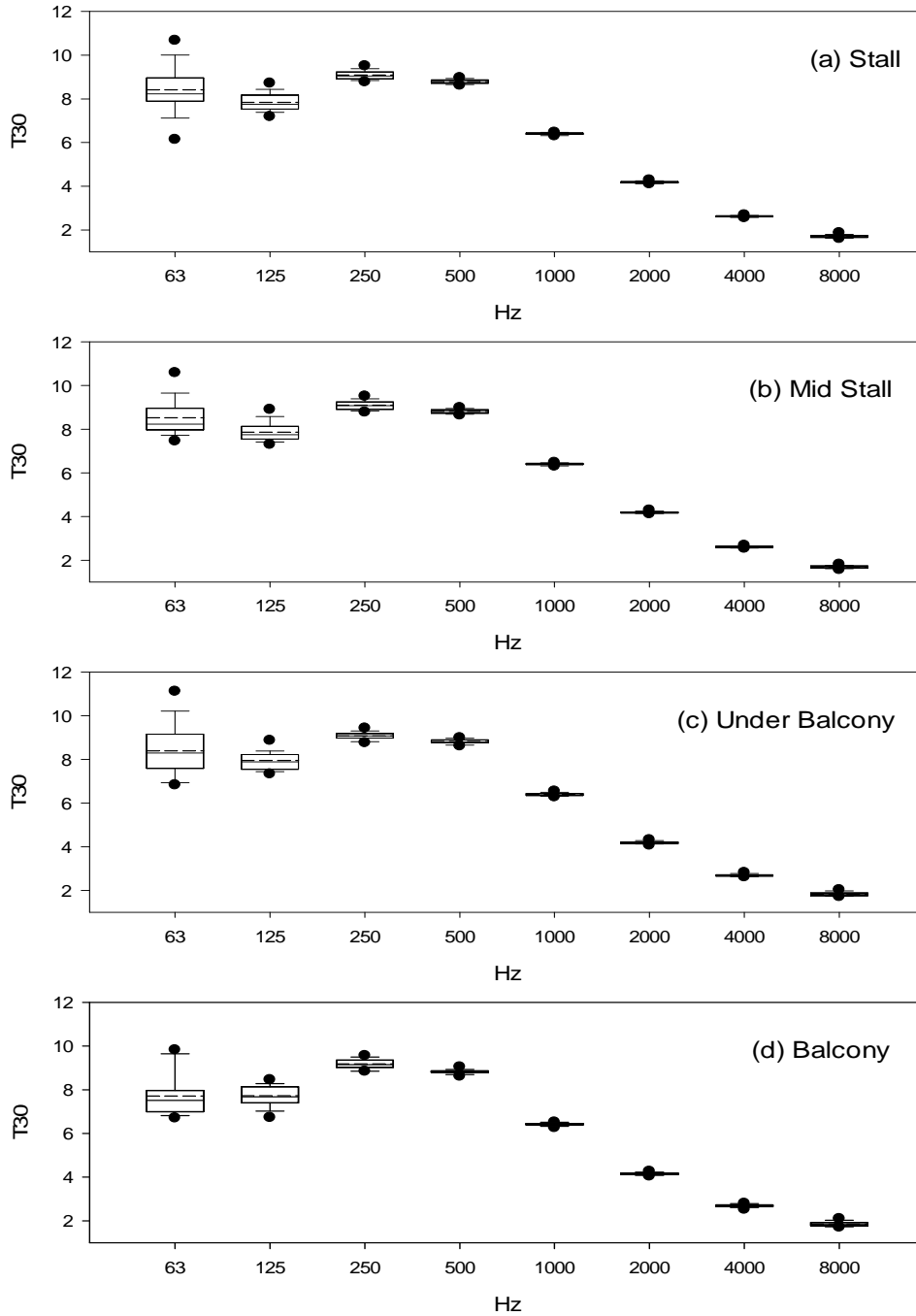


Figure 7-21 Measured T30 (in sec) spectrum of the scaled-model without balcony with a proscenium stage setting (Case 2)
 • : 5th and 95th percentiles; error bars : 10th and 90th percentiles; box edges : 25th and 75th percentiles; horizontal lines within boxes : median; horizontal dashed lines : mean values

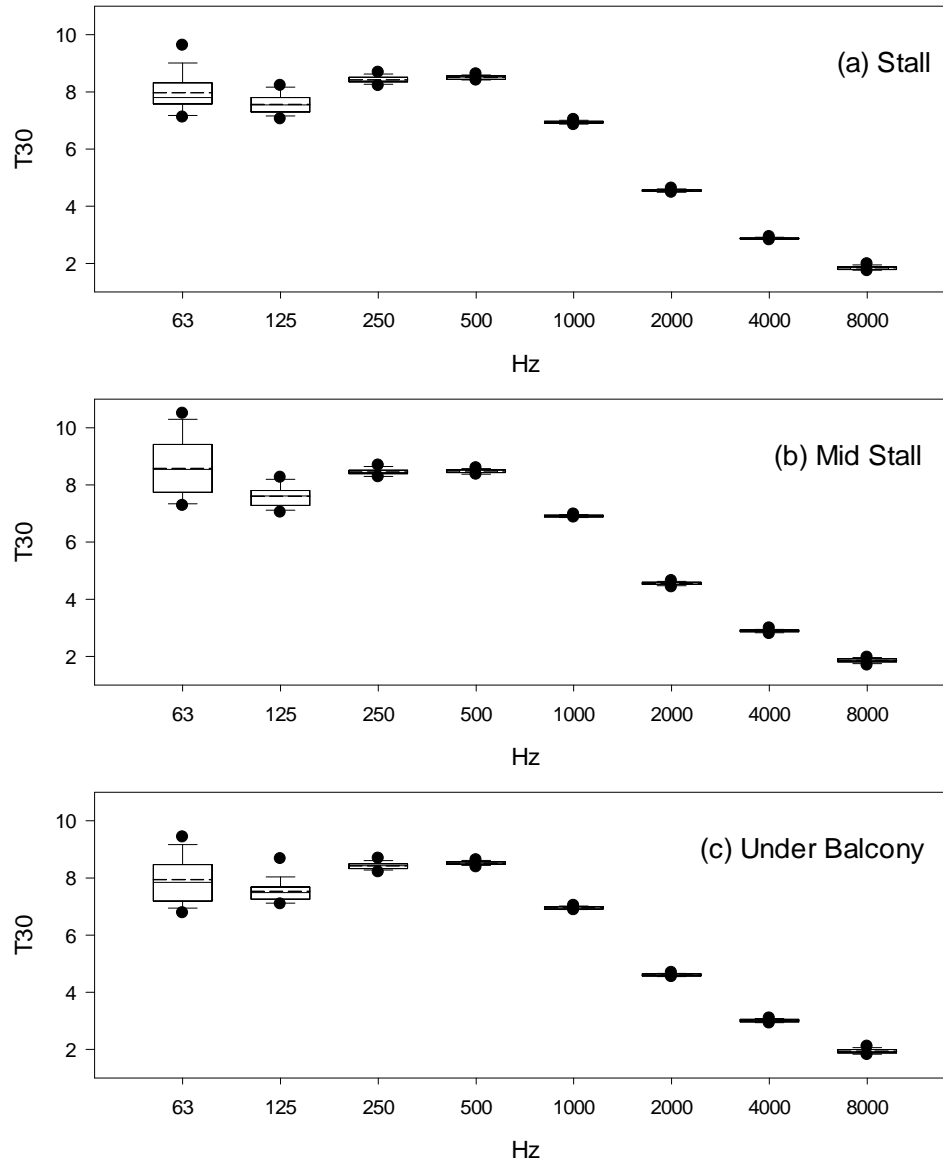


Figure 7-22 Measured T30 (in sec) spectrum of the scaled-model without balcony with a proscenium stage setting (Case 4)
 • : 5th and 95th percentiles; error bars : 10th and 90th percentiles; box edges : 25th and 75th percentiles; horizontal lines within boxes : median; horizontal dashed lines : mean values

7.4.3.2 Early energy ratios, Clarity and Definition

Figure 7-23 to Figure 7-26 plot the spectra of the measured C80s and D50s in the scale model with a concert setting with and without the balcony. The spectra of C80s and D50s in case 2 and case 4 were having the same trend as those in case 1 and case 3 respectively. The means of C80s range from around -7dB to around 6 dB while those of D50s from around 0.1 to approximately 0.65. They are both having larger ranges at 63Hz, decrease in ranges and have smaller means at 125Hz and 250 Hz. Their ranges and means increase with the frequency while maintaining small standard deviations. However, the variation at each zone at each frequency band is smaller than that under the concert setting. The plots of case 2 and case 4 show that the standard deviations are smaller than those in case 1 and case 3 respectively.

The standard deviations of C80 at 63Hz in the stall area are the largest among all locations and frequency. In case 2, with the sound canopy and the balcony, the C80s at the mid stall area varied the most, they decrease sharply from 63Hz to 250Hz and attain maxima at 8000Hz. This trend is observed in the stall area for the case without the balcony.

The standard deviations of D50s are the largest in the stall area among all locations and frequency, similar to the trend of C80s. One can conclude that the variations of the early energy within this area at 63 Hz are relatively large. While the C80 values are negative, the early energy content is yet larger than that of the late energy.

There are outlying data in the spectrum plots. When the whole set of energy ratios are plotted in contours, the values vary across all the stall area. While the C80s are higher under the balcony, the contours show patches of higher values comparing to the other parts of the hall. Also, the area along the centreline of the hall has slightly larger values. The D50s, the early to total energy ratios, also show that the early energy under the balcony in cases with the balcony are stronger in the stall area.

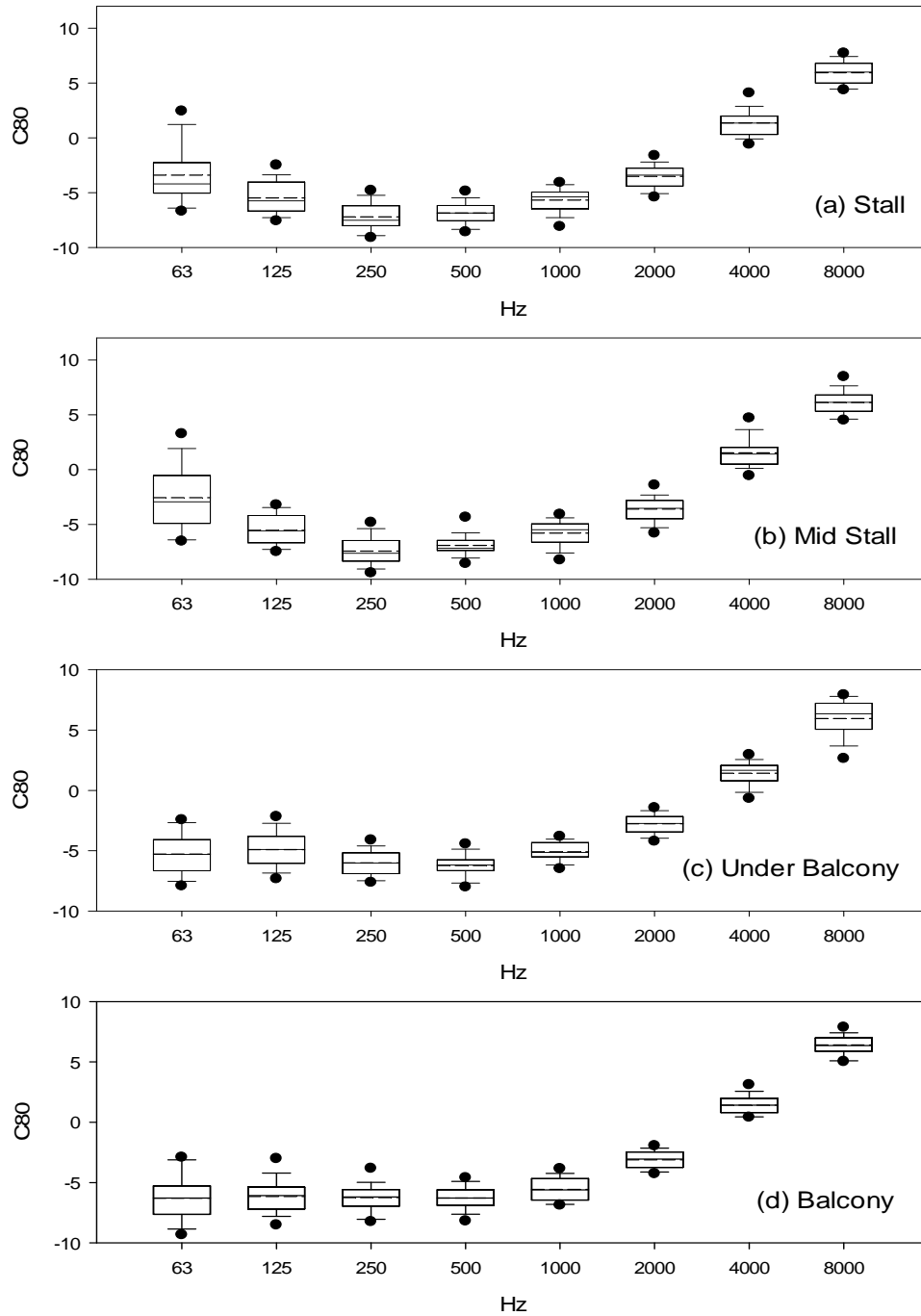


Figure 7-23 Measured C80 (in dB) spectrum of the scaled-model without balcony with a proscenium stage setting (Case 2)

• : 5th and 95th percentiles; error bars : 10th and 90th percentiles; box edges : 25th and 75th percentiles; horizontal lines within boxes : median; horizontal dashed lines : mean values

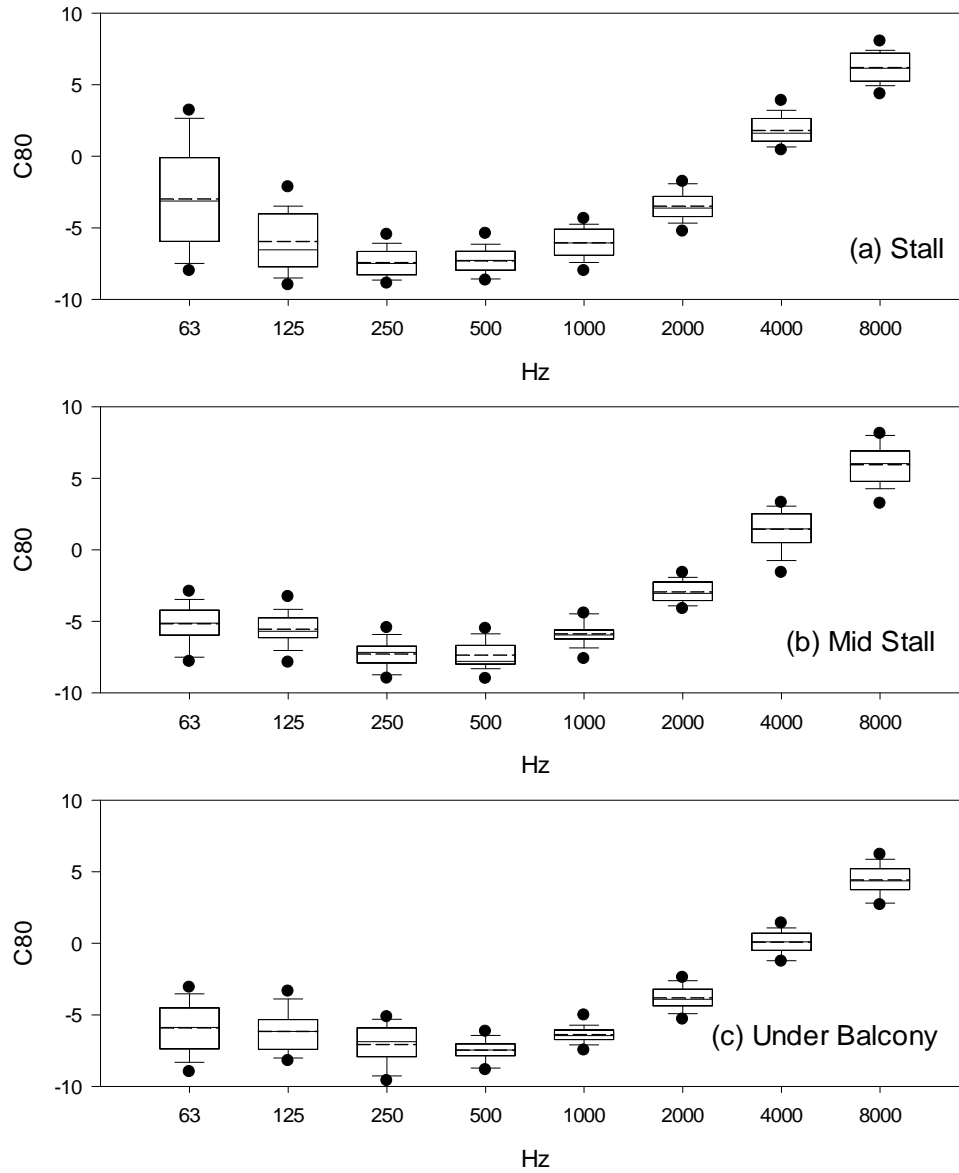


Figure 7-24 Measured C80 (in dB) spectrum of the scaled-model without balcony with a proscenium stage setting (Case 4)
 • : 5th and 95th percentiles; error bars : 10th and 90th percentiles; box edges : 25th and 75th percentiles; horizontal lines within boxes : median; horizontal dashed lines : mean values

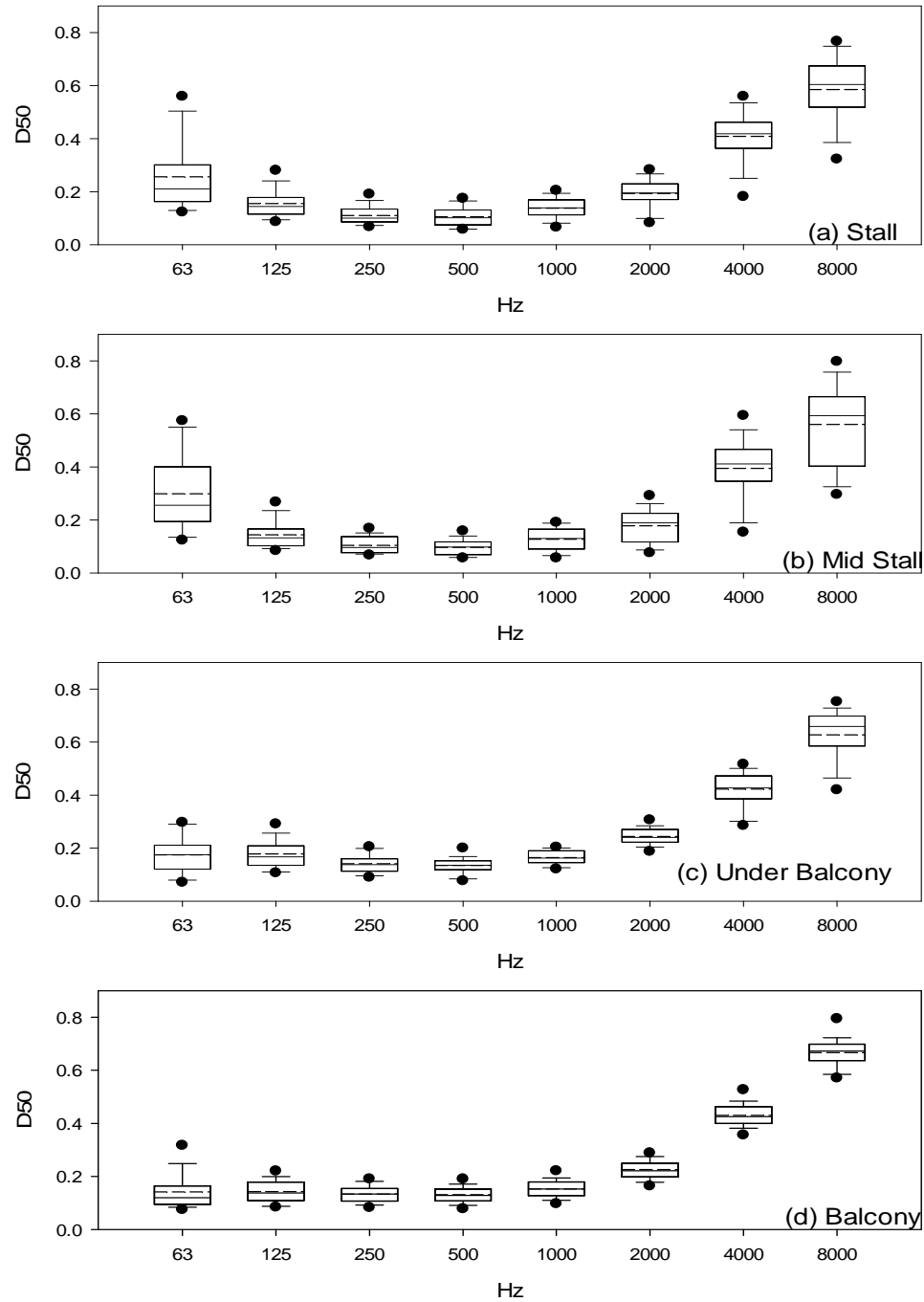


Figure 7-25 Measured D50 spectrum of the scaled-model without balcony with a proscenium stage setting (Case 2)

• : 5th and 95th percentiles; error bars : 10th and 90th percentiles; box edges : 25th and 75th percentiles; horizontal lines within boxes : median; horizontal dashed lines : mean values

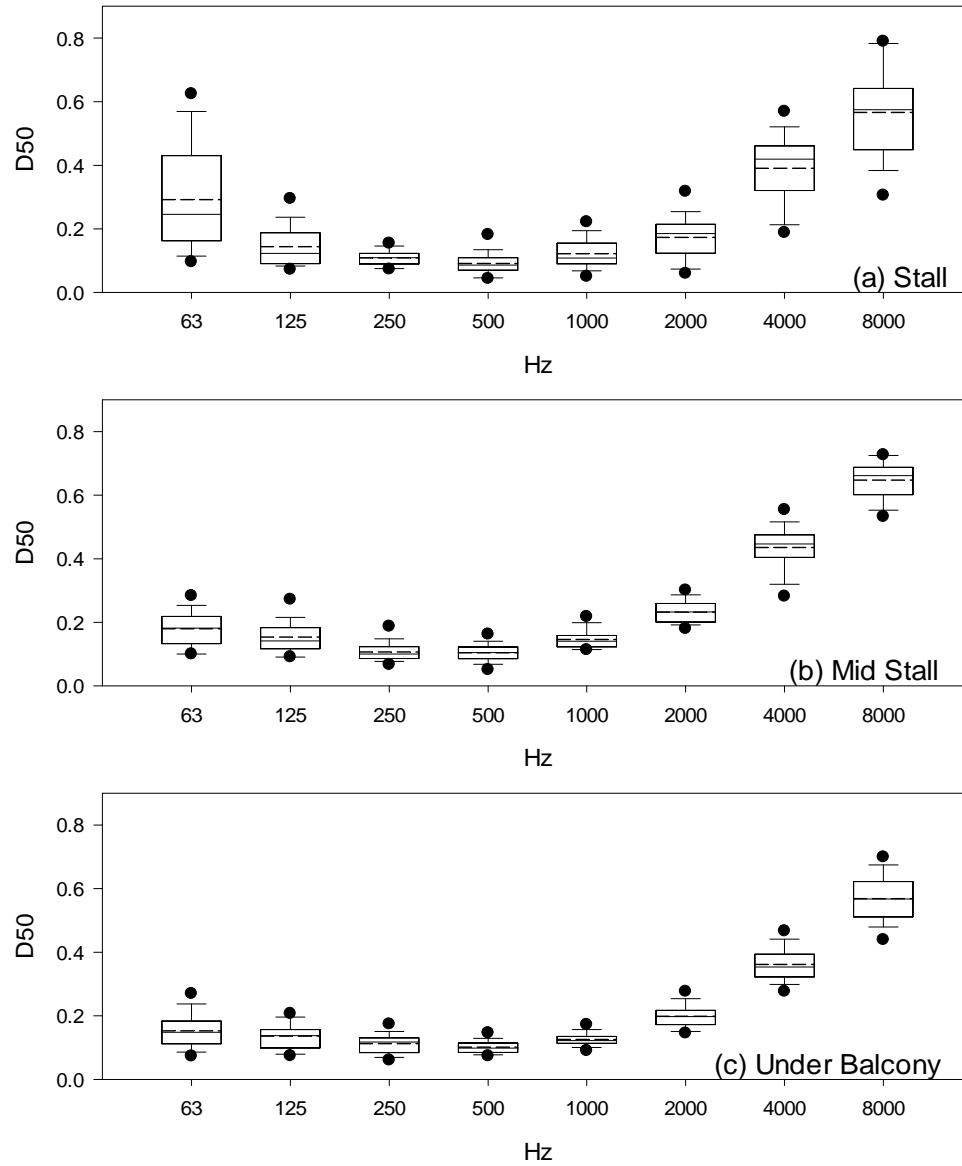


Figure 7-26 Measured D50 spectrum of the scaled-model without balcony with a proscenium stage setting (Case 4)
 • : 5th and 95th percentiles; error bars : 10th and 90th percentiles; box edges : 25th and 75th percentiles; horizontal lines within boxes : median; horizontal dashed lines : mean values

7.5 Balcony Effect

To look at the balcony effect [105] from the measured data, cases with and without the balcony of the same stage setting are compared respectively. The balcony effect of each parameter is defined as follow:

Balcony Effect, BE = with balcony – without balcony

In addition to the mean and standard deviation summary, the Box and Whisker diagram of the BE are also plotted. The BE is divided by the standard deviation of each frequency band. From these diagrams, the degree of changes and distributions of the balcony effect at each frequency of each parameter can be clearly observed.

Include the equation of the ratio equation

$$\text{Balcony Effect ratio} = \frac{\text{with balcony} - \text{without balcony}}{\text{with balcony}}$$

7.5.1 Proscenium Setting

The difference between the measured parameters from the scale model with a proscenium stage setting with and without the balcony is presented using the term Balcony Effect here. Negative values refer to situations that the removal of the balcony increases the measured values. The balcony effect ratios are also calculated and compared with the just noticeable differences as suggested in ISO3382 [13] so as to determine whether the changes are noticeable. The plots of the spectrum of data only show the BE at the stall, mid-stall and under-balcony area. Those on the balcony are neglected.

7.5.1.1 Early Decay Time and reverberation time

From Figure 7-27 and Figure 7-28 plot the spectra of BEEDT and BET30 respectively. The results here show the differences between cases with and without the balcony under the proscenium stage setting. One can see from the plots that most of the boxes are on the negative side, indicating that the balcony reduces EDT from the stall to under balcony area.

The BE is divided by the mean of the EDT of each frequency to observe the relative changes in the values. The just noticeable difference of EDT is relatively 5% [13] as suggested in ISO standard. With the ratio of the mean BE to the mean EDT with a balcony,

as shown in Table 7-2, the BE effect in the hall is very audible. The changes in the mid stall to the under balcony area are more significant than that in the front stall.

Figure 7-28 shows the spectrum of the measured reverberation time T30 while Table 7-3 shows the ratio of mean BE of T30s to mean T30s. The majority of the data are negative. The reverberation time decreases with the removal of the balcony. The balcony effects are smaller in magnitude at higher frequencies while it has greater impacts at low frequencies.

Table 7-2 The ratio of mean BE of EDT to the mean of values with the balcony measured

Zones	Mean BE/ with balcony mean							
	63	125	250	500	1000	2000	4000	8000
Front Stall	-0.11	-0.17	-0.15	-0.08	-0.13	-0.11	-0.11	-0.06
Mid Stall	-0.07	-0.18	-0.13	-0.09	-0.12	-0.14	-0.19	-0.21
Under-balcony	-0.12	-0.17	-0.14	-0.12	-0.15	-0.18	-0.20	-0.20
Overall	-0.11	-0.17	-0.14	-0.10	-0.14	-0.15	-0.17	-0.16

Table 7-3 The ratios of mean BE of T30 to the mean of values with the balcony measured

Zones	BE mean/mean							
	63	125	250	500	1000	2000	4000	8000
Front Stall	-0.05	-0.12	-0.09	-0.05	-0.05	-0.09	-0.09	-0.14
Mid Stall	0.08	-0.01	-0.09	-0.04	-0.04	-0.09	-0.11	-0.14
Under-balcony	-0.29	-0.13	-0.14	-0.06	-0.05	-0.11	-0.13	-0.17
Overall	-0.14	-0.10	-0.12	-0.05	-0.05	-0.10	-0.12	-0.15

Table 7-4 The ratios of mean BE of T60 to the mean of values with the balcony measured

Zones	BE mean/mean							
	63	125	250	500	1000	2000	4000	8000
Front Stall	-0.12	-0.10	-0.05	-0.02	-0.07	-0.10	-0.12	0.01
Mid Stall	-0.01	-0.09	-0.05	-0.03	-0.07	-0.10	-0.14	0.01
Under-balcony	-0.15	-0.16	-0.07	-0.04	-0.09	-0.12	-0.15	0.04
Overall	-0.11	-0.13	-0.06	-0.03	-0.08	-0.11	-0.14	0.03

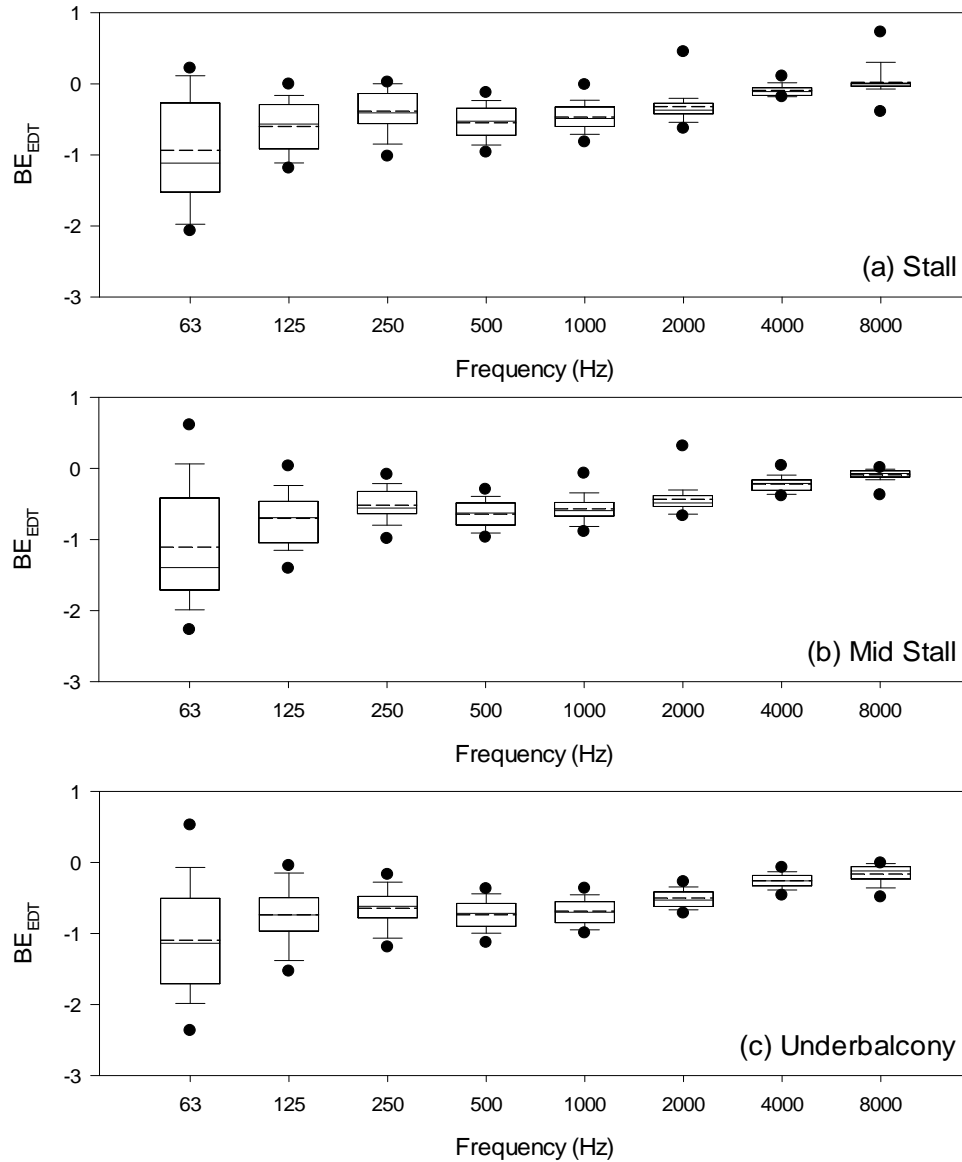


Figure 7-27 The balcony effect in EDT (in sec) spectrum of the scaled-model with balcony with a proscenium stage setting (Case 1 – Case 3)

- : 5th and 95th percentiles; error bars : 10th and 90th percentiles; box edges : 25th and 75th percentiles; horizontal lines within boxes : median; horizontal dashed lines : mean values

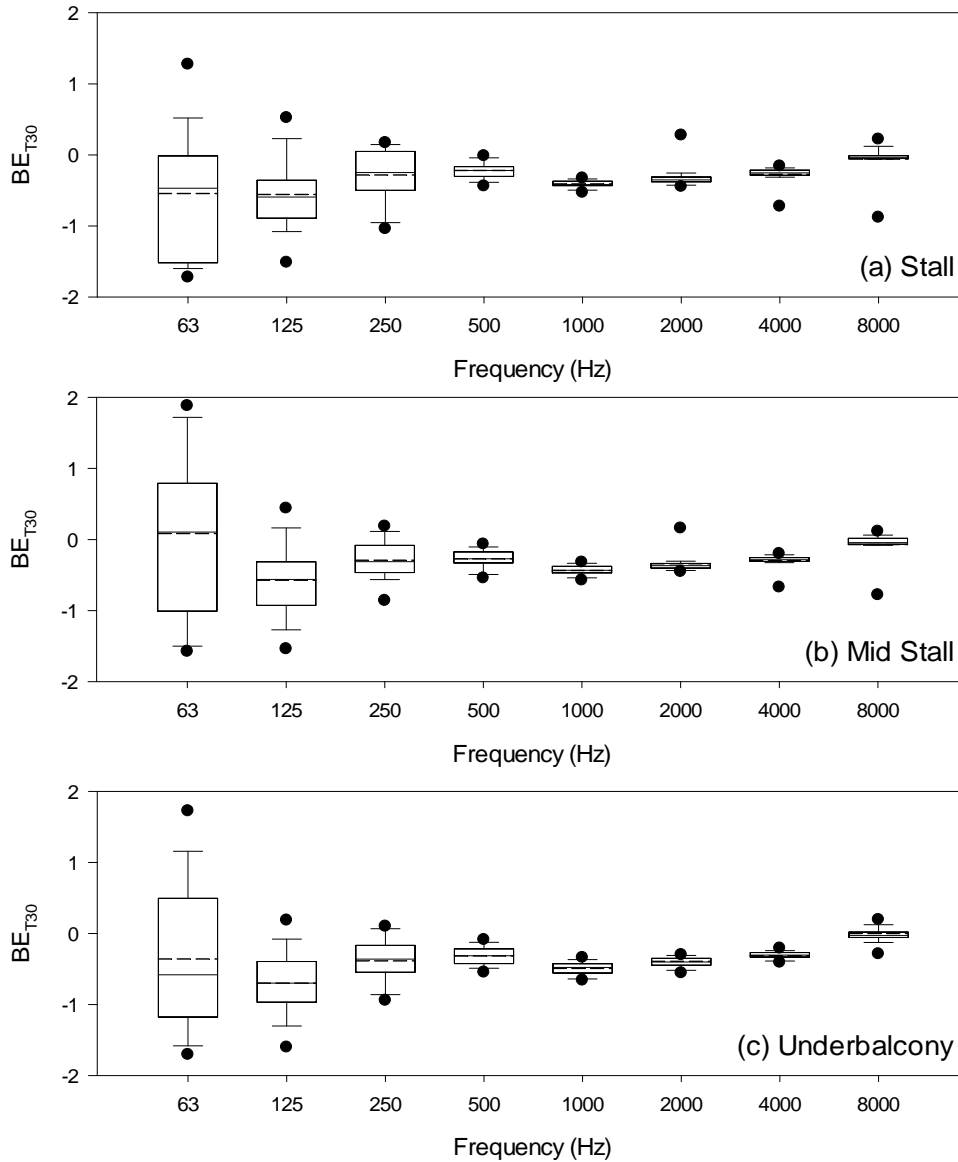


Figure 7-28 The balcony effect in T30 (in sec) spectrum of the scaled-model with balcony with a proscenium stage setting (Case 1 – Case 3)

• : 5th and 95th percentiles; error bars : 10th and 90th percentiles; box edges : 25th and 75th percentiles; horizontal lines within boxes : median; horizontal dashed lines : mean values

7.5.1.2 Early energy ratios, Clarity and Definition

Figure 7-29 shows the spectra of the balcony effects of C80, BEC80 with the proscenium stage setting. The balcony adds early energy to the whole hall in average. However, the interquartile ranges from the box plots show that the balcony effects on the whole hall diverges. Those at the stall area are around 0 and the values are more to the positive side while moving up to the under balcony area. The ranges from these plots and the ratio of BE shown in Table 7-5 suggest that C80 and the energy change after the removal of the balcony is significant, especially at the seats under the balcony.

The ratios in the underbalcony area are the largest among all zones. The existence of the balcony acts as a lower ceiling to the seats underneath. This lower ceiling is at a level that the direct sound from the stage can be reflected to the seats within the first few reflections before the reflections from the main ceiling arrives. This contributes to the early energy content to the seats in this area. Without the balcony, the first few reflections come from the main ceiling which is at twice the distance further than the balcony soffit.

BE_{C80} with a proscenium setting are slightly larger at lower frequencies and higher frequencies in all zones. The means of BE_{C80} at seats before the balcony are around 0 while those under the balcony are mostly positive. This suggests that the balcony brings extra early energy to the seats, especially under the balcony. However, the change in the energy content and ratio in the stall and mid-stall area varies. The variation of the BE_{C80} decreases with the distance from the balcony.

Figure 7-30 shows the spectrum of the balcony effects to D50 in the scale model with a proscenium setting. The pattern of the spectrum of BE_{D50} is similar to that of BE_{C80}. The result of D50 also shows that the balcony increases the amount of early energy to the seats under the balcony. This can be achieved more efficiently when the seats under the balcony are sloped like those in Hall A so that the balcony soffit is at the right position for early reflection.

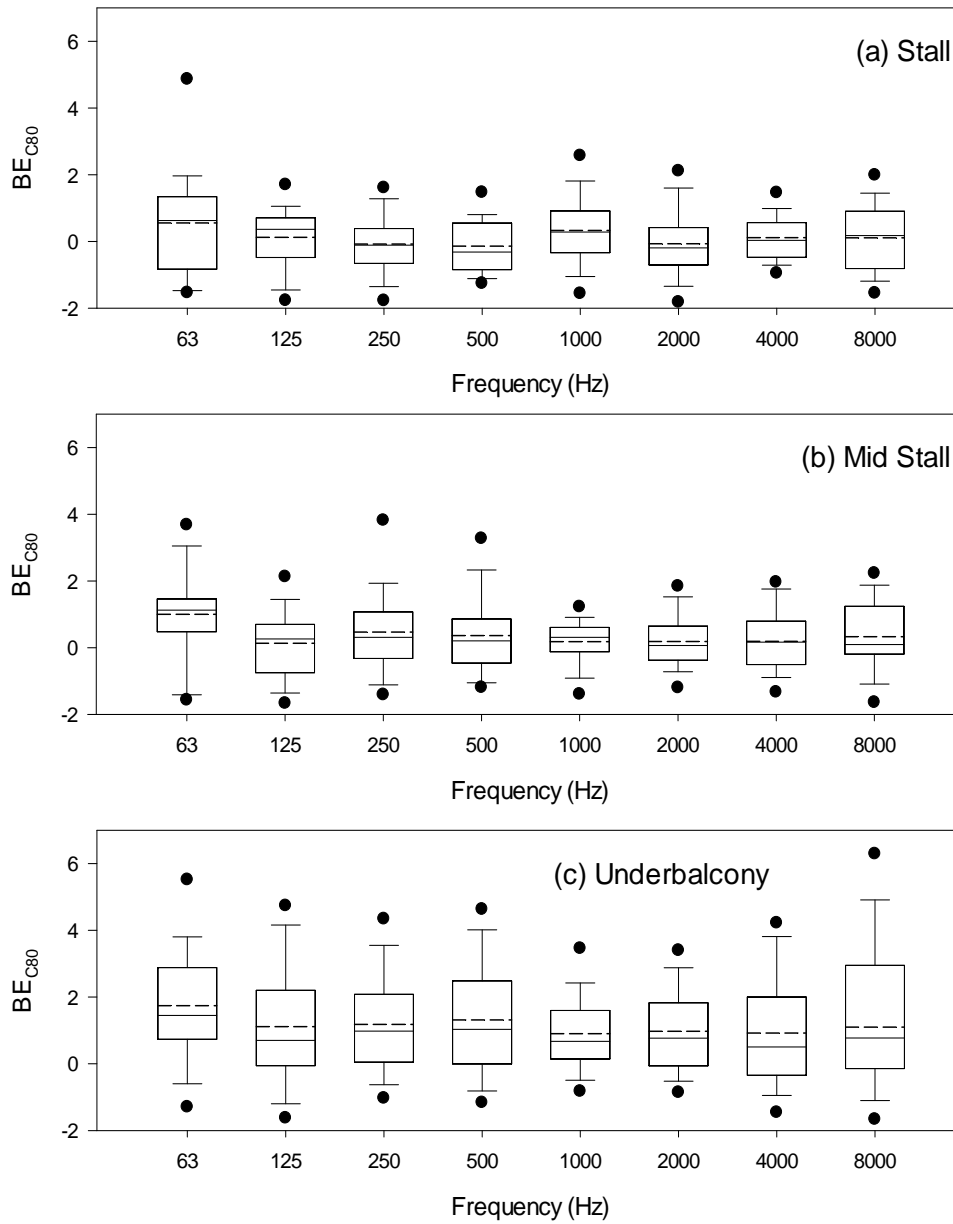


Figure 7-29 The balcony effect in C80 (in dB) spectrum of the scaled-model with balcony with a proscenium stage setting (Case 1 – Case 3)
 • : 5th and 95th percentiles; error bars : 10th and 90th percentiles; box edges : 25th and 75th percentiles; horizontal lines within boxes : median; horizontal dashed lines : mean values

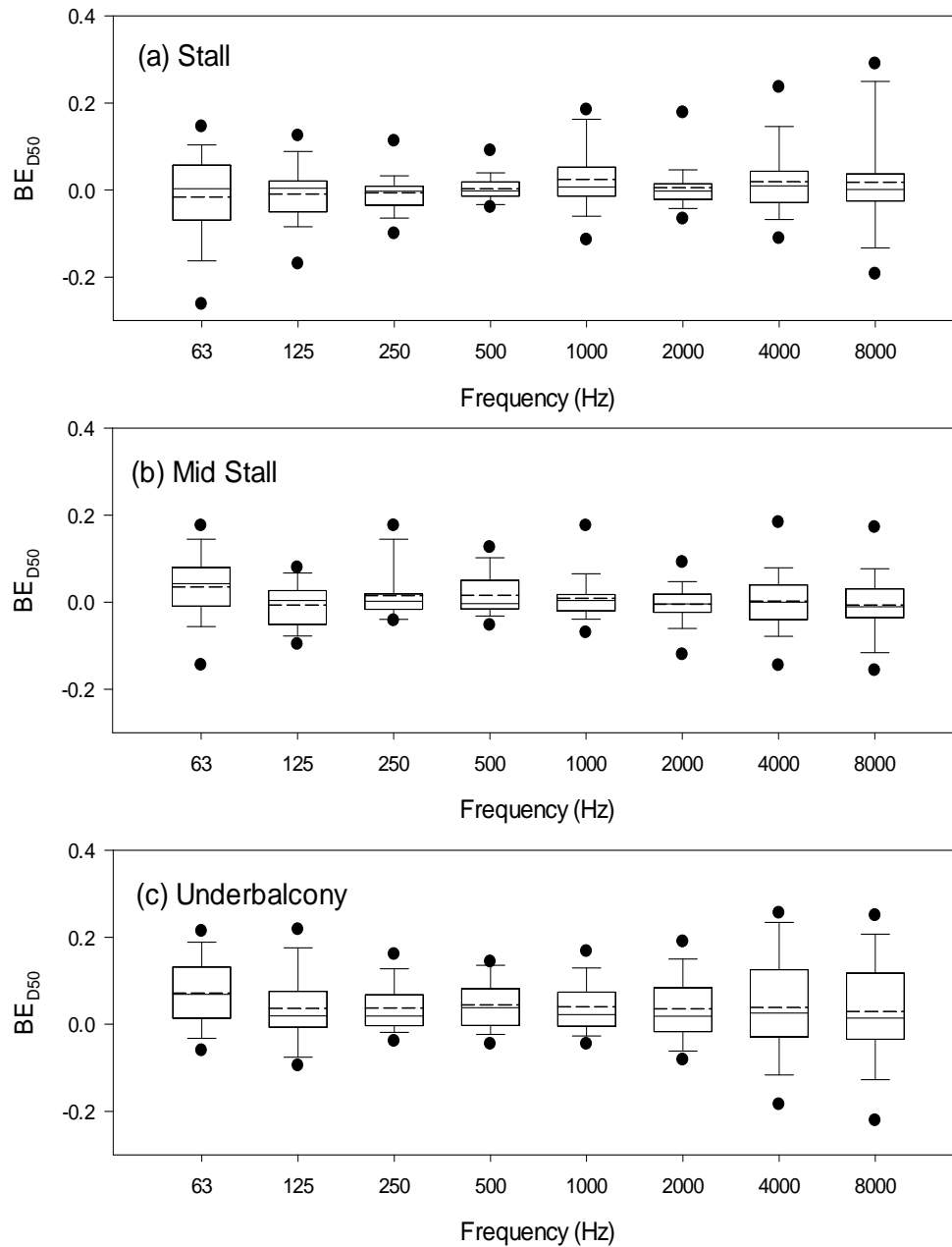


Figure 7-30 The balcony effect in D50 spectrum of the scaled-model with balcony with a proscenium stage setting (Case 1 – Case 3)

- : 5th and 95th percentiles; error bars : 10th and 90th percentiles; box edges : 25th and 75th percentiles; horizontal lines within boxes : median; horizontal dashed lines : mean values

Table 7-5 The ratios of mean BE of C80 to the mean of values with the balcony measured

Zones	BE mean/mean							
	63	125	250	500	1000	2000	4000	8000
Front Stall	1.00	0.11	0.04	0.06	-0.02	0.03	0.00	-0.02
Mid Stall	-0.41	0.08	-0.13	-0.12	-0.03	-0.10	0.03	0.04
Under-	-0.72	-0.43	-0.36	-0.57	-0.48	-1.88	0.47	0.19
Overall	-0.54	-0.15	-0.18	-0.24	-0.21	-0.51	0.28	0.11

Table 7-6 The ratios of mean BE of D50 to the mean of values with the balcony measured

Zones	BE mean/mean							
	63	125	250	500	1000	2000	4000	8000
Front Stall	-0.08	-0.06	-0.04	0.01	0.13	0.03	0.04	0.02
Mid Stall	0.13	-0.03	0.12	0.12	-0.03	-0.03	-0.02	-0.02
Under-	0.25	0.26	0.25	0.31	0.24	0.20	0.12	0.06
Overall	0.10	0.11	0.15	0.21	0.17	0.12	0.07	0.03

7.5.2 Concert Setting

With the concert stage setting, the balcony effects determined from Case 2 and Case 4 are giving different trends from those in proscenium setting. The trend and the values are different in this setting.

7.5.2.1 Early decay time and reverberation time

Figure 7-31 and Figure 7-32 show the spectra of the balcony effects on the early decay time and reverberation T30 in a concert hall setting respectively. Similar to the previous sections, the results here are separated into three zones for comparisons.

The interquartile ranges of BE_{EDT} at all frequencies and all locations are mostly negative. This implies that the balcony is shortening the early decay time in the hall in general. The range at each frequency with the balcony, especially at 63Hz with the sound canopy, is smaller than that without the balcony. The means of the BE_{EDT} show increasing trends with frequencies.

Unlike BE_{EDT} , BE_{T30} has a very different variation pattern. From 63Hz up to 500Hz, the mean and the median of the data are positive, followed by significant decreases to negative at 1000Hz and then they increase up to around zero till 8000Hz.

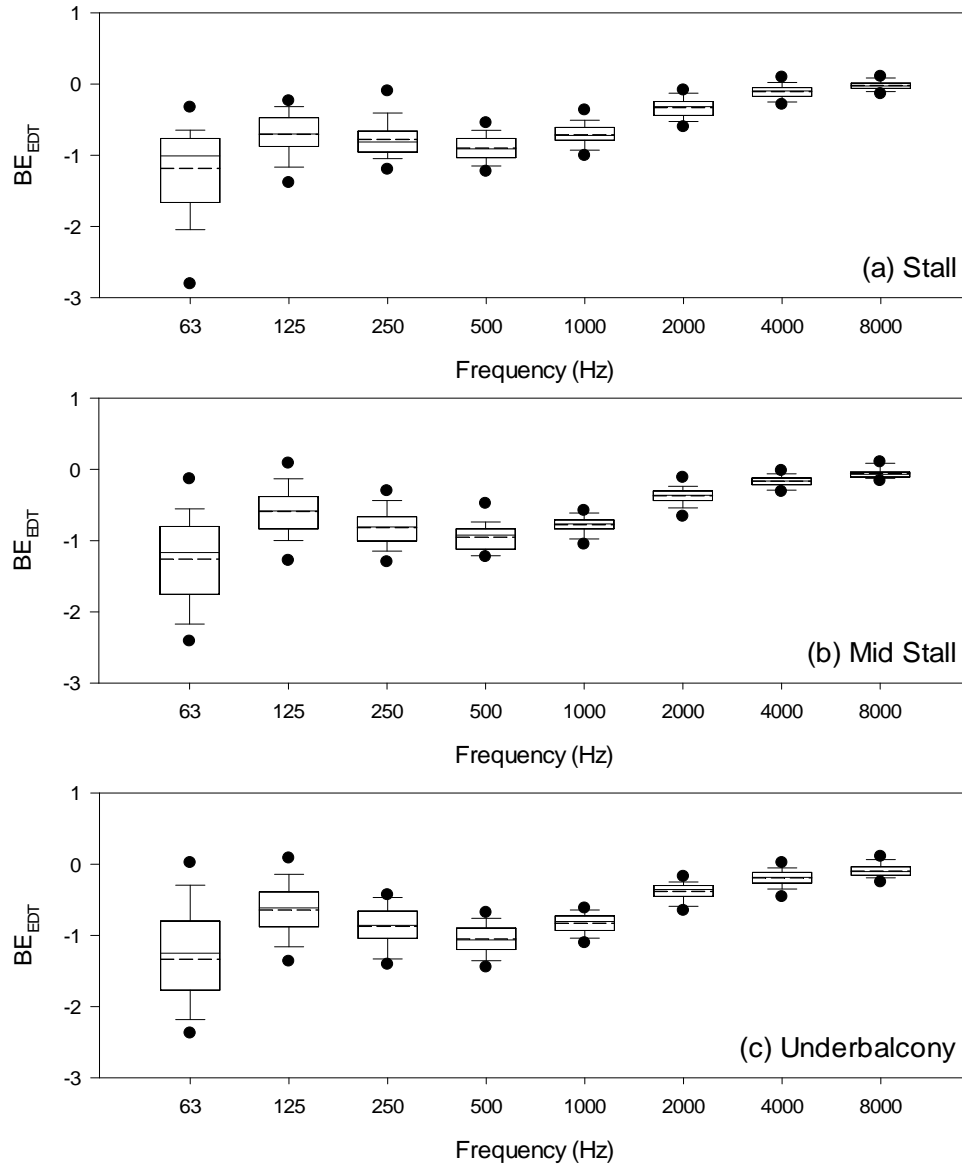


Figure 7-31 The balcony effect in EDT (in sec) spectrum of the scaled-model with balcony with a proscenium stage setting (Case 2 – Case 4)

- : 5th and 95th percentiles; error bars : 10th and 90th percentiles; box edges : 25th and 75th percentiles; horizontal lines within boxes : median; horizontal dashed lines : mean values

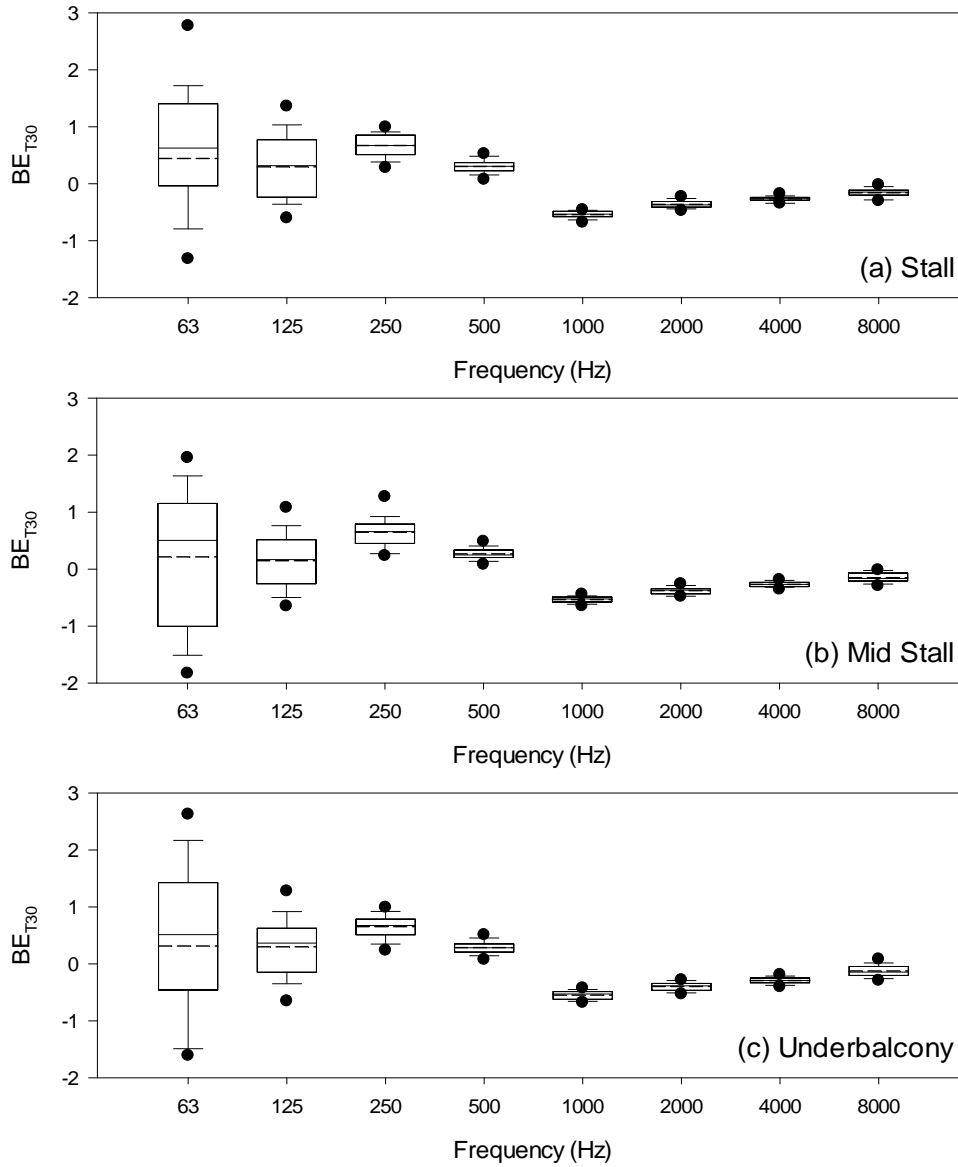


Figure 7-32 The balcony effect in T30 (in sec) spectrum of the scaled-model with balcony with a proscenium stage setting (Case 2 – Case 4)

• : 5th and 95th percentiles; error bars : 10th and 90th percentiles; box edges : 25th and 75th percentiles; horizontal lines within boxes : median; horizontal dashed lines : mean values

Table 7-7 The ratios of mean BE of EDT to the mean of values with the balcony measured in concert setting

Zone	BE mean/ mean EDT							
	63	125	250	500	1000	2000	4000	8000
Front Stall	-0.16	-0.11	-0.11	-0.12	-0.12	-0.09	-0.06	-0.02
Mid Stall	-0.21	-0.08	-0.11	-0.13	-0.14	-0.11	-0.11	-0.08
Under-balcony	-0.16	-0.10	-0.12	-0.15	-0.15	-0.11	-0.12	-0.14
Overall	-0.17	-0.10	-0.11	-0.14	-0.14	-0.10	-0.10	-0.09

Table 7-8 The ratios of mean BE of T30 to the mean of values with the balcony measured in concert setting

Zone	BE mean/ Mean T30							
	63	125	250	500	1000	2000	4000	8000
Front Stall	0.06	0.04	0.07	0.03	-0.08	-0.09	-0.10	-0.09
Mid Stall	-0.05	0.02	0.07	0.03	-0.08	-0.09	-0.10	-0.09
Under-balcony	0.06	0.05	0.07	0.03	-0.09	-0.10	-0.12	-0.06
Overall	0.04	0.04	0.07	0.03	-0.09	-0.09	-0.11	-0.07

Table 7-9 The ratios of mean BE of T60 to the mean of values with the balcony measured in concert setting

Zone	BE mean/ mean T60							
	63	125	250	500	1000	2000	4000	8000
Front Stall	0.07	0.05	0.14	0.18	0.03	-0.08	-0.09	-0.08
Mid Stall	-0.05	0.04	0.13	0.16	0.04	-0.08	-0.09	-0.07
Under-balcony	0.06	0.07	0.13	0.17	0.03	-0.08	-0.09	-0.04
Overall	0.04	0.06	0.13	0.17	0.03	-0.08	-0.09	-0.06

The BE ratios of EDT, T30 and T60 are calculated. Some of the values are more than 10% of the means with the balcony. Therefore, one can conclude that the BE of EDT and reverberation times are noticeable by audience.

7.5.2.2 Energy ratios, Clarity and Definition

Figure 7-33 and Figure 7-34 plots the spectra of the balcony effects of C80 and D50 in each zone at different frequencies respectively. The means and medians of BEC80 at all zones are positive at 1000Hz or below while those at higher frequencies are negative. The interquartile ranges of BEC80 are large, the results in Table 7-11 shows that the BE ratio cannot reflect the true deviation of the BEC80. From the mean and the standard deviation in Table 7-10, the standard deviations suggest that the variation of BEC80 should be audible. BEC80s are higher and having larger ranges under the balcony in concert hall

setting. This shows that a large number of seats decreases C80 after the removal of the balcony. The balcony provides more early energy to the hall, especially to the area under the balcony.

Figure 7-34 shows the spectra of D50s in this case at different frequencies in each zone in the scale model. The trend of BE_{D50} with concert hall setting are similar to that of BE_{C80} but with a smaller ranges while the values of D50 are smaller. It is still observed that the balcony increases the early energy to the whole hall, especially to the seats underneath the balcony. However, the BE_{D50} s are having a larger range at 8000Hz which indicates that the balcony is bringing a larger change to D50 in the scale model, especially under the balcony. Table 7-12 shows the ratios of the BE_{D50} to mean D50 with balcony at respective zones and locations. The values of the ratios are more than 10%, showing that the removal of the balcony produces significant changes.

Table 7-10 Mean and standard deviation of BE of C80 in Concert setting

		Frequency (Hz)							
		63	125	250	500	1000	2000	4000	8000
Front Stall	Mean	0.43	0.41	0.00	0.40	0.25	-0.12	-0.28	-0.09
	SD	<u>2.60</u>	<u>2.66</u>	<u>1.19</u>	<u>0.93</u>	<u>1.27</u>	<u>1.35</u>	<u>1.24</u>	<u>0.95</u>
Mid stall	Mean	0.74	0.29	0.41	0.48	0.26	-0.47	-0.22	-0.22
	SD	<u>1.75</u>	<u>2.07</u>	<u>1.43</u>	<u>1.05</u>	<u>1.40</u>	<u>0.95</u>	<u>1.21</u>	<u>1.64</u>
Under-balcony	Mean	0.66	1.12	1.05	1.28	1.37	1.12	1.44	1.63
	SD	<u>2.16</u>	<u>2.15</u>	<u>2.00</u>	<u>1.12</u>	<u>1.06</u>	<u>1.17</u>	<u>1.40</u>	<u>2.10</u>
Overall	Mean	0.61	0.75	0.60	0.86	0.81	0.43	0.59	0.74
	SD	<u>2.21</u>	<u>2.30</u>	<u>1.73</u>	<u>1.12</u>	<u>1.31</u>	<u>1.37</u>	<u>1.56</u>	<u>1.94</u>

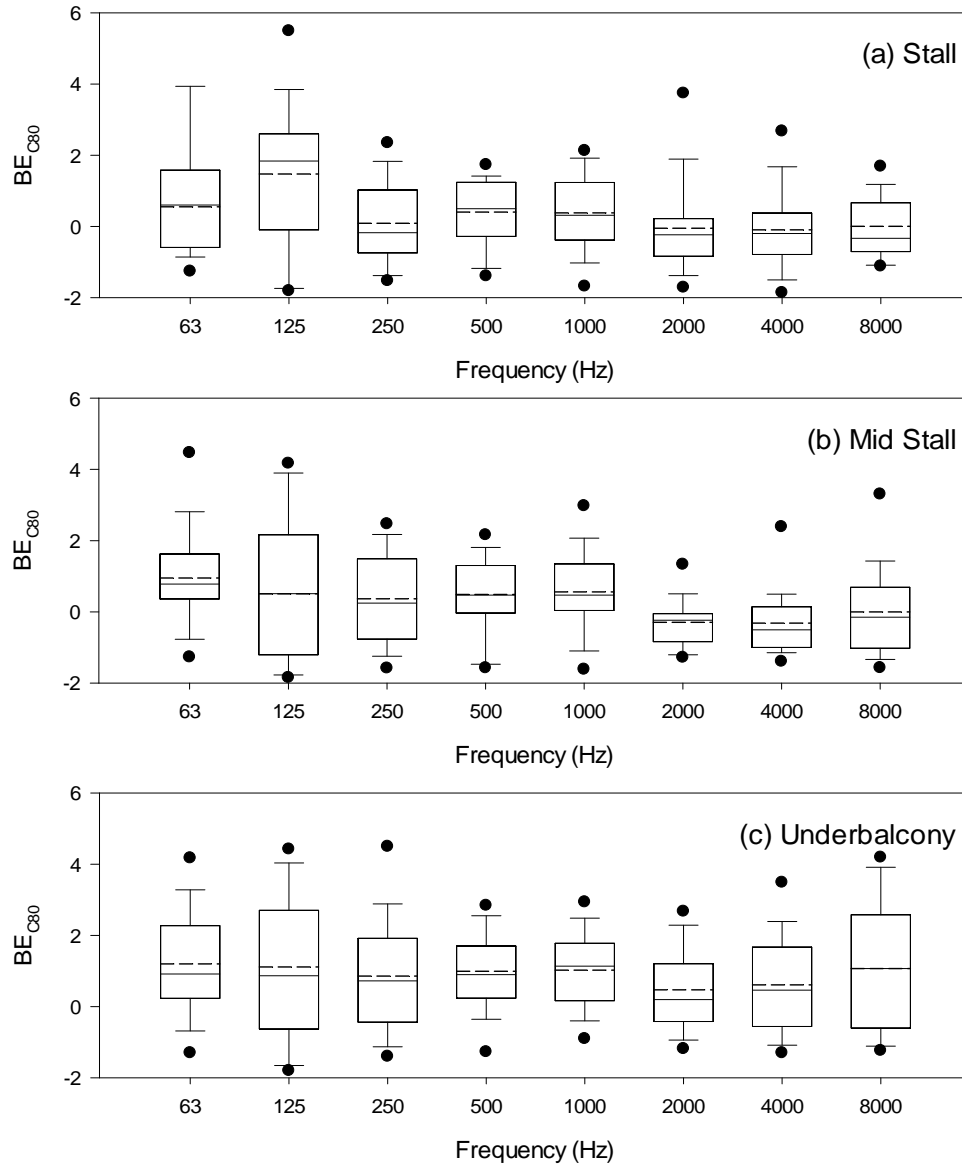


Figure 7-33 The balcony effect in C80 (in dB) spectrum of the scaled-model with balcony with a proscenium stage setting (Case 2 – Case 4)

• : 5th and 95th percentiles; error bars : 10th and 90th percentiles; box edges : 25th and 75th percentiles; horizontal lines within boxes : median; horizontal dashed lines : mean values

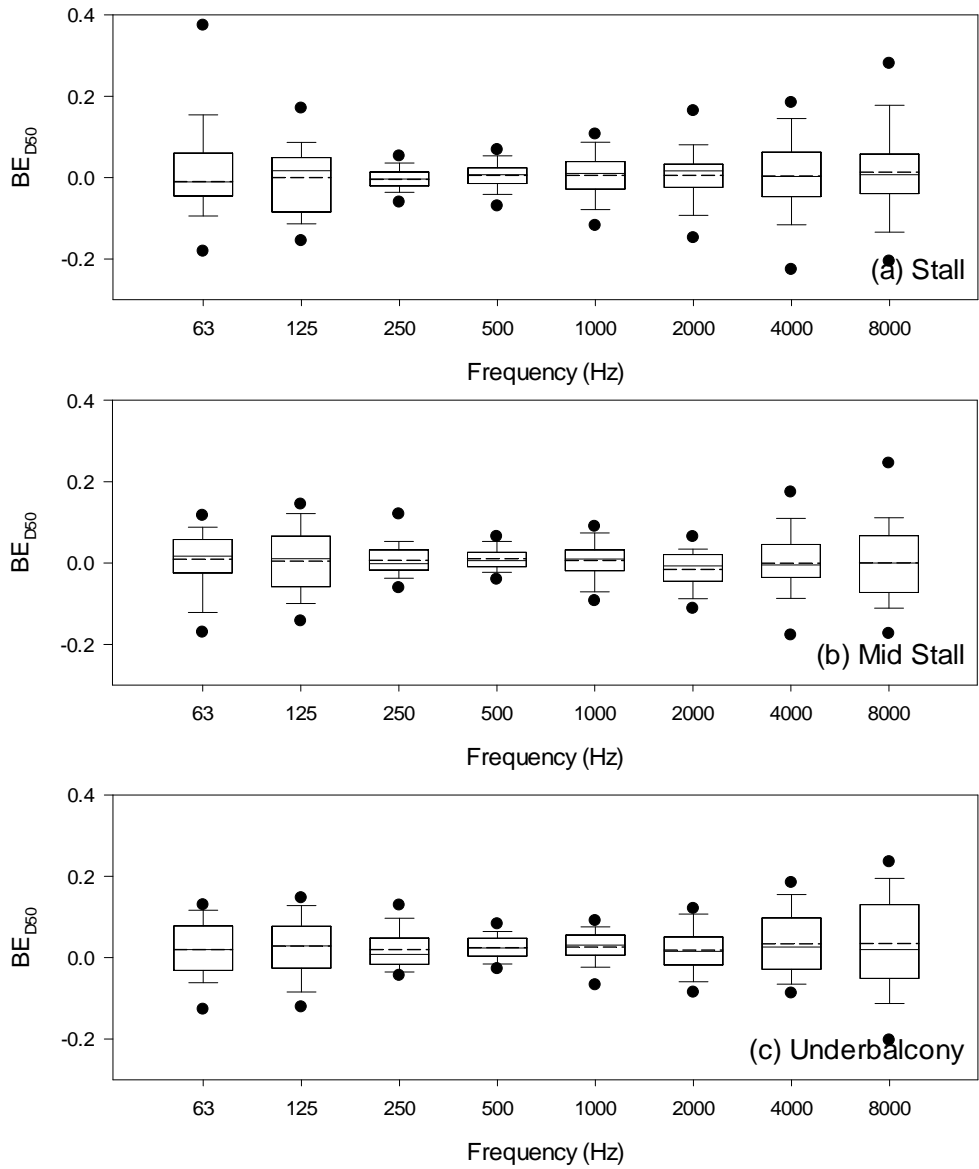


Figure 7-34 The balcony effect in D50 spectrum of the scaled-model with balcony with a proscenium stage setting (Case 2 – Case 4)

• : 5th and 95th percentiles; error bars : 10th and 90th percentiles; box edges : 25th and 75th percentiles; horizontal lines within boxes : median; horizontal dashed lines : mean values

Table 7-11 The ratios of mean BE of C80 to the mean of values with the balcony measured in concert setting

Zone	BE mean/ mean C80							
	63	125	250	500	1000	2000	4000	8000
Front Stall	-0.17	-0.07	0.00	-0.06	-0.04	0.03	-0.18	-0.01
Mid Stall	-0.17	-0.06	-0.06	-0.07	-0.05	0.14	-0.18	-0.04
Under-balcony	-0.13	-0.22	-0.17	-0.21	-0.27	-0.42	0.95	0.27
Overall	-0.14	-0.14	-0.09	-0.13	-0.15	-0.14	0.40	0.12

Table 7-12 The ratios of mean BE of D50 to the mean of values with the balcony measured in concert setting

Zone	BE mean/ mean D50							
	63	125	250	500	1000	2000	4000	8000
Front Stall	0.02	0.00	-0.04	0.06	0.04	0.03	0.01	-0.01
Mid Stall	0.09	0.11	0.10	0.10	0.01	-0.10	0.00	-0.03
Under-balcony	0.13	0.22	0.21	0.25	0.26	0.20	0.15	0.10
Overall	0.08	0.14	0.13	0.17	0.15	0.10	0.08	0.04

7.6 Effects on the early energy and reflections

7.6.1 Proscenium setting

One would expect that when the RT increases, more reflections are expected to occur and the late energy content will increase. Hence, the clarity C80 and definition D50 will decrease and vice versa. However, from the measurement data here, this prediction is found at the seats under the balcony, but not all the seats in the stall and mid stall area.

While all the BE of EDT and RTs are negatives in all seats, those of C80 are positive at 13 out of 43 measurement points under the balcony in all frequency bands. At mid frequencies 250Hz and 500Hz, there are more than 90% points having an increased C80s and there are more than 70% points having increases at the other frequencies. This is rather expected. The same trend also appears in D50s in this case under the balcony. The percentages of points having such changes are slightly higher. Such observation suggests that the ratio of the late energy has decreased thus the early energy ratios increase. However, the situation is not the same at seats right in front of the stage, which are not covered by the balcony. In the stall area and mid-stall area, respectively, there are more than 30% and 50% of seats where decreases in C80 and D50 are observed. The seats at the boundary of each zone are more likely to have decreases in early energy ratios at different frequencies. The closer to the stage, the further from the balcony edge, and thus the decreases are more obvious.

7.6.2 Concert hall setting

The concert stage setting brings a totally different but with a more observable trend. The changes in reverberation times and energy ratios are not the same across the whole spectrum. The changes at 500Hz and below are different from those at 2000Hz or above. That at 1000Hz appeared as a transition frequency as shown in Figure 7-31 and Figure 7-32. When the BE of decay time in Figure 7-32 and BE of energy ratios in Figure 7-33 and Figure 7-34 are compared, one can observe that the low to mid frequency zone and the high frequency zone are both having reverberation times increasing or decreasing with energy ratios. In details, the number of seats having observable changes across the whole spectrum is larger than that in proscenium setting. From Figure 7-31 and Figure 7-32, one can see that the BEs of EDTs and T30s are both negative at most seats at 2000Hz or above. This means that the balcony increases both values at the same time. Energy ratio C80s at 2000Hz or above are having both positive and negative BEs.

The balcony imposes different changes to the early decay time and the reverberation time at each seat. However, whether the combination will increase or decrease the early energy ratios, C80 and D50, depends on the location and the geometrical characteristics of the seat.

Figure 7-35 and Figure 7-36 compare the impulse response measured at three different seats in the scale model with concert hall setting with and without the balcony. The traces are from -10 milliseconds to 200 milliseconds. Figure 7-35 shows the impulse response at seat M31. At this seat, a strong impulse is found at time 0 with a series of reflections starting from 20 milliseconds. The energy shown in case 2 is decreasing but there is a strong impulse at around 120 milliseconds. Measurement point M31 was located at the mid stall area close to the side wall on the right when seeing from the audience to the stage. On its right, there was a recessed gallery below the major sidewall of the hall. From the measured data, the BE_{EDTs} and BE_{T30s} , as well as BE_{C80s} at this seat are negative. While this seat was much closer to reflectors and with a very reverberant internal environment, a large number of small reflections can be seen from Figure 7-35 in cases with and without the balcony. It is obvious that the reflections in Figure 7-35(a) are not as sharp as those in Figure 7-35(b). Meanwhile, there are less minor reflections at this measurement point as shown in Figure 7-35(b) without the balcony. Hence, the C80 increases after removing the balcony. One can conclude that the balcony can enhance the

reflections at seats with reflectors nearby. Thus, it decreases the early energy ratios at these measurement points while the late reflections are increased by the presence of the balcony. The balcony does not change the characteristics of the impulse received at this seat significantly.

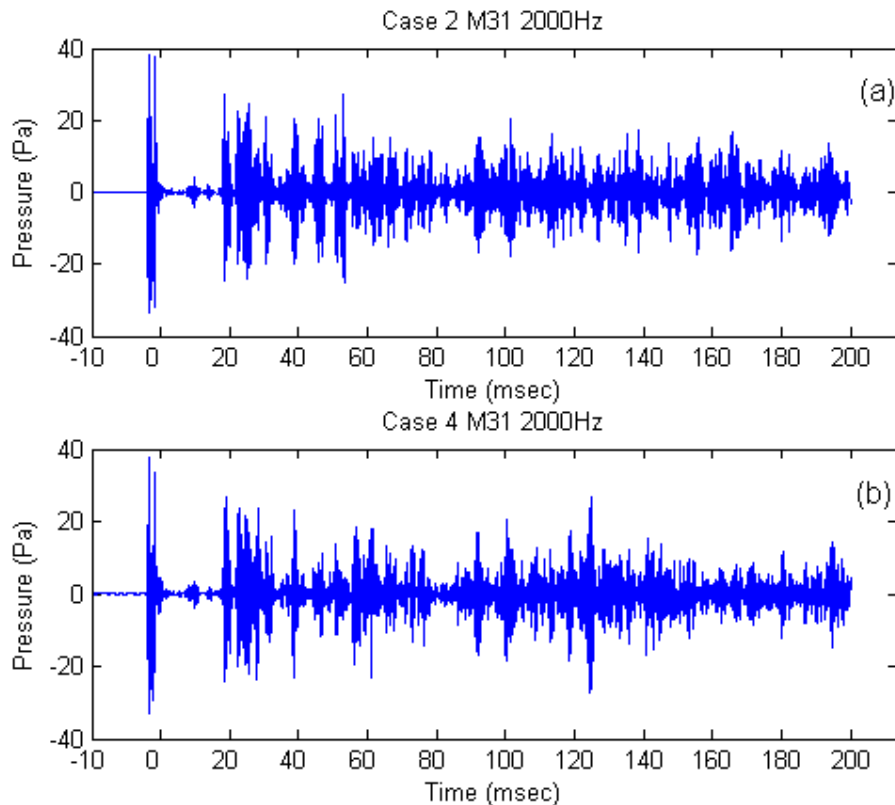


Figure 7-35 Impulse response measured at M31 in mid-stall on the side within the first 200msec. (a)case 2 concert setting with balcony; (b) case 4 concert setting without the balcony

Differently, the balcony has changed the pattern of the impulses measured at points O28 as shown in Figure 7-36. O28 was another point at the mid-stall area but this location was located closer to the centre line of the scale model than point M31. It was located in the middle between the hall's centre line and its side wall. This point was also closer to the balcony edge, which is expected to be more influenced by the balcony. Both the balcony effect on EDT and T30 are negative while those of energy ratios are positive. The balcony shortens the EDTs and T30s but increases the C80s. While C80 is the ratio of energy to late energy received at a point, the EDTs and Reverberation times here are decreasing at different ratio that allows the C80 to increase rather than maintaining the same ratio or decreasing. As shown in Figure 7-36, the form of the impulse of case 2 with balcony and case 4 without balcony show shifts in reflections with a very different pattern. The first

reflection in Figure 7-36(a) is very distinguishable, this enhances higher C80 value measured with the balcony. The other more distinguishable reflections, starting from around 15 milliseconds, are much higher than those associated with small reflections. This also helps give higher energy ratios. In Figure 7-36(b), removing the balcony has brought more small reflections before and after the strongest reflection at around 35 milliseconds. It can be seen that the removal of the balcony has increased the internal volume of the scale model and thus increases the reverberations inside. The time gap between the strongest and second strongest reflection in Figure 7-36(a) and Figure 7-36(b) are very similar. One may say that the balcony has made the reflections to arrive earlier to those seats closer to the balcony edge. In such case, the balcony, especially its edge facing the stage is bringing earlier reflections to the seats in front even back to the stage. This increment in clarity and definition not only enhances the hearing experience of the audience but also the ensembles of the performers at the stage front.

Figure 7-37 shows the impulse response measured at point Y16 under the balcony with and without the balcony. This seat was located along the centre line of the hall. The headroom at this location was relatively low in case 2, therefore, the effect of the balcony is expected to be higher than those of the other seats mentioned above. The balcony effects of EDT and T30 are both negative at this location while the effect of C80 is positive. It can be clearly seen that the energy content or reflections with the balcony is higher than that without the balcony. These reflections are more even with the balcony than that without the balcony. The balcony has also maintained the energy after each reflections instead of decreasing it after each peaks like those without the balcony. Similar to the patterns at seat O28, the balcony has helped to bring the reflections to an earlier time. It has also helped shortening the time gap between each reflections. In Figure 7-37(a), the times of the second and third reflection in case 2 are at around 15ms and 30ms respectively while those of case 4 in Figure 7-37(b) are 30ms and almost 100ms. The stronger reflections at the early time 50ms or 80ms, the higher the energy ratios are.

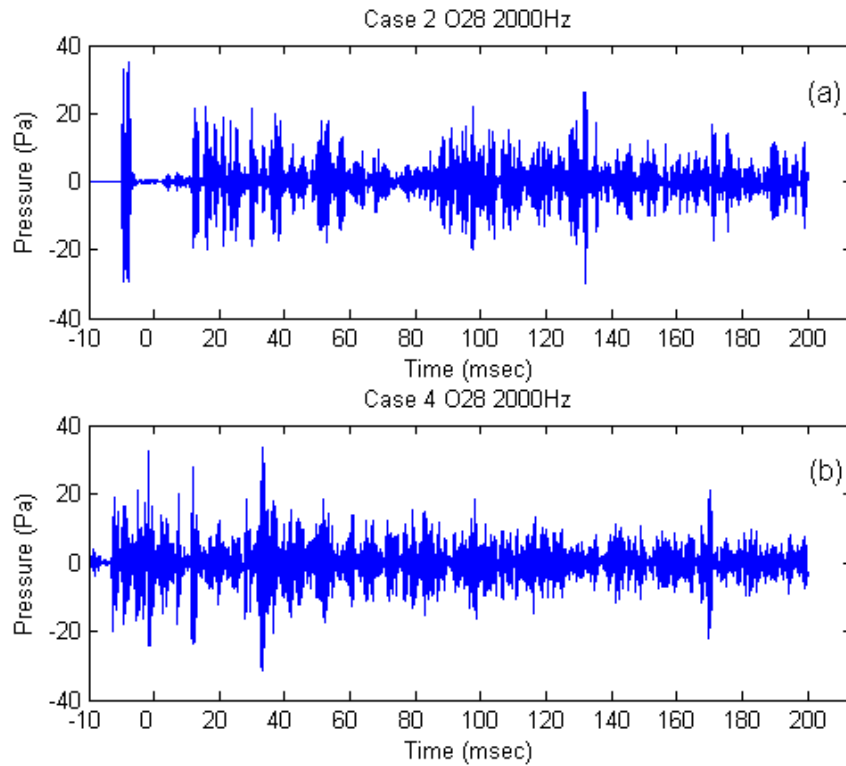


Figure 7-36 Impulse response measured at O28 in mid-stall in the middle within the first 200msec. (a)case 2 concert setting with balcony; (b) case 4 concert setting without the balcony

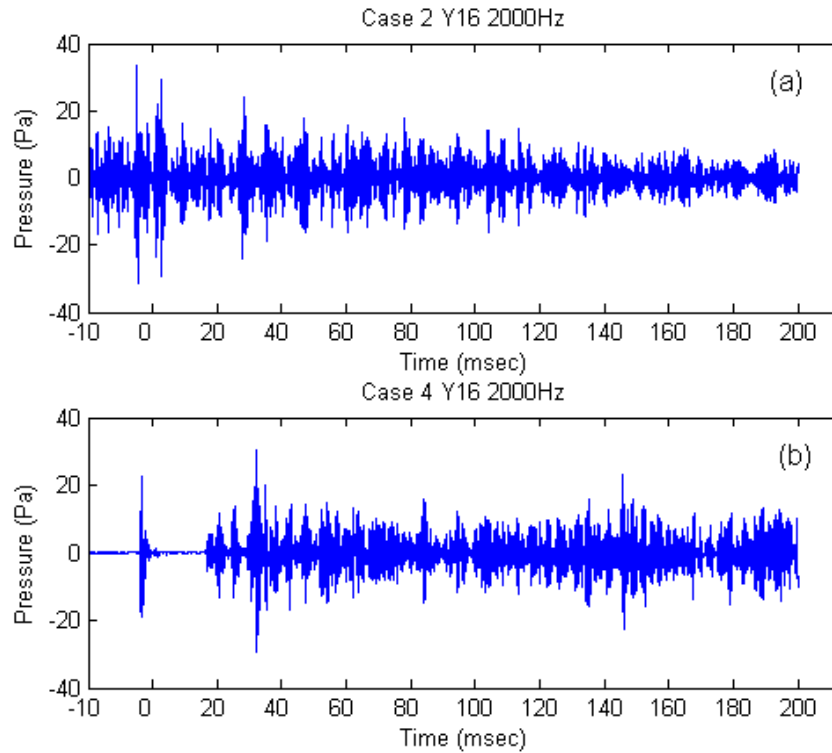


Figure 7-37 Impulse response measured at Y16 under the balcony within the first 200msec. (a)case 2 concert setting with balcony; (b) case 4 concert setting without the balcony

7.7 3D ray tracing model for comparison

The scale model experiment show the differences of the acoustical parameters with and without the balcony in the same hall. However, it would require much more resource in experimenting with other balcony setting. Therefore, a ray tracing 3D computer simulation of Hall A was done to investigate one more case: concert stage setting with a smaller balcony which is $\frac{1}{2}$ of the original depth of the real hall. Room Acoustic software, Odeon version 12.1, was used for this simulation. This computer model was constructed at real dimension as Hall A in Chapter 4. Three different cases of three different balcony size (100% depth, 50% depth, 9%) were used. All the receiver locations used in Chapter 4 were included in the simulation. The receiver points on the balcony were also kept in the simulation with a reduced size balcony and without the balcony. All the interior surfaces were assigned with material from the Odeon library with similar properties as the real finishes in Hall A. This makes the simulation result totally different from the scale model results. Therefore, the results cannot be directly compared with those from the scale model, only the trend can be compared. The simulation results here are also separated into the four different zones used in the previous chapters.

The simulated parameters are with smaller and similar ranges in each case across the whole frequency spectrum. The mean and the standard deviation of each parameter are calculated for each zone with the three different balcony sizes. In general, all the standard deviations are with 1-2 JND suggested by ISO-3382 [13]. The standard deviation of C80 and D50 are directly comparable to the suggested values 1dB and 0.05 respectively. Those of EDT and T30 are divided by their respective mean and compared with the 5% stated in the standard.

The means and the standard deviations of the simulated C80 with a full balcony are calculated. This setting is the one with the most diverged results. The standard deviations at the stall area are still within 2 JNDs. The simulated values on the balcony are having a small deviation, relatively. The standard deviations of the other parameters with other balcony size are very likely to be less than the suggested JND. This means that the variation on the balcony is small enough to be not noticeable. The results also show that the closer to the stage, from seats under the balcony to the seats in the stall area close to the stage, the results are more diverged and they exceed 1 JND.

7.7.1 Balcony effect in 3D simulation model

7.7.1.1 Effect of removing the balcony

The balcony effects of EDT, T30, C80 and D50 are determined using the simulated results from the full size balcony setting with the reduced balcony and removed balcony setting respectively. In both cases, the BE of the simulated T30 and EDT have very different patterns from those obtained from the scale model experiment. Those of early energy ratios C80 and D50 are quite similar but with different ranges. Hereinafter, the BE denoted with ‘half’ is referring to the comparison between the full and $\frac{1}{2}$ balcony while that denoted by ‘0’ is comparing the full balcony case and the removed balcony case.

Figure 7-38 shows the spectrum of the BET30,0 simulated with and without the balcony. The ranges of 1000Hz are the largest. The mean values of $BE_{EDT,0}$ show a monotonic increasing trend rather than a decreasing-then-increasing trend with increasing frequency. The means of $BE_{EDT,0}$ at low frequencies in all zones are negative while those starting from 250Hz are positive. The absorption material assigned in the computer model simulated the values with reasonable ranges, especially at low frequencies. The absorption material on the back wall of the hall greatly increases the total absorption in the hall which has shortened the T30 in this case while the balcony may reflect and scatter the energy in the real hall.

The simulated $BE_{C80,0}$ and $BE_{D50,0}$ have similar means and ranges with those measured in the scale model. The BE of the energy ratios have extended ranges starting from negative while the means in mid frequencies at around 500Hz and 1000Hz are negative in the mid stall and under balcony area.

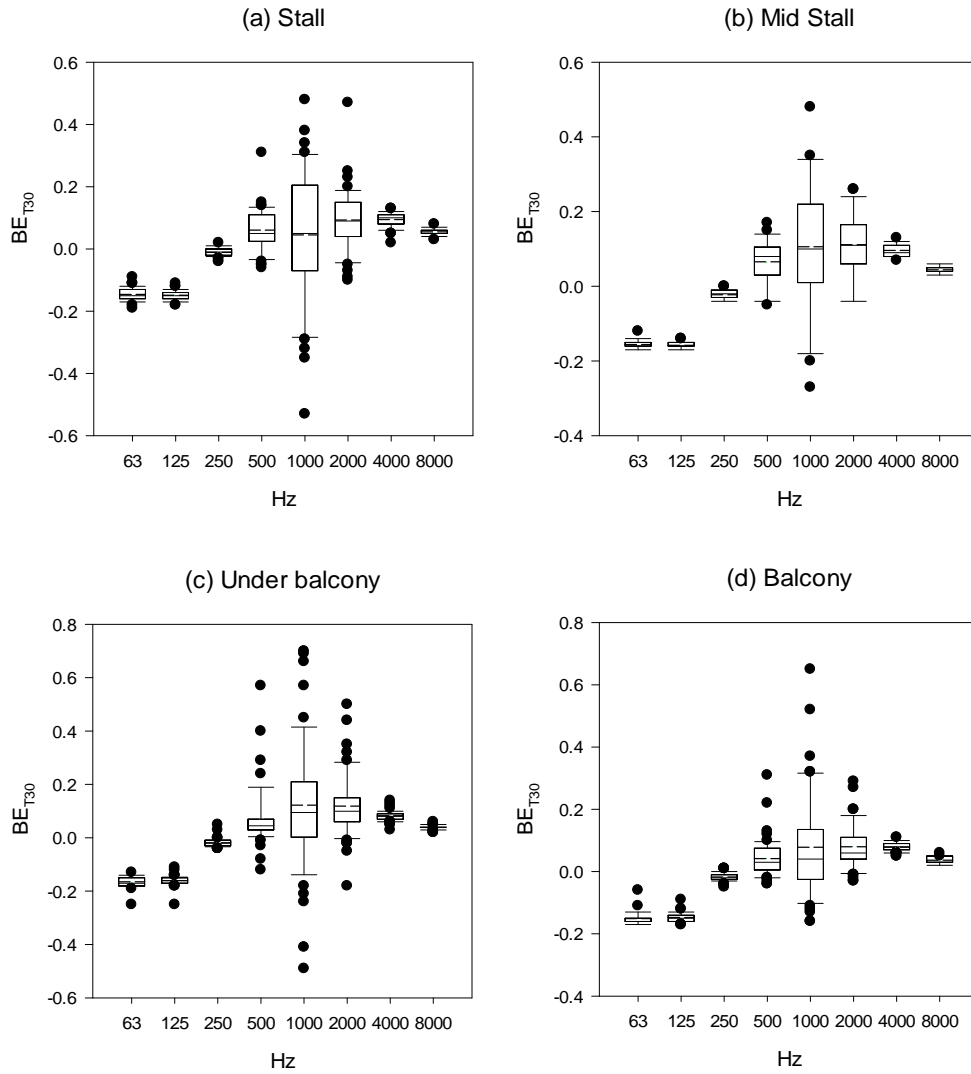


Figure 7-38 The balcony effect in T30 (in sec) spectrum of the ray-tracing model with a concert stage setting, comparison between with and without balcony.

• : 5th and 95th percentiles; error bars : 10th and 90th percentiles; box edges : 25th and 75th percentiles; horizontal lines within boxes : median; horizontal dashed lines : mean values

7.7.1.2 Effect of a reduced size balcony

The EDTs, T30s, C80s and D50s simulated in the half-sized balcony show similar trends of balcony effect as those simulated without the balcony. $BE_{T30, \text{half}}$ has similar trend as $BE_{T30, 0}$ but with larger ranges and smaller means. At 500Hz to 2000Hz in the mid-stall and under-balcony area, the corresponding means and the interquartile ranges change from positive to negative while the range at 1000Hz decreases and the other two increase. The minor decrease in values tends to suggest that the T30 with this half balcony are slightly longer than those without a balcony or with the full size balcony. It may be due to the increase of the volume while minimizing the balcony inside the model but the balcony structure itself can still provide sufficient amount of reflection.

$BE_{EDT, \text{half}}$ have similar ranges as those without the balcony. Those at the stall area are almost the same. While the means of $BE_{EDT, \text{half}}$ are very close to 0 especially at 250Hz or above, the change of the balcony may not affect the early energy decay at the seats close to the stage. Those at mid stall and under the balcony are having shifted ranges to the negative side at 250 to 2000 Hz. A large portion of the seats in these areas have long EDT with the shortened balcony than the full size balcony. This suggests that the balcony helps reflect the early energy to these areas.

Figure 7-39 and Figure 7-40 show the spectra of the balcony effect of early energy ratios C80 and D50 simulated with the half balcony. The general trends follow those simulated without a balcony. However, the means are slightly smaller at the stall area while the values simulated at mid stall and under the balcony are higher than those without the balcony. It appears that the change of balcony size does not bring a big change to the values at the seats close to the stage. The means from 250Hz onwards shifted from negative to positive which means the balcony is bringing more early energy to the simulated seats.

Comparing with the $BE_{EDT, \text{half}}$, it seems that the size of and the distance from the balcony do not affect the early energy in the front stall area much. However, reducing the balcony depth has brought longer EDTs to mid-stall and under-balcony area and enhanced the early energy ratios in these areas. The balcony structure acts as a large reflector to reflect and scatter the early energy.

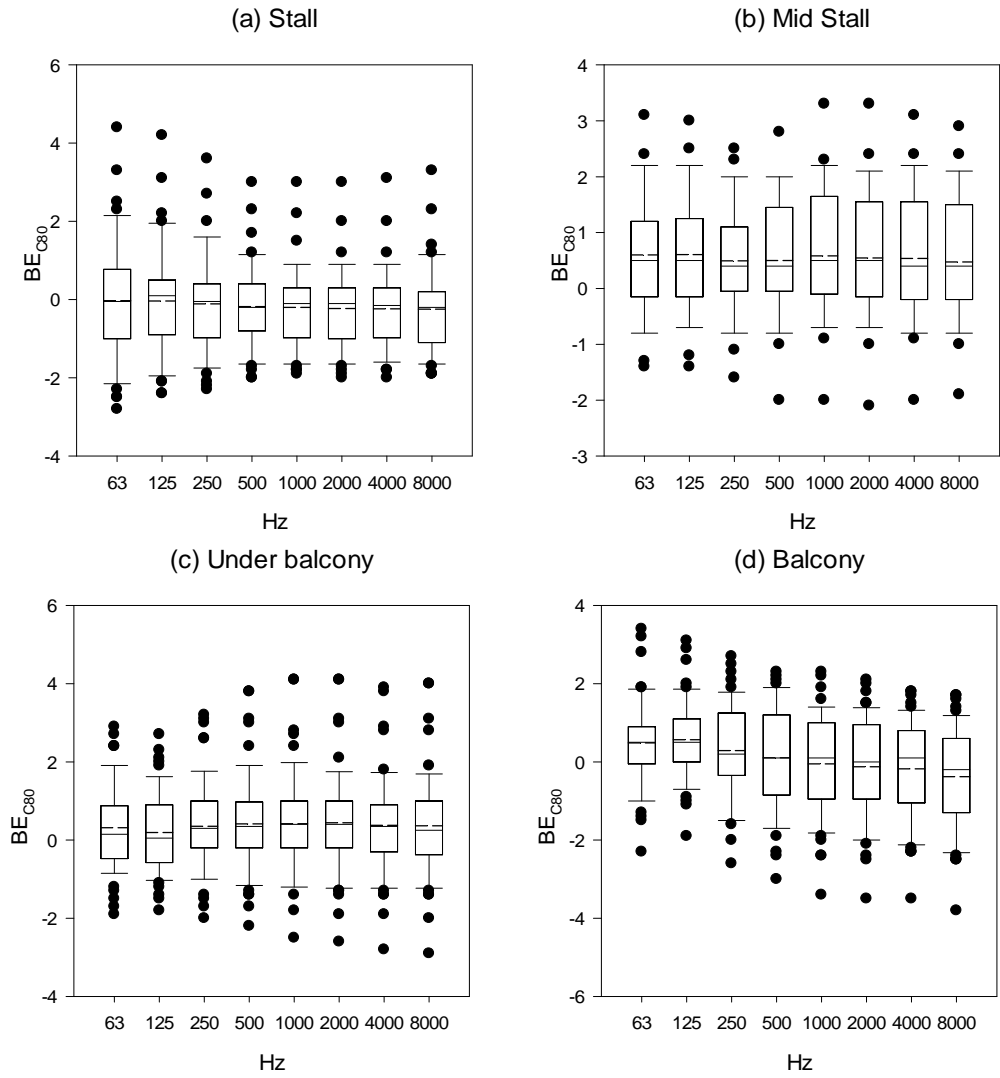


Figure 7-39 The balcony effect in C80 (in dB) spectrum of the ray-tracing model with a concert stage setting, comparison between a full balcony and a half-ly reduced balcony
 • : 5th and 95th percentiles; error bars : 10th and 90th percentiles; box edges : 25th and 75th percentiles; horizontal lines within boxes : median; horizontal dashed lines : mean values

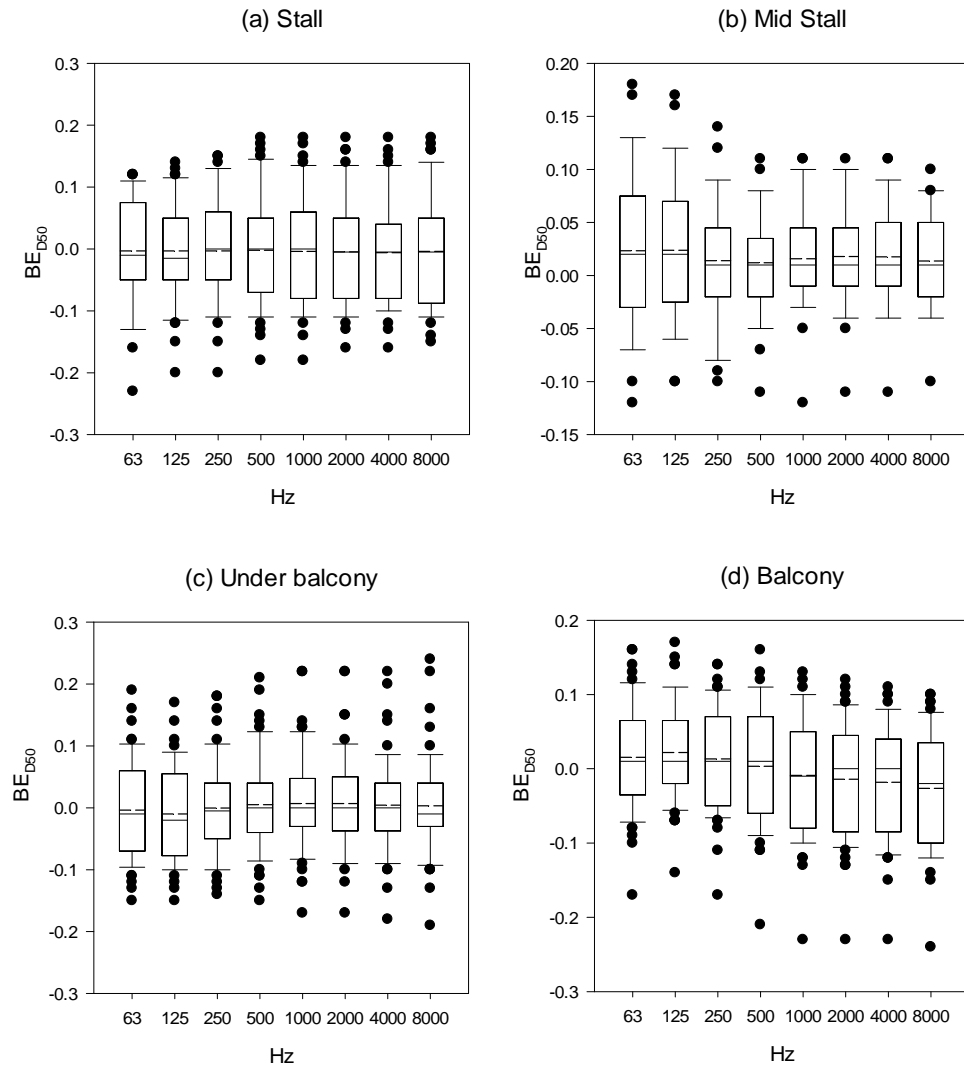


Figure 7-40 The balcony effect in D50 spectrum of the ray-tracing model with a concert stage setting, comparison between a full balcony and a half-ly reduced balcony
 • : 5th and 95th percentiles; error bars : 10th and 90th percentiles; box edges : 25th and 75th percentiles; horizontal lines within boxes : median; horizontal dashed lines : mean values

7.8 Conclusions

A 1/10 scale model study was done to investigate the effect of the balcony to the acoustics in a performance hall. The model was built with reference to the architecture of Hall A, an auditorium with a balcony seating more than 1000 audience. The experiment was classified into four cases, covering the concert setting and proscenium setting, with and without the balcony. The same set of measurement points was used in the four cases (120 for cases with balcony and 86 for cases with balcony). A spark source was used as the high-frequency sound source.

The measured results were with very long decay time and reverberation time. The effects of the balcony were studied. Though, the concert setting and the proscenium settings gave different results, they would have some common trends in altering the C80 and D50 values. This shows that the balcony has brought extra early energy to the seats under the balcony.

The presence of the sound canopy causes different acoustical parameters to behave differently at different frequencies, e.g. some parameters will increase at low frequencies and decrease at higher frequencies.

A 3D simulation model of Hall A was built to study the effect of the balcony size. In addition to the full size balcony and without balcony, a reduced size balcony of $\frac{1}{2}$ of the full size depth was also simulated. Ray-tracing based room acoustic software, Odeon was used for the simulation.

From the results of the scale model experiment and the ray-tracing simulation, it can be seen that the balcony does not affect the T30, EDT, C80 and D50 at the seats closer to the source in a performance hall. If the reverberant sound field is very strong in the hall, the balcony will help increase the amount of reflection in the hall. The statistical results and the plots of the impulse response in the previous sections also suggested that the balcony has helped to bring reflections earlier by shortening the first reflection time at the seats ranging from mid-stall to underneath the balcony. The balcony can also shorten the time gap between each reflection. These benefits of the balcony structure helps increase the early energy to the seats before and under the balcony. However, the change in early energy ratios, C80 and D50, also depend on the changes in the absorption area due to the change of the balcony.

The scale model experiment and the ray-tracing simulation worth further studies to enhance the results. The interior surfaces of the scale model was untreated and left with a smooth finish. This should have contributed to the very long RT measured, (up to 7s) which was not realistic in practice.

In this scale model, the boxes hovering the left and right hand side of the front stall area were omitted. Such omission tends to reduce the reflections to the front stall area but expose the seats underneath to more reflections. The sidewalls in the present study were also taken as smooth surfaces which simplify the reflectors with no absorption treatment while maintaining the angle diverging from the stage. This smooth surfaces increase the reflection over the front stall area. All the seating area are smoothed out and no scale down chairs were placed in the scale model. This would change the scattering coefficients of the audience and its absorption. The unmatched absorption on the scale model with respect to the real hall would affect the reflection pattern of the hall. The increased amount of reflection lengthens the decay time in the hall, widens the time gap between each reflection and increases the early energy content. As a whole, it tends to increase the total energy received at each receiver point.

The modification in the interior of this scale model limits the use of the data. The measured data can only present the effects of the balcony in the form of comparing the variation pattern and trends as well as the ratio of difference between cases, with and without the balcony.

The current results can yet be able to be generalized for other hall designs. One can still use the balcony effect ratio to compare and normalize results from simulations. With further analysis or simulation, one can incorporate the balcony ratio to compare the difference of simulated hall results. Future studies using scale model should also include absorption material in the model. This will provide more comprehensive results.

The construction of the scale model can be improved using new technology like 3D printer to improve the accuracy of small construction details and reduce the time cost for construction. With these kinds of delicate technology the exact dimension of the scale model can be printed which would also ensure the dimension and the airtightness of the model.

Chapter 8 Conclusions and Recommendation for Future Work

8.1 Conclusions

Chapter 2 stated the background of this research and reviewed the development in large performance hall researches worldwide over the years. This chapter also gave a brief account on the acoustical parameters involved in the present study. The impulse response method for measuring hall acoustical parameters was discussed in detail. The theory and application of the neural network analysis were also explained in the chapter.

Chapter 3 fully explained the sound source, equipment setup and methodology of carrying out the real hall measurement as well as the scale model experiment. The number of measurement cases, the construction of the scale model, and the characteristics of the spark source used in the scale model experiment were also discussed in this chapter..

Chapter 4 is one of the major parts of this study. Four different halls, namely Hall A, Hall B, Hall C and Hall D, with a total of seven full sets of data were collected. The results of this chapter are fundamental for the calculations and modelling building in the next few chapters. The binaural measurement results of the hall measurements were presented and discussed in this chapter. However, through simple plotting and curve fitting with physical parameter of the halls, not much straight-forward correlation can be found among the measured parameters from the measured results. Therefore, the calculation for finding the point of first reflection thus the path difference between direct and the first reflection was proposed. This geometrical parameter was then used together with the other parameters in the neural network analysis in Chapter 5.

Neural network analysis (NNA), presented in Chapter 5, is an important analysis in this study. Four training schemes were adopted with a relatively simple NNA prediction algorithm. The results of Hall A and Hall B were used in building, training and testing the network. The spherical coordinates of the measurement points were used as the inputs to the neural network algorithm. Both the concert and proscenium settings were included in the present study. A simple framework for the evaluation of performance hall acoustics has been established, this framework is good for halls with similar level of reverberance.

The regression analysis presented in Chapter is a compliment to the Neural Network Analysis in Chapter 5. The data from Chapter 4, divided into the four schemes used in Chapter 5, were analysed in an attempt to establish a systematic framework for predicting the early interaural cross-correlation coefficients (IACCE₃) through simple regression models with as little geometrical hall parameters and measurements as possible. For simplicity, the regression models generated were formed by linear combinations of polynomials of these parameters without any inclusion of cross-products of different parameters. The results of this study has shown that a simple model for predicting IACCE₃ to within engineering tolerance in acoustically symmetrical halls is feasible.

Chapter 7 summarizes the results of a 1/10 scale down model experiment of Hall A. The scale model was made of varnished wood panels. With a 2-feet tall raised platform below, access was allowed underneath the balcony and therefore around 120 measurements were carried out within a reasonable time period. Four different cases: with a concert or a proscenium setting, with and without balcony respectively have been measured. A scaled down sound canopy was also installed to the stage in the scale model for converting from proscenium setting to concert setting. The floor and the ceiling soffit of the balcony were taken down to covert the cases from with balcony to without balcony.

The two different hall settings in the scaled model give different results on the balcony effect. The balcony effects of each acoustical parameters are not consistent across all frequencies in each setting. In the concert setting, the sound canopy and the balcony, have brought extra early energy to the seats under the balcony. A 3D ray-tracing model was also built to simulate the additional case with a reduced-size balcony.

Contrasting the scale model results with the computer simulation results, the balcony was found to result in more reflections to the hall while bring reflections to an earlier time to the seats before the structure and even minimising the time gap between each reflection received at seats underneath. This may help improve the early energy ratios in the hall. In general, the balcony helps provide early energy to the seats under the balcony.

In this study, four halls were measurement intensively. The acoustical parameters measured in Halls A and B were further processed with neural network analysis and regression analysis. The possibility of predicting the hall parameters using geometrical and reduced amount of measured data were tested with this two approaches. It is found

that with an appropriate scheme in selecting the data from centre and perimeter of each hall zone, neural network analysis can predict the hall parameters accurately. The regression analysis approach can also predict the parameters successfully and even performed better than the neural network approach. These two prediction approaches so developed enable more efficient and reliable investigation of hall acoustics using a sufficiently small number of measurements.

8.2 Limitations of the present study

More extensive measurements were aimed to be performed for the real hall measurements and survey part, however, due to the ballooning demand in hall bookings all over Hong Kong, only measurements inside the listed halls were facilitated. At the same time, the access to hall information like recorded drawings was limited. Important information like absorption of the hall can hardly be found. While the number of halls measured was small, only Hall B can be used to justify the usefulness of neural network and regression analysis prediction approach in rectangular and fan-shaped halls.

The scale model experiment was done without any absorption treatment on the internal surfaces. This greatly affected the reflections inside the scale model thus the use and interpretation of the measured data. This also limited the comparison of results with those simulated using ray-tracing method. Also, due to the limit of space in the campus, the scale model was taken down into piece after the measurement was completed. Hence, further scale model experiments will be beneficial for deeper understanding of the subject

8.3 Recommendations for future work

More halls should be measured to expand the data pool. The larger and more comprehensive the data pool, the higher the chance of being able to generalize the prediction approaches for parameters. The types and use of halls can be extended to modern church halls with balconies and other performance halls with multiple balconies.

Effort can be used to find out the absorption properties and the detailed design of the halls. This can facilitate the understanding of the measured results. More scale model experiments should be carried out with absorption included for more in-depth understanding of the sound propagation phenomena and possible generalization work.

More ray-tracing simulation should also be done to investigate the effects of changing the balcony design while keeping the absorption in the hall as constant for easier comparison.

Subjective hall evaluation can be considered for future research. Other than western music, halls in Hong Kong are also used for Chinese music, which are totally different from western music in nature. This may bring differences in evaluating and correlating the subjective and objective parameters.

BIBLIOGRAPHIC REFERENCES

- [1] M. R. Schroeder, "Toward better acoustics for concert halls," *Phys. Today*, vol. 33, no. 10, p. 24, Dec. 1980.
- [2] L. L. Beranek, "Acoustics and the concert hall," *J. Acoust. Soc. Am.*, vol. 57, no. 6, pp. 1258–1262, 1975.
- [3] "ISO 9613-1:1993 - Acoustics -- Attenuation of sound during propagation outdoors -- Part 1: Calculation of the absorption of sound by the atmosphere." [Online]. Available: http://www.iso.org/iso/catalogue_detail.htm?csnumber=17426. [Accessed: 15-Jul-2015].
- [4] L. L. Beranek, *Concert Halls and Opera Houses: Music, Acoustics, and Architecture*, 2nd ed. New York: Springer, 2004.
- [5] L. E. Kinsler, *Fundamentals of acoustics*. New York : Wiley, c1982., 1982.
- [6] L. L. Beranek, *Concert and Opera Halls : How They Sound*. Woodbury, N.Y.: Published for the Acoustical Society of America through the American Institute of Physics, 1996.
- [7] M. R. Schroeder, B. S. Atal, G. M. Sessler, and J. E. West, "Acoustical Measurements in Philharmonic Hall (New York)," *J. Acoust. Soc. Am.*, vol. 40, no. 2, p. 434, Jul. 1966.
- [8] M. R. Schroeder, "Computer Models for Concert Hall Acoustics," *Am. J. Phys.*, vol. 41, no. 4, p. 461, Jul. 1973.
- [9] E. N. Gilbert, "An iterative calculation of auditorium reverberation," *J. Acoust. Soc. Am.*, vol. 69, no. 1, p. 178, Jan. 1981.
- [10] E. N. Gilbert, "Ray statistics in reverberation," *J. Acoust. Soc. Am.*, vol. 83, no. 5, p. 1804, May 1988.
- [11] M. Barron, *Auditorium acoustics and architectural design*, 2nd ed. London ; New York: Spon Press, 2010.

- [12] R. Thiele, "Richtungsverteilung und Zeitfolge der Schallrückwürfe in Räumen," *Acta Acust. united with Acust.*, vol. 3, no. 4, pp. 291–302, 1953.
- [13] ISO3382:1-2009, "Part 1: Performance spaces (ISO3382-1:2009)," vol. BS EN ISO. BSI Group, UK, 2009.
- [14] V. L. Jordan, *Acoustical Design of Concert Halls and Theatres: a personal account*. London: Applied Science Publishers LTD., 1980.
- [15] V. L. Jordan, "Acoustical Criteria for Auditoriums and Their Relation to Model Techniques," *J. Acoust. Soc. Am.*, vol. 47, no. 2A, p. 408, Aug. 1970.
- [16] *BS ISO 226:2003 Acoustics — Normal equal-loudness-level contours*. ISO, 2003.
- [17] J. S. Bradley, "Using ISO 3382 measures, and their extensions, to evaluate acoustical conditions in concert halls," *Acoust. Sci. Technol.*, vol. 26, no. 2, pp. 170–178, 2005.
- [18] M. Barron, "Using the standard on objective measures for concert auditoria, ISO 3382, to give reliable results," *Acoust. Sci. Technol.*, vol. 26, no. 2, pp. 162–169, 2005.
- [19] T. Hidaka, L. L. Beranek, S. Masuda, N. Nishihara, and T. Okano, "Acoustical design of the Tokyo Opera City (TOC) concert hall, Japan," *J. Acoust. Soc. Am.*, vol. 107, no. 1, pp. 340–354, 2000.
- [20] J. Nannariello and F. R. Fricke, "A neural-computation method of predicting the early interaural cross-correlation coefficient (IACCE3) for auditoria," *Appl. Acoust.*, vol. 63, no. 6, pp. 627–641, Jun. 2002.
- [21] Y. Ando and M. R. Schroeder, *Concert hall acoustics*, no. v 17. Berlin ; New York: Springer-Verlag, 1985.
- [22] L. L. Beranek, "Concert hall acoustics - 2008," *J. Audio Eng. Soc.*, vol. 56, no. 7–8, pp. 532–544, 2008.
- [23] A. Marshall, "Spatial responsiveness in concert halls and the origins of spatial impression," *Appl. Acoust.*, vol. 62, no. 2, pp. 91–108, Feb. 2001.

- [24] J. S. Bradley and G. A. Soulodre, "The influence of late arriving energy on spatial impression," *J. Acoust. Soc. Am.*, vol. 97, no. 4, pp. 2263–2271, 1995.
- [25] L. Beranek, "The sound strength parameter G and its importance in evaluating and planning the acoustics of halls for music," *J. Acoust. Soc. Am.*, vol. 129, no. 5, p. 3020, 2011.
- [26] H. Sakai, Y. Ando, N. Prodi, and R. Pompoli, "TEMPORAL AND SPATIAL ACOUSTICAL FACTORS FOR LISTENERS IN THE BOXES OF HISTORICAL OPERA THEATRES," *J. Sound Vib.*, vol. 258, no. 3, pp. 527–547, 2002.
- [27] A. Cocchi, M. Garai, and C. Tavernelli, "BOXES AND SOUND QUALITY IN AN ITALIAN OPERA HOUSE," *J. Sound Vib.*, vol. 232, no. 1, pp. 171–191, 2000.
- [28] P. John, "Introduction to Pitch Perception," in *Music, cognition, and computerized sound: an introduction to psychoacoustics*, P. R. Cook, Ed. Cambridge, Mass.: The MIT Press, 1999, pp. 57–70.
- [29] M. Max, "What is loudness?," in *Music, cognition, and computerized sound: an introduction to psychoacoustics*, P. R. Cook, Ed. Cambridge, Mass.: The MIT Press, 1999, pp. 71–78.
- [30] J. Parmanen, "A-weighted sound pressure level as a loudness/annoyance indicator for environmental sounds – Could it be improved?," *Appl. Acoust.*, vol. 68, no. 1, pp. 58–70, Jan. 2007.
- [31] J. M. Grey, "Multidimensional perceptual scaling of musical timbres," *J. Acoust. Soc. Am.*, vol. 61, no. 5, p. 1270, 1977.
- [32] M. Max, "Introduction to Timbre," in *Music, cognition, and computerized sound: an introduction to psychoacoustics*, P. R. Cook, Ed. Cambridge, Mass.: The MIT Press, 1999, pp. 79–87.
- [33] L. L. Beranek, "Audience and Seat Absorption in Large Halls," *J. Acoust. Soc. Am.*, vol. 32, no. 6, pp. 661–670, Jul. 1960.

- [34] L. L. Beranek, "Audience and Chair Absorption in Large Halls. II," *J. Acoust. Soc. Am.*, vol. 45, no. 1, pp. 13–19, 1969.
- [35] L. L. Beranek, "Analysis of Sabine and Eyring equations and their application to concert hall audience and chair absorption," *J. Acoust. Soc. Am.*, vol. 120, no. 3, pp. 1399–1410, 2006.
- [36] T. Hidaka, N. Nishihara, and L. L. Beranek, "Relation of acoustical parameters with and without audiences in concert halls and a simple method for simulating the occupied state," *J. Acoust. Soc. Am.*, vol. 109, no. 3, pp. 1028–1042, Mar. 2001.
- [37] N. Nishihara, T. Hidaka, and L. L. Beranek, "Mechanism of sound absorption by seated audience in halls," *J. Acoust. Soc. Am.*, vol. 110, no. 5, pp. 2398–2411, 2001.
- [38] L. L. Beranek and T. Hidaka, "Sound absorption in concert halls by seats, occupied and unoccupied, and by the hall's interior surfaces," *J. Acoust. Soc. Am.*, vol. 104, no. 6, pp. 3169–3177, 1998.
- [39] C. Haan and F. R. Fricke, "An evaluation of the importance of surface diffusivity in concert halls," *Appl. Acoust.*, vol. 51, no. 1, pp. 53–69, May 1997.
- [40] C. Hann and F. Fricke, "Surface Diffusivity as a Measure of the Acoustic Quality of Concert Halls," *Mech 94 Int. Mech. Eng. Congr. Exhib. Prepr. Pap. Resour. Eng. Vol. 3 Conf. 3; Noise Vib.*, p. 79, 1994.
- [41] T. Hidaka and L. L. Beranek, "Objective and subjective evaluations of twenty-three opera houses in Europe, Japan, and the Americas," *J. Acoust. Soc. Am.*, vol. 107, no. 1, pp. 368–383, 2000.
- [42] M. Barron, "Balcony overhangs in concert auditoria," *J. Acoust. Soc. Am.*, vol. 98, no. 5, p. 2580, 1995.
- [43] H. FURUYA, "Acoustical characteristics of the sound field under balcony in auditoria: A study using a scale model technique.," *Summ. Tech. Pap. Annu. Meet.*, 1999.
- [44] Y. Y.-M. Kwon and Y. Shimizu, "Under-balcony acoustics in concert halls: Vertical energy loss at the listener and acceptable view angles deduced from its

- effects,” *J. Acoust. Soc. Am.*, vol. 111, no. 5, p. 2331, 2002.
- [45] H. Furuya and K. Fujimoto, “An acoustical design criterion for balcony configuration in auditoria. II. A consideration on the directional characteristics of early reflections by computer simulation,” *J. Acoust. Soc. Am.*, vol. 100, no. 4, p. 2706, 1996.
- [46] K. Fujimoto, “An acoustical design criterion for balcony configuration in auditoria. I. Acoustical characteristics measured under the balcony and the effects on auditory envelopment,” *J. Acoust. Soc. Am.*, vol. 100, no. 4, p. 2706, 1996.
- [47] W. Chiang, W. Lin, and K. Wu, “Improving sound qualities at the seats under deep balcony overhangs,” *J. Acoust. Soc. Am.*, vol. 120, no. 5, p. 3054, 2006.
- [48] N. Edwards and D. Kahn, “Why do traditional opera houses work so well for opera?,” *J. Acoust. Soc. Am.*, vol. 103, no. 5, p. 2784, 1998.
- [49] Y. W. Lam, “A comparison of three diffuse reflection modeling methods used in room acoustics computer models,” *J. Acoust. Soc. Am.*, vol. 100, no. 4, pp. 2181–2192, 1996.
- [50] M. Hodgson, “Evidence of diffuse surface reflections in rooms,” *J. Acoust. Soc. Am.*, vol. 89, no. 2, pp. 765–771, 1991.
- [51] T. M. Chan and W. M. To, “Modelling of Scattering from Balcony Fronts,” *Build. Acoust.*, vol. 9, pp. 219–231, 2002.
- [52] M. R. Schroeder, “New Method of Measuring Reverberation Time,” *J. Acoust. Soc. Am.*, vol. 37, no. 3, p. 409, Jul. 1965.
- [53] C. S.W., *Shift-Register Sequences*. San Francisco: Holden-Day, 1967.
- [54] M. R. Schroeder, “Integrated-impulse method measuring sound decay without using impulses,” *J. Acoust. Soc. Am.*, vol. 66, no. 2, p. 497, Aug. 1979.
- [55] H. Kuttruff, “Comments to ‘Comparison of Reverberation Measurements Using the ISO and the Schroeder-Kuttruff-Method,’” *Acta Acust. united with Acust.*, vol. 34, no. 1, p. 46, 1975.

- [56] A. Lundeby, T. E. Vigran, H. Bietz, and M. Vorländer, “Uncertainties of Measurements in Room Acoustics,” *Acta Acust. united with Acust.*, vol. 81, pp. 344–355, 1995.
- [57] Griesinger D., “Beyond MLS- occupied hall measurement with FFT techniques.,” in *101st AES Convention*, 1996.
- [58] N. A., “On the acoustical characteristics of a balloon,” in *Proceedings of the 16th ICA*, 1998.
- [59] D. Sumaracpavlovic, D. Sumarac-Pavlovic, M. Mijic, and H. Kurtovic, “A simple impulse sound source for measurements in room acoustics,” *Appl. Acoust.*, vol. 69, no. 4, pp. 378–383, Apr. 2008.
- [60] B. H. Repp, “The sound of two hands clapping: An exploratory study,” *J. Acoust. Soc. Am.*, vol. 81, no. 4, p. 1100, Apr. 1987.
- [61] W. M. Wright, “Propagation in air of N waves produced by sparks,” *J. Acoust. Soc. Am.*, vol. 73, no. 6, p. 1948, 1983.
- [62] R. Wyber, “The design of a spark discharge acoustic impulse generator,” *IEEE Trans. Acoust.*, vol. 23, no. 2, pp. 157–162, 1975.
- [63] D. D. Rife and J. Vanderkooy, “Transfer-Function Measurement with Maximum-Length Sequences,” *J. Audio Eng. Soc.*, vol. 37, no. 6, pp. 419–444, 1989.
- [64] Aoshima N and Igarashi J., “M-sequence signal applied to the correlation measurement of acoustic system,” *J. Acoust. Soc. Japan*, vol. 24, pp. 197–206, 1968.
- [65] Y. Suzuki, “An optimum computer-generated pulse signal suitable for the measurement of very long impulse responses,” *J. Acoust. Soc. Am.*, vol. 97, no. 2, p. 1119, Feb. 1995.
- [66] N. Aoshima, “Computer-generated pulse signal applied for sound measurement,” *J. Acoust. Soc. Am.*, vol. 69, no. 5, p. 1484, May 1981.
- [67] X. Pelorson, J.-P. Vian, and J.-D. Polack, “On the variability of room acoustical

parameters: Reproducibility and statistical validity,” *Appl. Acoust.*, vol. 37, no. 3, pp. 175–198, Jan. 1992.

- [68] T. H. Sato F, Hirano J, Sakamoto S, “Comparison between the MLS and TSP methods for room impulse response measurement under time-varying condition,” in *Proceedings of international national symposium on room acoustics: RADS2004*, 2004, p. B05.
- [69] M. Barron, “ISO 3382 - How good are the acoustics really?,” in *Proceedings of the international national symposium room acoustics: RADS2004*, 2004, p. B01.
- [70] I. B. Witew, G. K. Behler, and M. Vorländer, “Subjective limens for lateral fraction and later lateral strength,” in *Proceedings of the international national symposium room acoustics: RADS2004*, 2004, p. B02.
- [71] T. Hidaka, “Supplemental data of dependence of room acoustical parameters on source and receiver positioning,” in *Proceedings of international national symposium room acoustics: RADS2004*, 2004, p. B03.
- [72] J. S. Bradley, “Using ISO3382 measures to evaluate acoustical conditions in concert halls,” in *Proceedings of international national symposium room acoustics: RADS2004*, 2004, p. B04.
- [73] R. Orłowski, “The relevance of ISO 3382 in auditorium design and measurement,” in *Proceedings of international national symposium room acoustics: RADS2004*, 2004, p. B06.
- [74] T. Hidaka, “Supplemental data of dependence of objective room acoustical parameters on source and receiver positions at field measurement,” *Acoust. Sci. Technol.*, vol. 26, no. 2, pp. 128–135, 2005.
- [75] I. B. Witew, G. K. Behler, and M. Vorländer, “About just noticeable differences for aspects of spatial impressions in concert halls,” *Acoust. Sci. Technol.*, vol. 26, no. 2, pp. 185–192, 2005.
- [76] T. Akama, H. Suzuki, and A. Omoto, “Distribution of selected monaural acoustical parameters in concert halls,” *Appl. Acoust.*, vol. 71, no. 6, pp. 564–577, Jun. 2010.

- [77] S. Haykin, *Neural Networks. A comprehensive Foundation*. New York: Prentice-Hall, 1998.
- [78] J. Nannariello and F. R. Fricke, "A neural network analysis of the effect of geometric variables on concert hall G values," *Appl. Acoust.*, vol. 62, no. 12, pp. 1397–1410, Dec. 2001.
- [79] A. C. Gade, "Prediction of room acoustical parameters," *J. Acoust. Soc. Am.*, vol. 89, no. 4B, p. 1857, Aug. 1991.
- [80] J. Nannariello and F. R. Fricke, "The use of neural network analysis to predict the acoustic performance of large rooms Part I. Predictions of the parameter G utilizing numerical simulations," *Appl. Acoust.*, vol. 62, no. 8, pp. 917–950, Aug. 2001.
- [81] J. Nannariello and F. R. Fricke, "The use of neural network analysis to predict the acoustic performance of large rooms Part II. Predictions of the acoustical attributes of concert halls utilizing measured data," *Appl. Acoust.*, vol. 62, no. 8, pp. 951–977, Aug. 2001.
- [82] L. Yu and J. Kang, "Modeling subjective evaluation of soundscape quality in urban open spaces: An artificial neural network approach.," *J. Acoust. Soc. Am.*, vol. 126, no. 3, pp. 1163–74, Sep. 2009.
- [83] Dirac, "Acoustics Engineering - Dirac." [Online]. Available: <http://www.acoustics-engineering.com/html/dirac.html>. [Accessed: 24-Aug-2015].
- [84] H. Kuttruff, *Room Acoustics*. Oxon: Spon Press, 2009.
- [85] *Signal Processing Toolbox 6 User's Guide*, 6th ed. Massachusetts: The MathWorks, Inc., 2002.
- [86] J. Nannariello and F. Fricke, "Introduction to neural network analysis and its application to building services engineering," *Build. Serv. Eng. Res. Technol.*, vol. 22, no. 1, pp. 58–68, Feb. 2001.
- [87] N. Genaro, A. Torija, A. Ramos-Ridao, I. Requena, D. P. Ruiz, and M. Zamorano, "A neural network based model for urban noise prediction.," *J. Acoust. Soc. Am.*,

vol. 128, no. 4, pp. 1738–46, Oct. 2010.

- [88] H. Demuth, M. Beale, and M. Hagan, *Neural Network Toolbox 5 User's Guide*. Massachusetts: The MathWorks, Inc., 2007.
- [89] “Lee Hysan Concert Hall.” [Online]. Available: <http://www.macostar.com/wordpress/wp-content/uploads/2012/11/m326-7446.jpg>. [Accessed: 24-Aug-2015].
- [90] M. Barron, “Energy relations in concert auditoriums. I,” *J. Acoust. Soc. Am.*, vol. 84, no. 2, p. 618, 1988.
- [91] Y. Ando and M. Imamura, “Subjective preference tests for sound fields in concert halls simulated by the aid of a computer,” *J. Sound Vib.*, vol. 65, no. 2, pp. 229–239, Jul. 1979.
- [92] T. Hidaka, L. L. Beranek, and T. Okano, “Interaural cross-correlation (IACC), lateral fraction (LF), and low- and high-frequency sound levels (G) as measures of acoustical quality in concert halls,” *J. Acoust. Soc. Am.*, vol. 97, no. 5, p. 3319, 1995.
- [93] W. Reichardt, O. A. Alim, and W. Schmidt, “Abhängigkeit der grenzen zwischen brauchbarer und unbrauchbarer durchsichtigkeit von der art des musikmotives, der nachhallzeit und der nachhalleinsatzzzeit,” *Appl. Acoust.*, vol. 7, no. 4, pp. 243–264, Oct. 1974.
- [94] M. BARRON and A. MARSHALL, “Spatial impression due to early lateral reflections in concert halls: The derivation of a physical measure,” *J. Sound Vib.*, vol. 77, no. 2, pp. 211–232, Jul. 1981.
- [95] T. Okano, L. L. Beranek, and T. Hidaka, “Relations among interaural cross-correlation coefficient (IACC(E)), lateral fraction (LFE), and apparent source width (ASW) in concert halls,” *J. Acoust. Soc. Am.*, vol. 104, no. 1, pp. 255–265, 1998.
- [96] a Carvalho, “Relations between rapid speech transmission index (RASTI) and other acoustical and architectural measures in churches,” *Appl. Acoust.*, vol. 58,

- no. 1, pp. 33–49, Sep. 1999.
- [97] S. K. Tang, “Speech related acoustical parameters in classrooms and their relationships,” *Appl. Acoust.*, vol. 69, no. 12, pp. 1318–1331, Dec. 2008.
- [98] U. Berardi, E. Cirillo, and F. Martellotta, “A comparative analysis of acoustic energy models for churches,” *J. Acoust. Soc. Am.*, vol. 126, no. 4, pp. 1838–49, Oct. 2009.
- [99] R. San Martin and M. Arana, “Predicted and experimental results of acoustic parameters in the new Symphony Hall in Pamplona, Spain,” *Appl. Acoust.*, vol. 67, no. 1, pp. 1–14, Jan. 2006.
- [100] P. Evjen, J. . Bradley, and S. . Norcross, “The effect of late reflections from above and behind on listener envelopment,” *Appl. Acoust.*, vol. 62, no. 2, pp. 137–153, Feb. 2001.
- [101] A. Kuusinen, J. Pätynen, S. Tervo, and T. Lokki, “Relationships between preference ratings, sensory profiles, and acoustical measurements in concert halls,” *J. Acoust. Soc. Am.*, vol. 135, no. 1, pp. 239–250, Jan. 2014.
- [102] T. HOTEHAMA, S. SATO, and Y. ANDO, “DISSIMILARITY JUDGMENTS IN RELATION TO TEMPORAL AND SPATIAL FACTORS FOR THE SOUND FIELD IN AN EXISTING HALL,” *J. Sound Vib.*, vol. 258, no. 3, pp. 429–441, Nov. 2002.
- [103] M. Sakurai, “a Diagnostic System Measuring Orthogonal Factors of Sound Fields in a Scale Model of Auditorium,” *J. Sound Vib.*, vol. 232, no. 1, pp. 231–237, Apr. 2000.
- [104] Y. Jurkiewicz, T. Wulfrank, and E. Kahle, “Architectural shape and early acoustic efficiency in concert halls (L),” *J. Acoust. Soc. Am.*, vol. 132, no. 3, pp. 1253–6, Sep. 2012.
- [105] H. Furuya, “An acoustical design criterion for balcony configuration in auditoria. II. A consideration on the directional characteristics of early reflections by computer simulation,” *J. Acoust. Soc. Am.*, vol. 100, no. 4, p. 2706, 1996.